Universitat Autònoma de Barcelona

Development and application of control strategies in an aerobic biotrickling filter for H2S removal from biogas streams: experimental and modelling study

Luis Rafael López De León

Universitat Autònoma de Barcelona

School of Engineering

Department of Chemical, Biological and Environmental Engineering

Development and application of control strategies in an aerobic biotrickling filter for H_2S removal from biogas streams: experimental and modelling study

PhD Thesis

Supervised by:

Dr. David Gabriel Buguña

Luis Rafael López De León

April, 2016

Title: Development and application of control strategies in an aerobic biotrickling filtre for H_2S removal from biogas streams: experimental and modelling study

Presented by: Luis Rafael López De León

Supervisor: David Gabriel Buguña

Doctoral Programme in Environmental Science and Technology, specialty in Environmental Technology.
ICTA – Institut de Ciència i Tecnologia Ambientals.

Departament d'Enginyeria Química, Biològica i Ambiental
Escola d'Enginyeria.
Universitat Autònoma de Barcelona, Bellaterra.

Part of this work has been done at Ghent University (Ghent, Belgium) under the supervision of Prof dr. ir Eveline Volcke

The Spanish Government provided financial support through the Ministerio de Economia project CTM2012-37927-C03-01. The Department of Chemical, Biology and Environmental Engineering is a unit of Biochemical Engineering of the Xarxa de Referència en Biotecnologia de Catalunya (XRB), Generalitat de Catalunya.

DAVID GABRIEL BUGUÑA, professor agregat del Departament d'Enginyeria Química, Biològica i Ambiental de la Universitat Autònoma de Barcelona

CERTIFICA:

Que l'enginyer químic **LUIS RAFAEL LÓPEZ DE LEÓN** ha realitzat sota la nostra direcció el treball titulat: "**Development and application of control strategies in an aerobic biotrickling filter for H_2S removal from biogas streams: experimental and modelling study**" el qual es presenta en aquesta memòria i que constitueix la seva tesi per a optar al Grau de Doctor per la Universitat Autònoma de Barcelona.

I perquè en prengueu coneixement i consti als efectes oportuns, presentem a l'Escola d'Enginyeria de la Universitat Autònoma de Barcelona l'esmentada Tesi, signant el present certificat a

Bellaterra, 7 d'abril de 2016

David Gabriel Buguña

This work is dedicated to my mother Maria Clementina, joy and happiness of my life. Also to my father Ricardo. My brothers José, Elba, Rodrigo and Manolo. To Mabel, my all. Thanks for being unconditionally with me along this journey. And especially in memoriam of my aunt, Yolanda "tia tutu" who supported me until her last breath.

Acknowledgements

CONTENTS

Summary. v

Resum. vi

Resumen. vii

List of Abbreviations. viii

Chapter 1

MOTIVATIONS AND THESIS OVERVIEW 3

Chapter 2

INTRODUCTION

Desulfurization of biogas 9
Modelling of biofiltration reactors 21
Process control theory 26

Chapter 3

OBJECTIVES 41

Chapter 4

MATERIALS AND METHODS

Description of equipments 45
Design and operational parameters of BTFs 54

Chapter 5

CHARACTERIZATION OF MANIPULATED VARIABLES IN AN AEROBIC BIOTRICKLING FILTER FOR BIOGAS DESULFURIZATION

Abstract 65
Introduction 67
Materials and methods 69
Biotrickling filter set up
Abiotic tests
Startup under co-current BTF operation
Biotic experimental conditions
Results and discussion 72
Effect of TLV and air supply in co-current and counter-current abiotic conditions
Startup under co-current BTF operation

Effect of TLV regulation on H_2S removal in co-current flow pattern
Effect of Air flow rate regulation on H_2S removal in co-current flow pattern
Effect of TLV in oxygen transport and biotrickling filter performance
H_2S removal and oxygen consumption along the packed bed height
Conclusions 88

Chapter 6

APPLICATION OF TITRIMETRY AS A MEASURED VARIABLE ON CONTROL LOOPS IN DISCONTINOUS AND CONTINOUS PROCESSES

Abstract 93
Introduction 95
Materials and methods 97
Biological HP determination in BTF for biogas desulfurization under aerobic conditions
Titrimetry application in a discontinuous process
Results and discussion 106
Observed and biological HPR for an aerobic desulfurizing BTF
Titrimetry application in a discontinuous process
Conclusions 119

Chapter 7

MODELLING AEROBIC BIOTRICKLING FILTERS FOR BIOGAS DESULFURIZATION THROUGH A TWO-STEP SULFIDE OXIDATION MECHANISM

Abstract 123
Introduction 125
Materials and methods 127
Experimental setup and operating conditions
Model development 130
Biotrickling filter model
Modeling of biological and chemical conversions of sulfides
Model implementation
Results and discussion 137
Sensitivity analysis
Model parameters estimation
Model Validation
Conclusions 150

Chapter 8

MODEL-BASED ANALYSIS OF CONTROL STRATEGIES IN AN AEROBIC BIOTRICKLING FILTER FOR BIOGAS DESULFURIZATION

Abstract 153
Introduction 155
Materials and methods 158
Empirical Mass transfer correlations
Framework for analysis of open-loop behavior: Effect of H_2S –LR changes due to H_2S inlet concentration and biogas flowrate changes on BTF performance
Framework for analysis for Closed-loop behavior: Effect of H_2S LR changes due to H_2S inlet concentration and biogas flowrate changes on BTF performance
Controllers tuning
Added value of feedback control strategies on biogas desulfurization in aerobic BTFs
Results and discussion 168
Selection of a suitable oxygen mass transfer correlation
Analysis of open-loop behavior: Effect of H_2S LR changes due to H_2S inlet concentration and biogas flowrate changes on BTF performance
Control strategies evaluation to face variable H_2S LR inlet changes
Model Validation
Added value of AFR-CL and TLV-CL control strategies for an aerobic BTF for biogas desulfurization
Conclusions 191

Chapter 9

APPLICATION OF FEEDBACK AND FEEDFORWARD CONTROL STRATEGIES BASED ON TRICKLING LIQUID VELOCITY REGULATION IN AEROBIC BIOTRICKLING FILTERS FOR BIOGAS DESULFURIZATION

Abstract 195
Introduction 196
Materials and methods 198
Experimental conditions for evaluation of feedback control strategy
Experimental conditions for evaluation of feedforward control strategy
Results and discussion 204
Controller parameters re-adjustment to experimental conditions
Evaluation of feedback control facing changes in the H_2S inlet concentration

Evaluation of feedback control facing changes in the biogas flowrate
Evaluation of feedforward control facing changes in the biogas flowrate
Evaluation of feedforward control facing changes in the H_2S inlet concentration
Overall assessment of feedback and feedforward control strategies
Conclusions 217

Chapter 10

GENERAL CONCLUSIONS AND FUTURE WORK 221

Chapter 11

REFERENCES. 229

SUMMARY

Industrial application of biotrickling filters (BTF) for biogas desulfurization under aerobic conditions requires the development and application of control strategies in order to achieve a robust, stable and reliable operation under variable hydrogen sulfide (H_2S) loading rates (LR) conditions. Controlling this type of biological reactors is highly difficult since their controllability depends on several parameters such as O_2 transfer, biological activity, biofilm structure, and LR variability among others. Therefore, before the implementation of control strategies, these systems must be deeply studied to characterize the different variables involved in control loops. In this thesis, not only experimental work under different operational conditions has been performed to understand biogas desulfurization under aerobic conditions in BTFs, but a model-based study has been also included in order to test and evaluate different control strategies before its experimental implementation.

The abiotic study of gas-liquid flow pattern performed before BTF start-up, indicated that co-current flow pattern was the most suitable configuration in order to improve the O_2 mass transport from the gas to the liquid phase, which was evaluated through the standard oxygen transfer rate (SOTR). Moreover, it was demonstrated that trickling liquid velocity (TLV) regulation provided higher SOTR values when compared to air flowrate (AFR) regulation. This result was later confirmed in biotic tests, where the effect in BTF performance of TLV and AFR regulation was quantified. TLV showed a high influence over the main performance parameters such as removal efficiency (RE), elimination capacity (EC) and principally over sulfate selectivity, indicating that TLV is a suitable variable to manipulate in order to improve O_2 transport in the packed bed.

Afterwards titrimetry was evaluated as possible measured variable, in order to relate biological activity and operational changes through proton production (HP) and proton production rate (HPR). Titrimetry was applied for a continuous process as well in a discontinuous process, indicating that HP was a suitable indicator to use in processes monitoring, in order to provide further information of the process state rather for control purposes. Before implementing control strategies, a dynamic model describing physical-chemical and biological processes for the removal of high loads of H_2S from biogas streams in BTFs was developed and successfully calibrated and validated allowing a proper description of different operational scenarios. This model was used to evaluate the influence of different parameters over the main process variables through a sensitivity analysis, and mainly to determine the control limits, capabilities and added value of different feedback control strategies applied to biogas desulfurization in aerobic BTFs. Finally, feedback and feedforward control strategies based on TLV regulation were experimentally evaluated in a desulfurizing BTF under aerobic conditions. Control strategies were designed based in knowledge obtained in the characterization manipulated variables and with the model-based analysis. Application of control strategies based in TLV regulation showed to be a suitable tool in order to improve BTF performance through O_2 transport improvement, without increasing biogas dilution.

RESUM

L'aplicació industrial de biofiltres percoladors per la dessulfuració de corrents de biogàs en condicions aeròbies requereix del desenvolupament i aplicació d'estratègies de control per poder aconseguir una operació robusta, estable i fiable davant de condicions de carga de H_2S variables. El control d'aquest tipus de reactors es difícil ja que la seva controlabilitat depèn de diversos paràmetres com el transport O_2, l'activitat biològica,l' estructura de la bio-pel·lícula i la variabilitat de la carga entre altres. Degut a això, abans de la implementació experimental de les estratègies de control, el sistema ha de ser profundament estudiat per poder de caracteritzar les diferents variables que comprenen un llaç de control. En aquesta tesi, no només s'ha dut a terme un estudi experimental per poder entendre el funcionament dels biofiltres percoladors per a la dessulfuració aeròbia de corrents de biogàs, sinó que també s'ha inclòs un estudi utilitzant un model amb el objectiu d'avaluar les diferents estratègies abans de la seva implementació experimental.

L'estudi abiòtic sobre el tipus de configuració del flux gas-líquid realitzat prèviament a la posada en marxa del biofiltre percolador, va indicar que la configuració en paral·lel es la mes adequada per a millorar el transport gas-líquid d'oxigen, el qual va ser avaluat mitjançant la taxa estàndard de transport d'oxigen. A més a més, es va demostrar que la regulació de la velocitat de percolació era una variable més efectiva per tal de obtenir taxes de transferència d'oxigen mes altes si es comparava amb la regulació del cabal d'aeració. Aquest resultat va ser posteriorment confirmat durant els experiments biòtics, on l'efecte del rendiment del biofiltre percolador davant la regulació de la velocitat de percolació i del cabal d'aeració va ser quantificat. La regulació de la velocitat de percolació va demostrar tenir una major influència en els principals paràmetres de rendiment tal com l'eficiència d'eliminació, la capacitat d'eliminació i principalment sobre la selectivitat de sulfat, indicant ser una variable adequada per la millora del transport de O_2 en el llit empacat.

Posteriorment la tritimetria va ser avaluada com a possible variable mesurada, amb el fi de poder relacionar l'activitat biològica i els canvis operacionals amb la producció de protons i la taxa de producció de protons generat per la reacció biòlogica. La titrimetria va ser aplicada a tant a un procés en continu, com en un procés discontinu, indicant que la producció de protons es una variable més adequada per a la monitorització del procés que per l'aplicació en un llaç de control. Abans de la implementació experimental de les estratègies de control, un model dinàmic incloent els diferents processos fisicoquímics i biològics que formen part de la eliminació de altes carregues de H_2S en corrents de biogàs mitjançant biofiltres percoladors va ser desenvolupat, i satisfactòriament calibrat i validat. Aquest model va permetre l'avaluació de la influencia de diferents paràmetres sobre les principals variables operacionals mitjançant un anàlisi de sensibilitat, així com dels límits de controlabilitat, les capacitats màximes i conèixer el valor afegit de les estratègies de control en la dessulfuració de biogàs en biofiltres percoladors en condiciones aeròbies. Finalment, control retro-alimentat i anticipatiu basat en la regulació de la velocitat de percolació va ser experimentalment avaluat. Aquestes estratègies van ser dissenyades a partir de informació obtinguda durant la caracterització de les variables manipulades i amb el anàlisi realitzat amb el model. Les estratègies de control basades en la regulació de la velocitat de percolació van demostrar ser una eina efectiva per la millora del rendiment dels biofiltres percoladors en condicions aeròbies degut a una considerable millora del transport gas-líquid d'oxigen, sense la necessitat de diluir el corrent de biogàs.

RESUMEN

La aplicación industrial de biofiltros percoladores para la desulfuración de biogás en condiciones aerobias requiere del desarrollo y aplicación de estrategias de control con el fin de poder conseguir una operación robusta, estable y fiable en condiciones de carga variable de H_2S. El control de este tipo de reactores biológicos es difícil ya que su controlabilidad depende de parámetros como el transporte de O_2, actividad biológica, estructura de la biopelícula, y la variabilidad de la carga entre otros. Por ello, antes de realizar la implementación de las estrategias de control, el sistema debe de ser profundamente estudiado para caracterizar las diferentes variables que comprenden un lazo de control. En esta tesis, no solo trabajo experimentación en diferentes condiciones de operación ha sido realizado para entender la desulfuración de biogás en biofiltros percoladores en condiciones aeróbicas, sino que también un estudio utilizando un modelo también ha sido incluido con el fin de poder evaluar las diferentes estrategias antes de su implementación experimental.

El estudio abiótico sobre el tipo de patrón de flujo gas-liquido realizado previo a la puesta en marcha del biofiltro percolador, indico que el patrón en paralelo era la configuración más adecuada para mejorar el transporte gas-liquido de O_2, el cual fue evaluado utilizando la tasa de estándar de transferencia de oxígeno. Además, se demostró que la regulación de la velocidad de percolación era la variable más efectiva para poder obtener mayores tasas de transferencia de oxígeno si se comparaba con la regulación del caudal de aireación. Este resultado luego fue confirmado en los experimentos bióticos, donde el efecto en el rendimiento del biofiltro percolador de la regulación de la velocidad de percolación y del caudal de aireación fue cuantificado. La regulación de la velocidad de percolación demostró tener una mayor influencia en los principales parámetros de rendimiento tales como la eficiencia de eliminación, la capacidad de eliminación y principalmente sobre la selectividad de sulfato, indicando ser una variable manipulada adecuada para poder mejorar el transporte de O_2 en el lecho empacado.

Posteriormente la titrimetría fue evaluada como posible variable medida, con el fin de relacionar la actividad biológica y los cambios operacionales mediante la producción de protones y la tasa de producción de protones. La titrimetría fue aplicada tanto a un proceso continuo como un proceso discontinuo, indicando que la producción de protones era una variable adecuada más adecuada para la monitorización de procesos que para el control de procesos. Antes de la implementación experimental de las estrategias de control, un modelo dinámico incluyendo los procesos físico-químicos y biológicos envueltos en la eliminación de altas cargas de H_2S en corrientes de biogás mediante biofiltros percoladores fue desarrollado, y satisfactoriamente calibrado y validado. Este modelo permitió evaluar la influencia de diferentes parámetros sobre los principales parámetros operacionales a través de un análisis de sensibilidad, así como determinar los límites de controlabilidad, las capacidades máximas y conocer el valor añadido que tienen las estrategias de control en la desulfuración de biogás mediantes biofiltros percoladores en condiciones aerobias. Finalmente, control retroalimentado y control anticipativo basado en la regulación de la velocidad de percolación fueron experimentalmente evaluados. Dichas estrategias de control fueron diseñadas en base a la información obtenida durante la caracterización de las variables manipuladas y mediante el análisis realizado con el modelo. Las estrategias de control basadas en la regulación de la velocidad de percolación demostraron ser una herramienta efectiva para mejorar el rendimiento de los biofiltros percoladores debido a una mejora en el transporte de oxígeno, sin la necesidad de diluir la corriente de biogás.

NOMENCLATURE SECTION

List of abbreviations

AD	Anaerobic digestion
AFR	Air flowrate
ASM	Activated sludge models
BF	Biofilter
BDF	Backwards differentiation formulas
BNR	Biological nutrient removal
BTF	Biotrickling filter
BSM	Benchmarking simulation models
CSTR	Continuous stirred tank reactor
CHP	Combined heat and power
CAD	Centralized anaerobic digestion
DO	Dissolved oxygen
DOL	Dissolved oxygen load
DMFC	Digital mass flow controllers
EBRT	Empty bed residence time
EC	Elimination capacity
FSS	Fixed suspended solids

FW	Food waste
FL	Liquid recycling flow rate
GFR	Gas flow ratio
GHG	Greenhouse gases emissions
HP	Proton production
HPR	Proton production rate
HRT	Hydraulic retention time+
IC	Ionic chromatography
IAE	Integral absolute error
ISE	Integral squared error
ITAE	Integral time-weighted absolute error
LR	Loading rate
LCA	Life cycle analysis
MFC	Mass flow controller
MEMS	Microelectromechanical system
NitUR	Specific nitrite uptake rate
NDF	Numerical differentiation formulas
NSE	Nash-Sutcliffe efficiency
NUR	Nitrate uptake rate

ORP	Oxidation-Reduction potential
OUR	Oxygen uptake rate
P	Proportional
PI	Proportional integral
PID	Proportional integral derivative
PR	Pall ring
PHB	Poly-hydroxy-butyrate
PUF	Polyurethane foam
PID	Proportional Integral derivative
PVDF	Polyvylidene fluoride
RSC	Reduced sulfur compounds
RE	Removal efficiency
SP	Set point
SOB	Sulfur oxidizing or S-oxidizing bacteria/biomass
SO-NR	Sulfide-oxidizing nitrate-reducing
SOTR	Standard oxygen transfer rate
SUR	Thiosulfate uptake rate
TDS	Total dissolved sulfur
TIC	Total inorganic Carbon

TOC	Total organic Carbon
TSS	Total suspended solids
TLV	Trickling liquid velocity
VOC	Volatile organic compound
VSS	Volatile suspended solids
WWTP	Waste water treatment plant
1DoF	One degree of freedom
2DoF	Two degrees of freedom

List of symbols

a	Specific surface area per volume unit of packed bed, $m^2\ m^{-3}$
$C_{B,i}^{nvs,1}$	Concentration of component *i* at the biofilm surface in layer *nvs*, $g\ m^{-3}$
$C_{B,i}^{nvs,nb}$	Concentration of component *i* at the biofilm subdivision *nb* in layer *nvs*, $g\ m^{-3}$
$C_{B,SS}$	Concentration of sulfide in the biofilm phase, $g\ m^{-3}$
$C_{B,S}$	Concentration of elemental sulfur in the biofilm phase, $g\ m^{-3}$
$C_{B,TS}$	Concentration of thiosulfate in the biofilm phase, $g\ m^{-3}$
$C_{B,DO}$	Concentration of dissolved oxygen in the biofilm phase, $g\ m^{-3}$
C_{g,O_2}^{AC}	Oxygen inlet concentration in the aeration column, $g\ m^{-3}$
C_{g,O_2}^{out}	Oxygen outlet concentration in the aeration column, $g\ m^{-3}$

$C_{g,i}^{nvs}$	Concentrations of component i in the bulk gas in layer nvs, g m^{-3}
$C_{L,i}^{In}$	Concentration of compound i in the mineral medium, g m^{-3}
$C_{L,i}^{nvs}$	Concentrations of component i in the bulk liquid in layer nvs, g m^{-3}
$C_{L,i}^{P}$	Concentration of compound i in the purge flow, g m^{-3}
$C_{L,i}^{RE}$	Concentration of compound i in the recirculation flow, g m^{-3}
$C_{L,SO4}^{2-}$	Concentration of sulfate in the liquid phase, g m^{-3}
CC_{O2}	O_2 Consumption Capacitity, g O_2 m^{-3} h^{-1}
D_i	Diffusivity of component i in water, m^2 h^{-1}
$F_{L,In}$	Fresh liquid mineral medium flow rate, m^3 h^{-1}
$F_{L,P}$	Liquid purge flow rate, m^3 h^{-1}
F_L	Liquid flow rate, m^3 h^{-1}
H_i	Gas-liquid dimensionless Henry coefficient for component I, dimensionless
K_c	Controller gain
$K_L a'_{,O2,AC}$	Gas-liquid global mass transfer coefficient for O_2 in the aeration column, h^{-1}
$K_{L,i}$	Gas-liquid global mass transfer coefficient of component i, h^{-1}
K_{max}	Maximum intracellular S^0 stored to biomass, g S g^{-1} VSS
K	Substrate switch constant, g S m^{-3}
K_{TS}	Affinity constant for $S_2O_3^{2-}$ consumption, g S m^{-3}

k_{SS}	Affinity constants for sulfide, g S m^{-3}
k_{is}	Sulfide inhibition constant, g S m^{-3}
k_o	Affinity constants for oxygen, g DO m^{-3}
k	Kinetic constant for $S_2O_3^{2-}$ production under biotic conditions, h^{-1}
m_S^0	Cumulative mass of elemental sulfur, g
$m_{SO_4^{2-}}$	Sulfate net mass flow, g S-SO_4^{2-} h^{-1}
$m_{H_2S,inlet}$	Inlet net mass flow for hydrogen sulfide, g S-H_2S h^{-1}
m_{S^0}	Elemental sulfur net mass flow, g S-S^0 h^{-1}
$m_{S_2O_3^{2-}}$	Thiosulfate net mass flow, g S-$S_2O_3^{2-}$ h^{-1}
$pCSO_4^{2-}$	Sulfate production capacitity, g S-H_2S m^{-3} h^{-1}
pCS^0	Elemental sulfur production capacitity, g S-H_2S m^{-3} h^{-1}
$pCS_2O_3^{2-}$	Thiosulfate production capacitity (g S-H_2S m^{-3} h^{-1})
Q_{air}	Air flow rate, m^3 h^{-1}
Q_{biogas}	Biogas flowrate , m^3 h^{-1}
Q_{RE}	Liquid recycling flow rate (m^3 h^{-1})
Q_{total}	Total gas flowrate, m^3 h^{-1}
r_{Bj}	Rate equation for each biological process considered, g m^{-3} h^{-1}
V_{bed}	Packed bed volume, m^3
$V_{g,\ nvs}$	Empty volume of the packed bed of layer nvs m^3

$V_{L,nvs}$	Liquid volume of layer nvs, m^3
$V_{L,D}$	Volume of liquid in the sump of the BTF, m^3
$V_{L,\ AC}$	Liquid volume of the aeration column, m^3
$V_{g,\ AC}$	Gas phase volume of the aeration column, m^3
$Y_{X/S}$,	Biomass growth yield using S^0, g VSS g^{-1} S
$Y_{X/SS}$,	Biomass growth yield using S^{2-}, g VSS g^{-1} S
$Y_{X/TS}$,	Biomass growth yield using $S_2O_3^{2-}$, g VSS g^{-1} S
X	Biomass concentration, g X m^{-3}
υ_{ij}	Stoichiometric coefficient for compound i in process rate j, dimensionless

Greek letters

α	Kinetic constant for elemental sulfur accumulation
ε_g	Gas phase porosity
ε	Packed bed porosity
δ_L	Thickness of the water layer, m
$\delta_{B\text{-}nb}$	Thickness of one biofilm subdivision, m
φ	Dynamic hold-up
β	Kinetic constant for thiosulfate
$\mu_{max,1}$	Specific growth rates for SOB over S^{2-}, h^{-1}
$\mu_{max,2}$	Specific growth rates for SOB over S^0, h^{-1} g X $^{1/3}$ g $S^{-1/3}$

$\mu_{max,3}$	Specific growth rates for SOB over $S_2O_3^{2}$, h^{-1}
τ_I	Integral time constant, h
τ_D	Derivative time constant, h
$\eta_{H_2S\text{-}O_2}$	

Superscripts

nvs	Vertical layers
nb	Biofilm subdivisions
P	purge line
RE	Recycling line

CHAPTER 1

MOTIVATIONS AND THESIS OVERVIEW

1. MOTIVATIONS AND THESIS OVERVIEW

1.1 MOTIVATIONS

This thesis has been carried out in the Department of Chemical, Biological and Environmental Engineering of the UAB, in the Research Group on Biological Treatment and Valorisation of Liquid and Gas Effluents (GENOCOV) within the project "Monitorización, modelización y control para la opmitización de biofiltros percoladores de desulfuración anóxicos y aerobios" (MICROBIOFIN), ref. **CTM2012-37927-C03-01** funded by the Ministerio de Economía. The project proposes the use of a range of techniques such as titrimetry and respirometry to improve process monitoring and for defining the degradation mechanisms and obtaining the biological degradation rates.

The information obtained experimentally together with the formulation of theoretical models should serve to predict the behavior of bioreactors under different situations as well as to serve as a powerful tool for design, optimization and process control. In this sense, the project aims at establishing different control protocols and strategies that will permit a robust, stable and secure operation under optimal conditions. Among the abovementioned research topics, this thesis is particularly focused on understanding different variables involved in process control loops of a desulfurizing biotrickling filter operated under aerobic conditions through experimental studies and a model-based analysis. With the results obtained along this thesis, process is optimized through application of control strategies, fulfilling the objectives of the project.

1.2. THESIS OVERVIEW

In this first chapter of the thesis the motivations and thesis overview are presented. In Chapter 2, the general introduction is presented. In the introduction, technical and socio-economical aspects related to the importance of the use of renewable energies such as biogas, are presented. This leads to introduce the need of H_2S removal in biogas streams, and different technical alternatives for biogas desulfurization, specifically presenting the experimental expertise achieved in this field using biotrickling filters. Also information about the different mechanisms used to model this type of reactors is provided. Finally, the importance of control strategies in biological processes is discussed, particularly in biotrickling filters for biogas desulfurization under aerobic conditions. In Chapter 3 the

general and specific objectives of the thesis are stated. Chapter 4 is a compilation of all materials and methods employed in this thesis, and also the equations used to assess mass balances and the most important process variables.

Chapter 5, 6, 7, 8 and 9 contain the results obtained during the thesis. In chapter 5 main manipulated variables in an aerobic biotrickling filter for biogas desulfurization are characterized. Specifically, the effect of regulating the trickling liquid velocity and the air flowrate are studied. Results obtained in this chapter were further used in Chapter 6, 7 and 9. Specifically, in Chapter 6 application of titrimetric variables such as proton production and proton production rate as measured variables to be potentially applied in control loops in discontinuous and continuous process is studied. In this chapter, the two-step denitrification process associated to thiosulfate oxidation is used to study titrimetry in discontinuous process. Titrimetric data obtained from results of Chapter 5 were used to study the relation between operational changes and biological activity through titrimetry. Later in Chapter 7, a model describing physical-chemical and biological processes for the removal of high loads of H_2S from biogas streams in biotrickling filters was developed, calibrated and validated. The model described the reactor performance in terms of H_2S removal and predicted satisfactorily the main intermediate and final products produced during the biological oxidation process under steady and dynamic loading rate conditions.

Afterwards in Chapter 8, a model-based analysis of control strategies in an aerobic biotrickling filter for biogas desulfurization was performed. In Chapter 8, a range of feedback control strategies to control the outlet gas concentration of biogas in biotrickling filters is studied. Control strategies studied in this chapter derive from common actuations in real BTFs as well as from experimental results of the influence of the main manipulated variables in a aerobic BTF for biogas desulfurization at lab-scale (Chapter 5). Control strategies were simulated using the biotrickling filter model developed in Chapter 7. This chapter also pursues to determine the controllability limits of the process under variable loading rate conditions and to study the added value of these strategies in increasing the selectivity of sulfate production. In chapter 9, feedback and feedforward control strategies were experimentally tested in an aerobic biotrickling filter. Results obtained in Chapter 8 helped to plan and design part of the control strategies tested in this chapter, specifically for the feedback control. Feedforward control strategies are based on results obtained in

Chapter 5. In Chapter 10 the conclusions extracted from the results obtained in previous chapters are exposed and future research topics recommended. Finally, Chapter 11 contains the references used along this thesis.

CHAPTER 2

INTRODUCTION

2. INTRODUCTION

2.1. DESULFURIZATION OF BIOGAS

2.1.1. Global warming: global repercussion issue with individual contributors

Earth occupies a privileged position in the solar system called habitable zone, which is the zone where light and radiation emitted by the sun allows the existence of water in liquid phase and, therefore, the existence of life (Gonzalez and Richards, 2004). Venus, for example, a planet with similar beginning and characteristics than Earth (solid planet, covered with a gaseous atmosphere and with similar size) is located in the lower limit of the habitable zone. Nowadays, Venus has a composition of 96% of CO_2 and a surface temperature of 460 ºC (Chaisson and McMillan, 1999). So, what changed in Venus? Scientific community has concluded that the carbon cycle has failed to maintain the conditions in the planet, having as a result an uncontrolled greenhouse effect (Carroll and Ostlie, 2007).

Can this happen on Earth in a near future? At the time scale at which planets evolve (millions of years), the answer is a clear No. Planet Earth temperature is the result of the carbon cycle which is defined as the interaction between the carbon present in the atmosphere and that one present in the surface, which both are expected to be in equilibrium. Volcanic eruptions, cataclysms or even asteroids impacts have affected this equilibrium along planet Earth existence, being the carbon cycle the responsible to recycle the excess of carbon produced during this events (Shu, 1982). This recycling process occurs with different time scale (300,000 years) than the time scale (last 200 years) that anthropogenic emissions of carbon have occurred on Earth. This changes have been occurring with such an unfortunate acceleration that makes that natural carbon cycle cannot regulated them and, therefore, continuing preserving equilibrium of carbon cycle on Earth.

Anthropogenic activity has produced an increase in the concentration of carbon dioxide (CO_2) and methane (CH_4) in the atmosphere producing what is called the greenhouse effect. The greenhouse effect refers to the temperature increase of the Earth atmosphere due to the absorption-emissions process of the infrared radiation (Jou, 2013). In order to come into energy balance, the amount of infrared radiation energy given off by the Earth has to be equal to the amount of energy absorbed from sunlight. So if some

energy remains within the greenhouse gases (GHG) some other energy must be emitted by the Earth into the space. Thus, the Earth surface is heated and emits infrared radiation in order to be in energy balance and, therefore, completes the energy balance (Trenberth et al., 2008). GHG effects over Earth climate are already noticeable, long periods of hot or cold weather, storms, droughts that are not unconnected to social issues such as migrations, wars and economic breakdowns of countries based on natural resources. We may not want to end like Venus atmosphere in a close future, but the need of individual actions to stop climate change is necessary since global warming is of global concern for our present and future generations.

2.1.2. Green energy production against global warming related energies

Most of the world GHG emissions come from a relatively small number of countries. In year 2011, the top six GHG emitters were the United States, China, the European Union (EU), Russia, India and Japan (Fig. 2.1) (Boden et al., 2015). However, commitments to mitigate GHG emissions vary among countries and some important agreements, such as the 1st Kyoto protocol period 2008-2012 where CO_2 emissions must be reduced a 5.2 % compared to 1990 values signed, are not signed by some of the abovementioned countries (United Nations, 1998).

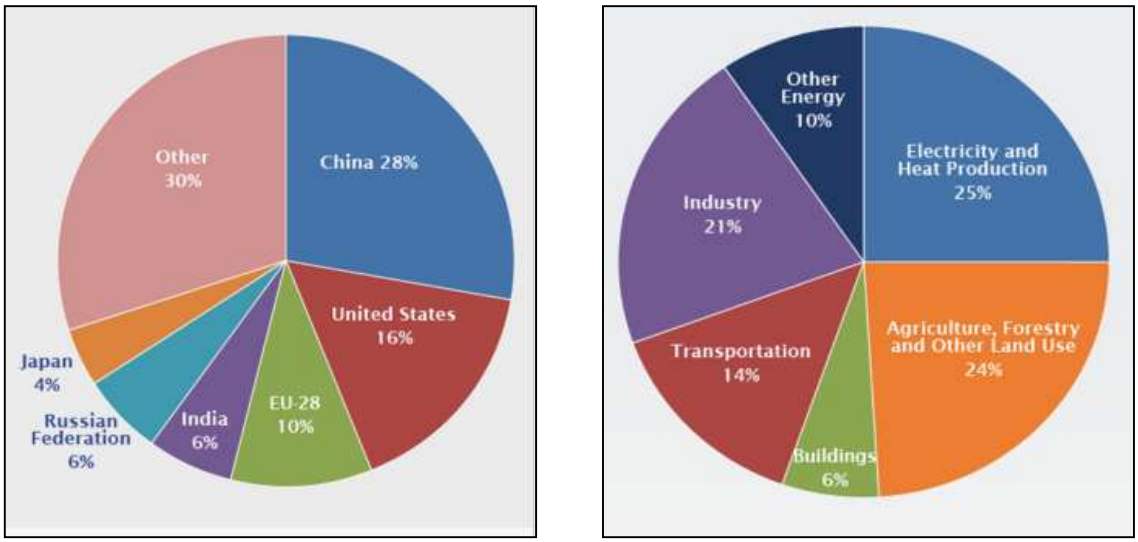

Figure 2.1. World Top Six GHG emitters and Top Six economical activities responsible of GHG emissions (Boden et al., 2015)

In the last decade, UE has applied regulations to reduce significantly GHG emissions by 20 % compared to 1990 values according to the 2nd commitment under the Kyoto protocol period 2013-2020 (European Commission, 2013). Actually the two economical activities responsible of 46% of GHG emissions production are related to energy generation industry (Fig 2.1). Firstly, GHG emissions from coal, natural gas and oil burning for electricity and heat production (25%) and secondly, GHG emissions related to general industry (21%) that burn fossil fuels on-site to produce energy (Boden et al., 2015). Therefore, regulation policies defined by EU points to increase significantly renewable technologies application (wind, solar, biomass and waste-to-power, geothermal and marine technologies) (Mc Crone, 2013).

Energy related to non-renewable sources is becoming too expensive or too environmentally damaging to retrieve. Besides there are many benefits that renewable energy provide, such as environmental benefits since they have a lower environmental impact than conventional energy technologies. Another important factor that must be considered of renewable energy is the economic factor. Actual energy market of many countries in the world depend on energy supply, such as oil, natural gas an nuclear energy from other countries, since their local production is not enough to cover their local demand (Eurostat, 2015). This may not be a problem if the energy providers would not be concentrated in a few number of countries, which is the case of the EU that around 33.5% of raw oil came from Russia or Norway in 2013 (Eurostat, 2015).

This energy dependency situation can be solved for energy depending countries by increasing their local production by generating more and more renewable energy. Actual energy dependency relies mainly on oil dependency, but this dependency will not turn out into a dependency of only one type of resource of renewable energy but several (British Petroleum, 2015). Appearance of renewable energies will lead to a distributed market were different types of energy sources, depending on local availability of natural resources (sunlight, wind, biomass, rivers and ocean waves), will be used and progressively substituted by non-renewable energies.

2.1.3. Biogas: a renewable energy source

One stream with high potential for green energy production is biogas. Biogas is a high-energy methane gas, and therefore highly usable, playing an important role in creating a sustainable society and reducing dependence on oil. Biogas is used in different

ways around the world, often for the production of electricity and heat, or directly for cooking and lightning in small communities (Intenational Gas Union, 2015). Sweden stands out as the country that mainly upgrades biogas for use as vehicle fuel (Swedish Gas Association, 2011). Different countries have invested in different types of biogas systems depending on widely different environment and energy programs. Denmark uses manure to a large extent as this has been a means of dealing with the overproduction of manure (Persson and Baxter, 2015). Germany, the UK and Sweden are examples of countries where (Swedish Gas Association, 2011) biogas production comes from collecting food waste (FW) (Persson and Baxter, 2015) since FW is a large portion of municipal solid waste in these countries (Zhang et al., 2014).

One example of the importance of biogas in the energy market in the world is that 14,000 TWh were produced from installations based on biogas in 2012; 37TWh were produced in Europe and 10 TWh in the USA (Intenational Gas Union, 2015). Worldwide countries are expected to increase biogas-based energy production, including composting waste from towns and industries, as a solution to reduce methane and GHG emissions to the atmosphere related to non-biogas-based energy production (Environmental Protection Agency, 2014)

Biogas can be used in the same way as natural gas, which consists of at least 90% of methane. 1 Nm^3 of upgraded biogas (97% Methane) has an energy content of 9.67 kWh while natural gas, 1 liter of petrol and 1 liter of diesel have 11 kWh, 9.1 kWh and 8.8 kWh, respectively (Swedish Gas Association, 2011). To be able to obtain this amount of energy from biogas, is important to understand from which processes biogas is obtained and which pre-treatments and upgrading treatments can be done in order to have a biogas with more quality (higher methane content) and more pure.

2.1.4. Roadmap from biogas production to energy production

Anaerobic digestion (AD) is a biological process that converts complex substrates into biogas (mixture of CO_2 and CH_4) and a digestate by microbial action in the absence of oxygen through four main steps, namely hydrolysis, acidogenesis, acetogenesis and methanogenesis (Ariunbaatar et al., 2014). AD is one of the oldest technologies, well-studied by several authors, for stabilizing organic wastes (Martín-González et al., 2011; Winkler et al., 2015). AD performance depends greatly on reactor configuration and on the source of organic matter present in the AD feedstock (Jenkins et al., 2008).

Additionally sometimes is required to apply a pretreatment to enhance anaerobic digestion performance (Barjenbruch and Kopplow, 2003; Hendriks and Zeeman, 2009). Common feedstocks used in AD are effluents with high loads of organic matter such as those produced from the food (Bouallagui et al., 2009; Lo et al., 2010), paper (Meyer and Edwards, 2014; Rintala et al., 2015) and chemical industry (Araya et al., 1999) or also from municipal wastes (Lo et al., 2010; Martín-González et al., 2010), animal manure (Álvarez et al., 2010; Cavinato et al., 2010) and others (Khalid et al., 2011).

Biogas produced by all above-mentioned activities is mainly composed by methane (35-75% v v^{-1}) with an energy production capacity between 15 and 30 MJ/Nm^3 (Abatzoglou and Boivin, 2009). Detailed biogas composition is presented in Table 2.1 (Montebello et al., 2013). Besides biogas, digestate is the other residue obtained during AD, which can be advantageously used in agriculture as fertilizer or soil conditioner (Murphy and Bochmann, 2011). Regarding energy recovery from biogas, there are various biogas utilization purposes, which mainly depend on CH_4 composition. Heat or steam production (Persson et al., 2006) or electricity production with combined heat and power production (CHP) are the lowest value chain of biogas utilization (Pöschl et al., 2010).

Denmark is one of the countries with a significant number of Centralized Anaerobic Digestion (CAD) facilities, where biogas is generated in CHP plants (circa 1MWe) achieving an electrical efficiency and thermal efficiency of 35% and 40%, respectively (Murphy et al., 2004). CHP presents the advantage that part of the generated heat can be used in the AD process or at other stage of the facility where heat is required. At the top of biogas utilization pathways is the utilization as vehicle fuel, production of chemicals (Persson et al., 2006) and upgrading and injection in the natural gas grids (Kristensson, 2007). In all this biogas utilization pathways, biogas quality is crucial in terms of CH_4 content and purity. Biogas upgrading process consists essentially in removing CO_2 from biogas in order to increase CH_4 content above 95%. After this transformation the final product is referred as biomethane (Ryckebosch et al., 2011).

In order to increase CH_4 content, many biogas upgrading technologies are nowadays available, such as pressurized water scrubbing (Tajima et al., 2004), chemical absorption (Lau et al., 2010), physical absorption (Persson et al., 2006), cryogenic distillation (Basu et al., 2010) and membrane separation (Yan et al., 2014). Removing

CO_2 and other impurities, gives biogas a great potential to supply green energy and therefore reduce our dependency of non-renewable energies.

Table 2.1. Main biogas impurities an their consequences

Component	Content	Effect
CH_4 (% v v^{-1})	50-75 35-75 60-68	Energy source
CO2 (% v v-1)	25-50 25-65 32-40 35-38	Lost of calorific power, corrosion in wet gas
H_2S (% v v^{-1})	0-0.5 0.0001-1.0 0.1-2.0	Corrosion in compressors, gas storage tanks and engines; SO_2 and SO_3 are formed due to combustion, which are more toxic than H_2S and cause corrosion with water
NH_3 (% v v^{-1})	0-0.05 <0.0005	Corrosion when dissolved in water; NOx emissions after burning
Water vapor (% v v^{-1})	1.0-5.0	Corrosion in compressors. Gas storage tanks and engines due to reaction with H_2S, NH_3 and CO_2 to form acids; Accumulation of water in pipes; Condensation and/or freezing due to high pressure.
Dust (µm)	>5	Clogging due to deposition in compressors and gas storage tanks
N_2 (% v v^{-1})	0.0-5.0	Lost of calorific power
Siloxanes (mg m^{-3})	0.0-50.0 200-700	Formation of SiO_2 and microcrystalline quartz due to combustion. Deposition at spark plugs, valves and cylinder heads abrading the surface

2.1.5. H_2S Removal in biogas streams

The most common impurities found in biogas (*see Table 2.1*) are H_2S and reduced sulfur compounds (RSC) coming from the anaerobic fermentation of S-Bearing organic

molecules (Abatzoglou and Boivin, 2009). H_2S concentration in biogas varies from 0.0001% (Abatzoglou and Boivin, 2009) up to 2 % (Syed et al., 2006) depending mainly on the anaerobic digestion feedstock. As shown in Table 2.1, other impurities lead to different effects if biogas is burned in their presence, from increasing NOx emissions due to the presence of NH_3 on biogas (Deublein and A. Steinhauser, 2008) to micro-crystalline silica formation on combustion engines due to the presence of siloxanes (Kymäläinen et al., 2012). Since the removal of impurities different than H_2S are out of the scope of this work, only H_2S removal will be extensively discussed. Removal of H_2S is strictly necessary to avoid corrosion of internal combustion engines during co-generation process as well as for proper performance of further biogas upgrading technologies (Cartwright, P.E., 2005). Upper limits between 250 ppm_v (Weiland et al., 2010) and 500 ppm_v of H_2S (Chaiprapat et al., 2015) are generally recommended to have a suitable biogas utilization. Ideally, H_2S-free biogas is desired to avoid the abovementioned corrosion of biogas engines and a fast degradation of engine lube oil.

The choice of the most adequate desulfurizing treatment is defined by several criteria such as process operating conditions (gas flow rate, contaminant concentration, temperature, etc.), pollutant characteristics (solubility, biodegradability, toxicity, flammability, etc.) and economic issues (investment and operational costs, valuable by-products recovery, etc.) (Devinny et al., 1999; Kennes and Veiga, 2001). In order to meet global GHG emissions reduction, the environmental impact related to each technology should be included (carbon footprint, energy required, waste generation), which can be assessed performing a life cycle analysis (LCA) (Ravina and Genon, 2016; Starr et al., 2012). Desulfurizing technologies can be divided into physical-chemical and biological technologies. The ones belonging to the first group are based on chemical absorption in aqueous solutions (Horikawa et al., 2004), chemical adsorption of H_2S on solid adsorbents (Maat et al., 2005) and scrubbing with solvents or other liquid phases (Couvert et al., 2010).

On the other hand, the alternative to physical-chemical technologies is biological desulfurizing technologies. Biological technologies are based on different species of chemotrophic bacteria serving as S-oxidizing agents in biofilters (BF) (Duan et al., 2006; Estrada et al., 2012), biotrickling filters (BTF) (Deshusses and Cox, 2002; Fortuny et al., 2008; López et al., 2016a) and bioscrubbers (van den Bosch et al., 2007). If both types of technologies are compared from an environmental point of view, biological technologies

for biogas desulfurization are more environmentally friendly technologies than physical-chemical technologies. Physical-chemical methods are characterized by high consumption of energy and chemicals, leading to other pollution problems such as generation of large amounts of CO_2, NO_x and other wastes (exhaust absorbents) (Devinny and Armstrong, 1999; Fernández et al., 2013). Another strong point for biological technologies are operational costs, which according to Estrada et al. (Estrada et al., 2012) biological techniques present an operating cost up to six times lower than physical-chemical treatments. Until some years ago, the main advantage of physical-chemical technologies was their high reliability and that they were able to work at higher contaminant concentrations and flow rates than biological technologies. At that moment, biological technologies still needed more intensive research in order to gain reliability and therefore increase their industrial application. Nowadays, biological technologies for biogas desulfurization continue their application range expansion, treating higher and higher H_2S concentrations and flowrates (Fortuny, 2009), while more and more knowledge is gained about the biology involved in the process, more specialized equipment is developed.

2.1.6. Biological removal of H_2S in biotrickling filters

Biogas desulfurization performed through BTFs is one of the most efficient biological alternatives to physical-chemical desulfurization treatments. In BTFs the contaminant is first transferred to the liquid phase to later on be transferred to the biofilm phase, where biological reaction occurs. Consequently, the pollutant treated in BTFs must necessarily be soluble in water, biodegradable and non-toxic to the microorganisms. In BTFs the biofilm layer grows on an inert packing material, therefore a continuous flow of water and nutrients is required, preventing drying and offering a means for precise control of nutrient content and medium pH (Devinny and Armstrong, 1999). In Fig. 2.2, a general schematic of a BTF is shown.

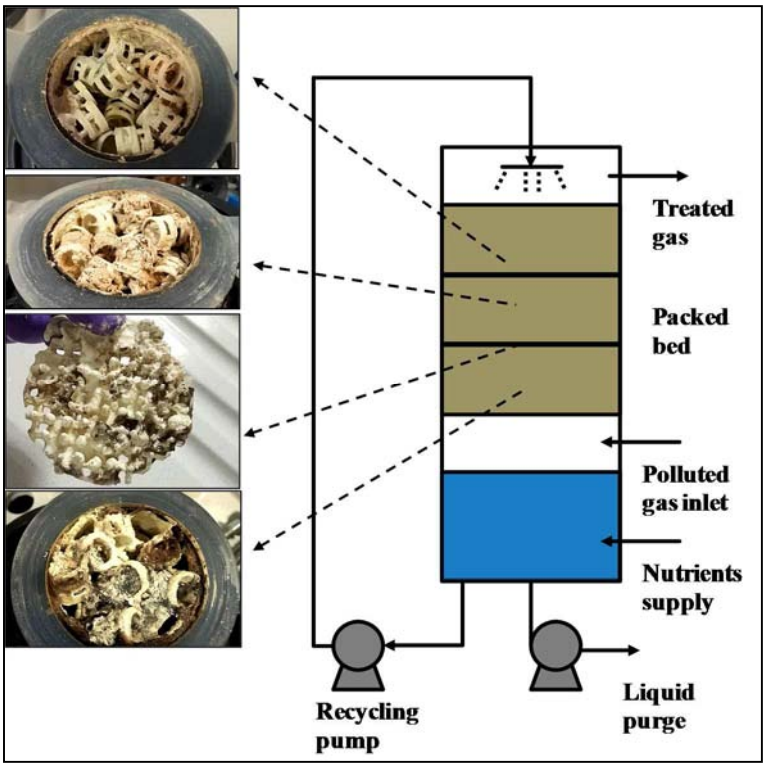

Figure 2.2. General schematic of a BTF for gas treatment operated under counter-current flow pattern

Biogas desulfurization in BTFs can be performed aerobically (Fortuny et al., 2010; Montebello et al., 2012), when the electron acceptor is oxygen (O_2) or under anoxic conditions (Fernández et al., 2013b), when the electron acceptor is nitrite (NO_2^-) or nitrate (NO_3^-). During aerobic biogas desulfurization in BTFs, besides having a proper H_2S gas-liquid mass transfer, O_2 must also be transferred in order to have enough O_2 to carry out the complete H_2S oxidation as shown in Eq. 2.1 and Eq. 2.2. In desulfurizing BTFs, the H_2S contained in biogas is converted, under aerobic or anoxic conditions, to elemental sulfur (S^0, an inorganic solid) and further to sulfate (SO_4^{2-}) by S-oxidizing bacteria (SOB). Biological oxidation reactions of H_2S by SOB are described by Munz et al. (Munz et al., 2009) by the following catabolic reactions:

$$HS^- + 0.5O_2 \rightarrow S^0 + OH^- \qquad [\Delta G^0 = -169 \text{ kJ mol}^{-1}] \tag{2.1}$$

$$S^0 + 1.5O_2 + H_2O \rightarrow SO_4^{2-} + 2H^+ \qquad [\Delta G^0 = -563.83 \text{ kJ mol}^{-1}] \tag{2.2}$$

According to Eq. 2.1 and Eq. 2.2, if the H_2S/O_2 ratio is higher than 2, S^0 is the main oxidation product and if the H_2S/O_2 ratio is lower than 0.5 the reaction ends up on SO_4^{2-} formation. Hence the supply of O_2 is a crucial step in order to avoid S^0 production since massive accumulation of S^0 can lead to bed clogging due to an excess of solids accumulation in the BTF bed. Total solids accumulation is directly related to the increase of pressure drop inside BTFs bed (Andreasen et al., 2012), leading to a significant reduction of BTFs operational life time.

As shown in Fig. 2.2, when the polluted gas inlet is located at the bottom of the reactor and the trickling liquid enters from the top of the BTF, is said that the BTF is operated under counter-current flow pattern. Alternatively, BTFs can be also operated under a co-current flow pattern, when flowing both gas and liquid in parallel from top to bottom of the BTF. In this work comparison between co-current and counter-current flow pattern was studied in order to find the most advantageous operating configuration for biogas desulfurization under aerobic conditions in BTFs. Study was based on the improvement of the H_2S/O_2 ratio, which in the case of aerobic BTF for biogas desulfurization, is a key parameter to consider in order to achieve complete H_2S oxidation.

On the left part of Fig. 2.2 different pictures of the packed bed of an aerobic lab-scale BTF working at high H_2S LR with an unfavorable H_2S/O_2 ratio are shown. A gradient in the amount of elemental sulfur accumulated in the bed according the position of the BTF bed is observed. Since in the first bed (top section) the highest H_2S LR is received, more solids are accumulated than in the last section of the bed (bottom section), where the packed bed has barely biofilm on it.

Regarding to the distribution of the packing material in BTFs, inert packing material can have a structured (Fortuny et al., 2008) or random distribution (López et al., 2016a; Montebello et al., 2012) in the BTF bed. Selecting the adequate packing material is also crucial to have a proper performance of the BTF, since gas-liquid mass transfer in the packed bed of BTFs depends on system specific constants that may be defined by the packing material characteristics such as the distribution of the packing material in the packed bed, water hold-up in the reactor or water distribution profile, specific surface area per unit volume (a), porosity (ε) and diameter of the packing material among others.

Fortuny et al. (Fortuny et al., 2008) found that the irregular structure of polyurethane foam (PUF) hindered solids flushing, inducing S^0 accumulation in the packed bed and pressure drop increase in the BTF. Acidic desulfurization induces the degradation of metallic Pall rings used as packing material by Montebello et al. (Montebello et al., 2014), which lead to a larger solid sulfur production and a gradual loss of sulfate selectivity (López et al., 2016a).

2.1.7. Main limitations of industrial application of biological H_2S removal in BTF: Main drawbacks

Despite a lot of experimental effort has been done in order to gain knowledge about BTFs for biogas desulfurization, there are still some technical aspects to improve that slow down the industrial application of this emerging, biological technology. Several experimental studies have been carried out in our research group in the field of biogas desulfurization using BTFs as shown in Table 2.2.

Table 2.2. Range of designs, operational conditions and strategies tested in our research group.

H_2S_{in} (ppm_v)	EC_{max} ($g\ H_2S\ m^{-3}\ h^{-1}$)	$O_{2supplied}$	$S\text{-}SO_4^{2-}/S\text{-}H_2S_{removed}$ (%)	pH	Packing	G/L flow pattern	Reference
8000	190	Gas pipe	12	6	HD-Qpack structured	Counter current	(Fortuny et al., 2008)
8000	175	Gas pipe	clogging	6	PUF	Counter current	(Fortuny et al., 2008)
8000	201	Diffuser	57	6.5	HD-Qpack structured	Counter current	(Montebello et al., 2010)
8000	223	Diffuser	56	2.5	Metallic Pall rings	Counter current	(Montebello et al., 2014)
2500	72	Diffuser	52	1.9	Plastic Pall rings	Co-Counter current	(Rodriguez et al., 2014)
2500	54	Jet-Venturi	61	1.7	Metallic Pall rings	Co-Counter current	(Rodriguez et al., 2012)
8000	215	Diffuser	52	6.5	Plastic Pall rings	Co-current	(López et al., 2016a)

Studies have been focused on studying different pollutants loads (Fortuny et al., 2008), different oxygen mass transfer devices (Rodriguez et al., 2014, 2013, 2012), pH conditions (Montebello et al., 2010), gas-liquid flow pattern (López et al., 2016a), and different packing materials (Fortuny et al., 2008) as well as different electron acceptors (Montebello et al., 2012).

The main drawback related with the industrial application of aerobic desulfurizing BTFs is bed clogging caused by S^0 accumulation. As it was mentioned above, this situation occurs when high loads of H_2S are treated under limiting dissolved oxygen concentrations. When desulfurization is carried out under anoxic conditions (Fernández et al., 2013b), the solution to this problem only relies in the availability of a rich nitrogen stream, since NO_2^- or NO_3^- are already dissolved. Since the solubility of O_2 in water is 80 times lower than the solubility of H_2S in water (Sander, 2014), large amounts of O_2 are necessary to ensure complete H_2S oxidation. However, increasing airflow rate in the BTF impacts negatively in the percentage of CH_4 present in the biogas, reducing the calorific capacity of the final biogas stream obtained due to a dilution (Chaiprapat et al., 2011; Walsh et al., 1988). For this reason it is important to improve O_2 gas-liquid mass transfer efficiency of the system.

Fortuny et al. (Fortuny et al., 2008) and Montebello et al. (Montebello et al., 2012) obtained low sulfate selectivity values using conventional diffuser or open-end pipe based devices. However, recent studies have shown the suitability of the implementation of Venturi-based devices for intensive gas-liquid mass transfer (Rodriguez et al 2012, Rodriguez et al 2014). In Chapter 5 of the present thesis the effect of the two manipulated variables, trickling liquid velocity (TLV) and air flowrate was studied in order to regulate the dissolved oxygen load (DOL) to a BTF for biogas desulfurization working at high H_2S LR. The capability of this variables to increase oxygen consumption along the bed without the need of diluting the biogas stream was evaluated.

Therefore the main goal to accomplish in aerobic biogas desulfurization in BTFs is to reduce S^0 production when high H_2S LR are treated through improving O_2 gas-liquid mass transfer efficiency without reducing biogas calorific capacity. So then, more reliable process with longer operational periods without less periodicity of maintenance tasks to unclog the bed would be obtained making a profitable process at the time of comparing with physical-chemical technologies.

2.2. MODELLING OF BIOFILTRATION REACTORS

The importance of modeling biological processes relies on the fact that models allow testing new ideas and theories, in order to make the process more efficient and reliable. The representation of the model may be different from discipline to discipline but in basic sciences such as physics, biology or chemistry, is essentially a mathematical representation. The mathematical model has the advantage of summarizing a theory in a precise and concise symbolic language. Lately more accurate simulations are obtained thanks to technological development that allow solving simultaneously a number of mathematical expressions with low error associated and in a short time. By simulation we mean the production of a mathematical or computational model of a system or subsystem that seeks to represent or reproduce some properties that that systems displays (Kell and Knowles, 2006).

Once a model is calibrated and validated, this can be useful to determine the performance of the reactor under different operational conditions, without the need of unnecessary experimentation, thus saving time and money. Another important reason to develop models of biological processes is that allows analyzing which parts of the system contribute the most to some desired properties of interest, using techniques such as the sensitivity analysis. Such techniques are designed to indicate which parameters must be known with more precision and focus the effort on their estimation (Saltelli et al., 2000). However, before developing a model of a biological process, experimentation is needed in order to gain knowledge and understand the studied process. Experimentation allows obtaining valuable data to improve the consistency of model predictions with experimental data.

In the biofiltration field there are already several experimental studies that allow understanding the main physical-chemical and biological mechanisms that describe the processes studied. Consequently, several models have been already proposed. Process modeling has shown to be a crucial tool to evaluate the technical and economical feasibility of biological processes prior to full-scale implementation (Guerrero Camacho, 2014) and for the development of control strategies (Guerrero et al., 2014; Guisasola et al., 2010). Another important advantage of modeling biofiltration reactors is that extreme conditions such as sudden changes in the inlet concentration can be simulated, avoiding the risk of damaging microbial population. Also personal risk is reduced, especially in

the gas treatment field, where high risk is involved when high pollutant concentrations are treated.

2.2.1. Biotrickling filter mechanisms

Several models have been proposed in literature to describe the removal of different pollutants through biofiltration reactors (such as BF and BTF) like volatile organic compounds (VOCs) (Álvarez-Hornos et al., 2009; Meena et al., 2015) and ammonia (Baquerizo et al., 2005; Cortus et al., 2008) under transient and steady-state conditions. Accordingly to the phases present in the biofiltration reactor, models can be divided as two-phase models (gas and biofilm) appropriate for BF models (Meena et al., 2015; Salehahmadi et al., 2012) and three-phase models (gas, liquid and biofilm) adequate for BTF (Kim and Deshusses, 2003; López et al., 2016b). The mechanisms for two-phase models are the same as those for three-phase models, except that liquid advective flow does not exist and only the mass transport at the gas-liquid interface is modeled instead of mass transport at both the gas-liquid and liquid-biofilm interfaces (Li et al., 2002). The main phenomena and mechanism typically considered in three-phase models for BTFs of gaseous pollutants compounds are graphically represented in Fig. 2.3 and described below as a function of the different phases.

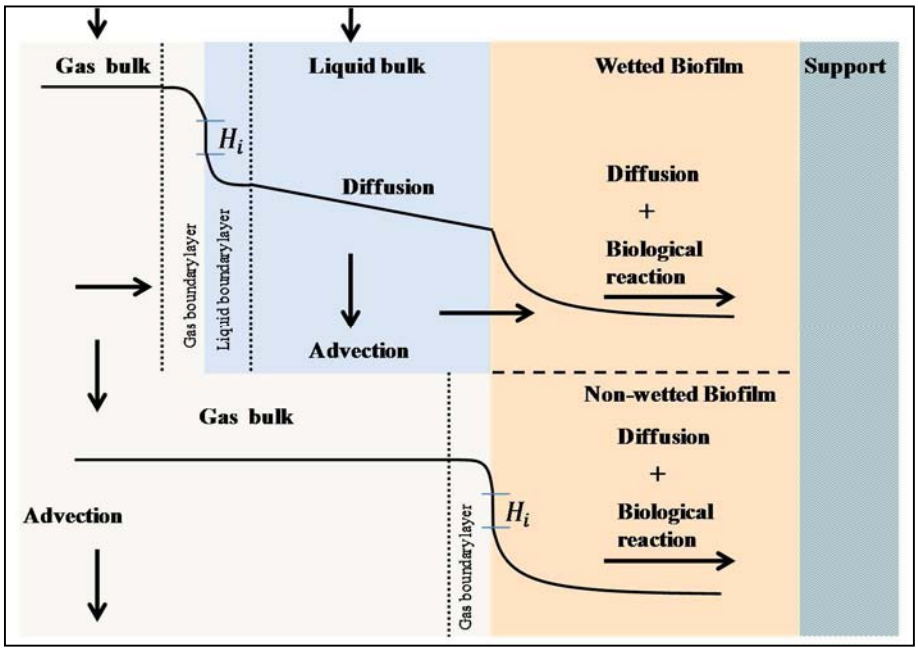

Figure 2.3. General schematic of the phenomena in a BTF for gas treatment under a co-current flow pattern.

Gas phase transport

The first phenomena to consider in a BTF is the advective transport of the gas bulk. Prior to gas-liquid mass transport of the contaminant, as well as oxygen in aerobic BTFs, gas bulk tortuously flows through the pores of the packed bed. Most BTFs models consider that transport of the gas bulk in the axial direction can be modeled as plug flow without axial nor radial dispersion (Devinny and Ramesh, 2005; Li et al., 2002; Sharvelle et al., 2008). However, some works in the literature have included axial dispersion (Hodge and Devinny, 1995; Silva et al., 2012). Nonetheless, Dorado et al. (Dorado et al., 2010) confirmed that the assumption of neglecting axial dispersion was correct for a BTF for toluene removal working at high residence times as is commonly done in most BTFs for biogas desulfurization. Hodge and Devinny (Hodge and Devinny, 1995) also found that axial dispersion is only significant in BTFs operated at residence times of a few seconds (Hodge and Devinny, 1995). Moreover, radial dispersion is neglected since typically there are no radial gradients in concentration (Deshusses et al., 1995).

Regarding the phase transfer mechanism from gas to liquid, a first approach is to consider that the liquid phase is stagnant. With the first approach, molecular diffusion of a laminar layer of gas near the liquid interface is considered to be the only transport mechanism (Devinny and Ramesh, 2005). Therefore this process may be limited by diffusion in the water phase, while water pores are relatively small. Moreover, molecular diffusion constants in water are lower than in air. Considering diffusion as the only mass transport limitation, the gas-phase interfacial resistance is neglected due to dispersion caused by advection in the gas phase that tends to mix the gas phase. Some authors, instead of considering the abovementioned mechanism, directly neglected the liquid phase, based on the fact that the liquid trickling rate is low, and, hence, the liquid film is assumed to be thin (Alonso et al., 1997). Therefore the three-phase model is transformed into a two-phase model, where direct gas-biofilm transport occurs mainly controlled by diffusion resistance in the biofilm surface (Devinny and Ramesh, 2005).

However, some investigators have observed mass transfer resistance at the interfaces (Kim and Deshusses, 2003), most likely to occur when contaminant solubility is high and biodegradation is fast. In this case, the mass flux at the gas-liquid interface is defined by the double-film theory proposed by Whitman et al. (Whitman, 1923). Consistent with the double film theory two interfaces resistances, gas-phase interface and

liquid-phase interface are added to obtain a global resistance. It is common practice to refer the resistance as a global coefficient. As is shown in Fig. 2.3, the gas-phase and liquid-phase interfaces resistance occur in the zone called gas boundary layer and liquid boundary layer, respectively.

The double film theory states that the mass transfer velocity into the interface is equal to the mass transfer from the interface. This velocities are equal to the product of a global mass transfer coefficient times the driving force. For example, the driving force from the gas-phase interface is defined as the concentration difference between the concentration of the gas in equilibrium with the liquid bulk, according to Henry's law, and the concentration of the gas phase. The global mass transfer resistance can be determined as the sum of gas and liquid interface resistances, which can be calculated through empirical correlations (Billet and Schultes, 1999; Onda et al., 1968) or experimentally (Dorado et al., 2009; Kim and Deshusses, 2008).

Liquid phase transport

Besides the operational functions of the liquid phase in BTFs such as providing nutrients to microorganisms, transport of biodegradation metabolites and for pH regulation, the liquid phase in BTFs for the removal of high loads of H_2S plays an important role at the time of defining the gas-liquid mass transport properties. As abovementioned, some models neglect the existence of a liquid layer since they consider this layer thin enough to not offer any mass transfer resistance (Alonso et al 1997). Other models attempt to have a more realistic approach and consider that the biofilm layer is not completely wetted and that some non-wetted portions of the biofilm exist (Bonilla-Blancas et al., 2015; Kim and Deshusses, 2003) as shown in Figure 2.3.

Conservative models assume a completely wetted biofilm neglecting direct transport to the biofilm (López et al., 2016b; Sharvelle et al., 2008), considering that assigning a fraction of wetted and non-wetted biofilm would introduce more uncertainties to model predictions. Liquid layer thickness is one of the hardest parameters to determine at the moment of defining model parameters, and even if there are some correlations to estimate the thickness of the liquid layer (Alonso et al., 2001; Li et al., 2002), the latter is generally estimated through fitting of experimental data to model predictions (Bonilla-Blancas et al 2015, López et al 2016).

Liquid phase advective transport through the BTF bed is commonly discretized as a sequence of continuous stirred tank reactor (CSTR) (Baltzis et al., 2001; Deshusses et al., 1995). Once the gaseous compounds are in the liquid phase, mass transfer from the liquid phase to the biofilm phase occurs. Modelers typically represent mass transfer resistance in the liquid-biofilm interface with Fick's law considering that the whole thickness of the liquid phase acts as the liquid boundary layer for mass transport resistance (Devinny and Ramesh, 2005; López et al., 2016b). Other works define the mass flux in the liquid-biofilm interface with mass transfer coefficients (Bonilla-Blancas et al., 2015; Kim and Deshusses, 2003; López et al., 2016b).

Biofilm phase transport

Molecular diffusion described by Fick's law is the main mechanism to represent species transport through the biofilm phase in BTFs (Kim and Deshusses, 2003; Li et al., 2002). Diffusion coefficients determined in pure water are commonly used, which is a good starting point. However, the effective diffusion in the biofilm is reduced compared to the diffusion coefficient in water due to the presence on microbial cells, extracellular polymers and abiotic particles or gas bubbles trapped in the biofilm (Stewart, 2003). Thus, the use of diffusion constants determined in pure water instead of that in a biofilm may result in inappropriate results. The relation between the effective diffusion coefficient in the biofilm and the coefficient measured in pure water is known as relative effective diffusion.

The relative effective diffusion depends on the biomass density in the biofilm and the physical-chemical properties of the solute. Its value can be experimentally determined (Stewart, 2003) or using more sophisticated methods (Wood et al., 2002). Other authors have proposed correlations to relate diffusion coefficients in the biofilm with diffusion coefficients measured in water (Fan et al., 1990). However, latest technological developments have allowed applying avant-garde methodologies to determine more accurately and precisely biofilm's effective diffusivity by the use of microsensors based on microelectromechanical systems (MEMS) (Guimerà et al., 2014).

Biodegradation mechanism

A Monod-type kinetic expression is often used to describe substrate consumption (Kim and Deshusses, 2003; Li et al., 2002) in desulfurizing systems, being H_2S the only

rate-limiting substrate. However, different authors have shown that the treatment of high-loads of H_2S, such as those found in biogas desulfurization processes, may lead to substrate inhibition or oxygen-limiting conditions. A multi-substrate type equation with a Haldane term for H_2S and a Monod term depending on the dissolved oxygen (DO) concentration inside the biofilm have been shown to describe well experimental oxygen uptake rate (OUR) and H_2S uptake rate profiles (Bonilla-Blancas et al., 2015) during the characterization of H_2S-oxidizing biofilms in BTFs. Some authors have also proposed the use of a kinetic equation in which the ratio of elemental sulfur/sulfate produced is based on the DO concentration (Roosta et al., 2011). A product selectivity function for elemental sulfur or sulfate based on the sulfide oxidation activity and the OUR has been also considered by other authors (Gonzaléz et al., 2014; Mannucci et al., 2012). It is well-known that elemental sulfur, the main intermediate product of H_2S biological oxidation, is formed due to O_2 transport limitations inside the BTF bed (López et al., 2016a; Montebello et al., 2012). Lately, a multi-step oxidation kinetic model including not only H_2S oxidation end products, but also intermediate products such as thiosulfate and elemental sulfur (S^0) have been proposed in literature by Mora et al. (Mora et al., 2016).

2.3. PROCESS CONTROL THEORY

According to Baeza (Baeza, 2016), control is defined as a set of operations oriented to supervise the state of a system to generate, as a function of the deviation of its desired state, control actions needed to reduce or eliminate these deviations. Among control theory, the expected operation mode for the control system can be done through the specification of a certain closed-loop reference model. Most usual control structures found in chemical and biochemical systems may include feedforward control, feedback control, or both as shown in Fig. 2.4 adapted from Baeza (Baeza, 2016). To have a proper design of a control loop, this must be able to deal with the two types of disturbances: setpoint disturbances and load disturbances. If the input signal of the closed-loop controller is the setpoint value (R), then the process operates in Servocontrol mode. The objective of a servocontrol control loop is to adjust properly the manipulated variable to reach a new setpoint as fast and accurately as possible.

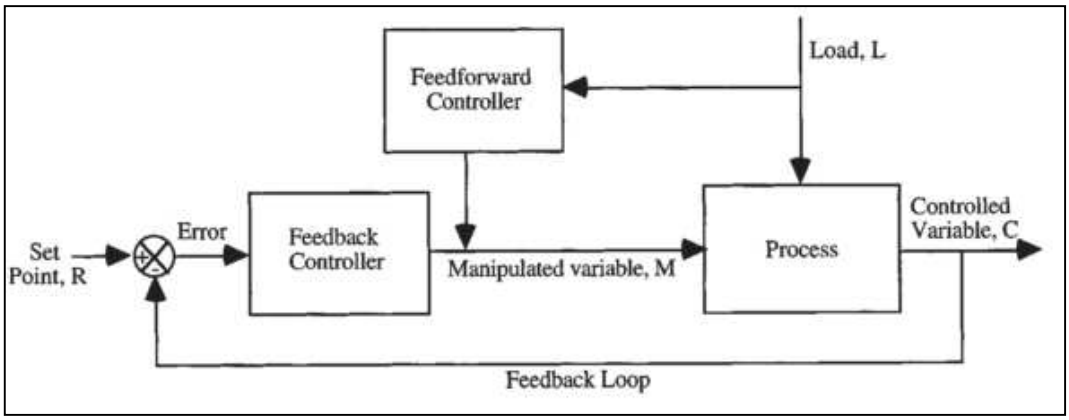

Figure 2.4. Block diagram for a combined feedforward+feedback control loop.

Besides servocontrol, control strategies should also be able to overcome undesired or unexpected load disturbances (L), in this case the input variable to the controller is the disturbance signal and therefore the process is operated under regulatory control.

The objective of regulatory control is to perform suitable changes in the manipulated variable in order to return the controlled variable to its setpoint. Undesired changes in the inlet streams are mainly related to downstream processes, so knowledge about previous step of the controlled unit also results useful at the time of determining the most adequate control strategy. Almost all control loops must content with different disturbances; therefore regulatory control is of primary importance. Servo-control is most commonly applied in batch processes than for continuous processes which are designed for operating with a fixed set point (Luyben and Luyben, 1997).

2.3.1. Feedback control

In a feedback control loop, the controlled variable C is compared to the set point R, with the difference (Eq. 2.3), deviation or error (ε) acted upon by the controller to move the manipulated variable M in such a way that the error is minimized .

$$\varepsilon = y_{SP} - y_m \qquad (2.3)$$

Where $y_{SP}$is the set point (R) value and y_m is the value measured of the controlled variable (C), according to Fig. 2.5. The simplest type of controller used in feedback control loops is the on/off controller. The manipulated variable only has two levels, acting over the system with a prefixed value (on) and without action over the system (off). They

are commonly applied for temperature, pressure and liquid level in pumped storage systems (Perry et al., 1997). Due to the cycling nature of the response of an on/off controller, this type of controller is not recommendable for biological processes that requires a constant controller action in order to achieve a stable and reliable operation.

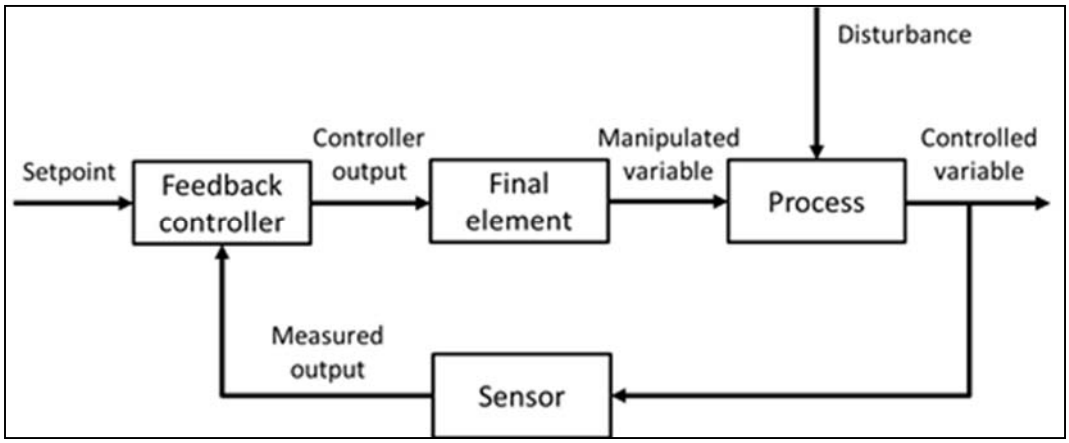

Figure 2.5. Block diagram for a feedback control loop.

The performance of an on/off controller can be highly improved using typical proportional integral derivative (PID) controllers. This type of controller is able to solve satisfactorily almost 80% of conventional control applications. The output of a PID controller is calculated by Eq. 2.4.

$$c(t)=c_s+K_c\cdot\varepsilon(t)+\frac{K_c}{\tau_I}\int_0^t\varepsilon(t)+K_c\cdot\tau_D\cdot\frac{d\varepsilon(t)}{dt} \quad (2.4)$$

The first contribution is the bias of the controller (c_s), which is the controller output selected to have no error in the controlled variable when the system is working under steady-state operation without disturbances. The three other terms are calculated as a function of the error. The proportional term is calculated multiplying a selected proportional gain (K_c) by the current error. The integral term is obtained with the integral of the error from the initial time to the current time, multiplied by the proportional gain and divided by the integral time constant (τ_I). Finally, the derivative term takes into account the rate of change of the error multiplied by the proportional gain and by the derivative time constant (τ_D). The procedure used for the selection of this parameters is

known as the controller tuning problem (Stephanopoulos, 1984). According to Stephanopoulos (Stephanopoulos, 1984) there are three general approaches we can use for tuning PID controller parameters.

The first and simplest approach is the use of semi-empirical rules which have been proven in practice. This procedure may be more applicable for chemical processes than for biological processes since changes in the manipulated variable on chemical processes have an intuitive result on the controlled variable. The result of this methodology would always produce a poorly tuned controller. The second approach to the tuning problem is a compromise between purely heuristic trial-and-error techniques and the more rigorous analytical techniques through the use of simple performance criteria. Simple performance criteria are based on some characteristic features of the closed-loop response of a system and the most often quoted like overshoot, rise time, settling time, decay ratio and frequency of oscillation of the transient. For the simple criteria above, the decay ratio has been the most popular by the practicing engineers (Stephanopoulos, 1984). Experience has shown that a 1/4 decay ratio is a reasonable trade-off between a fast rise and a reasonable settling time. Although nowadays is not recommended since is considered a too oscillating response for most of control applications (Baeza, 2016).

A large number of mathematical and heuristic techniques for selecting appropriate values for the controller parameters have been developed over the last years (Åström and Hägglund, 2004; Cohen and Coon, 1953; Ziegler and Nichols, 1942). One of the most applied methods for tuning PID controllers are the Ziegler-Nichols tuning rules (Ziegler and Nichols, 1942), which are a compromise between purely heuristic trial-and-error techniques and rigorous analytical techniques (Ziegler and Nichols, 1942). The first Ziegler-Nichols method is based on the idea of connecting a controller to the process, increase the gain until the system starts to oscillate, and then reduce the gains by an appropriate factor known as the ultimate gain method, also known as the Ziegler-Nichols Closed Loop Method (Ziegler and Nichols, 1942) .The Ziegler-Nichols closed loop method is based on experiments executed on closed loop and can be only applied to processes having a time delay or having dynamics of order higher than 3. The second Ziegler-Nichols method is based on measurements of the open loop response to measure some features of the open loop response and to determine controller parameters based on these features, known as the Ziegler-Nichols Open Loop method or also known as the process reaction curve (Ziegler and Nichols, 1942). This last method is based on open

loop testing on a steady-state process to take it into a new steady-state due to a step change on the final control element and to record the results of the process output. Then information related to the transient response and of the new steady-state are used to determine the controller parameters.

The third approach is the analytical approach. This approach relies heavily on the mathematical model of the process and its experimental application, which may be time consuming. If the mathematical model is so complicated that cannot be easily obtained, then the analytical approach to the design of a PID controller is not possible. The most usual criteria are the time-integral performance criteria, which considers the shape of the complete closed-loop response, from time zero until the steady-state has been reached. The time-integral criteria are based on the entire response of the process, unlike the simple criteria that use only isolated characteristics of the dynamic response (e.g. decay ratio, settling time, overshoot) (Stephanopoulos, 1984). The most used are Integral of the Square Error (ISE), Integral of the Absolute value of the Error (IAE) and Integral of the Time-Weighted Absolute Error (ITAE)

Parameters optimization can be performed for servo-control or for regulation, providing different tuning for obtaining the best response in one of these operational modes. This is the conventional PID controller, which only consider one degree of freedom (1DoF), because it does not allow adjusting independently the closed loop response for servo-control and regulation. However, there are alternatives proposals for the 1DoF PID controller that allows to alternatively tune the controller for somewhere in between the servo and the regulator operating mode (Alcántara et al., 2010), named PID controllers with two-degrees of freedom (2DoF). This work is focused on the closed-loop response for regulation control, consequently only the 1DoF PID controller tuning methodologies are studied. Stephanopoulos et al. (Stephanopoulos, 1984) proposed a systematic manner to design PID feedback controllers. Firstly, an appropriate performance criterion must be defined. Then, the performance criterion must be computed using a proportional (P) controller, proportional integral (PI) controller or aproportional integral derivative (PID) controller with the best settings for the adjusted parameters of the feedback controller. Finally, the controller which gives the best value for the performance criterion must be selected.

2.3.2. Feedforward control

In the other hand, feedforward control uses measurements of disturbance variables to position the manipulated variables in such a way to minimize any resulting deviation. A block diagram for a feedforward control loop is presented in Fig. 2.6. Disturbance variables could be either measured loads or the set point. As discussed in the previous section, an error must be detected in a controlled variable before the feedback controller can take action to change the manipulated variable, which means that disturbances must affect the system before the feedback controller can react. This is what is principally changed in the feedforward control loop.

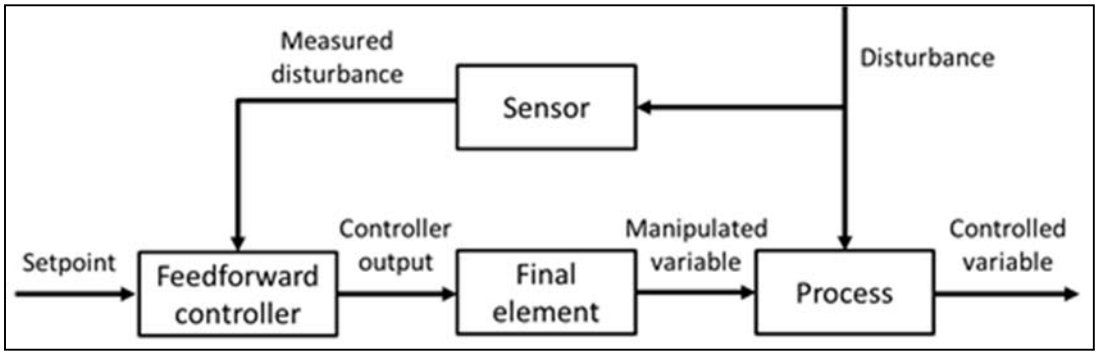

Figure 2.6. Block diagram for a feedforward control loop

The objective of a feedforward control loop is to take an appropriate action before a disturbance reaches the process. Thus a corrective action is taken as soon as a disturbance is about to affect the system instead of waiting for the disturbance to propagate all through the process before a correction is made (feedback control) (Luyben and Luyben, 1997). A feedforward controlled is based on simplified mechanistic models of the system, which is in charge of calculating the variation of the manipulated input required to avoid any changes in the controlled output. According to Perry et al. (Perry et al., 1997), in order to determine the appropriate settings for the manipulated variable the mathematical model must relate principally the effect of the manipulated variable on the controlled variable and the effect of the disturbance on the controlled variable.

If the feedforward controller is perfectly designed, the control system is able to modify the manipulated variable in order to avoid any deviation in the controlled variable. In practice, the model used to build the feedforward controller is not perfect and it has

limitations of precision and dynamics, which produces deviations between the setpoint and controlled output (Baeza, et al., 2016). Moreover, the model could also not include other non-measured disturbances.

Feedforward control is usually combined with feedback control to eliminate any offset resulting from inaccurate measurements and calculations (feedback failure) and unmeasured load components (feedforward failure) as shown in Figure 2.7. This control structure is more complex, and requires more instrumentation for measuring the controlled variable and disturbance but only uses one final element.

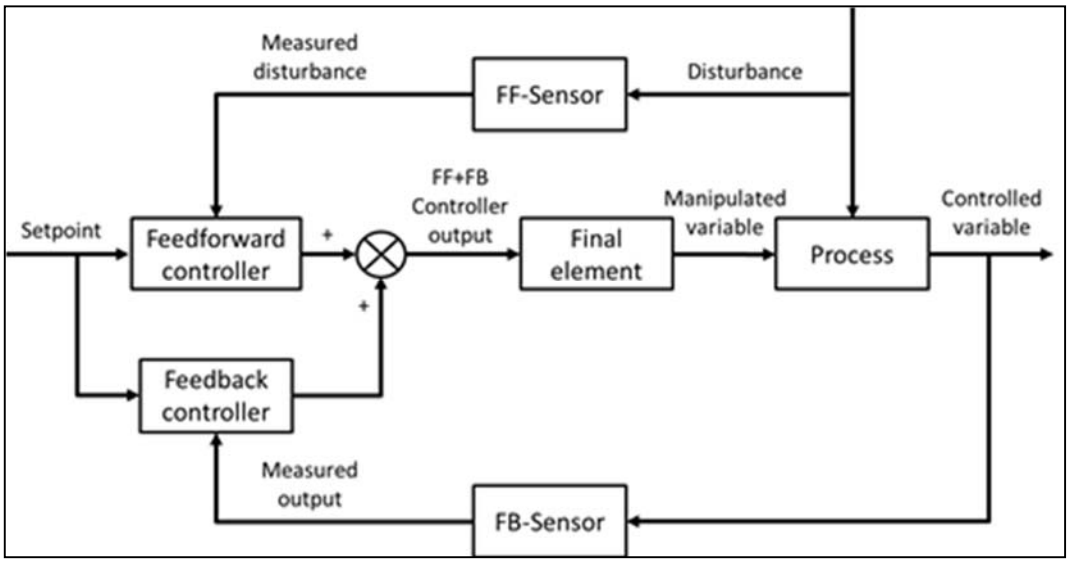

Figure 2.7. Block diagram for a combined feedforward and feedback control loop

2.3.3. Process control in biological processes

Compared to other biological process, the wastewater treatment field is one of the most advanced regarding process control implementation. This has been achieved thanks to mathematical modelling, which has been extensively studied and applied in the improvement of the enhanced biological nutrient removal (BNR) process (Baeza et al., 2002; Corriou and Pons, 2004; Guerrero et al., 2014; Isanta et al., 2013) carried out at wastewater treatment plants (WWTP). There are several parameters and variables to monitor and regulate at WWTPs in order to control the process. As an example, oxidation-reduction potential (ORP) measurements to optimize aeration system (Caulet et al., 1998), internal recycle flow-rate (Baeza et al., 2004, 2002) as well as external flow rates as a function of the influent flow-rate (Baeza et al., 2002), DO concentration through aeration

(Bartrolí et al., 2010; Jemaat et al., 2013) or nitrate set-point (Guerrero et al., 2014). Regarding the type of controllers and control loops applied, different strategies have been developed to achieve low effluent concentrations at reasonable operational costs and to reduce perturbations on the process (Baeza et al., 2002). Most typical perturbations on WWTPs are changes in the nutrients inlet loading rate due to changes in the nutrients concentration (Guerrero et al., 2014) or due to changes in the inlet flow rate caused by meteorological events such as dry and storm weather (Santin et al., 2015)

In order to standardize the simulation procedure and evaluation of all types of control strategies applied on WWTPs, standardized simulation protocols named Benchmarking Simulation Models (BSM) have been developed (Alex et al., 2008; Spanjers et al., 1998). In Figure 2.8 a general schematic of a default control strategy of BSM No1 (BSM1) is presented.

This simulation benchmark includes an standardized simulation protocol and evaluation procedure including plant layout, simulation models and model parameters, detailed description of disturbances to be applied during testing and evaluation criteria for testing the relative effectiveness of simulated strategies (Alex et al., 2008). Application of such protocol is only possible due to the existence of internationally accepted activated sludge models (ASM) (Henze et al 1987). Subsequently to the first ASM (ASM1), several improvements have been introduced by different authors to expand ASM1 to ASM2 (Henze et al., 1987), then to ASM3 (Gujer et al., 1999) in order correct a number of shortcomings that have emerged from its application, as thoroughly assessed by Gernaey et al. (Gernaey et al., 2004).

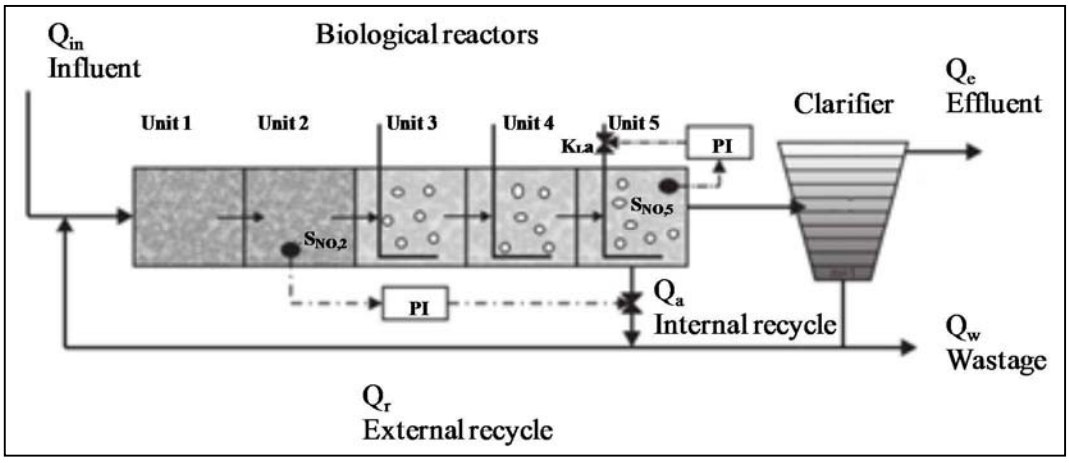

Figure 2.8. Schematic of default control strategy of BSM1 (Adapted from Santin et al., 2015).

Another process where process control has been successfully applied is in AD. Process control has enabled quick process stabilization with less operation and less maintenance inconvenient. Besides poor design and maintenance costs in AD reactors, generation of H_2S, inhability to maintain optimum pH and low biogas yield are the main reasons to implement a control system in AD processes in order to avoid cessation of AD reactors operation (Nguyen et al., 2015). In AD a variety of process control strategies have been developed that range from simple on/off and PID control (García-Diéguez et al., 2011) up to model-adaptive control (Rincón et al., 2012), fuzzy logic (knowledge-based control) (Nguyen et al., 2015) and artificial neural network schemes (Holubar et al., 2002) and their combination (Waewsak et al., 2010). Regarding the manipulated variables in AD process, these depends on the reactor configuration, but there are some of them that are present in the majority of cases. The key manipulated variables in AD process are especially non-biological parameters such as pH (Heredia-Molinero et al., 2014), alkalinity (Wilcox et al., 1995) and feeding rate (Jimenez et al., 2015), which is the most common and widely used to control disturbances in AD system. Some of the most common disturbances in AD process are Carbon/Nitrogen ratio shifting, load shocks by sludge-surplus mixing and foaming problems (Nguyen et al., 2015).

In real scale AD, simple feedback closed loop like PID control is preferable and mostly adopted. Advanced monitoring techniques are most discarded at all, but are most typically use to reinforce these robust control schemes. However, identification of the optimal controller constants for the PID algorithm is still the main challenge for AD systems since AD process is a dynamic and non-linear system. Overall, control process has clearly improved AD performance, demonstrating the importance of its application to compensate the different disturbances, regardless the type of AD reactor, the type of control strategy or the manipulated variable.

Regarding other waste treatment technologies, composting of solid waste is another biologically-based process which has been widely studied. Several studies have been published to comparing different methods to optimize the main key parameter: the aeration rate (Lau et al., 1992; Puyuelo et al., 2010). This knowledge allowed the development of control strategies in composting process, improving the quality process and minimizing environmental impact (Guardia et al 2006). In composting process, oxygen flow-rate is commonly supplied as a function of temperature and OUR measures using feedback controllers (Puyuelo et al., 2010). However, the prediction of better

aeration requirements is still necessary for an optimal design of composting process control. Besides process control, composting process improvement has also been focused through the characterization of waste through biodegradability studies (Tremier et al., 2005).

2.3.4. Process control in biotrickling filters for biogas desulfurization

BTFs have shown to be environmentally friendly, and an economically and technically efficient strategy to perform biogas desulfurization (Fortuny et al., 2008; Tomàs et al., 2009). However, in order to achieve a robust and reliable operation, process control is needed in BTFs in order to mitigate the effect causedd by daily variations of H_2S LR in the biogas stream, which can be due to many factors like seasonal or daily variations (Gabriel and Deshusses, 2003b; Gabriel et al., 2004). H_2S LR load variations may be due to biogas flow rate changes or due to biogas composition. An increase on biogas flow rate variations mainly related to shock loads (sludge surplus) on upstream processes (AD) (Nguyen et al., 2015; Rodriguez et al., 2014). Often biogas composition variations are mainly related to changes in the feedstock of AD (Soreanu et al., 2010). Biogas production fluctuation may lead to pressures below or above the biogas utilization equipment requirements, affecting negatively the performance of these equipment's or leading to dangerous situations. Thus, adding a storage facility in biogas utilization plants is a suitable solution to smooth out variations in biogas productions (Walsh et al., 1988).

However some storage systems would also need a conditioning step before biogas storage, principally to remove H_2S since this compound is extremely corrosive and its corrosiveness increases with increasing system pressure (Walsh et al., 1988). There are some installations that also have biogas storage tanks before biogas treatment, in order to also provide a constant pressure to the BTF (Rodriguez et al., 2014). There are more considerations to be studied, such as volume, pressure and location, in order to determine the type of storage facility for a biogas storage facility. In the other hand, dealing with variations on biogas composition is much more difficult, being totally necessary conditions step in order to increase lifespan of biogas utilization equipment like combustion engines where energy recovery from biogas is performed (Pipatmanomai et al., 2009; Walsh et al., 1988). When these variations occur and any action is taken in order to avoid or attenuate its effect on the BTF performance, long-term operation is considerably affected. Each type of disturbance has a different effect on BTF

performance. When biogas flow rate increases, empty bed residence time (EBRT) is reduced (Montebello et al., 2012), affecting mass transfer efficiency, and therefore increasing the amount of H_2S present in the outlet biogas stream and leading to a decrease in the lifespan of the cogeneration engines due to an increase in the amount of H_2S in the biogas. In the other hand, as previously mentioned in section 2.1.6, when H_2S inlet concentration increase, the O_2/H_2S ratio in the BTF decreases leading to bed clogging due to an excessive production of elemental sulfur.

Therefore, it is clear that the process must be regulated in favor of increasing the long-term stability of the desulfurization process. There are two variables that offer some regulation possibility: the air flowrate and the TLV. The first one is the most common actuation in some of the BTF actually installed in order to control the percentage of air in the outlet gas mixture as well as for security reasons to control the internal pressure of the reactor (Rodriguez, 2013). However, it is also common to regulate the airflow rate in order to increase the amount of air and therefore favor the complete H_2S oxidation, using conventional blowers or more efficient devices such as jet-venturi devices (Rodriguez et al., 2014, 2012). Increasing the airflow rate has the main drawback of reducing the calorific power of the biogas stream burned in the cogeneration engines, and increasing the explosion risk of the gaseous mixture. Air flowrate regulation effect on an aerobic BTF for biogas desulfurization operated under different H_2S LR conditions was studied in Chapter 5. In the other hand TLV regulation offers several advantages in front of airflow rate regulation, the principal is that improves gas-liquid mass transport efficiency along the packed bed leading to higher sulfate production and therefore reducing elemental sulfur in the packed bed without any biogas dilution (López et al., 2016a). In Chapter 5 TLV regulation effect is evaluated for different H_2S LR conditions. TLV regulation was also included in Chapter 8 in a theoretical study of control strategies in an aerobic BTF for biogas desulfurization. Afterwards in Chapter 9, TLV is also coupled to a feedback and feedforward control loops in order to regulate separately, H_2S disturbances on the inlet concentration and the biogas flow rate.

In BTFs for biogas desulfurization, the most common on-line monitored variables are the liquid medium pH, internal pressure of the BTF, liquid level, DO, and gas phase compounds (O_2 and H_2S) compositions. Besides the important information that this variables can provide about the process, some of them can also be used for process control purposes. The most important measured variables are the O_2 and H_2S percentage in the

outlet biogas stream, thus becoming primary control loops variables. In the other hand, pH, internal pressure and liquid level can be also coupled to a control loop in order to achieve a more stable operation, but they may be part of secondary loops. Primary control loops are those that have a direct relation with the overall process performance, while secondary control loops may provide complementary backup or be more related to safety reasons. However, if the information regarding pH control is treated through titrimetric techniques, pH can also be part of a primary loop and therefore contribute to overall process improvement. Titrimetry is the indirect measurement of the proton production through the monitoring of the amount of base or acid dosage necessary to maintain a constant pH where pH-affecting reactions are taking place (Marcelino et al., 2009; Spanjers et al., 1996). Titrimetry has also been commonly used to monitor biological processes such as organic matter degradation, denitrification and phosphorous removal (Gernaey et al., 2002; Guisasola et al., 2007b). The advantage of titrimetric monitoring is that provides online information about process performance through the determination of the biological proton production (HP_{bio}) from the observed proton production (HP_{obs}). However, in order to determine HP_{bio} from HP_{obs} the contribution to the pH of the different species present in the medium is required ($HP_{contributions}$), being this the main drawback for relating titrimetric variables with operational conditions in order to couple titrimetric variables in a control loop, especially at low H_2S LR loads. In Chapter 6 this techniques is applied in order to evaluate the application of titrimetry as measured variable in control lops.

CHAPTER 3

OBJECTIVES

3. OBJECTIVES

The general objective of this thesis was the development and application of control strategies in an aerobic biotrickling filter for biogas desulfurization.

Biotrickling filters have already shown to be technically and economically feasible compared to physical-chemical technologies to perform biogas desulfurization under aerobic conditions. However, control strategies are needed in order to achieve a robust, reliable and stable operation in full-scale installations. The following specific objectives were proposed in order to evaluate different control strategies and the added value that these can provide to desulfurizing biotrickling filters.

- To evaluate the main manipulated variables available in an aerobic biotrickling filter for biogas desulfurization in order to improve oxygen supply in the recycling line and the oxygen consumption along the packed bed, and therefore improve sulfate production.

- To assess the use of titrimetric techniques to study the representativeness of the information behind the biological proton production of an aerobic biotrickling filter and extend the use of titrimetric techniques to discontinuous process to help to identify the stoichiometric of sulfide-oxidizing microbial population.

- To develop, calibrate and validate a dynamic model of an aerobic BTF for the removal of high loads of H_2S from biogas streams to describe intermediate and final products obtained from H_2S oxidation under stationary, transient and dynamic feeding periods.

- To determine the controllability limits for a desulfurizing biotrickling filter under aerobic conditions and to examine the added value of these strategies in increasing selectivity of sulfate production.

- To evaluate experimentally feedback and feedforward control strategies in a lab-scale desulfurizing biotrickling filter under aerobic conditions.

CHAPTER 4

GENERAL MATERIALS AND METHODS

4. GENERAL MATHERIALS AND METHODS

4.1. DESCRIPTION OF EQUIPMENTS

4.1.1. Biotrickling filter set up

The main experimental setup used during this work is a lab-scale biotrickling filter (BTF) for biogas desulfurization under aerobic conditions. This experimental setup has been already used in two previous PhD thesis. Fortuny et al. (Fortuny, 2009) as a first development of a bioreactor for energy-rich gases desulfurization and Montbello et al. (Montebello, 2013) who studied the aerobic biotrickling filtration for biogas desulfurization. However, many improvements have been introduced in order to adapt the experimental setup to achieve the objectives defined in this thesis. In order to have a clearer picture of the experimental set up operation, the description of the lab-scale BTF has been divided in the following sections: general characteristics of the reactor, gas phase and liquid phase dynamics, gas phase sampling and liquid phase sampling and process monitoring control.

General characteristics of the reactor

This work has been conducted in a BTF reactor with an ancillary unit for air supply. The reactor diameter was 7.14 cm with a packed bed volume of 2.80 L. Polypropylene Pall rings of 16 mm diameter (MACH engineering products, USA) with a specific surface are of 354 $m^2 m^{-3}$ were randomly distributed inside the packed bed. Random distribution was preferred over structured packing materials such as HD-QPack, since as it was previously stated by Fortuny et al. (Fortuny et al., 2008), Fortuny et al. (Fortuny et al., 2011) and Montebello et al. (Montebello et al., 2012), this structure did not favor preservation of S-oxidizing biomass (SOB) sampling. Biomass samples were taken in order to perform a kinetic and stoichiometry characterization of aerobic sulfur oxidizing bacteria through LFS respirometry (Mora et al., 2016). From an industrial point of view, replacement of a deteriorate section of the packed bed can be easily done if a random configuration of the packing material is used instead of a structured packed bed. Regarding to the material of the packed bed, polypropylene was selected due to its resistance to work under a wide pH range since metallic pall rings can be degraded under acidic conditions (Montebello et al., 2014), affecting thus the overall performance of the BTF. An Empty Bed Residence Time (EBRT) of 118 s and an average Hydraulic

Retention time (HRT) of 30 ± 4 h were maintained during reference conditions. Montebello et al. (Montebello et al., 2013) defined an EBRT reference value of 131 s, since when lower EBRT values were applied lower RE and higher amounts of elemental sulfur were produced. The difference between the EBRT of Montebello et al. (Montebello et al., 2013) and the one used in this work is due to a smaller packed bed volume. In Fig. 4.1 detailed description of the experimental set up is presented.

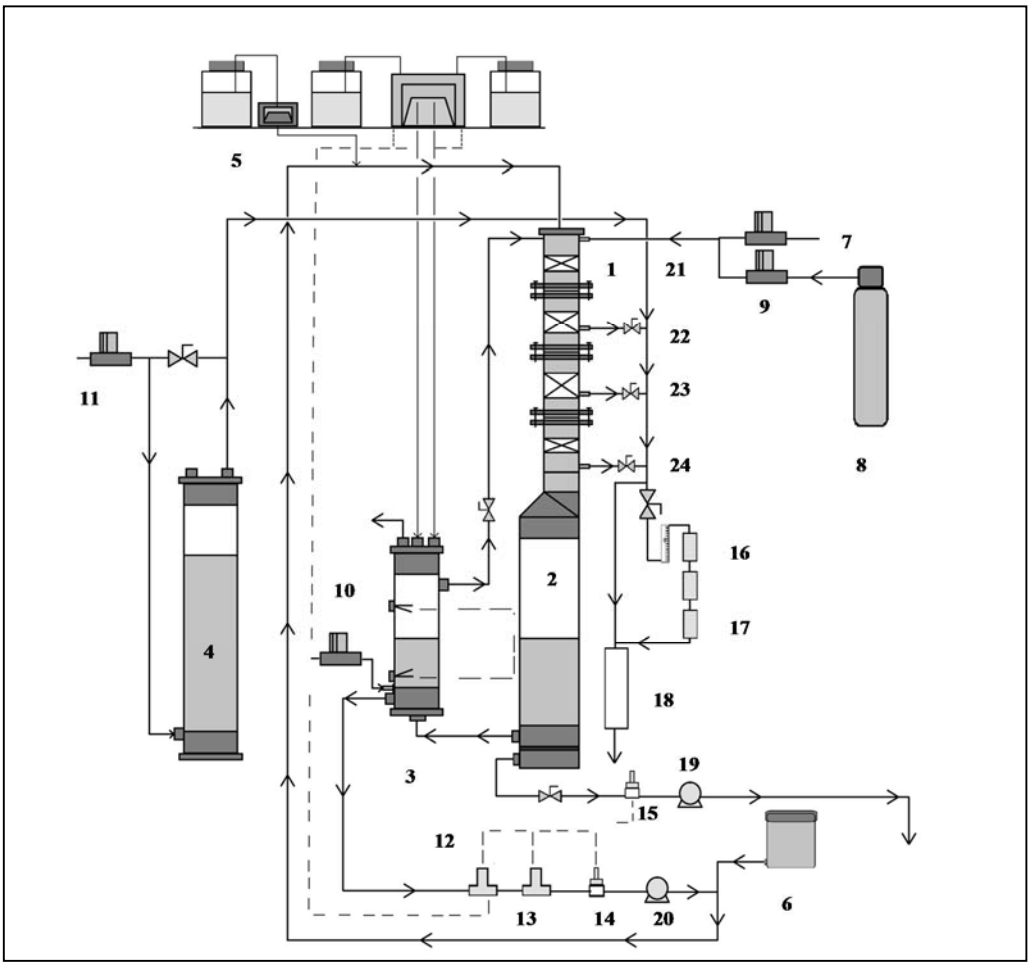

Figure 4.1. Schematic of the co-current biotrickling filter set-up: (1) main reactor, (2) purge column, (3) aeration column , (4) humidification column, (5) bicarbonate supply, (6) acid and base pumps, (7) N_2 DMFC, (8) H_2S cylinder, (9) H_2S DMFC, (10) Air DMFC , (11) Dilution air DMFC, (12) pH sensor, (13) ORP sensor, (14) recycle DO sensor (15) purge DO sensor, (16) H_2S gas sensor, (17) O_2 gas sensor, (18) NaClO trap, (19) purge pump, (20) recycling pump, (21) gas inlet, (22) gas sampling port h=0.24 m, (23) gas sampling port h=0.51 m, (24) gas outlet (h=0.7).

The selection of some operational parameters, such as EBRT and HRT, was based on previous experience in the research group (Fortuny et al., 2011; Montebello et al., 2013, 2010).

Gas phase and liquid phase dynamics

Pure N_2 and H_2S (Carburos Metalicos, Spain) flows were mixed with digital mass flow controllers (DMFC) (Bronkhorst, The Netherlands) to create a synthetic biogas stream that under reference conditions contained 2000 ppm_v of H_2S (56 g S-H_2S m^{-3} h^{-1}). Air was supplied to the liquid phase by continuous aeration at an O_2/H_2S supplied ratio of 41.2 (v v^{-1}) using DMFC (Bronkhorst, The Netherlands). Air flow is first fed to an ancillary unit to increase the dissolved oxygen (DO) concentration in the liquid phase coming from the purge column. The reactor is prepared to work under co-current flow pattern or under counter-current flow pattern. In Fig. 4.2 of both configurations are presented. In counter-current flow mode, excess oxygen from the aeration column and biogas mimics were fed from the bottom of the packed bed column, while in co-current flow mode the excess oxygen gas flow, the recirculation liquid flow and the biogas mimics flow were fed from the top of the BTF.

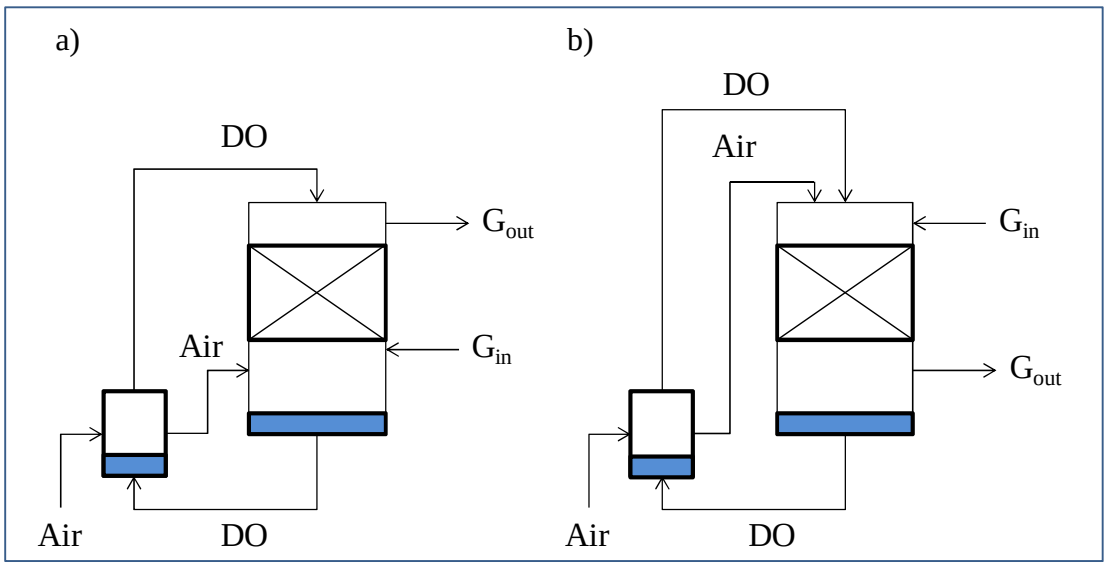

Figure 4.2. Schematic of the (a) counter-current and (b) co-current configurations.

The liquid volume of the ancillary unit for air supply was 1.53 L. A cylindrical airstone diffuser (Marina A961-Rolf C. Hagen Inc, Canada) of 2.84 cm diameter was used in the oxygenation column to oxygenate the outlet liquid stream from the purge column. Once the outlet liquid stream is oxygenated in the aeration column, it is recycled to the

top of the BTF using a diaphragm dosing pump (Alldos Primus 221, Germany). The DO concentration in the recycle and purge line were monitored in-situ for all the experiments with DO probes (CellOx® 325 – WTW, Germany). The BTF was also equipped with on-line monitoring of pH, oxidation-reduction potential (ORP) (pH 5333-Crison instruments). Besides monitoring pH, this was also controlled around 6.5 and 7 using an ON/OFF control system by automated addition of NaOH (Panreac, Spain) 1M or HCl (Panreac, Spain) 1 M using peristaltic pumps (Watson Marlow OEM 400FS/M1, Sweden). Liquid phase was renewed by automated dosage of mineral medium with peristaltic pump (Masterflex II L/S, Germany) at a rate of 2.2 L d^{-1}. Mineral medium composition is detailed in Table 4.1.

Table 4.1. Mineral medium composition

Compound	**Concentration**	**Units**
K_2HPO_4	0,15	g L^{-1}
KH_2PO_4	0,12	g L^{-1}
NH_4Cl	1,00	g L^{-1}
$CaCl_2$	0,02	g L^{-1}
$MgSO_4 \cdot 7H_2O$	0,20	g L^{-1}
Trace Elements	1,00	ml L^{-1}
Trace Elements		
Compound	**Concentration**	**Units**
HCl	6,7	ml
$FeCl_2 \cdot 4H_2O$	1,5	mg L^{-1}
H_3BO_3	0,06	mg L^{-1}
$MnCl_2 \cdot 4H_2O$	0,1	mg L^{-1}
$CoCl_2 \cdot 6H_2O$	0,12	mg L^{-1}
$ZnCl_2$	0,07	mg L^{-1}
$NiCl_2 \cdot 6H_2O$	0,025	mg L^{-1}
$CuCl_2 \cdot 2H_2O$	0,015	mg L^{-1}
$NaMoO_4 \cdot 2H_2O$	0,025	mg L^{-1}
$EDTA.Na_2O_8 \cdot 2H_2O$	4.3	mg L^{-1}

All reagents were off analytical grade. Trace elements, added in a proportion of 1 mL of trace elements per liter of mineral medium, were prepared according to (Norbert Pfenning, Friedrich Widdel, 1981). Since SOB is autotrophic bacteria, sodium bicarbonate ($NaHCO_3$) 3M was automatically added as inorganic carbon source using an peristaltic pump (Masterflex L/S, Germany) at a rate of 1.8 L d^{-1} . In order to maintain a

constant volume in the reactor, continuous liquid purge was automatically performed with a peristaltic pump (Masterflex II L/S, Germany) at a rate of 2.77 L d^{-1}.

Gas phase sampling

During operation under reference conditions gas phase concentration was measured only from the main outlet gas stream, but when experiments where performed, gas concentration was also measured through three sampling ports located along the BTF height at 0.24 m, 0.51 and 0.7. Gas samples were monitored on-line with an electrochemical gas sensor for H_2S (Sure-cell, Euro-Gas Management Services, UK), and oxygen (O_2 SL sensor, Euro-Gas Management Services, UK) and a silicon-based non-dispersive infrared (NDIR) sensor for CO_2. (GMP343 Vaisala Carbocap, Finland). Since H_2S sensor measure range is limited between 0-200 ppm_v, biogas mimic outlet from the BTF was diluted with air previously humidified, in order to be able to measure higher H_2S concentrations (Fig. 4.3).

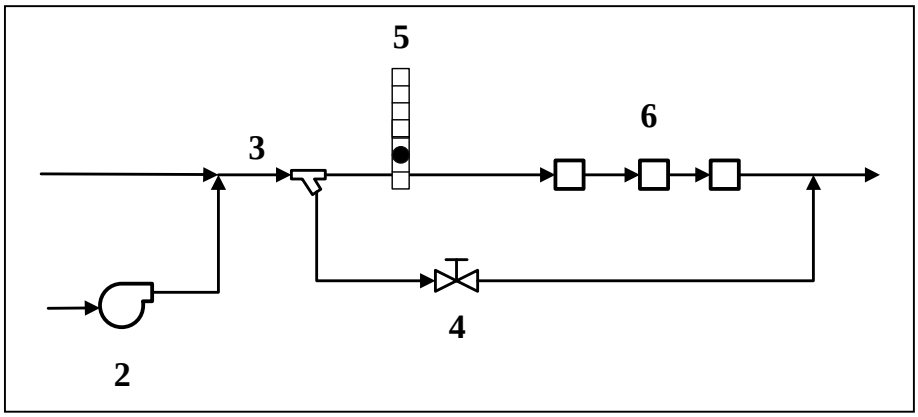

Figure 4.3. Schematic of the BTF gas measurement system: (1) Biogas mimic inlet ,(2) Dilution air, (3) Diluted biogas mimic, (4) regulation valve, (5) rotameter, (6) H_2S , O_2 and CO_2 gas sensor.

Regarding the diluted biogas flow rate, once the biogas mimic is mixed with the dilution air, a fraction of the diluted biogas mimic is purged to the final outlet stream and one fraction is passed through the gas sensors as detailed in Fig. 4.3. For safety reasons, piping, junction accessories and valves for H_2S lines were in polyvylidene fluoride (PVDF) (MAZZER CHEMI-PVD 6", Accesair, Spain). Gas lines for air and N_2 were in polyamide 12 (PA 6" Accesair, Spain).

Liquid phase sampling

Liquid samples were periodically taken from liquid purge in order to measure the ionic composition and the total inorganic carbon (TIC) of the liquid purge. Since bicarbonate and CO_2 were used as carbon source for SOB, TIC was measured using a TIC/TOC 1020 analyzer (IO Analytical, USA) equipped with a non-dispersive infrared detector and a furnace maintained at 680 ºC. By this way, dissolved inorganic carbon was analyzed in order to avoid carbon source limitation during all the experiments. Besides purge samples, fresh mineral medium and $NaHCO_3$ samples were also analyzed in order to also quantify the ionic composition and TIC of both solutions.

H_2S oxidation products as sulfate and thiosulfate were analyzed off-line using ion chromatography (IC) with a suppressed conductivity detector using a Dionex ICS-2000 HPLC system with an IonPac AS18-HC column (4x250 mm - Dionex, USA). Before analyzing liquid samples, they were filtered with disposable 0.22 µm syringe filter driven units (Millipore, Germany) in order to remove any biomass or impurity present in the sample. Liquid samples were diluted with Mili-Q Water (18 MΩ cm^{-1}) in a 1:10 ratio for IC analysis or 1:10 for TIC analysis. After conditioning the sample, 200 ml of sample was stored in a plastic container at 4ºC to be used until 24 hours after the sample collection or at -20 ºC for preserving the sample for long storage periods. About liquid lines material, polyamide 12 and silicone rubber tubes were used for piping in the liquid lines, since the liquid medium was not corrosive.

When the trickling liquid velocity (TLV) was regulated, total suspended solids (TSS) were analyzed in order to study if TLV could also help to remove solids such as elemental sulfur accumulated in the BTF bed. Samples were obtained from the liquid purge and from the solids accumulated at the bottom of the purge column. TSS were performed according to Standard Methods (APHA, 2005). By this way, an aliquot of liquid sample (V_s) was firstly filtered through a pre-weighed standard glass microfiber filter (W_1) of 0.7 µm (GF/F grade, Whatman, USA) and dried at a constant temperature of 105 ºC until constant weight. The increase of weight (W_2) represents the organic and inorganic matter in suspension in the sample. The relation between the weight increase (W_1-W_2) and the sample volume is the concentration of TSS. After this first step the sample is ignited at 550 ºC. The loss of weight represents the VSS content in the sample.

The inorganic suspended material, or fixed suspended solids (FSS), is calculated from the difference between TSS and VSS.

Process monitoring and control

As it has been mentioned in previous sections, many gas and liquid phase variables are monitored online by different sensors (Fig. 4.4).

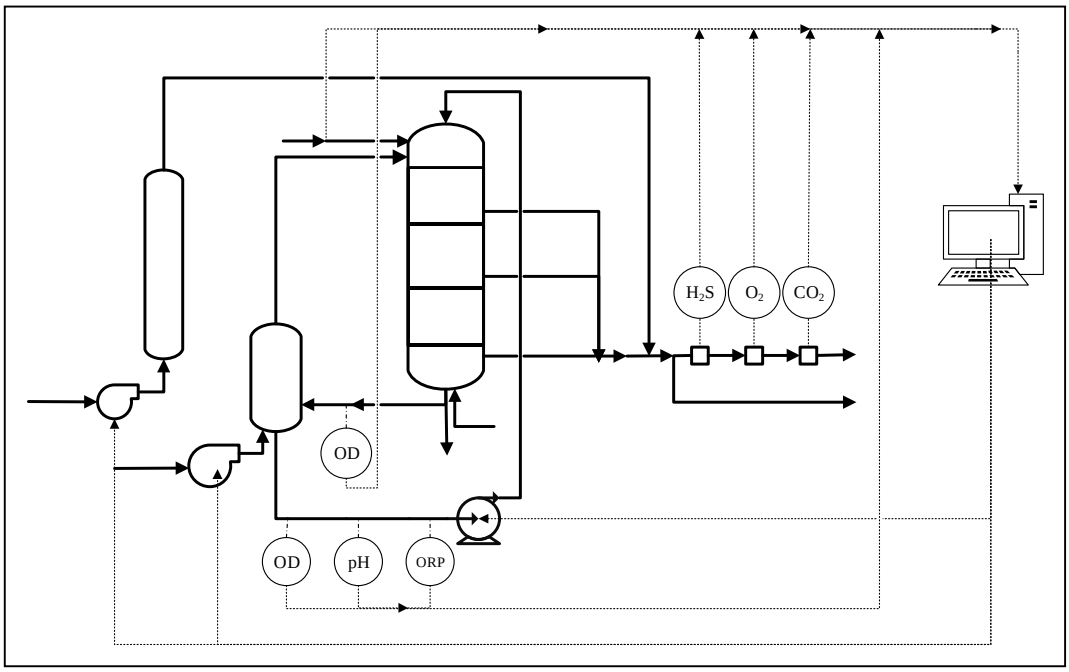

Figure 4.4. Schematic of monitoring signals on the co-current biotrickling filter set-up

Data was collected with a data acquisition card (Advantech PCI-1711) connected to a PC LabWindows CVI 2010 software named AddControl (Fig. 4.5) developed in our research group, and used in different lab-scale setups to monitor and control biological processes (Fortuny, 2009; Guerrero Camacho, 2014; Montebello, 2013). Through the data acquisition card several analogic and digital inputs and outputs for actuation over the dosing pumps and over digital mass flow controllers. In order to be able to test control strategies (Chapter 8 and Chapter 9), some improvements were done in the BTF setup with respect to the previous design (Montebello et al.,2013) to be able to measure and communicate the main instruments to the PC.

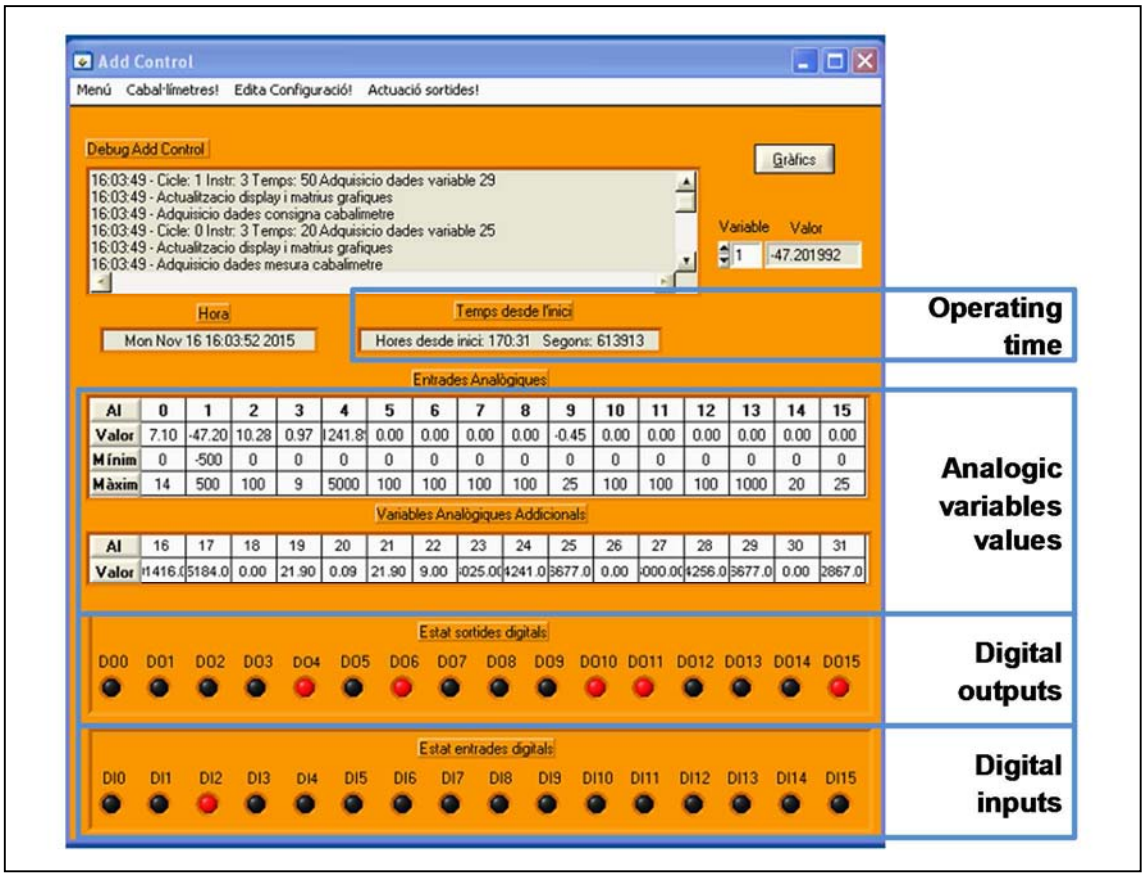

Figure 4.5. Screenshot of the software AddControl used to monitor and control the BTF

These improvements were: changing the previous diaphragm recycling pump (Alldos Primus 221, Germany) which only had the manual regulation option, into an automatic diaphragm recycling pump (Grundfos DDI 150-AR-PV, Germany). The previous AddControl version (Guerrero, 2014) only include DO control with a proportional integral (PI) controller that acted over the air mass flow controller (Bronkhorst, The Netherlands). Therefore in order be able to regulate TLV following a feedback control loop where the controlled variable can be the H_2S or O_2 outlet concentration, a PI controller was coupled to the AddControl version used in this work. This control loop will be further detailed in Chapters 8 and 9.

4.1.4. Respirometer experimental set up

Parallel to BTF operation, abiotic respirometric tests were performed (*Chapter 6, section 6.2.1*), in order to determine the proton production (HP) related only to CO_2 stripping and therefore be able to determine the biological HP from the observed HP of

biotic respirometric tests for the kinetic parameter determination of SO-NR microbial population (Mora et al., 2014a).

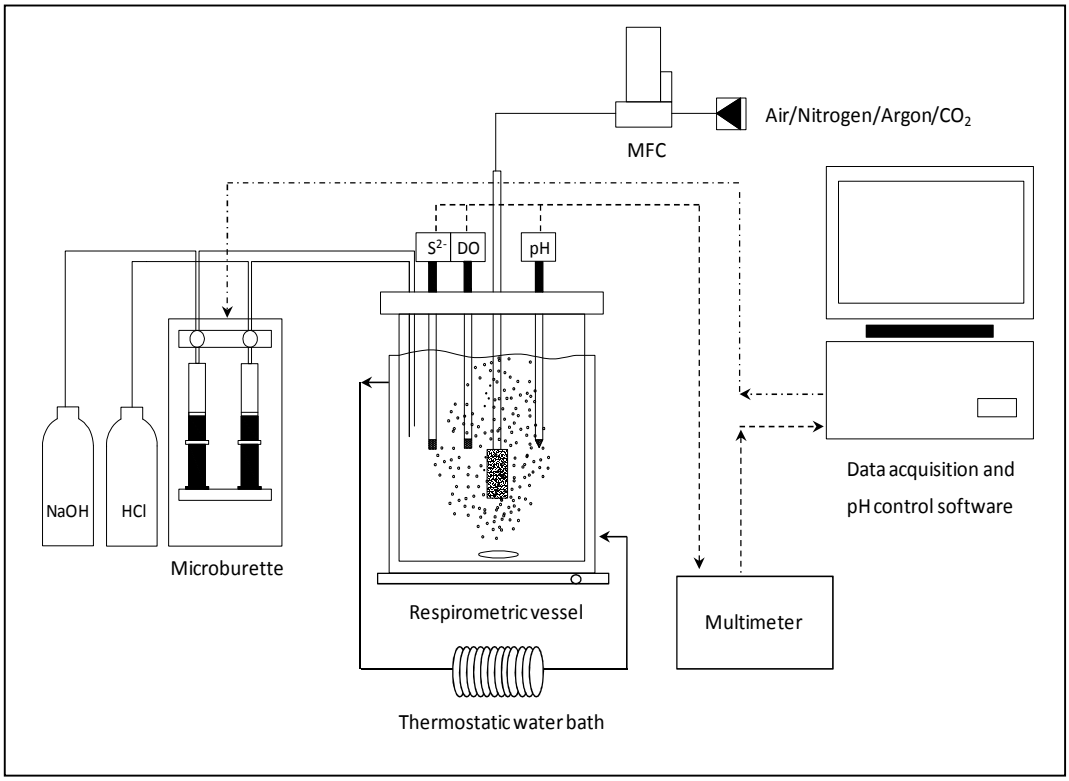

Figure 4.6. General schematic of the homogeneous respirometer

Abiotic anoxic stripping tests were carried out in a stirred respirometer with a capacity of 350 mL (Fig. 4.6.). Temperature and pH were monitored and controlled continuously during anoxic tests. Both parameters were monitored through a pH electrode with temperature probe integrated (SenTix 82, WTW, Germany), and also an additional probe was also eventually used to monitor dissolve oxygen concentration (CellOx 325, WTW, Germany). Both, the electrode and the oxygen probe were connected to a bench top multimeter (Inolab Multi 740, WTW, Germany) for data monitoring. In both reactors the pH was controlled trough the automatic addition of diluted HCl and NaOH solutions with a dispensing burette (Multi-Burette 2S-D, Crison Instruments, Spain). Temperature was controlled by means of a circulating thermostatic water bath (Polystat24, Fisher Scientific, Spain). In Table 4.2. further information about the vessel used is provided.

Table 4.2. Detailed characteristics of the respirometric vessel RV-1 (*from Mora et al., 2014a*)

Parameter	Value
Working volume	350 mL
Vessel material	Glass
Cover	Stainless steel cover
Diffuser	Stainless steel diffuser
Other characteristics	Jacketed vessel

4.2. DESIGN AND OPERATIONAL PARAMETERS OF BTFs

Many parameters can be used to describe biotechnological waste gas treatment, but as is explained in Langenhove and De Eyder et al. (Langenhove and De Eyder, 2001), for some parameters identical values can be obtained at different operational conditions. Hence, the following expressions are usually applied to describe correctly the design and operational parameters of a BTF:

$$LR = \frac{C_{g,H2S\ in} \cdot Q_{biogas}}{V_{bed}} \quad (4.1)$$

where:

LR	Loading rate of H_2S (g S-H_2S m^{-3} h^{-1})
$C_{g,H_2S,in}$	H_2S concentration at the inlet of the BTF (g S-H_2S m^{-3})
Q_{biogas}	Biogas flow rate (m^3 h^{-1})
V_{bed}	Empty volume of the packed bed (m^3)

The loading rate of H_2S gives the relation between the amount of pollutant contained in the biogas stream and the volume of packed bed.

$$EBRT = \frac{V_{bed}}{\left(Q_{biogas} + Q_{air}\right)} \quad (4.2)$$

where:

EBRT	Empty bed residence time (s)
V_{bed}	Empty volume of the packed bed (m^3)
Q_{biogas}	Biogas flow rate (m^3 h^{-1})
Q_{air}	Air flow rate (m^3 h^{-1})

Empty bed residence time indicates the time that the total gas flow rate is in contact with the packed bed. In this case for the EBRT calculation, air flow rate must be also included. In order to determine the true residence time of the gas phase in the packed bed, the porosity of the packed bed must be included in the expression:

$$\tau = EBRT \cdot \varepsilon \quad (4.3)$$

where:

τ	Real residence time (s)
EBRT	Empty bed residence time (s)
ε	Packed bed porosity (m^3 void volume m^{-3} packed volume)

Mainly LR and EBRT are the most used parameters to characterize the design and operation of a BTF. In order to evaluate the BTF performance, there are also several parameters used in literature that describe the effectiveness of the biotechnological waste gas treatment. Effectiveness of BTFs can be evaluated in terms of H_2S removal efficiency (RE) according to Eq. 4.4.

$$RE = \frac{C_{g,H2S\ in} - C_{g,H2S\ out}}{C_{g,H2S\ in}} \cdot 100\% \quad (4.4)$$

where:

RE	Removal efficiency (%)
$C_{g,H_2S,in}$	H_2S concentration at the inlet of the BTF (g S-H_2S m^{-3})
$C_{g,H_2S,out}$	H_2S concentration at the outlet of the BTF (g S-H_2S m^{-3})

RE provides the percentage of H_2S removed from the gas phase but does not include any parameter related to the BTF size or to the packed bed. Hence a variable able to be compared with other reactors is necessary. Therefore the Elimination Capacity (EC) is defined as follows:

$$EC = LR \cdot RE \quad (4.5)$$

where:

EC	Elimination capacity of H_2S (g S-H_2S m^{-3} h^{-1})
LR	Loading rate of H_2S (g S-H_2S m^{-3} h^{-1})
RE	Removal efficiency (%)

EC represents the mass of H_2S removed from the gas phase per unit volume of reactor and time. When the BTF performance is 100% RE, then the EC is equal to the LR. EC can be used to define critical and maximum performance of the reactor through the critical EC ($EC_{critical}$) and the maximum EC (EC_{max}). When the EC begins to be lower than the LR, therefore the $EC_{critical}$ is reached. If the LR is still increased, subsequently an overall EC_{max} is achieved. In addition, it is also common in BTF for waste gas treatment to know the TLV of operation, which is described by the following expression:

$$TLV = \frac{FL}{S} \tag{4.6}$$

where:

TLV	Trickling liquid velocity (m h^{-1})
FL	Liquid recycling flow rate (m^3 h^{-1})
S	Section of the reactor (m^2)

In BTFs for biogas desulfurization under aerobic conditions, besides evaluating BTF performance through gas phase parameters (RE, EC), it is also crucial to evaluate sulfur species selectivity since long-term operation of the reactor will depend on these values. With the objective of determining sulfur species selectivity, overall mass balances for sulfur species involved in the process were performed as follows: two sulfur species, sulfate and thiosulfate were measured by IC while biological S^0 was determined by difference between total amount of H_2S removed $\left(m_{H_2S,removed}\right)$ and the net mass flow of the abovementioned measured species $\left(m_{SO_4^{2-}}, m_{S_2O_3^{2-}}\right)$ taking into account that no dissolved sulfide was detected at any time. Equations 4.7 to 4.10 were used for calculations:

$$m_{H_2S,removed} = \left(C_{g,H_2S,in} - C_{g,H_2S,out}\right) \cdot Q_{biogas} \tag{4.7}$$

where:

$m_{H_2S,removed}$	Total amount of H_2S removed (g S-H_2S h^{-1})

$C_{g,H_2S,in}$ H_2S gas outlet concentration (g S-H_2S m^{-3})
$C_{g,H_2S,out}$ H_2S gas inlet concentration (g S-H_2S m^{-3})
Q_{biogas} Biogas flow rate (m^3 h^{-1})

$$m_{SO_4^{2-}} = \left(C_{L,SO_4^{2-},out} - C_{L,SO_4^{2-},in}\right) \cdot Q_{L,P} \quad (4.8)$$

where:
$m_{SO_4^{2-}}$ SO_4^{2-} net mass flow (g S-SO_4^{2-} h^{-1})
$C_{L,SO_4^{2-},out}$ SO_4^{2-} liquid outlet concentration (g S-SO_4^{2-} m^{-3})
$C_{L,SO_4^{2-},in}$ SO_4^{2-} liquid inlet concentration (g S-SO_4^{2-} m^{-3})
$Q_{L,P}$ Liquid purge flow rate (m^3 h^{-1})

$$m_{S_2O_3^{2-}} = \left(C_{S_2O_3^{2-},out} - C_{S_2O_3^{2-},in}\right) \cdot Q_{L,P} \quad (4.9)$$

where:
$m_{S_2O_3^{2-}}$ $S_2O_3^{2-}$ net mass flow (g S-$S_2O_3^{2-}$ h^{-1})
$C_{L,SO_4^{2-},out}$ $S_2O_3^{2-}$ liquid out let concentration (g S-$S_2O_3^{2-}$ m^{-3})
$C_{S_2O_3^{2-},in}$ $S_2O_3^{2-}$Liquid inlet concentration (g S-$S_2O_3^{2-}$ m^{-3})
$Q_{L,P}$ Liquid purge flow rate (m^3 h^{-1})

$$m_{S^0} = m_{H_2S,removed} - m_{SO_4^{2-}} - m_{S_2O_3^{2-}} \quad (4.10)$$

where:
m_{S^0} S^0 net mass flow (g S-S^0 h^{-1})
$m_{H_2S,removed}$ Total amount of H_2S removed (g S-H_2S h^{-1})
$m_{SO_4^{2-}}$ SO_4^{2-} Net mass flow (g S-SO_4^{2-} h^{-1})
$m_{S_2O_3^{2-}}$ $S_2O_3^{2-}$Net mass flow (g S-$S_2O_3^{2-}$ h^{-1})

Once the net mass flow of each sulfur specie is known, sulfur selectivity can be determined relating the net mass flow of each specie with the total sulfur mass at the BTF inlet as is described in the next expressions:

$$\% SO_4^{2-} = \left(\frac{m_{SO_4^{2-}}}{m_{H_2S,inlet}}\right) \cdot 100\% \quad (4.11)$$

where:

$\% SO_4^{2-}$	SO_4^{2-} selectivity (%)
$m_{SO_4^{2-}}$	SO_4^{2-} net mass flow (g S-SO_4^{2-} h^{-1})
$m_{H_2S,inlet}$	H_2S inlet net mass flow (g S-H_2S h^{-1})

$$\% S^0 = \left(\frac{m_{S^0}}{m_{H_2S,inlet}}\right) \cdot 100\% \quad (4.12)$$

where:

$\% S^0$	S^0 selectivitity (%)
m_{S^0}	S^0 net mass flow (g S-S^0 h^{-1})
$m_{H_2S,inlet}$	H_2S inlet net mass flow (g S-H_2S h^{-1})

$$\% S_2O_3^{2-} = \left(\frac{m_{S_2O_3^{2-}}}{m_{H_2S,inlet}}\right) \cdot 100\% \quad (4.13)$$

where:

$\% S_2O_3^{2-}$	$S_2O_3^{2-}$ selectivity (%)
$m_{S_2O_3^{2-}}$	$S_2O_3^{2-}$net mass flow (g S-$S_2O_3^{2-}$ h^{-1})
$m_{H_2S,inlet}$	H_2S inlet net mass flow (g S-H_2S h^{-1})

Since the above equations are not related to the reactor size or to the volume of packed bed, a production capacity is defined as the product between LR and the sulfur selectivity.

$$pCSO_4^{2-} = \% SO_4^{2-} \text{selectivity} \cdot LR \quad (4.14)$$

where:

$pCSO_4^{2-}$	SO_4^{2-}production capacitity (g S-H_2S m^{-3} h^{-1})
$\% SO_4^{2-}$	SO_4^{2-} selectivity (%)
LR	Loading rate of H_2S (g S-H_2S m^{-3} h^{-1})

$$pCS^0 = \% S^0 \cdot LR \quad (4.15)$$

where:

pCS^0= S^0 production capacitity (g S-H_2S m^{-3} h^{-1})

% S^0= S^0 selectivitity (%)

LR= Loading rate of H_2S (g S-H_2S m^{-3} h^{-1})

$$pCS_2O_3^{2-}=\%\ S_2O_3^{2-}\cdot LR \tag{4.16}$$

where:

$pCS_2O_3^{2-}$ $S_2O_3^{2-}$ production capacitity (g S-H_2S m^{-3} h^{-1})

LR Loading rate of H_2S (g S-H_2S m^{-3} h^{-1})

% $S_2O_3^{2-}$ $S_2O_3^{2-}$ selectivity (%)

In order to satisfy sulfur mass balances, sulfur production capacities must be equal to EC. It must be noticed that when H_2S inlet it is equal to zero, elemental sulfur accumulated is degraded (Montebello et al. 2010) and further oxidized to sulfate. In this case equation 4.15 hanges its sign and changes from S^0 production to S^0 consumption capacity. Once parameters describing sulfur species are introduced, expressions describing oxygen in the BTF are also here presented in the following expressions.

$$SOTR=\left(DO_{recycle}-DO_{purge}\right)\cdot Q_{recycle} \tag{4.17}$$

where:

SOTR Standard Oxygen transfer rate (Kg O_2 h^{-1})

$DO_{recycle}$ O_2 Dissolved concentration in the recycle line (g m^{-3})

DO_{purge} O_2 Dissolved concentration in the purge line (g m^{-3})

$Q_{recycle}$ Liquid recycling flow rate (m^3 h^{-1})

SOTR describes the mass rate of O_2 that is supplied from the gas phase to the liquid phase in the aeration column. This parameter is useful in order to quantify oxygen mass transfer in the aeration column in order to compare it with other aeration devices.

$$DOL=\left(DO_{RE}\right)\cdot Q_{RE} \tag{4.18}$$

where:

DOL	Dissolved Oxygen Load (Kg O_2 h^{-1})
DO_{RE}	O_2 Dissolved concentration in the recycle line (g m^{-3})
Q_{RE}	Liquid recycling flow rate (m^3 h^{-1})

The main difference between SOTR and DOL, is that DOL is used in order to describe the oxygen biologically available (dissolved) at the top of the reactor, and SOTR is only used in order to evaluate mass transfer in the aeration column as previously explained. Finally, in order to determine a possible observed S/O_2 ratio, O_2 consumption capacity is determined as follows:

$$CC_{O2}=\frac{C_{g,O2,in}\cdot Q_{L,inlet}-C_{g,O2,out}\cdot Q_{L,purge}}{V_{bed}} \quad (4.19)$$

where:

CC_{O2}	O_2 Consumption Capacitity (g O_2 m^{-3} h^{-1})
$C_{g,O2,in}$	O_2 gas inlet concentration (g O_2 m^{-3} h^{-1})
$C_{g,O2,out}$	O_2 gas outlet concentration (g O_2 m^{-3} h^{-1})
Q_{inlet}	Liquid inlet flow rate (m^3 h^{-1})
$Q_{L,P}$	Liquid purge flow rate (m^3 h^{-1})
V_{bed}	Volume of packed bed (m^3)

Finally the overall ratio of H_2S removal to O_2 consumption in g S-H_2S g^{-1} O_2 is described as follows:

$$\eta_{H_2S\text{-}O_2}=\frac{EC_{H_2S}}{CC_{O_2}} \quad (4.20)$$

where:

CC_{O2}	O_2 Consumption Capacitity (g O_2 $m^{-3}$$h^{-1}$)
EC	Elimination capacity of H_2S (g S-H_2S m^{-3} h^{-1})

4.1.3. Loading rate (LR) and Elimination Capacity (EC) nomenclature.

In Chapter 5, overall LR and EC are calculated based on total H_2S mass flow (g S-H_2S $h^{-1)}$ fed or removed, respectively, divided by the empty bed volume (m^3). In addition, LR and EC per each section were assessed, named as $LR_{section,i}$ and $EC_{section,i}$, respectively,

where subindex “section” refers to the LR of only one section of the BTF bed and subindex “i” refers to the number of the section. Number 1 referred to the top of the reactor and number 3 to the lower section.

CHAPTER 5

CHARACTERIZATION OF MANIPULATED VARIABLES IN AN AEROBIC BIOTRICKLING FILTER FOR BIOGAS DESULFURIZATION

5. CHARACTERIZATION OF MANIPULATED VARIABLES IN AN AEROBIC BIOTRICKLING FILTER FOR BIOGAS DESULFURIZATION

The main motivation of this chapter was to gain knowledge about the effect of the regulation of the two main manipulated variables in an aerobic biotrickling filter for biogas desulfurization, air flowrate and trickling liquid velocity, over process performance. Initially, abiotic experiments were performed in order to study the effect of flow pattern and the manipulated variables over oxygen gas-liquid mass transfer parameters. Abiotic tests results allowed determining the most suitable gas-liquid flow pattern, in terms of oxygen gas-liquid mass transfer, to be applied in biotic experiments. After biotrickling filter inoculation, loading rate changes due to H_2S inlet concentration increases were performed in order to quantify the effect of this perturbation when no regulation is performed. Later on, the same experimental conditions were applied, regulating first the trickling liquid velocity and later the air flow rate. This biotic tests allowed performing a comparison between the test with and with regulation. Especial attention is focused the effect of trickling liquid velocity regulation tests. Results obtained in this chapter were useful in the following chapters, from the evaluation of titrimetry application in continuous processes in Chapter 6 to obtain the data for the calibration of a model of an aerobic biotrickling filter for biogas desulfurization in Chapter 7.

Abstract

Biological oxidation in biotrickling filters for the treatment of high H_2S loads contained in biogas streams still requires further study to reduce elemental sulfur accumulation due to limited gas-liquid oxygen mass transfer inside biotrickling filters bed. Reduction of elemental sulfur accumulation may be improved by regulating the main manipulated variables related to oxygen mass transfer efficiency during biological hydrogen sulfide removal in biotrickling filters. Trickling liquid velocity was selected as the most appropriate variable to manipulate compared to air supply regulation, while co-current flow pattern was selected compared to counter-current flow in order to improve gas-liquid oxygen mass transfer. Then, trickling liquid velocity influence on the performance of a lab-scale biotrickling filter treating high loads of H_2S in a biogas mimics and operated in co-current flow at neutral pH and packed with plastic pall rings was investigated. Effect of trickling liquid velocity modulation between 4.4 and 18.9 m h^{-1} in biotrickling filter performance was compared with operation without trickling liquid velocity regulation, which resulted in an improvement of 10% on the elimination capacity and, most importantly, a 9% increase in the product selectivity to sulfate at a loading rate of 284 g S-H_2S m^{-3} h^{-1}. Concentration profiles along the biotrickling filter height evidenced that trickling liquid velocity regulation progressively lead to a better dissolved oxygen distribution and, thus, enhanced overall biotrickling filter performance

A modified version of this chapter has been published as:

L.R. López, T. Bezerra, M. Mora, J. Lafuente, D. Gabriel. Influence of trickling liquid velocity and flow pattern in the improvement of oxygen transport in aerobic biotrickling filters for biogas desulfurization. J Chem. Biotechnol. (2016). 91, 1031-139.

5.1. INTRODUCTION

Biogas conditioning has been performed reliably and effectively using biological technologies such as biotrickling filters (BTFs), which have been shown to perform well under different pollutant loads at lab-scale (Fortuny et al., 2008), pilot-scale (Rodriguez et al., 2014) and full-scale (Tomàs et al., 2009). Nevertheless, complete H_2S oxidation during biological desulfurization of biogas in BTFs still needs to be optimized to avoid elemental sulfur accumulation inside the BTF bed. Biological oxidation reactions of H_2S by sulfur-oxidizing bacteria (SOB) are described by Munz et al. (Munz et al., 2009) by the following catabolic reactions:

$$HS^- + 0.5O_2 \rightarrow S^0 + OH^- \qquad [\Delta G^0 = -169 \text{ kJ mol}^{-1}] \qquad (5.1)$$

$$S^0 + 1.5O_2 + H_2O \rightarrow SO_4^{2-} + 2H^+ \qquad [\Delta G^0 = -563.83 \text{ kJ mol}^{-1}] \qquad (5.2)$$

According to Eq. 5.1 and Eq. 5.2, the O_2/H_2S concentration ratio defines the end product formed during biological desulfurization. Since sulfate formation yields more energy for microbial growth than the formation of elemental sulfur (S^0), this reaction is preferentially carried out in the absence of biomass or oxygen limitation (Janssen et al., 1998). Since H_2S loads in real plant operation vary depending on many factors like seasonal or daily variations(Gabriel and Deshusses, 2003a; Gabriel et al., 2004), the abovementioned ratio must be maintained by controlling the oxygen supplied to the system to avoid S^0 formation and minimize the total solids accumulated in the BTF bed (Mannucci et al., 2012). Total solids accumulation is directly related to the increase of pressure drop inside BTF bed (Andreasen et al., 2012), leading to a significant reduction of BTF operational life time.

Many studies have focused on finding S^0 oxidation strategies to remove S^0 once accumulated such as S^0 wash-out through increasing trickling liquid velocity (TLV) (Fortuny et al., 2011) as well as oxidation of biologically produced S^0 during H_2S starvation periods (Fortuny et al., 2011, 2010) according to Eq. 5.2. However, few efforts have been done in order to control S^0 production through oxygen gas-liquid mass transfer optimization strategies during biological desulfurization in BTFs. Still many full-scale BTFs for biogas desulfurization supply the air flow directly to the biogas pipeline as a function of the biogas flow rate, which has been proven inefficient for proper BTF

performance. Air or pure oxygen directly supplied to the liquid phase of the BTF in the bioreactor sump with conventional blowers improves sulfate production (Rodriguez et al., 2014). Nevertheless, the common control action in such reactors consists in increasing the air flow rate, which dilutes biogas and is not effective enough in terms of oxygen transfer (Rodriguez et al., 2014).

In the last years, many automated control strategies have been applied in bioprocesses in order to increase process performance, to reduce operating costs and to upgrade effluent quality (Guerrero et al., 2011; Ruano et al., 2012; Steyer et al., 1999; Zhang et al., 2008). Air supply and TLV are the two sole process variables that allow regulating oxygen supply to BTFs to face H_2S load variations. Increasing the air supply to improve oxygen transport produces biogas dilution (Chaiprapat et al., 2015), which reduces its energy content and increases the explosive risks associated to an increase in the percentage of air in the fuel mixture, which ranges from 5 to 15 % of methane in air (Walsh et al., 1988) . Oppositely, TLV manipulation does not involve biogas dilution nor explosion risks. Instead, positive effects of TLV variation have been reported in H_2S removal in BTFs operated in counter-current flow (Jin et al., 2005; Kim and Deshusses, 2005; Walsh et al., 1988).

Although literature (Diks and Ottengraf, 1991; Hartmans and Tramper, 1991) suggests no significant differences in BTF performance irrespective of the flow pattern, performance of biogas upgrading BTFs in which oxygen is directly fed to the recycle line may depend strongly on the flow pattern, since the end product depends on the O_2/H_2S concentration ratio, which is radically different if the gas and liquid entrance are fed in co-current or in counter-current mode. Interestingly, BTFs used for biogas desulfurization research operate under a counter-current configuration (Fortuny et al., 2011; Montebello et al., 2012; Rodriguez et al., 2014). In BTFs operated in counter-current mode an unfavorable O_2/H_2S concentration ratio is obtained at the biogas inlet leading to high S^0 production due to oxygen lack for complete H_2S oxidation. A co-current configuration implies a favorable O_2/H_2S concentration ratio at the reactor inlet. Though some studies have focused on the effect of TLV and gas supply in BTF with co-current configuration for removing different contaminants as xylene and trichloroethene (TCE) vapors (Popat and Deshusses, 2010; Trejo-Aguilar et al., 2005), few studies have analyzed the effect of these variables on BTFs performance during H_2S desulfurization operated in co-current flow.

The aim of this Chapter was to evaluate the influence of the flow pattern and manipulated variables for improving the oxygen transport to reduce S^0 accumulation, but specifically focus on the study of the influence of the TLV on the performance of a BTF operated in co-current configuration for biogas desulfurization under aerobic conditions.

5.2. MATERIALS AND METHODS

5.2.1. Biotrickling filter set up

Experiments were conducted in a BTF reactor with an ancillary unit for air supply. Detailed information of the BTF set up can be found elsewhere (Fortuny et al., 2011; Montebello et al., 2012) and in Chapter 4 (*see section 4.1.1.)*. The reactor diameter was 7.14 cm with a packed bed volume of 2.80 L. Polypropylene Pall rings of 16 mm diameter (MACH engineering products, USA) with a specific surface area of 354 $m^2 m^{-3}$ were used. An Empty Bed Residence Time (EBRT) of 118 s and an average Hydraulic Retention time (HRT) of 30 ± 4 h were maintained during reference conditions.

Air was supplied to the liquid phase by continuous aeration at an O_2/H_2S supplied ratio of 41.19 (v v^{-1}) using digital mass flow controller (Bronkhorst, The Netherlands). Air flow is first fed to an ancillary unit to increase the dissolved oxygen (DO) concentration in the liquid phase. Exhaust air from the oxygenation column was fed at the top or bottom of the BTF under co-current or counter-current flow pattern, respectively. A figure of both configurations can be found in Chapter 4 (*see section 4.1.1*). The liquid volume of the ancillary unit for air supply was 1.53 L. A cylindrical airstone diffuser (Marina A961-Rolf C. Hagen Inc, Canada) of 2.84 cm diameter was used in the oxygenation column to oxygenate the outlet liquid stream from the purge column. Once the outlet liquid stream is oxygenated in the aeration column, it is recycled to the top of the BTF. The DO concentration in the recycle and purge line were monitored in-situ for all the experiments, pH was also controlled around 6.5 and 7 using an ON/OFF control system by automated addition of NaOH 1M or HCl 1 M. Furthermore, H_2S, oxygen and carbon dioxide (CO_2) in the gas phase were monitored on-line through three sampling ports located along the BTF height at 0.24 m, 0.51 and 0.7 m. Further details of gas and liquid phase sampling can be found in Chapter 4 (*see seccion 4.1.1.*).

5.2.2. Abiotic tests

A set of abiotic experiments were carried out in the BTF before inoculation to study the effect of TLV and the air-to-total gas flow ratio (GFR) as manipulated variables on oxygen transport as a function of the gas-liquid flow patterns. Before each experiment the BTF was loaded with fresh mineral medium. Then, continuous operation at one HRT was set by applying the variations on reference operational conditions presented in Table 5.1.

Table 5.1. Experimental conditions of abiotic tests

Test	Flow pattern	TLV *(m h^{-1})*	Q_{air} $Q_{total\ gas}^{-1}$ *(v v^{-1})*
A1	Co-current	4.4	0.15
A2		4.4	0.28
A3		4.4	0.46
A4		9.3	0.28
A5		14.5	0.28
A6	Counter-current	4.4	0.15
A7		4.4	0.28
A8		4.4	0.46
A9		9.3	0.28
A10		14.5	0.28

TLV was varied in the typical range of liquid velocity in BTFs while the GFR range was decided based on previous literature. Experiments allowed studying the effect on the Standard Oxygen Transfer Efficiency (SOTE) and on the Standard Oxygen Transfer Rate (SOTR**),** which were determined according to ASCE/EWRI 2-06 and further detailed in Rodriguez et al. (Rodriguez et al., 2013).

5.2.3. Startup under co-current BTF operation

Unspecific inoculation was performed using aerobic sludge obtained from the external recycle line of a local municipal wastewater treatment plant (Granollers, Barcelona). The sludge was diluted 1:1 with mineral medium, obtaining thus a final volatile suspended solids (VSS) concentration of 1.3 g L^{-1}. To attach biomass in the inert support, the liquid phase was not renewed thorough the first day of the startup phase. H_2S gas inlet concentration was maintained at 1000 ppm_v (28.2 g S-H_2S m^{-3} h^{-1}) over the first two days of the startup. Latter, H_2S concentration was increased to the reference inlet

concentration of 2000 ppm_v (56.3 g S-H_2S m^{-3} h^{-1}). The rest of operational parameters were maintained similar as the reference operational values mentioned in section 5.2.1

5.2.4. Biotic experimental conditions

After BTF startup, a set of biotic experiments were performed in order to assess the elimination capacity (EC) and the effect on sulfate selectivity according to the conditions shown in Table 5.2.

The first experiment was performed on day 114 after startup, namely constant TLV test, while the second experiment was performed on day 183, namely variable TLV test and the third experiment was performed on day 269, namely variable AFR test. The constant TLV experiment, which was equivalent to test the effect of TLV under open loop conditions from a control point of view, consisted on stepwise loading rate (LR) increments from 56.3 to 283.8 g S-H_2S m^{-3} h^{-1} as a consequence of H_2S inlet concentration increases. Through variable TLV experiments, which were equivalent to test the effect of TLV under close loop conditions from a control point of view, same stepwise LR increments were applied but modulating the TLV from 4.4 m h^{-1} to 18.9 m h^{-1} for the first three LR increments. Since 18.9 m h^{-1} corresponded to 100% of the total capacity of the recycling pump, TLV was kept constant at 18.9 m h^{-1} for the last two LR increments in the variable TLV experiment. Along variable GFR experiments, which were equivalent to test the effect of GFR under closed loop conditions from a control point of view, same stepwise LR increments were applied but modulating the air flow rate (AFR) from 400 ml/min to 2000 ml/min. At each LR step-wise increment AFR was increased 400 ml/min in order to maintain constant the O_2/H_2S volumetric ratio at 42.2 % v v^{-1}. Each LR stepwise increment was maintained for 24 h. In addition to liquid samples collected in the purge line, gas samples were collected through the sampling ports to study H_2S elimination and oxygen gas consumption profiles along the BTF height. As described in Chapter 4 (*see section 4.1.2*), data allowed calculating the overall LR and EC of the reactor as well as the $LR_{section,i}$ and $EC_{section,i}$ per each section of the packed bed. A H_2S starvation period of 7 days was set after each constant TLV and variable TLV experiments to reduce the amount of S^0 accumulated inside the bed.

Experiment	$[H_2S]$	$[H_2S]$ LR	O_2/H_2S	TLV	DOL	GFR	Biogas dilution
	(ppm_v)	*(g S-H_2S m^{-3} h^{-1})*	*(% v v^{-1})*	*(m h^{-1})*	*(g O_2 h^{-1})*	*(m^3 h^{-1})*	*(%)*
Constant TLV Constant GFR	2000	56.3	42.2	4.4	$8.3\cdot10^{-2}$	1.4	28.2
	4000	112.9	21.0		$7.3\cdot10^{-2}$		
	6000	169.6	14.0		$5.9\cdot10^{-2}$		
	8000	226.6	10.5		$2.9\cdot10^{-2}$		
	10000	283.8	8.4		$1.4\cdot10^{-2}$		
	0	0	-		$8.5\cdot10^{-2}$		
Variable TLV Constant GFR	2000	56.3	42.2	4.4	$9.0\cdot10^{-2}$	1.4	28.2
	4000	112.9	21.0	11.3	$1.6\cdot10^{-1}$		
	6000	169.6	14.0	18.9	$1.7\cdot10^{-1}$		
	8000	226.6	10.5	18.9	$1.4\cdot10^{-1}$		
	10000	283.8	8.4	18.9	$1.4\cdot10^{-1}$		
	0	0	-	4.4	$6.4\cdot10^{-2}$		
Constant TLV Variable GFR	2000	56.3	42.2	4.4	$6.6\cdot10^{-2}$	1.4	28.2
	4000	112.9			$7.2\cdot10^{-2}$	1.8	43.9
	6000	169.6			$7.2\cdot10^{-2}$	2.2	54.2
	8000	226.6			$7.3\cdot10^{-2}$	2.6	61.1
	10000	283.8			$6.7\cdot10^{-2}$	3.0	66.2
	0	0			$5.3\cdot10^{-2}$	1.4	28.2

5.3. RESULTS AND DISCUSSION

5.3.1. Effect of TLV and air supply in co-current and counter-current abiotic conditions

Fig. 5.1 (a and b) shows the SOTR and SOTE obtained in the aeration column under abiotic conditions for experiments in co-current and counter-current flow pattern, respectively. Results show that when TLV was increased, SOTR and SOTE showed a linear relationship for co-current liquid-gas flow pattern while both variables seemed to reach a plateau at TLV over 9 m h^{-1} for counter-current. When GFR was varied, SOTR remained invariant irrespective of the flow pattern configuration, while SOTE decreased in both cases due to the increase of the supplied air. The negligible variation of SOTR due to GFR changes was probably due to the short contact time of the air flow in the aeration column coupled to a low impact of air flow velocity changes in oxygen transport in the packed bed under the conditions tested. Oxygen transport efficiency obtained herein

(1.7 %) using the airstone diffuser is significantly lower than that obtained by Rodriguez et al. (Rodriguez et al., 2012) with different intensive gas-liquid contact devices, such as venturi ejector (9%), jet-venturi (8%) and membrane diffuser (7%).

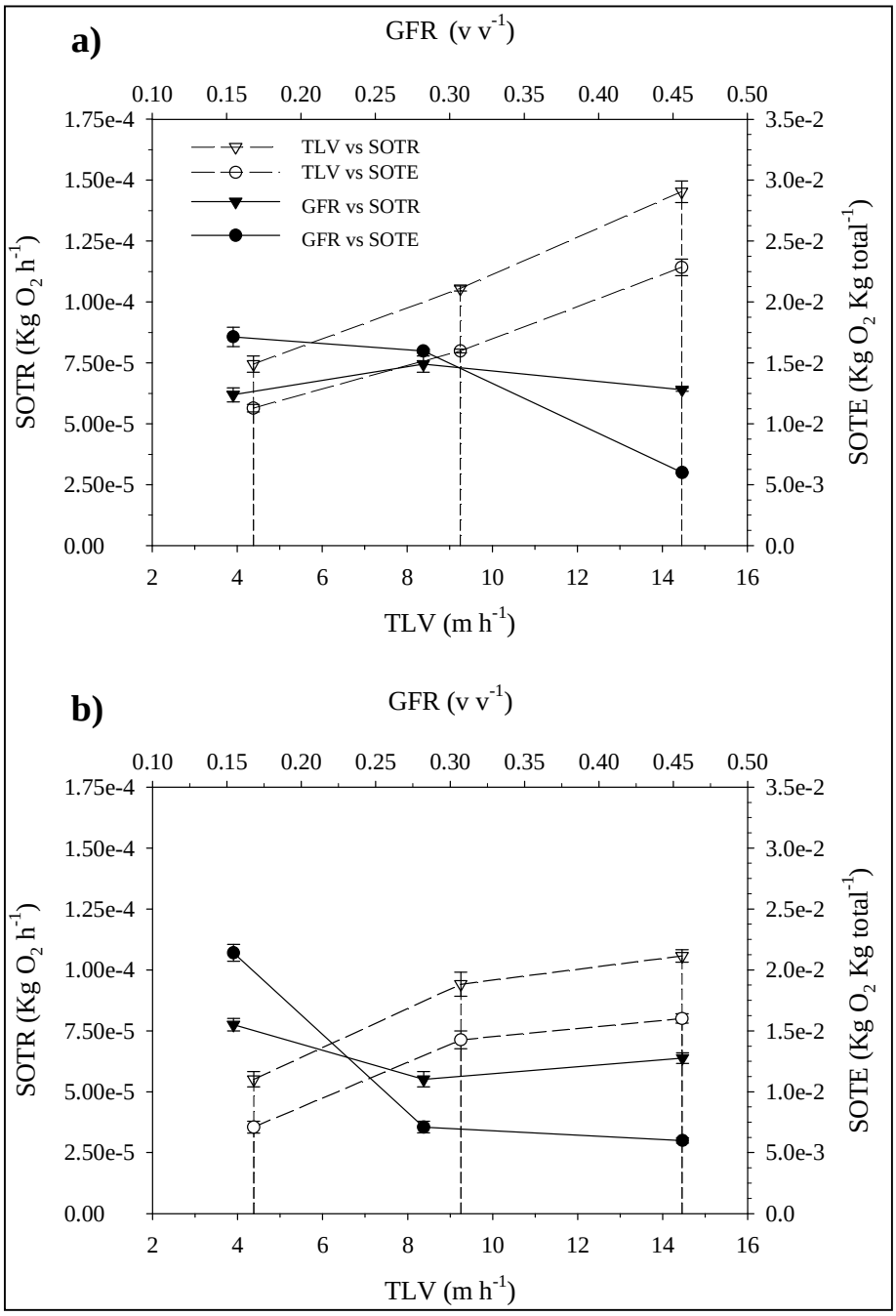

Figure 5.1. Effect of TLV (bottom x-axis) and GFR ratio (upper x-axis) on SOTR (left y-axis) and SOTE (right y-axis) for (a) co-current configuration and for (b) counter-current configuration under abiotic conditions.

Although a GFR shorter than 0.15 v v^{-1} would lead to a more efficient oxygen transport, i.e. larger SOTE, the amount of oxygen transferred (SOTR) in the aeration column would not increase significantly. In this sense, the TLV and flow pattern had a larger impact in the oxygen transport along the packed bed. Under abiotic conditions, oxygen mass transfer efficiency in the packed bed depended mainly on the gas-liquid flow pattern. The SOTR of the co-current flow pattern was larger compared to that of the counter-current flow (Fig. 5.1, a and b), particularly at TLV above 10 m h^{-1}, which indicated that the G-L transport in the packed bed column was more favorable in the case of the co-current flow pattern.

Because of the oxygen supply from top and bottom of the column in the counter-current mode, a greater oxygen concentration gradient along the reactor height existed in the co-current flow pattern, thus favoring oxygen transport between phases. A similar behavior in terms of oxygen gradients under biotic experiments was expected, which favored the O_2 absorption with a net oxygen flux towards the liquid phase due to biological oxygen uptake in the biofilm.

Differences in terms of SOTR between both flow pattern configurations were in the range of 10 to 23% at TLV in the range of 4 to 9 m h^{-1}, which were decisive for selecting a co-current flow pattern in the present work. In addition, Montebello et al. (Montebello et al., 2010) suggested that in a co-current operation the DOL/$[H_2S]_{removed}$ ratio would be favorable for sulfate production at the entrance of the reactor where H_2S concentration reaches its maximum value.

Results obtained under abiotic conditions demonstrate that TLV is a more suitable manipulated variable than air flow rate in an attempt to regulate the SOTR to define accurate control strategies in BTFs that would improve BTF performance at high H_2S loads. Increasing TLV not only increases the load of DO supplied (SOTR) but also improves penetrability of liquid through the BTF bed (Montebello et al., 2010), which results in an interesting strategy to improve H_2S removal and to reduce S^0 accumulation without the need of further dilution of biogas. Thus, TLV was designated to be the manipulated variable during biotic experiments in order to regulate the ratio DOL/$[H_2S]_{removed}$. Furthermore abiotic experiments were helpful to decide that co-current flow was the proper configuration to use under biotic conditions.

5.3.2. Startup under co-current BTF operation

After two days of operation, the BTF achieved a RE of 100%, which was maintained during all the startup period (Figure 5.2).

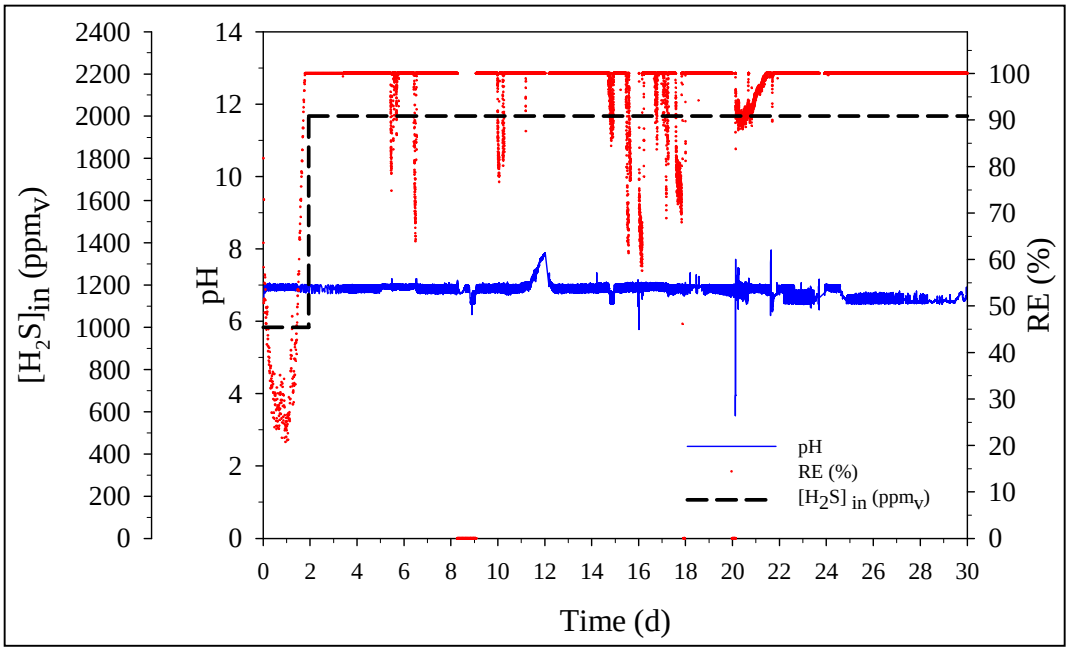

Figure 5.2. Startup of the BTF under co-current operation.

Short losses of performance happened due to operational problems with the ancillary aeration column. Once solved these operational problems, RE stabilized at 100%. The startup period lasted 3 days in terms of H_2S removal. However, 27 days were needed for 100% sulfate selectivity. During these 27 days no operational changes with respect to the reference operational conditions were made in order to maximize the sulfate production and removal efficiency. During steady-state conditions, the ratio between dissolved oxygen load (DOL) and the amount of H_2S removed ($H_2S_{removed}$) was maintained at 0.38 ± 0.01 (g O_2 g^{-1} S-$H_2S_{removed}$) to guarantee 100% sulfate selectivity and H_2S removal. After BTF startup (May 2013), the BTF was continuously operated along 35 months in a continuous mode without interruptions until March 2016. In fig. 5.3 elemental sulfur and sulfate production rate and sulfur mass balance during the first year of BTF operation is presented. Demonstrating stability of H_2S RE and of sulfate production rate of BTF after LR experiments.

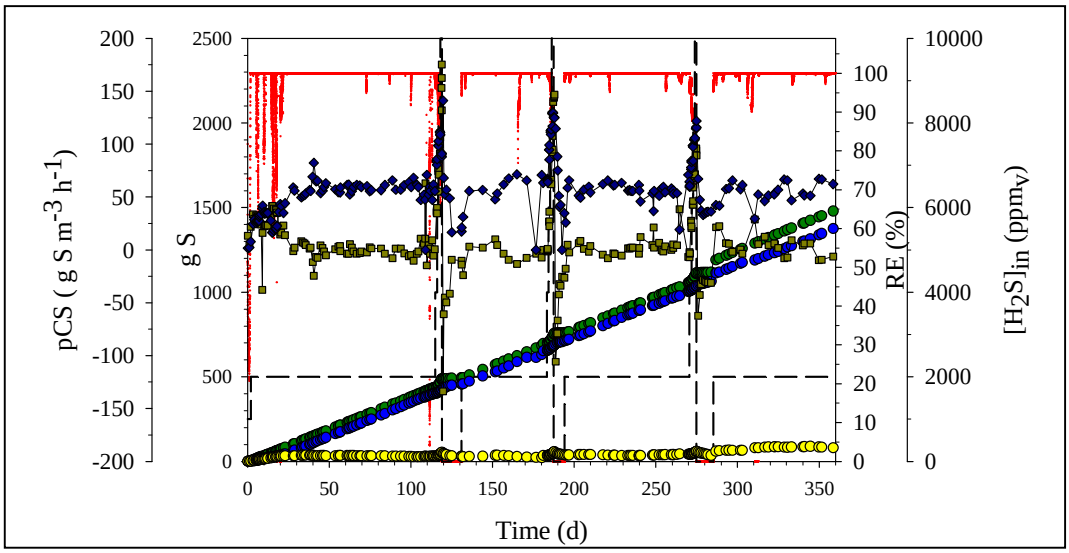

Figure 5.3. Elemental sulfur production rate (dark yellow squares), sulfate production rate (blue dark squares), removal efficiency (red dots), sulfur mass removed (dark green circles), sulfate mass produced (blue circles), elemental sulfur mass (yellow circles) and H_2S inlet profile during the first year of BTF operation

5.3.3. Effect of TLV regulation on H_2S removal in co-current flow pattern

Since BTFs reported in literature for biogas desulfurization often operate in up-flow, counter-current mode (Fernández et al., 2013a; Fortuny et al., 2011; Montebello et al., 2013; Namini et al., 2013), down-flow, co-current operation performance was first assessed at constant TLV prior to variable TLV test. Results of stepwise H_2S loading rate increments in constant TLV experiments are shown in Table 5.3 (a and b). In terms of H_2S removal, an average RE of 83.5±2.0% at a LR of 283.8 g S-H_2S m^{-3} h^{-1}, corresponding to a maximum EC (EC_{max}) of 237.0±2.7 g S-H_2S m^{-3} h^{-1}, was reached.

Lower EC_{max} of 140-150 g S-H_2S m^{-3} h^{-1} have been reported in analogous experiments performed in a BTF operated in up-flow, counter-current mode under neutral conditions (Fortuny et al., 2008; Montebello et al., 2010) using a structured polypropylene HD Q-PAC 4x4 mm grid with a specific surface area of 433 m^2 m^{-3}. Both reactor performances are comparable since operational conditions, design parameters and tests performed were similar.

A better performance was achieved in the present work for the BTF in co-current flow using Pall rings, a packing material with a lower specific surface area. Such result is consistent with previous works that report that the specific surface area of the packing

material is not a critical design parameter in biogas desulfurization (Bonilla-Blancas et al., 2015). Such high H_2S ECs have not been reported in neutrophilic desulfurization, which points at an improvement related with the co-current operation.

Only comparable results have been reported in biogas desulfurization in counter-current flow at acid pH (Montebello et al., 2014). An EC_{max} of 223 g S-H_2S m^{-3} h^{-1} was obtained in a BTF with similar operational conditions using a randomly packed bed with metallic pall ring (483 m^2 m^{-3}). In the constant TLV experiment no manipulated variable was modified, thus the DOL/$[H_2S]_{removed}$ ratio decreased in each H_2S LR step as shown in Table 5.3.a to determine the S^0 and SO_4^{2-} production capacities (pCS^0 and $pCSO_4^{2-}$ rates, respectively) a sulfur mass balance was calculated as described in Chapter 4 (*see section 4.1.2*). In terms of product selectivity, such unfavorable decrease of the DOL/$[H_2S]_{removed}$ ratio lead to an incomplete H_2S oxidation to sulfate due to an insufficient oxygen supply to the BTF bed.

While almost no S^0 production capacity (pCS^0) was found at an H_2S LR of 56.3 g S-H_2S m^{-3} h^{-1} (Table 5.3.a), increasing H_2S LR lead to increasing S^0 production rates and, concomitantly, a larger selectivity of oxidation products towards S^0 rather than to sulfate. At a LR of 226.6 g S-H_2S m^{-3} h^{-1} the sulfate production capacity was 102.8 g S m^{-3} h^{-1} while in previous works under counter-current flow were 12.2 and 79.8 g S m^{-3} h^{-1}, thus demonstrating the impact of the flow pattern when a decreasing DOL/$[H_2S]_{removed}$ ratio was applied.

Table 5.3.a. BTF performance results during biotic experiments under constant and variable TLV

Assay	**$[H_2S]$ LR** *($g\ S\text{-}H_2S\ m^{-3}\ h^{-1}$)*	**RE** *(%)*	**$[H_2S]$ EC** *($g\ S\text{-}H_2S\ m^{-3}\ h^{-1}$)*	**DOL $[H_2S]_{removed}^{-1}$** *($g\ O_2\text{-}\ g^{-1}\ S$)*	**$pCSO_4^{2-}$** *($g\ S\ m^{-3}\ h^{-1}$)*	**pCS^0** *($g\ S\ m^{-3}\ h^{-1}$)*	**$S^0/S\text{-}H_2S_{removed}$ (%)** *($g\ S^0\ g^{-1}\ S\text{-}H_2S_{RE}$)*	**$S\text{-}SO_4^{2-}/S\text{-}H_2S_{in}$ (%)** *($g\ S\text{-}SO_4^{2-}\ g^{-1}\ S\text{-}H_2S$ in)*
Constant TLV Constant AFR	56.3	100	56.3	0.39	55.7	0.6	1.00	99.0
	112.9	100	112.9	0.20	76.4	36.4	32.3	69.6
	169.6	97.6	165.6	0.12	93.5	69.5	42.5	56.9
	226.6	90.6	205.2	0.06	102.8	101.9	49.7	47.1
	283.8	83.5	237	0.02	82.5	148.5	64.7	30.8
	0 (initial rate)	-	-	-	133.2	-133.2	-	-
	0 (average rate)	-	-	-	67	-67	-	-
Variable TLV Constant AFR	56.31	100	56.3	0.36	56.4	-0.5	0	100.0
	112.9	100	112.9	0.32	84.2	28.0	23	78.7
	169.6	98.7	167.3	0.31	102.5	63.7	38.6	62.4
	226.6	95.3	215.3	0.24	117.8	105.8	45.5	54.9
	283.8	92.7	262.7	0.08	115.9	145.1	55.7	43
	0 (initial rate)	-	-	-	105.8	-105.8	-	-
	0 (average rate)	-	-	-	47.5	-47.5	-	-

Table 5.3.b. BTF performance results during biotic experiments under variable AFR.

Assay	**$[H_2S]$ LR**	**RE**	**$[H_2S]$ EC**	**DOL $[H_2S]_{removed}^{-1}$**	**$pCSO_4^{2-}$**	**pCS^0**	**$S^0/S\text{-}H_2S_{removed}$ (%)**	**$S\text{-}SO_4^{2-}/S\text{-}H_2S_{in}$ (%)**
	(g $S\text{-}H_2S$ m^{-3} h^{-1})	*(%)*	*(g $S\text{-}H_2S$ m^{-3} h^{-1})*	*(g O_2- g^{-1} S)*	*(g S m^{-3} h^{-1})*	*(g S m^{-3} h^{-1})*	*(g S^0 g^{-1} $S\text{-}H_2S_{RE}$)*	*(g $S\text{-}SO_4^{2-}$ g^{-1} $S\text{-}H_2S$ in)*
Constant TLV Variable AFR	56.3	100	56.3	0.29	60.1	-3.8	9.3	103.8
	112.9	98.2	110.9	0.18	84.0	26,6	13.9	74.4
	169.6	90.1	152.9	0.16	99.0	52.7	22.4	58.4
	226.6	83.7	189.7	0.13	110.1	77.3	28.9	48.6
	283.8	80.8	229.3	0.10	123.9	102.4	33.7	43.7
	0 (initial rate)	-	-		68.9	-68.9	-	-
	0 (average rate)	-	-		39.6	-39.6	-	-

It is worth mentioning that total dissolved sulfur (TDS) did not accumulate in the reactor since ORP during constant TLV experiment ranged from 200 mV to -200 mV (Montebello et al., 2010). Consequently, no biological limitation occurred since the total H_2S transferred to the liquid phase was then transferred to the biofilm to be consumed by the bacterial consortia. The fact that pCS^0 increased through the constant TLV experiment was clearly due to an oxygen gas-liquid mass transfer limitation.

5.3.4. Effect of Air flow rate regulation on H_2S removal in co-current flow pattern

At a first sight, results obtained due to AFR regulation (table 5.3b), indicate that it's a suitable variable in order to reduce elemental sulfur production in BTF. However, this results involve a considerable biogas dilution, as showed in table 5.2, since in order to maintain constant the O_2/H_2S volumetric ratio at 42.2 % v v^{-1} , biogas dilution passed from a 28.2 % to a 66 %. This means that if a biogas stream with an initial methane composition of a 60 % was treated, this composition would be reduced from 43% down to 20% due to aeration increase during the AFR experiment. Although that in abiotic conditions it was already observed that SORT was poorly improved, as showed in table 5.2 and also in table 5.3 were the DOL and the DOL $[H_2S]_{removed}^{-1}$ for the variable AFR experiment are presented, respectively. Trends of these variables are similar to those obtained for SOTR for abiotic tests A1 to A2 when AFR was varied in GFR tests.

A maximum DOL of 0.13 (g O_2- g^{-1} S) was obtained for AFR regulation, which means that increasing AFR did not improve the DOL significantly because during constant TLV and variable TLV experiments maximum DOL of 0.08 g O_2 h^{-1} and 0.17 g O_2 h^{-1} were achieved, respectively. When AFR was increased in the aeration column, the contact time between the gas and the liquid phase was reduced as well as gas-liquid oxygen mass transfer. In this sense, increasing AFR does not result in an efficient strategy in order to improve gas-liquid mass transfer in the aeration column to obtain higher DOL to finally achieve improved $pCSO_4^{2-}$ rates.

Aeration is needed in BTF in order to provide the oxygen present in air, however main control strategies for optimizing the process cannot be based in AFR regulation in order to improve oxygen transfer and therefore achieve complete H_2S oxidation. Strategies based on TLV regulation offers also significant improvement on H_2S gas

removal and also into obtaining more sulfur oxidized species. Therefore efforts should be directed into understanding the effect of TLV regulation.

5.3.5. Effect of TLV in oxygen transport and biotrickling filter performance

Unclear conclusions are reported in literature about the effect of TLV in BTFs. In a BTF operated at low EBRT for removal of low loads of H_2S, Jin et al. (Jin et al., 2005) reported that TLVs in the range between 0.6 m h^{-1} and 2.7 m h^{-1} the EC_{max} was negatively affected due to an increase of the resistance between gas phase and liquid/biofilm phase as a result of an increment of the thickness of the liquid phase on the biofilm. Contrarily, Fortuny et al. (Fortuny et al., 2011) found a net increase of sulfate production in the performance of a BTF for the removal of high loads of H_2S in a TLV range of 0.5 m h^{-1} to 19 m h^{-1}. According to Kim and Deshusses et al. (Kim and Deshusses, 2008), mass transfer coefficients may have decreased because the system approached the flooding conditions in the case of the low-loaded BTF, while in the highly-loaded BTF performance was positively favored by the TLV increment due to the increment of the water distribution along the BTF bed and, therefore, in the wettability of the biofilm and to an increase of the solids flushing (principally S^0) amongst others. Thus, analysis of the TLV influence deserves special attention if used for control purposes to determine its range of application and impact on system performance. In the present work the influence of TLV in the BTF performance was assessed during a variable TLV experiment, in which TLV was increased from 4.2 m h^{-1} to 18.9 m h^{-1}, for the first three LR increments from 56.3 g S-H_2S m^{-3} h^{-1} to 169.6 g S-H_2S m^{-3} h^{-1} and then maintained at 18.9 m h^{-1} for the last two increments as shown in Table 5.3.a.

Results in Table 5.3.a show that, compared to the results obtained in the constant TLV experiment, a sulfate production capacity ($pCSO_4^{2-}$) between 9.6% and 14.6% larger was attained in the variable TLV experiment along the first four LR increments, while a 40.5% increase in the $pCSO_4^{2-}$ was found for the last LR increment even when the TLV was maintained at 18.9 m h^{-1} (Table 5.3.a.). Except for the last load increase, the $DOL/[H_2S]_{removed}$ ratio was maintained at above 0.24 g O_2 g^{-1} S-$H_2S_{removed}$ along the variable TLV experiment, resulting in a higher sulfate selectivity, which ranged from 100% to 43% (Table 5.3.a). A 12.2% increase in the sulfate selectivity was found at the higher LR tested (283.8 g S-H_2S m^{-3} h^{-1}). Also, the H_2S EC and RE improved along the variable TLV experiment (Figure 5.4a), particularly during the higher LR tested.

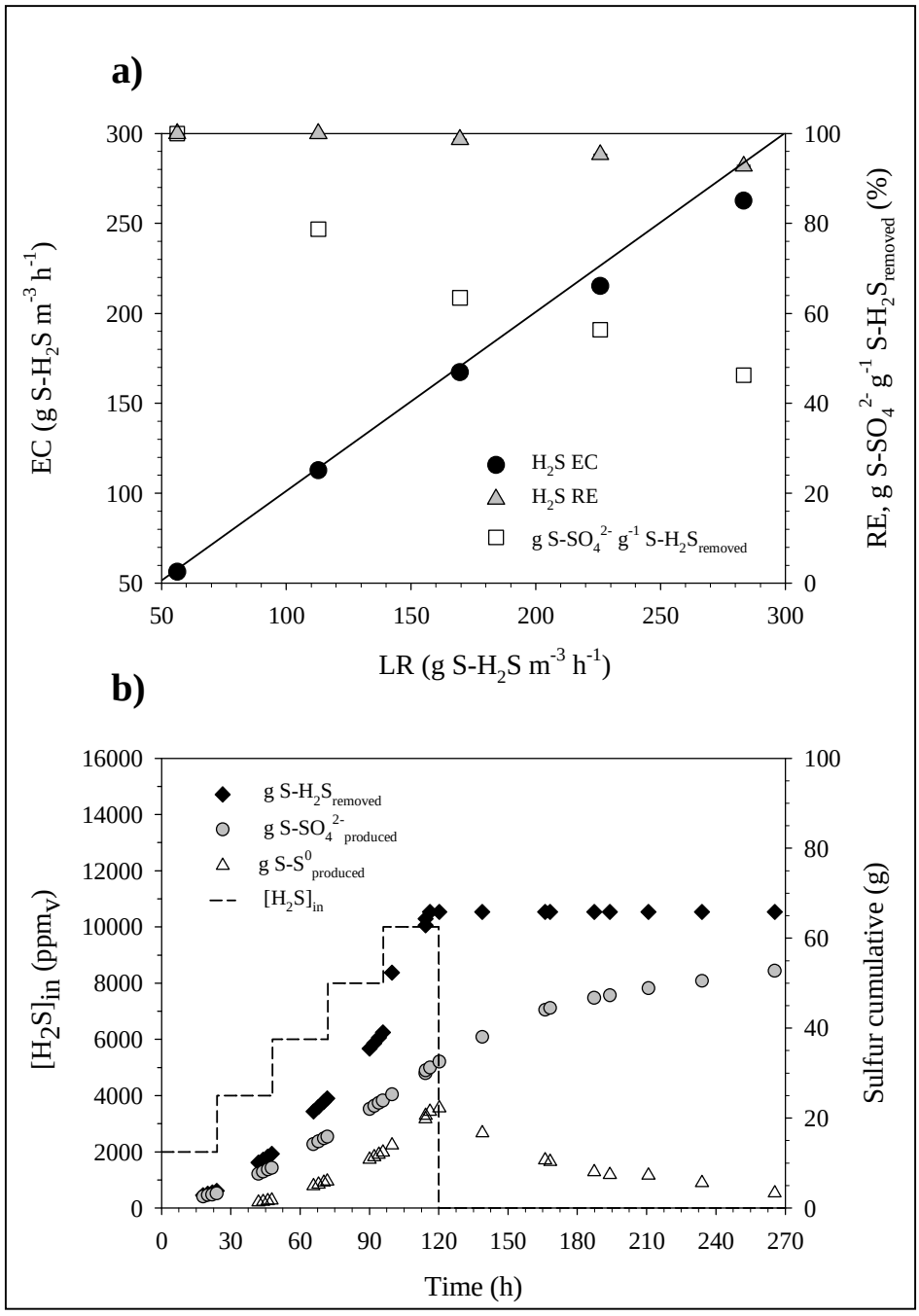

Figure 5.4. (a) Elimination capacity, removal efficiency and sulfate selectivity in front of H_2S loading rate and (b) Sulfur mass balance during the variable TLV experiment.

A higher EC_{max} of 262.7±1.5 g S-H_2S m^{-3} h^{-1} and an average RE of 92.7±0.2% were obtained during variable TLV experiment. Concerning to reactor hydrodynamics, no flooding conditions were observed since gas phase and liquid phase flowed co-currently during variable TLV experiment. Similar observations were also obtained by other authors from a co-current BTF for TCE removal (Popat and Deshusses, 2010). ORP

profiles from 150 mV to -100 mV in the variable TLV experiment also indicated that TDS did not accumulated in the liquid phase. Oxygen and sulfur mass balances were useful to quantify the ratio between the H_2S elimination capacity (EC_{H2S}) and the O_2 consumption capacity (CC_{O2}) (*see section 4.1.2 Chapter 4 for further detail on mass balances calculations*). Thiosulfate was measured and considered in the equations in order to close sulfur mass balances, however concentrations measured were below detection limit in all samples. Oppositely to most works in which the system is characterized as a function of the O_2 supplied (Rodriguez et al., 2014, 2012), the EC_{H2S}/CC_{O2} ratio provides useful information to understand the profitability of the system in O_2 usage to remove H_2S and to further visualize the influence of TLV in process stoichiometry.

Results during constant TLV and variable TLV experiments are shown in Figure 5.5 (a) and (b), respectively. Results show that the CC_{O2} progressively increased in all LR step changes in the variable TLV (Figure 5.5b). A plateau was reached in the case of the constant TLV experiment (Figure 5.5a). Such behavior leads to the reduced sulfate production rate ($pCSO_4^{2-}$) in the last step change, which was markedly lower in the case of the constant TLV experiment. Except for the last step change, similar CC_{O2} were calculated in both experiments, however, a lower EC_{H2S}/CC_{O2} ratio and a higher $pCSO_4^{2-}$ was calculated in the variable TLV experiment indicating that the same amount of O_2 transferred was used in a more efficient way to increase sulfate selectivity, i.e. to produce sulfate instead of elemental sulfur.

Such positive effect of TLV modulation, which improved oxygen distribution along BTF bed, allowed increasing oxygen profitability without the necessity of increasing oxygen supply, which is the most common control action in industrial BTFs (Chaiprapat et al., 2015). Interestingly, even in the case of complete sulfate production (LR of 56.3 g m^{-3} h^{-1}) the EC_{H2S}/CC_{O2} ratio were far from the theoretical ratio for sulfate production (0.5 g S/g O_2 according to Eqs. 5.1 and 5.2), indicating that probably other biological processes were consuming oxygen additionally to biological sulfide oxidation. Oxygen uptake processes such as nitrification and consumption of organic matter from endogenous biomass decay have been described to occur in desulfurizing BTFs operated at neutral pH (Gabriel and Deshusses, 2003b; Joseph S. Devinny, Marc A. Deshusses, 1998).

The total amount of oxygen supplied was the contribution of that supplied to the liquid phase in the aeration column plus the excess air from the aeration column that passed through the packed bed of the reactor. Thus, a variable named aeration column consumed oxygen ratio ($ACCR_{O2}$), which was defined as the ratio between the amount of oxygen of that supplied in the aeration column that was consumed with respect to the total amount of oxygen consumed. Fig. 5.5 shows that $ACCR_{O2}$ varied from 6% to 2% in the constant TLV experiment and from 6% to 19% in the variable TLV experiment. Such results stress the importance of the TLV regulation strategy in terms of directly incrementing the oxygen supply to lead to a greater overall BTF performance.

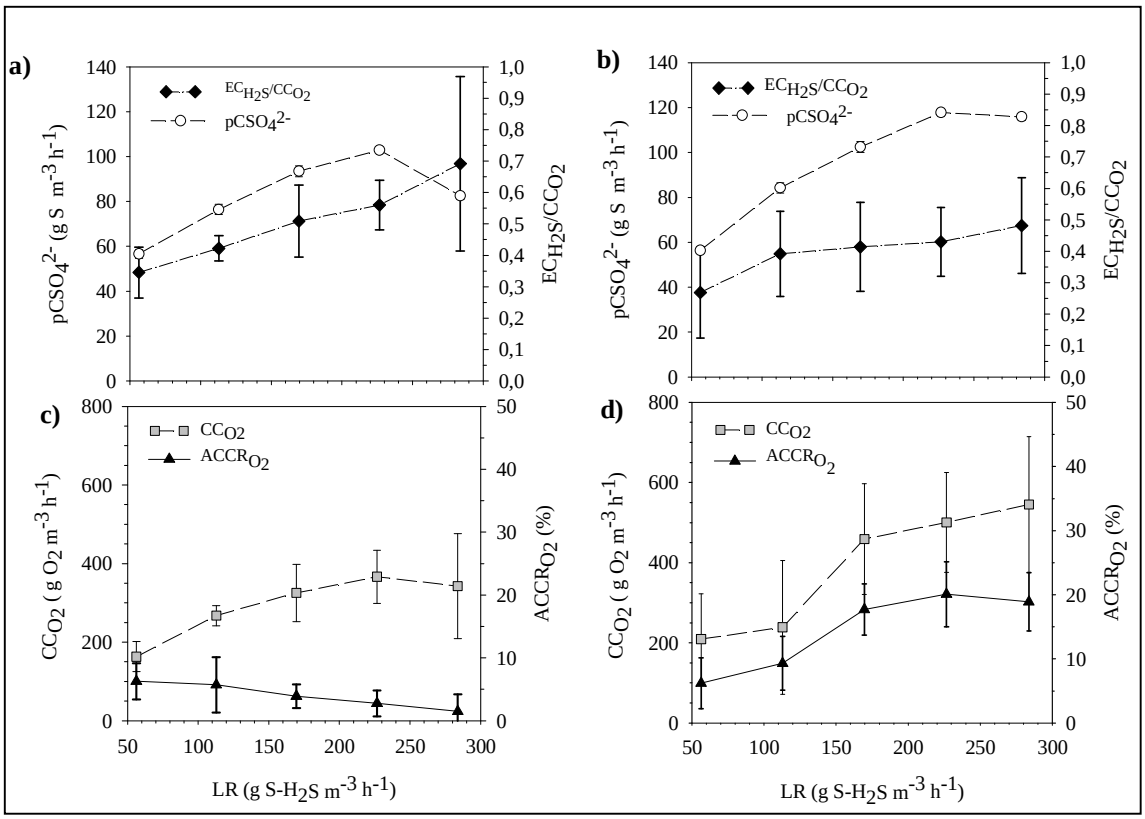

Figure 5.5. (a and b) Influence of TLV in the sulfate production rate ($pCSO_4^{2-}$) and in the EC_{H2S}/CC_{O2} ratio during constant TLV and Variable experiments. (c and d) Influence of TLV in the O_2 consumption capacity (CC_{O2}), and the aeration column consumed oxygen ratio ($ACCR_{O2}$), during constant TLV and variable TLV experiments.

Such performance improvement under a variable TLV regulation was attributed to an improved oxygen gas-liquid mass transfer both in the aeration column and in the packed bed coupled to a proper packing wettability and liquid distribution (Doan et al., 2008). Kraakman et al. (Kraakman et al., 2011) defined the wettability factor as the

percentage of wetted specific surface area of the total specific surface area of the packing material. Kim and Deshusses (Kim and Deshusses, 2008) also stated that not all the biofilm of the packing material is completely wetted by the trickling liquid. As a consequence of this, part of the pollutant is directly transferred from the gas phase to the biofilm phase, and another part of the pollutant is first transferred to the liquid phase, and then to the biofilm phase. Therefore mass transfer inside the BTF bed may be defined by different mechanisms as a function of TLV since wettability factor solely depends on TLV**.** Kim and Deshusses (Kim and Deshusses, 2008) also studied the effect of different TLV and gas velocities for different BTF packing, concluding that the k_La showed a strong linear relationship with TLV being the wettability factor and the liquid hold-up the governing factors for the effect of TLV.

In terms of solids, modulation of TLV can also help removing solids such as S^0 accumulated in the BTF bed. Total suspended solids (TSS) were measured in the liquid purge at each LR step. The ratio between the TSS and the total solids accumulated (TSA), which were calculated as the S^0 accumulated inside the BTF bed through mass balances, indicated the amount of TSS flushed due to TLV modulation with respect to the TSA. From the second LR step, the TSS/TSA ratio was 5.6 % (g TSS g^{-1} TSA), respectively, which indicated a low solids flushing at low TLVs. At a TLVs of 18.9 m h^{-1} the TSS/TSA ratio initially increased up to 16.3% (g TSS g^{-1} TSA) at a LR of 226.0 g S-H_2S m^{-3} h^{-1}. When the LR was further increased to 283.3 g S-H_2S m^{-3} h^{-1} keeping the TLVs at 18.9 m h^{-1} a TSS/TSA ratio of 7.1% (g TSS g^{-1} TSA) was obtained due to the pCS^0 increase, indicating that a beneficial effect was found in terms of S^0 flushing by increasing the TLV.

To further improve elemental sulfur removal and to verify in a co-current system the viability of the cleaning strategy pointed out in Jin et al. (Jin et al., 2005) for co-current systems, a H_2S starvation period of 7 days (Figure 5.4b) was decided after each constant TLV and variable TLV experiment at a TLV of 4.4 m h^{-1}, in which accumulated S^0 was rapidly oxidized to sulfate (Figure 5.4b). Table 5.3.a shows that, both the initial and average S^0 consumption rate (pCS^0) in the constant TLV experiment were higher than that of the variable TLV experiment, which correlated well with the larger amount of S^0 biologically available in the constant TLV experiment compared to that of the variable TLV test. Biomass in the BTF bed was able to consume 89.8% and 85.2% of the S^0 accumulated throughout each LR increase experiment showing that H_2S starvation

periods are a feasible strategy for S^0 removal for BTF maintenance also in BTF operated in co-current flow pattern.

5.3.6. H_2S removal and oxygen consumption along the packed bed height

During constant TLV and variable TLV experiments gas sampling was performed at different BTF heights to monitor H_2S and O_2 depletion. Results in Fig. 5.6 show the H_2S RE profile at three BTF heights (h=0.24 m, h=0.51 m and h=0.7 m) at each LR applied during constant TLV (Fig.5.6a) and variable TLV tests (Fig. 5.6b).

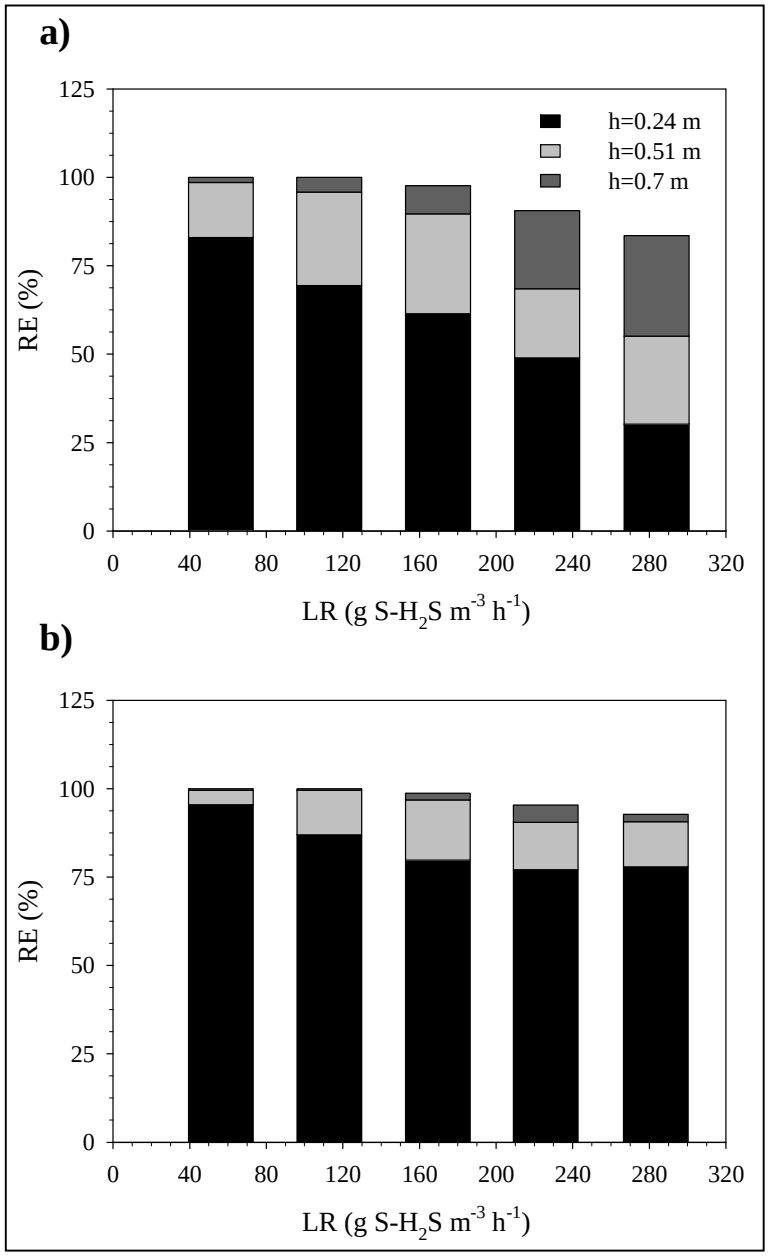

Figure 5.6. RE at different BTF heights as a function of the LR applied in the (a) Constant TLV and (b) Variable TLV experiments.

Fig. 5.6a shows that at the lowest LR of 56.3 g S-H_2S m^{-3} h^{-1} the first section was responsible for more than 83.0% of the EC of the BTF, while the second and third bed sections only contributed to 15.6% and 1.4%, respectively, of the total EC. A larger bioreactor capacity for pollutant removal in the sections closer to the pollutant inlet have been previously reported elsewhere due to a non-uniform biomass distribution along the packed bed (Lu et al., 2002). The RE of the second and third sections of the packed bed increased according to the LR increase up to 24.8 % and 28.4%, respectively, at the highest LR of 283.8 g S-H_2S m^{-3} h^{-1}, showing a significant increment in the biomass activity that demonstrates the capability of the bioreactor to adapt to progressive increasing loads.

When the TLV was increased in the variable TLV experiment (Fig.5.6), a relatively constant RE was obtained in the first section between the first (95.4%) and the last (77.9%) LR increment. A similar increase in the performance to that of the constant TLV experiment was found for the second section in the variable TLV experiment, while the third section slightly increased its capacity from 0.5% at a LR of 56.3 g S-H_2S m^{-3} h^{-1} to 2.1% at the highest LR applied (283.8 g S-H_2S m^{-3} h^{-1}). Results indicate that TLV regulation clearly improved the treatment capability of the first and second sections of the BTF by increasing the supply of DO at a TLV of 18.9 m h^{-1} during the last two LR increments. TLV experiments.

Since the LR applied to the section of the bed closer to the gas and liquid inlet ranged between a $LR_{section}$ of 164.2 g S-H_2S m^{-3} h^{-1} and 827.8 g S-H_2S m^{-3} h^{-1} results were compared in terms of the EC_{max} obtained during the constant TLV and the variable TLV experiment in each reactor section (Fig. 5.7). While the EC_{max} of BTF section 1 in the constant TLV experiment (Fig.5.7a) was in the range of EC_{max} found in previous works (Fortuny et al., 2011; Lu et al., 2002; Montebello et al., 2012), notorious differences were observed in EC_{max} of section 1 in the variable TLV Experiment (Fig.5.6b), in which a substantial improvement in the EC_{max} was observed due to TLV modulation obtaining EC_{max} up to 643.4 g S-H_2S m^{-3} h^{-1} and a RE of 77.88 ± 0.81 %. To the author's knowledge, no other previous works in BTFs have reported such high H_2S EC in BTFs for biogas desulfurization. Results showed that the co-current flow pattern coupled to the TLV regulation lead to a significant increase on the EC_{max} as well as to a larger DO penetration along the bed height thus improving the capabilities of the bioreactor for H_2S removal.

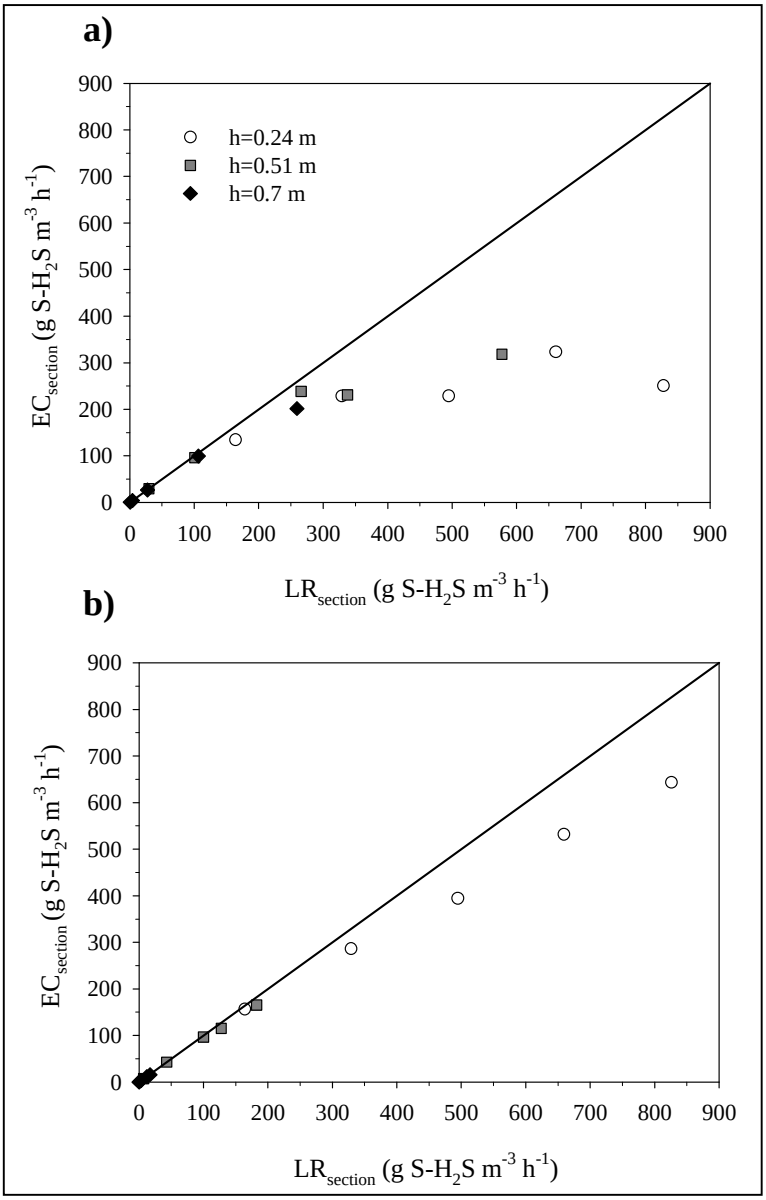

Figure 5.7. EC and LR per BTF at each section bed during (a) constant TLV and (b) variable TLV experiments.

5.4. CONCLUSIONS

The effect of TLV and air flowrate modulation in aerobic BTF for biogas desulfurization under different loading rate conditions was studied and the following conclusions were deduced from the work:

Irrespective of the flow configuration studied during abiotic experiments, a significant SOTR increase was observed when TLV was varied from 4.4 m h^{-1} to 18.9 m h^{-1} indicating that TLV is more recommended to be the manipulated variable over air supply for biotic experiments. Air supply increment demonstrate to be an inefficient strategy to increase SOTR and SOTE since, independently of the configuration studied, low SOTR and SOTE were obtained due to a significant reduction in the gas residence time inside oxygenation column, for experiments under abiotic conditions.

Efficient biogas desulfurization was effectively performed for a BTF packed with plastic pall rings at neutral pH and operated in co-current flow configuration. However when step-wise LR increment experiments were realized with a variable DOL/$[H_2S]_{removed}$ ratio the EC_{max} and sulfate selectivity obtained were significantly diminished due to oxygen lack.

Experiments when air flow rate was regulated during H_2S load periods allowed to conclude that the main performance parameters (RE, EC_{max} and sulfate selectivity) were barely improved respect the constant TLV experiment. Also, since EBRT is reduced during variable air flow rate experiments, results here obtained in terms of the main performance parameters were here greater than other BTF´s operated at low EBRT. Even variable air flow rate experiments shown to be a suitable variable in terms of effectivity, has the main drawback of biogas dilution. Therefore regulation of air flow rate cannot be the main strategy for improving biogas desulfurization under aerobic conditions, since it involves biogas dilution and its consequent loss of calorific power.

TLV influence over the main performance parameters (RE, EC_{max} and sulfate selectivity) was studied during variable H_2S load periods, indicating that TLV is a suitable variable to manipulate in order to regulate DOL to the BTF. Regulation of TLV along step-wise LR increments leads to a RE over 92. 7 % and an EC max of 262.7 g S-H_2S m^{-3} h^{-1}

Major finding obtained for the assessment of H_2S removal profile is that in the co-current configuration the major RE and oxygen consumption occurs in the first reactor bed and that during non-regulated experiments RE was distributed along the different BTF beds.

Although an airstone diffuser was used herein as oxygen mass transfer device to study the effect of TLV in the BTF performance, more effective devices such as jet-venturi devices are recommended in order to improve oxygen mass transfer to the liquid phase. However, results here obtained about performance improvement can be extrapolated to other BTFs no matter the aeration device used (airstone diffuser, membrane diffuser, jet venturi etc…). Certainly, using more efficient oxygen mass transport devices would produce different numerical results but similar conclusions in terms of profitability of the TLV regulation strategy.

CHAPTER 6

APPLICATION OF TITRIMETRY AS A MEASURED VARIABLE ON CONTROL LOOPS IN DISCONTINOUS AND CONTINOUS PROCESSES

6. APPLICATION OF TITRIMETRY AS A MEASURED VARIABLE ON CONTROL LOOPS IN DISCONTINOUS AND CONTINOUS PROCESSES

The main motivation of this chapter was to study the sensitivity of titrimetry when operational changes on discontinuous and continuous processes occurs. Firstly a methodology to quantify the different contributions affecting the protons equilibrium for both types of processes studied was developed, in order to obtain the proton production related only to biological activity a methodology to quantify the different contributions affecting the protons equilibrium for both types of processes studied was developed. Titrimetry was firstly applied into a discontinuous process, where the operational conditions and the pH affecting reactions are well defined, before applying the techniques to a more complex process such as biotrickling filter for aerobic biogas desulfurization. Then to study the application of titrimetry to a continuous processes, results obtained in the previous chapter during the constant TLV experiment were here used. Although the results obtained in this chapter showed that the proton production could be related qualitatively to operational changes, especially at high H_2S inlet loading rates, it has the inconvenient that liquid phase has a slower dynamic than gas phase dynamic. Therefore titrimetry application was not considered in future chapter of this thesis, even it can result helpful as a complementary variable for monitoring long term operations.

Abstract

In the present work titrimetry was coupled to a discontinuous and continuous process in order to evaluate it as a suitable measured variable on a control loop. Titrimetry, a well-established technique in the field of wastewater treatment is used in this chapter to relate the proton production and the proton production rate to the biologic activity of (a) an aerobic desulfurizing BTF (b) and respirometric tests used for kinetic parameter and the stoichiometry determination of a sulfide-oxidizing nitrate-reducing microbial population. The different contributions to the titration rate in each system have been identified and quantified. In one hand, biological proton production and proton production rate has been related to biological activity of sulfide oxidation by S-oxidizing biomass in a BTFunder variable H_2S loading rate due to concentration variations. Results indicate that titrimetry allows only to relate qualitatively operational changes and biological activity, especially at higher loading rate conditions than 168.9 g H_2S m^{-3} h^{-1}. On the other hand, the CO_2 global mass transfer coefficient for CO_2 stripping process occurring during anoxic respirometric tests was firstly characterized. Afterwards titrimetry and respirometric profiles were coupled to allowing the determination of the stoichiometric of two-step denitrification reaction.

A modified version of this chapter has been published as:

M. Mora, L.R. López, X. Gamisans, D. Gabriel, 2014b. Coupling respirometry and titrimetry for the characterization of the biological activity of a SO-NR consortium, *Chem. Eng. J.* 251, 111-115.

and presented as conference paper:

L.R. López, M. Mora, X. Gamisans, D. Gabriel, 2013. Application of repirometry and titrimetry under anoxic conditions for the characterization of carbon dioxide stripping and biological activity of a SO-NR consortium. 5th IWA specialized conference on Odours and Air Emissions Jointly with 10th Conference on Biofiltration for Air Pollution Control. San Francisco California, USA. March 2013.

6.1. INTRODUCTION

Common measured variables in control loops in biotrickling filters (BTFs) for biogas desulfurization under aerobic conditions are gas phase variables, such as H_2S or O_2 outlet gas concentrations (Rodriguez et al., 2014), since both present a faster dynamic than liquid phase variables such as S^0 and SO_4^{2-} production. However, controlling a multiphase process only through information related with a single phase can lead to long-term operational problems, since different dynamics occur in the rest of the phases that are not monitored. In addition, on-line monitoring of sulfate and elemental sulfur is of great difficulty. In this sense, monitoring of liquid phase variables such as titrimetric variables, in BTF for biogas desulfurization can provide complementary information related to pCS^0 and $pCSO_4^{2-}$ rates without the need of complex measurements of sulfur species. Titrimetry consists of the controlled addition of dilute acidic or alkaline solutions to maintain a constant pH in systems where a pH affecting reaction is taking place (Ficara et al. 2003). Titrimetry allows calculating two variables: the proton production linked to the process (HP) and the proton production rate (HPR) defined by Eq. 6.1 and Eq.6.2:

$$HP=C_{base}V_{base}-C_{acid}V_{acid} \quad (6.1)$$

$$HPR=\frac{HP}{dt} \quad (6.2)$$

Where V_{base} and V_{acid} stand for the accumulated base and acid dosage (mL), C_{base} and C_{acid} for the base and acid concentration (mM). HPR is calculated as the first derivate of HP with respect to time (Guisasola et al., 2007c). This technique can be applied to any biological or physico-chemical reactions affecting the proton concentration of the medium in continuous processes or in discontinuous processes. Regarding discontinuous processes, most studies have focused their efforts on studying the proton-producing or proton-consuming reactions in biological systems (Guisasola et al., 2007a). However, biological reactions are not the only ones that affect the pH in a bioreactor. Reactions involving carbon dioxide (CO_2), bicarbonate (HCO_3^-) and carbonate (CO_3^{-2}) equilibriums also result in pH variations. As an example, during the enhanced biological phosphorous removal (EBPR) process, CO_2 is continuously produced and continuously stripped (Guisasola et al., 2007c), and during the Anammox process, CO_2 is consumed and HCO_3^- produced (Yang et al., 2010). Particularly, when autotrophic biomass is studied through respirometric techniques, the

quantity of CO_2 present in the medium is crucial since lower biological activities are obtained under carbon limiting conditions (Torà et al., 2010). On the other hand, respirometry is defined as the measure and interpretation of the biological oxygen or nitrogen uptake rates (OUR and NUR, respectively) associated with the biological reactions under well-defined operating conditions (Gernaey et al., 2001). The application of tritrimetric and respirometric techniques separately to characterize sulfide-oxidizing suspended biomass (SOB) has already been reported for the study of reduced sulfur compounds oxidation in anoxic and aerobic conditions (Artiga et al., 2005; Munz et al., 2009).

Nevertheless, OUR and NUR occasionally do not provide enough information when different biological processes occur simultaneously during a respirometric test. In this situation, titrimetry is a relevant technique that can help to determine the stoichiometry and kinetics of the reactions implicated in the process since, coupled to respirometry, can be used to identify the rate of intermediates production (Munz et al. 2009). In addition, when nitrogen gas is sparged in the liquid phase, as occurs in respirometries under anoxic conditions, CO_2 stripping occurs, which affects the sensitivity of titrimetric data if high nitrogen gas or high CO_2 concentrations are used during respirometric tests (Guisasola et al., 2007a). For this reason the acquisition of titrimetric data is highly important when the characterization of biomass through respirometric tests with low biological activity or low concentration is performed. However, the application of titrimetric techniques for continuous complex processes such as biogas desulfurization in biotrickling filters has not been studied yet. During H_2S removal in BTFs under aerobic conditions, the pH of the biological suspension is mostly affected by the biological reactions that take place in the BTF but also by the different physical-chemical processes taking place due to the different dynamics in the equilibriums of the inorganic species in the BTF.

A preliminary assessment of titrimetric techniques application for biomass activity monitoring in H_2S removing reactors has been qualitatively assessed, clearly showing that it is possible to relate the volumes of added base or acid with an increase or decrease in the biological activity if other variables influencing the pH do not change or if they change in a known pattern (Fortuny et al., 2011). However, there is a literature lack about the application of titrimetry to biological processes under continuous conditions, specifically for BTF for biogas desulfurization under aerobic conditions.

The main challenge of the application of this technique under real scale application is to have a proper characterization of the main inlets to the BTF, since many acid or basic inorganic species can be fed through the make-up water line. Another challenge related to the application of titrimetry to BTF for biogas desulfurization is the difference between liquid and gas phase dynamics, since as was explained in chapter 4 both phases haves a different residence time. EBRT is of the order of seconds and HRT is in the order of hours and sometimes of days, which implies that changes that occur in the gas phase will be detected in the liquid phase with a certain time delay. Consider this two facts is key at the moment of developing a suitable methodology to use titrimetry as measured variable on a control loop.

The first aim of this study is (a) to use titrimetric techniques to study the representativeness of the information behind the biological HP/HPR of an aerobic desulfurizing biotrickling filter, during different operating conditions, towards the possible use of HP or HPR as a measured variable in the optimization and control of desulfurizing biotrickling filters and the second aim is (b) the application of titrimetry to model the CO_2 stripping that occurs during respirometric tests in order to relate the biological HP with the biological activity, stoichiometry and kinetics of the reactions resulting from the RSC biodegradation by a sulfide-oxidizing microbial population,

6.2. MATERIALS AND METHODS

6.2.1. Biological HP determination in BTF for biogas desulfurization under aerobic conditions

In order to characterize the biological proton production during biological biogas desulfurization in BTF under aerobic conditions, all the reactions that affect the pH of the suspension must be quantified. In the case of H_2S removing biotrickling filters under aerobic conditions, the subprocesses that contribute to proton production (or consumption) that will be studied regardless of the biological H_2S degradation are: i) H_2S deprotonation, ii) Nutrient supply as Mineral Medium (MM) dosage, iii) Inorganic carbon (IC) as $NaHCO_3$ dosage. In order to calculate the biological HP of the desulfurization process, the proton production or consumption of each contribution must be known. The biological HP can be calculated with Eq. 6.3 and the HP of each contribution as is described in Eq. 6.4:

$$HP_{biological}=HP_{observed}-HP_{contributions} \quad (6.3)$$

$$HP_{contributions}=HP_{H_2S}+HP_{NaHCO_3}+HP_{MM} \quad (6.4)$$

Where the HP with the sub-indexes H_2S, $NaHCO_3$, MM and $CO_{2\ stripping}$, refers to the contribution of H_2S deprotonation, $NaHCO_3$ dosage and MM dosage to the HP observed, respectively. The methodology detailed in Marcelino et al. (Marcelino et al., 2009) is applied to determine the numerical HP value of each specie at the operating pH. For this the concentration of each species on the equilibrium at the operating pH must be known. The titrimetric effect of H_2S deprotonation can be calculated considering H_2S equilibriums as described in the following equations (Eq. 6.5-6.7):

$$H_2S_{(g)} \xleftrightarrow{He} H_2S_{(aq)} \quad (6.5)$$

$$H_2S_{(aq)} \xleftrightarrow{pK_{a1}} HS^-_{(aq)} + H^+ \quad (6.6)$$

$$HS^-_{(aq)} \xleftrightarrow{pK_{a2}} S^{2-}_{(aq)} + H^+ \quad (6.7)$$

Eq. (6.5) indicates that H_2S absorption from the gas to the liquid phase is related with the Henry coefficient and has no titrimetric effect, while the two deprotonations of the H_2S depend on the logarithmic measurements of the acid dissociation constants (pKa_{S1}=7 and pKa_{S2}=13.9 for pure water at 25 ºC) (Steudel and Eckert, 2004) are described by Eq. 6.6 and Eq. 6.7, respectively. The titrimetric effect due to the H_2S deprotonation is given by the following expression (Eq. 6.8):

$$HP_{H_2S}=[H_2S]_{removed}\cdot\left(f_{HS^-}+2\cdot f_{S^{2-}}\right) \quad (6.8)$$

Where $[H_2S]_{removal}$ is the total amount of H_2S removed from the gas phase in (mol S-H_2S). f_{HS^-} and $f_{S^{2-}}$ are the sulfide and sulfur fractions at the equilibrium, represented by Eq. 6.9 and Eq. 6.10 respectively:

$$f_{HS^-} = \frac{10^{pKa_{S1}-pH}}{10^{pKa_{S2}-pH} + 10^{pKa_{S1}+pKa_{S2}-2pH} + 1} \quad (6.9)$$

$$f_{S^{2-}} = \frac{1}{10^{pKa_{S2}-pH} + 10^{pKa_{S1}+pKa_{S2}-2pH} + 1} \quad (6.10)$$

Titrimetric effect of carbon species equilibriums must be also considered, since $NaHCO_3$ is dosed to the BTF in order to provide an inorganic carbon source for SOB which are autotrophic microorganisms. The following expressions describe equilibriums related to $NaHCO_3$ dosage (Eq. 6.11 to Eq. 6.12):

$$CO_{2(g)} + H_2O_{(aq)} \overset{He}{\longleftrightarrow} CO_{2(aq)} + H_2O_{(aq)} \overset{pk_{C1}}{\longleftrightarrow} H^+ + HCO^-_{3(aq)} \quad (6.11)$$

$$HCO^-_{3(aq)} \overset{pk_{C2}}{\longleftrightarrow} CO^{2-}_{3(aq)} + H^+ \quad (6.12)$$

Where pKc_1=6.4 and pKc_2=10.9 for water at 25 ºC (Perry et al., 1997). Depending on the pH of operation, $NaHCO_3$ dosage can lead to medium basification due to CO_2 production (Eq. 6.11) or to medium acidification due to carbonate production (Eq. 6.12). If afterwards CO_2 is produced, CO_2 is stripped from the liquid phase to the gas phase, and this will lead to extra basification of the medium due to an equilibrium displacement to CO_2 production. The titrimetric effect due to the carbon equilibrium species is given by the following expression (Eq. 6.13):

$$HP_{NaHCO_3} = [TIC]_{consumed} \cdot \left(f_{CO_3^{2-}} - f_{CO_2} \right) \quad (6.13)$$

Where $[TIC]_{consumed}$ refers to the total amount of TIC consumed in (mol C) and is determined by Eq. 6.14. $f_{CO_3^{2-}}$ and f_{CO_2} are the carbonate and CO_2 fractions in the equilibrium represented by Eq. 6.15 and Eq.6.16 respectively:

$$[TIC]_{consumed}=(C\text{-}NaHCO_3)_{dosed}-(C\text{-}NaHCO_3)_{L,out}-(C\text{-}CO_2)_{G,out} \quad (6.14)$$

$$f_{CO_3^{2-}}=\frac{10^{pKa_{c2}-pH}}{10^{pKa_{c2}-pH}+10^{pKa_{c1}+pKa_{c2}-2pH}+1} \quad (6.15)$$

$$f_{CO_2}=\frac{10^{pKa_{c1}-pH}}{10^{pKa_{c2}-pH}+10^{pKa_{c1}+pKa_{c2}-2pH}+1} \quad (6.16)$$

Where $(C-NaHCO_3)_{dosed}$ is the inorganic carbon dosed as bicarbonate in (mol C-$NaCO_3$), $(C-NaHCO_3)_{L,out}$ is the inorganic carbon as bicarbonate in the liquid purge in (mol C-$NaCO_3$) and $(C\text{-}CO_2)_{G,out}$ refers to the CO_2 present in the gas outlet and refers to the total amount of TIC consumed in (mol C-CO_2). Finally, with respect to the species added in the MM (*see section 4.1.1.*) in order to supply nutrients to the biomass, the only species that produces or consumes protons at the operating pH are the potassium hydrogen phosphate (K_2HPO_4), the potassium di-hydrogen phosphate (KH_2PO_4) and ammonia chloride (NH_4Cl). The following expressions describe equilibriums related to species present in the MM with titrimetric effect (Eq. 6.17 to Eq. 6.20)

$$H_3PO_4 \xleftrightarrow{pk_{m1}} H_2PO_4^- + H^+ \quad (6.17)$$

$$H_2PO_4 \xleftrightarrow{pk_{m2}} HPO_4^{2-} + H^+ \quad (6.18)$$

$$HPO_4^{2-} \xleftrightarrow{pk_{m3}} PO_4^{3-} + H^+ \quad (6.19)$$

$$NH_4^+ \xleftrightarrow{pk_{n1}} NH_3 + H^+ \quad (6.20)$$

Where pKm_1=2.2 and pKm_2=7.2 for the K_2HPO_4 and pkn_1=9.24 for the NH_3 for pure water at 25 ºC (Perry et al., 1997). The titrimetric effect due to the ionic species present in the MM is given by the following expressions (Eq. 6.21) :

$$HP_{MM}=[K_2HPO_4]_{dossed}\cdot\left(-2\cdot f_{H_3PO_4}-f_{H_3PO_4^-}+f_{PO_4^{3-}}\right)+[KH_2PO_4]_{dossed}\cdot\left(-f_{H_3PO_4}-f_{HPO_4^-}+f_{PO_4^{3-}}\right)$$
$$+[NH_4Cl]_{dossed}\cdot\left(f_{NH_3}\right) \quad (6.21)$$

Where $[K_2HPO_4]_{dossed}$, $[KH_2PO_4]_{dossed}$, and $[NH_4Cl]_{dossed}$ refers to the total amount of K_2HPO_4, KH_2PO_4 and NH_4Cl dosed in the MM in (mol P) and (mol N), respectively. $f_{H_3PO_4}$, $f_{H_3PO_4^-}$, $f_{PO_4^{3-}}$, $f_{HPO_4^-}$and f_{NH_3} are the phosphorous species fractions and nitrogen species fraction respectively represented by Eq.6.22 to Eq. 6.30 :

$$f_{H_3PO_4}=\frac{10^{pKa_{m2}-pH}+10^{pKa_{m1}+pKa_{m2}+pKa_{m3}-3pH}}{10^{pKa_{m3}-pH}+10^{pKa_{m2}+pKa_{m3}-2pH}+10^{pKa_{m1}+pKa_{m2}+pKa_{m3}-3pH}+1} \quad (6.22)$$

$$f_{H_2PO_4^-}=\frac{10^{pKa_{m2}+pKa_{m3}-2pH}}{10^{pKa_{m3}-pH}+10^{pKa_{m2}+pKa_{m3}-2pH}+10^{pKa_{m1}+pKa_{m2}+pKa_{m3}-3pH}+1} \quad (6.23)$$

$$f_{PO_4^{3-}}=\frac{1}{10^{pKa_{m3}-pH}+10^{pKa_{m2}+pKa_{m3}-2pH}+10^{pKa_{m1}+pKa_{m2}+pKa_{m3}-3pH}+1} \quad (6.24)$$

$$f_{PO_4^{3-}}=\frac{1}{10^{pKa_{m3}-pH}+10^{pKa_{m2}+pKa_{m3}-2pH}+10^{pKa_{m1}+pKa_{m2}+pKa_{m3}-3pH}+1} \quad (6.25)$$

$$f_{NH_3}=\frac{1}{1+10^{pKa_1-pH}} \quad (6.26)$$

Experimental conditions

Titrimetric data was obtained from a lab-scale BTF for biogas desulfurization under aerobic conditions (*see section 4.1.1. for further description of the setup*). Specifically,

titrimetric data was obtained from the constant TLV experiment according to table 6.2 (*See table 5.2 of chapter 5 for further detail*). The aims of such constant TLV experiment were the assessment of EC as well as sulfate selectivity when step-wise LR increments were performed. LR increments from 56.3 to 283.8 g S-H_2S m^{-3} h^{-1} were produced as a consequence of H_2S inlet concentration increase as showed in table 6.1.

Table 6.1. Experimental conditions of constant TLV experiment

Exp	**[H_2S]** *(ppm_v)*	**[H_2S] LR** *(g S-H_2S m^{-3} h^{-1})*	**O_2/H_2S** *(% v v^{-1})*	**TLV** *(m h^{-1})*	**DOL** *(g O_2 h^{-1})*	**Previous Operation** *(days)*
Constant TLV	2000	56.3	42.2	4.4	8.32E-02	114
	4000	112.9	21.0		7.39E-02	
	6000	169.6	14.0		5.86E-02	
	8000	226.6	10.5		2.99E-02	
	10000	283.8	8.4		1.39E-02	

Thus, the O_2/H_2S volumetric ratio was progressively reduced along the experiment as a consequence of H_2S increase at a constant airflow rate. H_2S LR changes performed during constant TLV experiment were maintained during 24 hours, in order to study the effect of changes in the gas phase over the liquid phase, and therefore be able to relate titrimetric data to LR changes. The total amounts of the different volumes of NaOH, HCL, MM and $NaHCO_3$ added to the BTF during the different experiments were needed to determine the HP of the contributions ($HP_{contributions}$). Acid and Base volumes were acquired and registered automatically by a software programmed in LabWindows in order to control the pH, and monitor other variables in the BTF such as DO, ORP from the liquid phase and H_2S, O_2 and CO_2 from the gas phase. MM and $NaHCO_3$ volumes were registered manually every 2 hours along the experiment.

The pH was controlled using an ON/OFF control rule between 6.5 (low set point, LSP) and 7 (high set point, HSP). Thus, if the pH of the liquid phase was lower than the LSP a basic solution was dosed to increase the pH up to the LSP value. Instead, if the pH was

higher than the HSP the control system dosed an acidic solution to decrease the pH down to the HSP value. From acid and base volumes dosed by the pH control system, the observed HP (HP_{obs}) was determined according to Eq. 6.1. Since the concentration of each species dosed to the BTF was previously known, the $HP_{contributions}$ were calculated according to Eq. 6.4 to finally determine the biological HP (HP_{bio}) from the HP_{obs} and $HP_{contributions}$ according to Eq. 6.3. The biologiccal HPR (HPR_{biol}) can be determined from the HP_{bio} according to equation 6.2, however the resulting HPR_{bio} must be treated in order to reduce the noise associate to the signal Therefore, two different methodologies were used to filter the signal.:(a) a running average to smooth the HPR signal using Sigma plot (11.0 version), namely methodology A. In order to determine HPR value through a running average, experimental data was divided in a total of 200 intervals with a sampling portion of 0.001.

(b) HPR was determined as the slope of a simple lineal regression using time interval of one hour was fixed as time interval to determine the HPR_{bio}, namely methodology B. Afterwards for both methodologies, average HPR_{bio} values were determined as the HPR_{bio} average of the last 4 hours of each H_2S concentration step. Later on, the methodology showing lowest standard deviation values on the average HPR_{bio} calculation, was selected in order to compare HPR_{bio} values with the most common operational parameters such as RE, EC, pCS^0 and $pCSO_4^{2-}$ rates were also studied.

6.2.2. Titrimetry application in a discontinuous process

In this work, titrimetry was coupled to the respirometric study of the two-step denitrification associated to thiosulfate oxidation with SO-NR oxidation (Mora et al., 2014a) in order to obtain more information about biological activity. Since respirometric tests were performed under anoxic conditions, OUR can not be measured and therefore a secondary measure is needed, being titrimetric variables (HP and HPR) suitable for biological processes on-line monitoring.

Carbon dioxide stripping tests under abiotic conditions

In order to determine the biological HP of respirometric tests of a SO-NR microbial population from the observed HP, it is necessary to quantify and model the CO_2 stripping that occurs during respirometric test. To properly model the CO_2 stripping the CO_2 global mass transfer coefficient $(K_L a_{CO_2})$must be assessed in abiotic tests (Mora et al. 2014c). The same respirometer set up (*See section 4.1.2*) used during the respirometric tests for the kinetic

parameter determination of a SO-NR microbial population (Mora et al., 2014a) was used here. Abiotic tests were carried out in a 20 mM buffer solution and at a gas flow rate of 20 ml min^{-1} in order to develop the stripping tests according to respirometric tests conditions described in Mora et al. (Mora et al., 2014a). Once the pH was stable after the buffer solution was added to the respirometer, anoxic conditions were achieved by sparging nitrogen in the liquid phase. Later, the nitrogen flow was switched to flow through the headspace of the respirometer. A known pulse of 70 g L^{-1} $NaHCO_3$ was added in order to monitor and analyze the CO_2 stripping.

Carbon dioxide stripping model development

A bibliographic model described elsewhere (Ficara et al., 2003) was chosen to describe the CO_2 stripping during respirometric tests. This model describes the response of the titration system to the production of protons, CO_2, $NaHCO_3$ and CO_3^{-2} due to any biological or physical-chemical reaction affecting the pH according to Eq. 6.27

$$sS \rightarrow P + bHCO_3^- + cCO_2 + dCO_3^{2-} + hH^+ \quad (6.27)$$

Where b, c, d and h are positive when the corresponding chemical species is produced or negative when it is consumed, meanwhile S is the substrate converted into product (P). The model integrates the mass balances and equilibrium equations of each species of the system. Eq. 6.28 corresponds to the HPR due to the physical-chemical or biological reactions taking place while Eq. 6.29 corresponds to the HPR due to the CO_2 unbalance.

$$r_t(1) = r_p \left[(b-h+2\cdot d) - (b+c+d) \cdot \left(\frac{10^{pH-pk_{C1}} \cdot \left(1+2\cdot 10^{pH-pk_{C2}}\right)}{\left(1+10^{pH-pk_{C1}} \cdot \left(10^{pH-pk_{C2}}\right)\right)} \right) \cdot e^{-\alpha \cdot t} \right] \quad (6.28)$$

$$r_t(2) = \alpha \cdot 10^{pH-pk_{C1}} \cdot \left(1+2\cdot 10^{pH-pk_{C2}}\right) \cdot \left([CO_2]_0 - [CO_2]_{eq}\right) \cdot e^{-\alpha \cdot t} \quad (6.29)$$

$$\alpha = \frac{K_L a}{\left(1+10^{pH-pk_{C1}} \cdot \left(10^{pH-pk_{C2}}\right)\right)} \quad (6.30)$$

Where $[CO_2]_{eq}$ is the CO_2 concentration at equilibrium with the initial gas phase composition defined by Henry's law. Dimensionless Henry's constant of 0.83 for CO_2 was used (Sanders, 1999). $[CO_2]_0$ is the concentration of CO_2 at time zero. pK_{c1} and pK_{c2} are the dissociation constants for the. α is a constant parameter, described by Eq. 6.30 and contains the parameter to be determined, the CO_2 global mass transfer coefficient ($K_La,_{CO2}$)

Carbon dioxide global mass transfer coefficient parameter determination

The methodology employed to determine the $K_L a_{CO_2}$ was based on the model described in the previous section and HP measurements. Later, HPR is determined by calculating the first derivative of HP as explained (Eq. 6.2). The proton production can be obtained integrating the HPR described by Eq. 6.29. Sampling of the liquid phase is not required in this methodology since the control software described in chapter 4 (*see section 4.1.1*) acquires continuously the volumes of acid and base added to maintain a constant pH. Therefore, the HP or HPR of the test can be calculated. Integration of Eq. 6.29 was performed with a routine with a variable step- Runge-Kutta method (ODE45) programmed in Matlab (R2011b) to obtain a model describing the HP. This function is used to optimize properly the experimental HP data using an optimization tool (fminsearch). Finally the corresponding $K_L a_{CO_2}$ is obtained as result of the optimization process.

Carbon dioxide stripping model validation

The validation of the model is the final step of the modeling process of the CO_2 stripping. To this aim, titrimetric data from respirometric tests of a SO-NR microbial population under anoxic conditions were used. Known pulses of thiosulfate, nitrate and nitrite were added in each of the periods of the test (Table 6.2). During the tests the system was continuously sampled to obtain the respirometric profiles from off-line analysis of all the species involved in the process. Estimation of nitrite, nitrate and thiosulfate uptake rates (NitUR, NUR and SUR respectively) and further the study of the biological reactions mechanisms were performed from the abovementioned profiles.

Table 6.2. Initial concentrations of nitrite, nitrate and thiosulfate for each period of the respirometric test

Period	**Time (min)**	**Process**	**Nitrite** *(mg N-NO_2^- L^{-1})*	**Nitrate** *(mg N-NO_3^- L^{-1})*	**Thiosulfate** *(mg S-$S_2O_3^{2-}$ L^{-1})*
I*	0 - 90	NitUR	20.8	0	330.0
II*	90 - 240	CO_2 Stripping	0	0	268.6
III*	240 - 380	NUR + NitUR	24.2	12.1	267.7

Further information of respirometric test conditions can be found in Mora et al. (Mora et al., 2014). Biological HP was assessed by subtracting the HP due to CO_2 stripping from the observed HP (Eq. 6.31):

$$HP_{biological}=HP_{observed}-HP_{stripping} \quad (6.31)$$

Where HP_{bio}, $HP_{observed}$ and $HP_{striping}$ are the biological HP, observed HP and the HP related to CO_2 stripping, respectively.

6.3. RESULTS AND DISCUSSION

6.3.1. Observed and Biological HPR for an aerobic desulfurizing biotrickling filter

During the constant TLV experiment, acid and base were dosed in order to maintain a constant pH (Fig.6.1.) Acid and base profiles obtained during constant TLV experiment were closely related to the H_2S LR increase since no regulation in the oxygen supply was applied, which helped to characterize the process and determine the biological activity limits under the conditions tested. During the first 24 hours, sulfate production was favored and almost no S^0 production capacity (pCS^0) was found at an H_2S LR of 56.3 g S-H_2S m^{-3} h^{-1} as is presented in Chapter 5 (*see Table 5.3a*). Since during constant TLV experiment the O_2/H_2S volumetric ratio is variable, H_2S LR increase lead to an increase in the pCS^0 production rate due to an insufficient oxygen supply to the BTF bed during H_2S concentration steps. At time 72h, the S^0 selectivity was close to 50 % and became the main oxidation product with a selectivity value of 64.7% at time 96h (*See Table 5.3a*).

Despite base was dosed along the first two H_2S LR step-wise increments, large base dose only occurred from the third H_2S LR step-wise increment until hour 89, when acid was dosed again until the end of the experiment. Titrimetric data such as $HP_{observed}$ and HP_{bio} results interesting when this change in the predominance of the main oxidation product takes place since clear changes in acid and base trend can be easily observed and related to process changes. The ON/OFF control rule, lead to periods where the system switched from the LSP and the HSP due to biological activity changes. If the pH lays in-between this range no base and acid dosage occurs. This situation is not favorable from a titrimetric point of view, since

no information is received during that period, leading to wrong interpretation and determination of the results. During the first 24 hours of the constant TLV experiment acid was mostly dosed, with a punctual base dosage, in order to compensate proton consumption reactions.

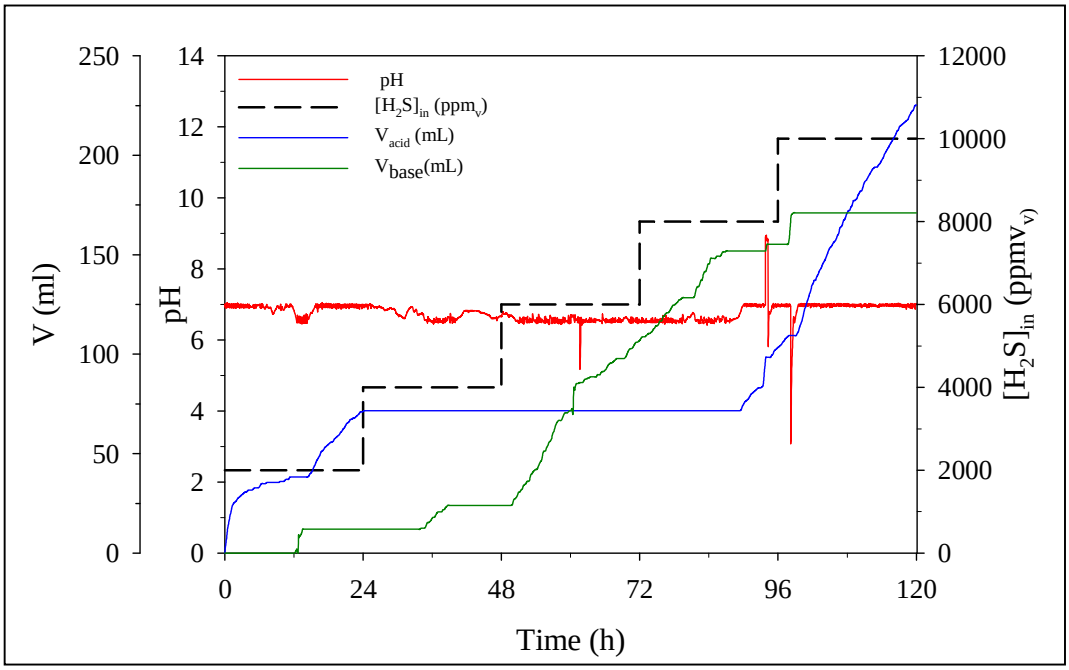

Figure 6.1. Raw titrimetric data during constant TLV experiment: acid dosage (blue solid line), base dosage (green solid line), H_2S inlet concentration (black dashed line) and pH (red solid line).

During the second step-wise H_2S concentration increase, bad quality of titrimetric data due to a pH switch between the LSP and the HPS from hour 24 until hour 34 and from hour 38 until hour 48 was found (Fig.6.1). Such data was not useful from a titrimetric point of view. Another type of pH control may result more useful, like a proportional integral (PI) controller in order to have a more accurate pH control and therefore titrimetric data. Raw titrimetric data must be transformed into titrimetric variables such as $HP_{observed}$ which is the result of the sum of $HP_{contribution}$ and HP_{bio} as is described in Eq. 6.2.

In order to discuss the HP_{obs} and HP_{bio} value (Fig. 6.2 a), $HP_{contribution}$ is also analyzed simultaneously in Fig. 6.2b. In Fig.6.2b the percentage of contribution to the $HP_{contribution}$ of each specie is presented. At low H_2S LR, biological proton production contribution activity

to the $HP_{observed}$ is very low, hence subprocesses related to proton consumption are predominant.

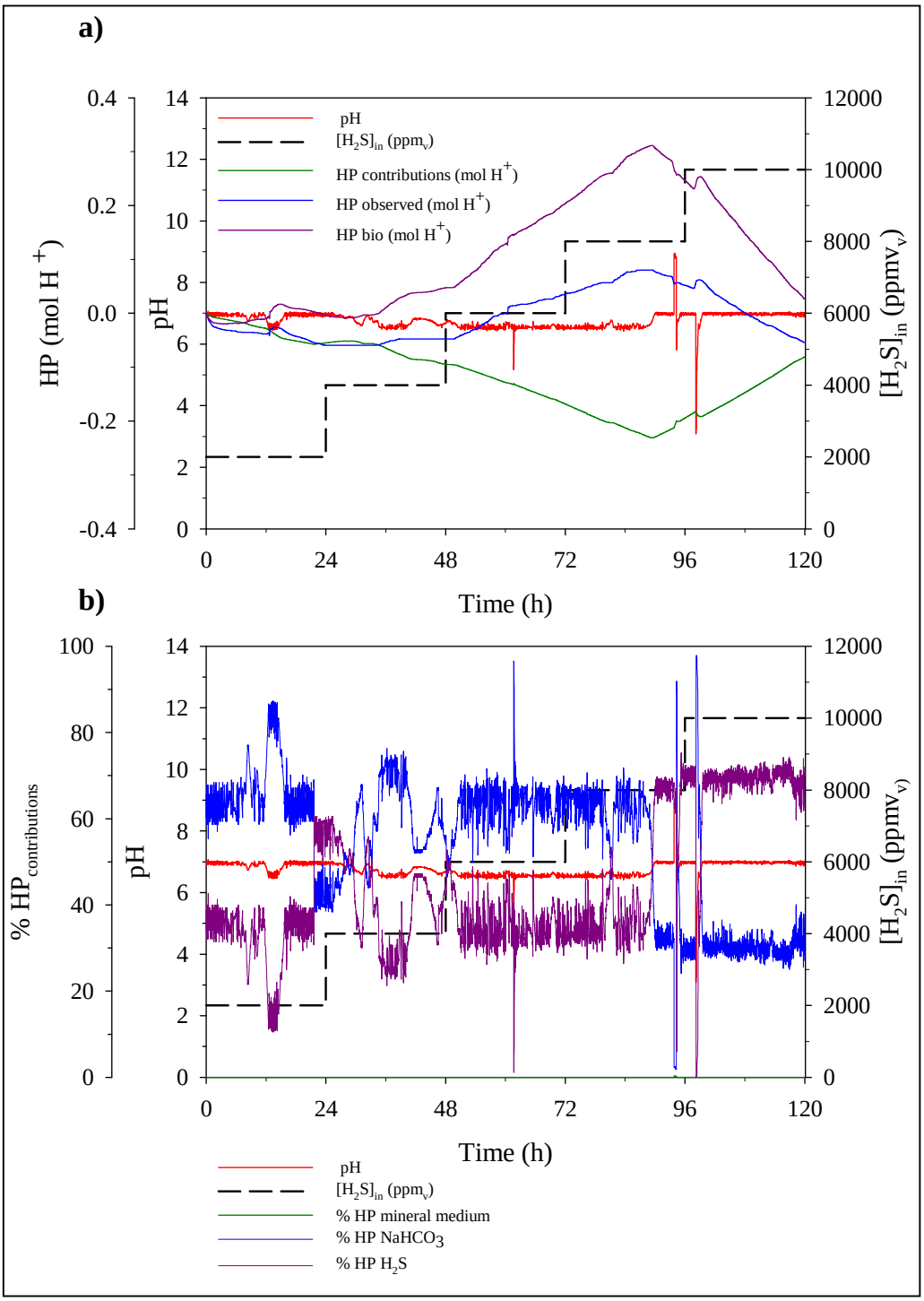

Figure 6.2. (a) Cumulative HP obtained for the constant TLV experiment. $HP_{observed}$ (blue solid line), $HP_{contributions}$ (green solid line), HP_{bio} (purple solid line), inlet H_2S concentration (black dashed line) and pH (red solid line) and (b) contribution percentage to the $HP_{contribution}$ of each specie is presented. MM percentage contribution (green solid line), $NaHCO_3$ percentage contribution (blue solid line), H_2S percentage contribution (purple solid line), inlet H_2S concentration (black dashed line) and pH (red solid line).

As shown in Fig. 6.2a, during the first 24 hours the main contributors to the $HP_{contributions}$ were H_2S and $NaHCO_3$ equilibriums, resulting in a negative $HP_{contributions}$ as result of predominance of CO_2 stripping which is a proton consuming process over H_2S dissociation, which resulted in positive HP. HP_{bio} became positive at the end of the first period (0-24 h), which means that proton production was the predominant process due to biological activity. This result was in coherence with sulfate selectivity for the constant TLV experiment, as showed in the next pages in Fig. 6.4b. Quality of titrimetric data during the second period (from hour 24 until hour 48) is not useful since pH was controlled between the LSP and the HSP band, and therefore no clear conclusions can be obtained about $HP_{observed}$ and $HP_{contributions}$ and operational conditions.

During the first two concentration steps tested, where the process is close to reference conditions, changes in the process cannot be clearly reflected on the HP_{bio} since other production/consumption of protons related to other sub processes is still masking HP_{bio}. It is not until the third concentration step change at hour 48 when biological activity increases, as reflected on the HP_{bio} magnitude. During the third concentration step the percentage of contribution of the different species changed dramatically. Base was dosed to a larger extent and the percentage of contribution of the different species to the $HP_{contributions}$ shows that H_2S was the predominant specie over $NaHCO_3$ contribution. However, a clear switch in the HP trend was found at time 89h.

Such behavior was mainly due to a reduction in the proton production related to biological activity. Such proton production decrease is in coherence with the pCS^0 rates obtained during the constant TLV experiment in which the S^0 selectivity increased from 1% (t=24 h) to 42.5% (t=72h). Such HP_{bio} decrease occurred since S^0 became the predominant end product over SO_4^{2-} production of H_2S oxidation (64.7% of S^0 selectivity), hence protons were mainly consumed resulting in a negative slope of the HP_{bio}. When this sudden changes of HP_{bio} trends occurs, it is also useful to analyze HPR in order to complement information provided by the HP. Fig. 6.3(a) shows the HPR_{bio} calculated along the constant TLV experiment. During the first H_2S LR stepwise increase, peaks in both HPR profiles are observed due to punctual base dosage.

Despite the noisy behavior, a positive HPR_{bio} with a slight trend to increase was observed along the first three H_2S steps. Clearly positive HPR_{bio} due to a positive HP_{bio} slope reflected that the process was mainly producing SO_4^{2-} over S^0. A positive HPR_{bio} does not

imply a positive or negative HP_{bio} but provides information about the process evolution, whether towards a proton producing or towards a proton consuming process. On Fig. 6.3 is presented the result of HPR_{bio} values obtained of applying Eq. 6.2 for HP_{bio} values.

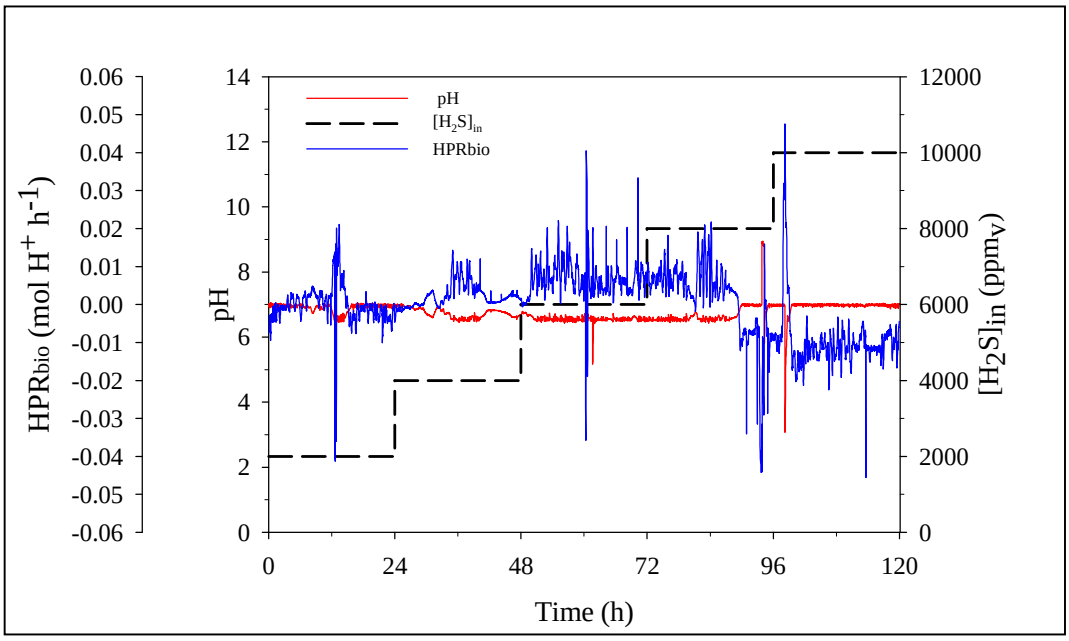

Figure 6.3. HPR_{bio} values for the constant TLV experiment. HPR_{bio} estimation according Eq. 6.2 (blue solid line), inlet H_2S concentration (black dashed line) and pH (red solid line).

From Fig. 6.3 it can be seen that HPR_{bio} signal must be treated in order to be able to relate with operational values. As it was mentioned above, a better type of pH controller would be more suitable than the used during TLV constant experiments. Contrarily to HP_{bio} that provides punctual information about biological activity, HPR_{bio} provides information about how biological activity is changing with the time in the BTF. In order to be able to find a clearer relation between operational changes and HPR_{bio}, the signal obtained (Fig 6.3) must be treated in order to reduce the noise associated to the signal.

HPR_{bio} obtained from applying methodology A and B are presented in Fig. 6.4 (a and b), respectively. From Fig. 6.4 (a) it can be observed a more smoothed HPR_{bio} signal after applying a running average method, although still some HPR_{bio} peaks, corresponding to noise on the pH signal and not to operational changes, are still observed. When HPR_{bio} is estimated as the slope of a linear regression using a time span of one hour (Fig. 6.4b), HPR_{bio} trend is slightly smoothed specially during the last two H_2S inlet concentration steps

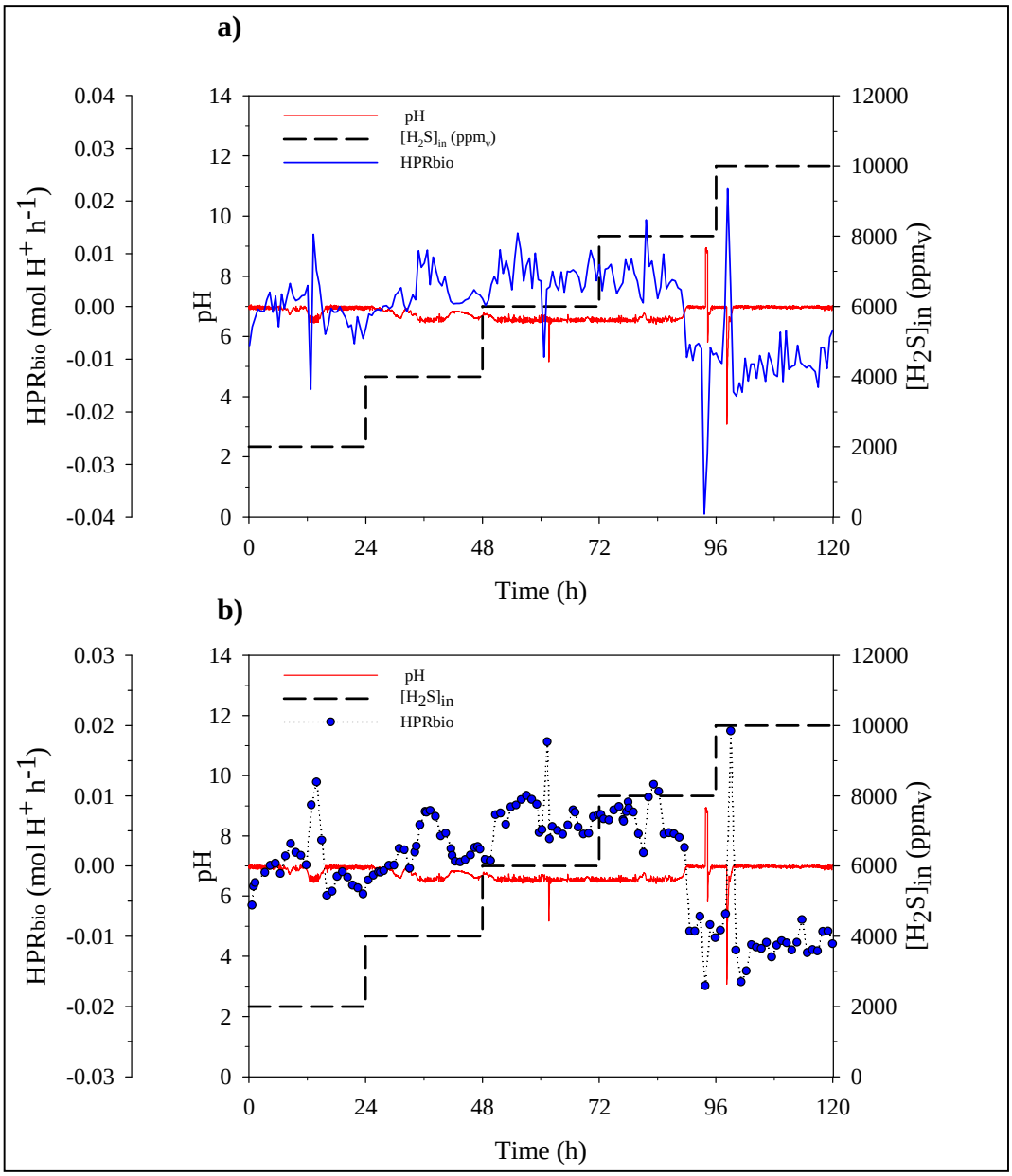

Figure 6.4. (a) HPR_{bio} values for the constant TLV experiment. Average HPR_{bio} estimation through a running average (blue solid line), inlet H_2S concentration (black dashed line) and pH (red solid line) and (b) Average HPR_{bio} estimation as linear regression slopes using 1 hour as time span (blue dots-black doted line), inlet H_2S concentration (black dashed line) and pH (red solid line)

. Since the peaks observed on HPR_{bio} signal for both methodologies are due to external noise non related to operational changes, this values are not considered at the moment of calculating HPR_{bio} averages. From Fig. 6.4 (a and b) a clearer trend than the obtained on Fig. 6.3 can be observed along H_2S inlet concentration steps. In order to have one representative value for the main operational parameters at each H_2S concentration value during constant TLV experiment, an average value for each operational parameter was estimated as the average of the parameters values during the last 4 hours at each step.

Therefore to have a proper comparison between the main operational parameters and HPR_{bio}, the average values of HPR_{bio} for the last 4 hours were also calculated for both methodologies and presented in Fig. 6.5a. Also the relative difference between both average HPR_{bio} values is presented. Along the first H_2S inlet concentration steps, the percentage of difference between both methodologies is below the 32% indicating that the methodology for estimating the average HPR_{bio} is not that determinant.

Significate differences are observed during the last H_2S inlet concentration step, indicating that at high H_2S LR where the biological contribution to the proton production has a bigger weight, the methodology used influence more in the result. Regarding the deviation of the HPR_{bio} obtained with each methodology, methodology A present higher error bars than methodology B, especially during the last three H_2S concentration steps.

Methodology B present more suitable results in terms of accuracy, been this important since at the highest H_2SLR the most important changes in terms of HP_{bio} and HPR_{bio} occurs, such as the change after hour 72 where a change in the predominance on the selectivity of the final product happens. Hence, average HPR_{bio} values obtained with methodology B are selected to be compared with the main operational parameters. The average HPR_{bio} per H_2S inlet concentration step are presented in Fig. 6.5b, together with the main operational parameters describing BTF performance. Average HPR_{bio} trend of the first 72 hours indicates that proton production increase along H_2S LR step.

The negative HPR_{bio} value of the first 24 hours of the constant TLV experiment is not in agreement with sulfate selectivity that indicates that proton production should be the main process occurring. This mismatch between HPR_{bio} value and sulfate selectivity shows that HPR has low sensitivity at low H_2S LR conditions, since biological proton production is lower compared to the contribution of other species

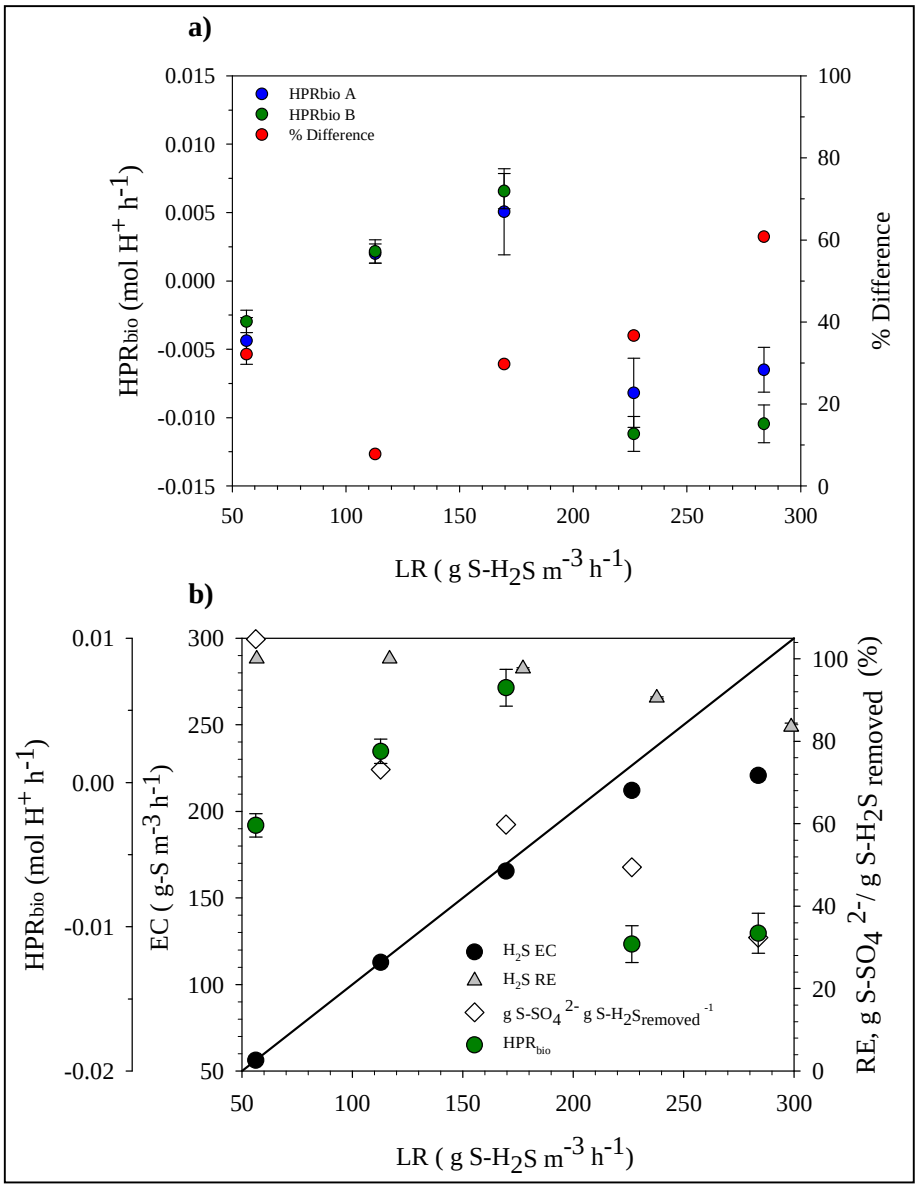

Figure 6.5. (a) Average HPR_{bio} values for the constant TLV experiment. Average HPR_{bio} estimation through methodology A (blue solid line), average HPR_{bio} estimation through methodology B (blue dots-black dotted line), inlet H_2S concentration (black dashed line) and pH (red solid line) and (b) Elimination capacity (black circles), removal efficiency (grey triangles), sulfate selectivity (white diamonds) and selected average HPR_{bio} (green circles) in front of H_2S loading rate during the constant TLV experiment.

Once H_2S LR increase, HPR_{bio} values are in agreement with sulfate selectivity that is over 56.95%, indicating that protons produced due to sulfate production are majority in front of protons consumed by elemental sulfur production. HPR_{bio} values drops to negative values once sulfate selectivity is lower than 50%, indicating that protons are consumed due to elemental sulfur production predominance over sulfate production. Average HPR_{bio} relation with sulfate selectivity is presented in Fig. 6.6.

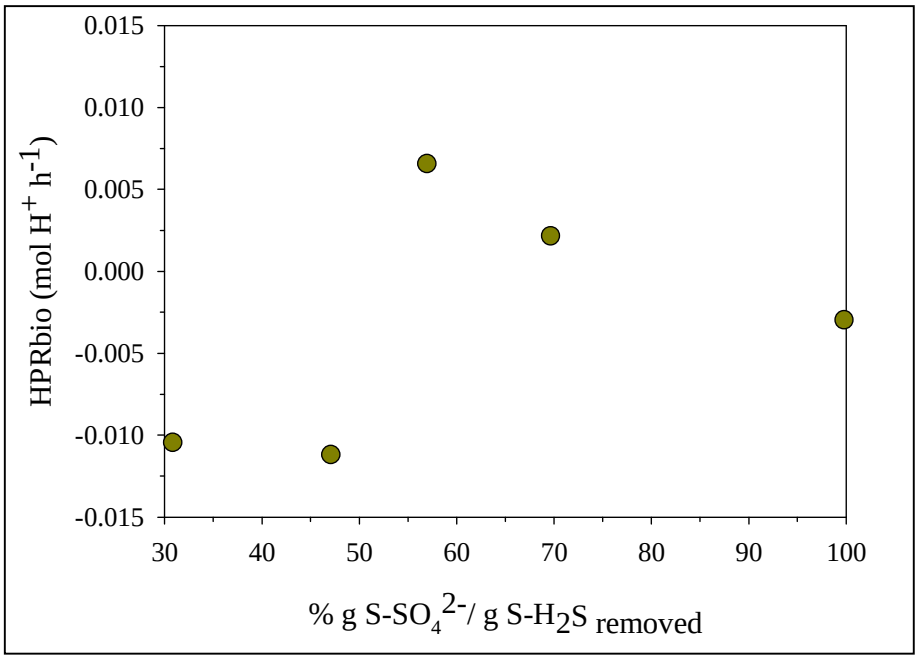

Figure 6.6. Average HPR_{bio} and sulfate selectivity relation for the constant TLV experiment. Average HPR_{bio} estimation through methodology B (dark yellow circles).

As is presented in Fig. 6.6 average HPR_{bio} relation with sulfate selectivity is clear, since for sulfate selectivity values higher than 50% positive HPR_{bio} values are obtained, while for lower sulfate selectivity's values lower than 50 % HPR_{bio} takes negative values. HPR_{bio} results in a suitable indicator that the process performance has decreased and that principally S^0 is produced over SO_4^{2-} production.

Overall, the HP appeared to be a sensitive variable to monitor process performance and operational conditions changes. Especially at high loads when proton production related to biological activity has a greater weight over other process contributing to HP_{obs}, as it occurs during the last two concentration steps. $HP_{contributions}$ determination requires a certain knowledge of the process, such as the liquid medium composition and the gas-liquid mass transfer phenomena's of the dissolved species.

Liquid medium characterization should not be a problem since this is already characterized upstream in the WWTP. Therefore to have a proper biological proton production estimation, continuous feedback of liquid medium composition is needed. Regarding the gas-liquid mass transfer phenomena's occurring in the BTF, such as CO_2 stripping, this can be predicted by using mass-transfer correlations, since this mainly depends on the liquid and gas flow rates

Gas phase dynamics on a BTF is defined by the value of the EBRT, which commonly is set at around 1 to 2 minutes. This means that a change in the inlet may be reflected in the outlet in a time scale of minutes. Consequently, any variable used as a measured variable must be sensitive in this time scale. The HPR signal has the inconvenient to have a background noise associated to the pH control, and therefore changes related to biological activity must be bigger than this background noise. In order to remove this background noise from the HPR signal, a mathematical treatment of the raw titrimetric data is needed in order to have a clearer signal, which depending on the application field can result in a detriment at the time of implementing it as a possible process variable in a control loop.

6.3.2. Titrimetry application in a discontinuous process

Estimation of CO_2 global mass transfer coefficient

Results obtained during the CO_2 stripping test performed at a constant pH, temperature and nitrogen flow are presented in Fig. 6.7.

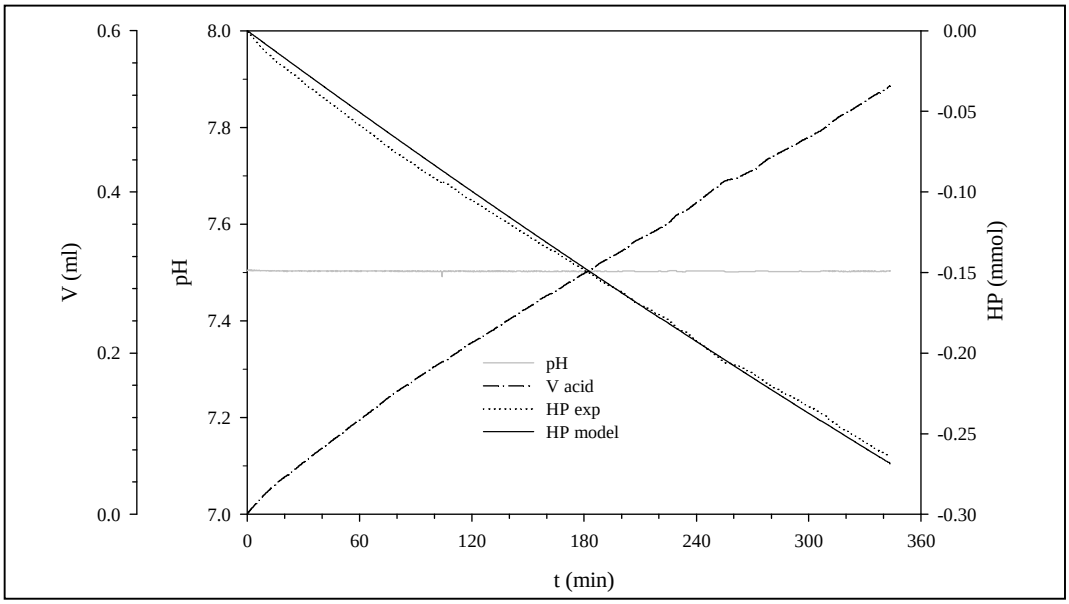

Figure 6.7. Modeling of the titrimetric profile obtained from the stripping test performed at 20 ml N_2 min^{-1}

A satisfactory correspondence between the experimental HP and the modeled HP was obtained, resulting in a $K_La,_{CO2}$ estimation of 0.475 h^{-1}. The $K_La,_{CO2}$ estimated was between one and two order of magnitude lower than other K_La reported in systems where air is

sparged in the liquid phase (Ficara et al., 2003). Therefore, this result was satisfactory since stripping of CO_2 was highly minimized when nitrogen was sparged in the headspace of the respirometer. Moreover, the minimization of the carbon source stripping avoids not only its limitation during the respirometric test but also a lower interference in the observed HP value.In consequence, increased sensitivity and reliability are obtained from titrimetric data. Regarding to titrimetric data, a negative HP value is obtained along the abiotic test due to acid dosage in order to compensate protons that are consumed during CO_2 stripping process.

CO_2 stripping model validation

At time 0, a NO_2^- pulse of 20.8 mg N- NO_2^- L^{-1} and 330 mg S-$S_2O_3^{2-}$$L^{-1}$ of $S_2O_3^{2-}$ was added and degraded during the next 90 minutes being acid addition the consequence of the autotrophic denitrification process being nitrite the electron acceptor during thiosulfate oxidation (Fig. 6.8). From these periods a nitrite uptake rate (NitUR) of 0.394±0.001 mmol NO_2^- h^{-1}, a thiosulfate uptake rate (SUR_{Nit}) (thiosulfate uptake rate associated to nitrite reduction) of 0.185±0.004 mmol $S_2O_3^{2-}$ h^{-1} and a ratio NitUR/SUR_{Nit} of 2.13±0.04 mol NO_2^- /mol $S_2O_3^{2-}$ were calculated (Table 6.3) Elemental sulfur production was not detected since SUR was similar to sulfate production rate being accomplished the sulfur mass balance.

Therefore, the HPR_{bio} used to calculate the ratio HPR_b/NitUR (0.178 mol H^+/mol NO_2) was that obtained from period IIIb since $K_L a_{CO_2}$ was underestimated during period I as explained before. Using the values presented above, the stoichiometry of the denitrification from nitrite, using CO_2 and HCO_3^- as carbon sources and considering a biomass growth associated could be estimated (Eq. 6.33).

Table 6.3. Experimental HPR and Nitrite, Nitrate and Tiosulfate uptake rates obtained from the respirometric profiles

Period	**NitUR** *(mmol NO_2^- h^{-1})*	**NUR** (*mmol NO_3^- h^{-1})*	**SUR_{Nit}** *(mmol $S_2O_3^{2-}$ h^{-1})*	**SUR_N** *(mmol $S_2O_3^{2-}$ h^{-1})*	**HPR_{Nit}** *(mmol $S_2O_3^{2-}$ h^{-1})*
I	0.395	--	0.185	--	0.131
IIIa	0.402	0.343	0.194	0.130	0.074
IIIb	0.393	--	0.192	--	0.070

Then, from minute 90 to minute 240 no other pulse was done and stripping was the sole process taking place in the respirometer. During this period the stripping of CO_2 was the unique running process being $HP_{observed}$ equivalent to the HP of CO_2 stripping (HP_{CO_2}).

The validation of the CO_2 stripping modeling and the $K_La,_{CO2}$ estimation with a biotic test was achieved during this period.

At minute 240 a new pulse of 24.2 mg N L^{-1} of NO_2^- and 12.1 mg N L-1 of NO_3^- and 267.7 mg S-$S_2O_3^{2-}L^{-1}$ of $S_2O_3^{2-}$ was added was performed (IIIa), being nitrate and nitrite simultaneously used as electron acceptors. A positive HP_{bio} was observed during this period (IIIa), which is a consequence of the base dosage resulted from the proton production generated by denitrification from nitrate.

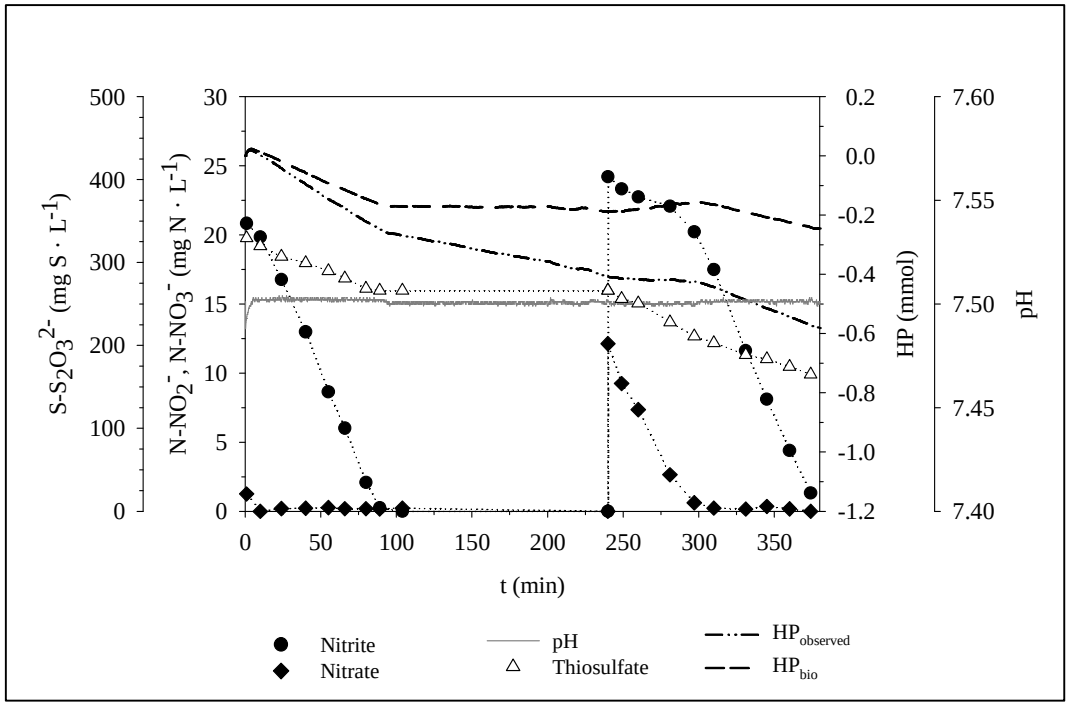

Figure 6.8. Respirometric and titrimetric profiles obtained from the autotrophic thiosulfate oxidation and denitrification

It was observed that NitUR was higher than NUR since nitrite was consumed during nitrate reduction. It is not the usual result since many authors have reported that nitrite reduction is the slower step of denitrification process being nitrite accumulated (Betlach and Tiedje, 1981; Campos et al., 2008). Finally, nitrate was totally depleted at minute 300 being the denitrification from nitrite the unique biological reaction taking place thus causing proton consumption and consequently acid dosage to the system. Similar NitURs were obtained during the whole period III regardless the presence of nitrate in the medium.

Based on this observation, the stoichiometry of the first reaction (Eq. 6.32) was solved by using firstly the stoichiometric ratio $NitUR/SUR_{Nit}$, obtained from period IIIb, and calculating the SUR related uniquely to nitrate reduction rate to nitrite through Eq. 6.31 (SUR_N = 0.130 mmol $S_2O_3^{2-}$ h^{-1}).

$$SUR_N = SUR_{(period\ IIIa)} - NitUR_{(period\ IIIa)} / [NitUR / SUR_{Nit}]_{(period\ IIIb)} \quad (6.31)$$

As a result of determining the HPR_{bio} at period IIIb, NUR/SUR_N and HPR_{bio}/NUR ratios (2.626 mol $S_2O_3^{2-}$ /mol NO_3^- and 0.569 mol H^+/mol NO_3^-, respectively) could be determined and the two-step denitrification with thiosulfate oxidation completely defined. (Eq 6.32 to Eq 6.33).

$$S_2O_3^{2-} + 2.626NO_3^- + 0.043CO_2 + 0.644\ HCO_3^- + 0.137\ NH_4^+ + 0.631H_2O \rightarrow$$

$$0.137C_5H_7O_2N + 2.626NO_2^- + 1.494H^+ + 2\ SO_4^{2-} \quad (6.32)$$

$$S_2O_3^{2-} + 2.070NO_2^- + 0.028CO_2 + 0.419HCO_3^- + 0.089NH_4^+ + 0.400H^+ \rightarrow$$

$$0.089\ C_5H_7O_2N + 1.035\ N_2 + 0.275\ H_2O + 2\ SO_4^{2-} \quad (6.33)$$

The biomass-substrate yields ($Y_{x/s}$) for each electron acceptor used were obtained from the stoichiometric coefficients as well as the yield associated to the complete denitrification (Eq.6.34).

$$S_2O_3^{2-} + 1.16NO_3^- + 0.035CO_2 + 0.519\ HCO_3^- + 0.110\ NH_4^+ + 0.124H_2O \rightarrow$$

$$0.110C_5H_7O_2N + 0.578N_2 + 0.435\ H^+ + 2\ SO_4^{2-} \quad (6.34)$$

On previous works, bibliographic biomass yields were used in order to solve the two-step denitrification stoichiometry Mora et al. (Mora et al., 2014b). The biomass yield obtained (0.101 g biomass/g $S_2O_3^{2}$) on the abovementioned work by Mora et al. (Mora et

al., 2014b) for the complete denitrification associated to thiosulfate oxidation of the suspended SO-NR mixed culture in a CSTR was similar to that founded here (0.111 g biomass/g $S_2O_3^{2}$). Hence, one important finding of this work is that the use of titrimetric data in a single respirometric test per electron acceptor allowed solving both reactions by reducing the degrees of freedom of the system with no additional experimental tests. Further information about estimation of nitrite, nitrate and thiosulfate uptake rates (NitUR, NUR and SUR respectively) and further the study of the biological reactions mechanisms can be found in (Mora et al., 2014c)

6.4. CONCLUSIONS

From the results obtained in this chapter it can be concluded that titrimetry is a powerful tool that allows relating the biological HP and HPR with biological activity occurring in the aerobic desulfurizing BTF during different operational changes. pH affecting species were satisfactorily quantified in order to determine biological HP and HPR from observed HP and HPR.

In this sense, in order to have a proper prediction of biological HP and HPR it was confirmed that a good pH control system is required. ON/OFF control law has showed that erroneous titrimetric conclusions can be obtained if the pH is controlled between the LSP and the HSP band. Quantification of pH affecting species allowed to identify the main species affecting proton equilibrium, and therefore to have a better understanding of the observed HP. In this sense, CO_2 stripping and H_2S dissociation were the main pH affecting species.

From both titrimetric variables determined, HP and HPR, HP has shown to be more suitable variable for process monitoring in order to detect biological activity changes along the operation of a real scale BTF for biogas desulfurization. HPR demonstrated to be a more complex variable, not only for the previous treatment of the data in order to obtain a clearer signal, but principally because of the difference between the dynamics of the liquid and gas phase that makes this variable not appropriate to be considered as a measured variable in a control loop.

Also this work allowed concluding that titrimetry and respirometry are useful tools separately but powerful when used together. The biological proton production was calculated from titrimetric measurements once characterized the CO_2 stripping process that

occurred during the autotrophic denitrification conducted in the respirometer. Titrimetry also permitted, not only estimating the $K_L a_{CO_2}$ from the integration of the mass balances and equilibrium equations of each HP affecting species of the system, but calculating several stoichiometric ratios between the biological HPR and the substrate and electron acceptor uptake rates obtained from the respirometric measurements by reducing DOF of the system with additional experimental data.

The application of these techniques allowed obtaining not only the stoichiometry of the two-step autotrophic denitrification and thiosulfate oxidation, but also the biomass-substrate yields and the biological activities when nitrate and/or nitrite were used as electron acceptors. Finally, the application of respirometry and titrimetry gives the possibility to obtain microbial kinetic parameters, which could be incorporated in those generic models used to design, evaluate and optimize the desulfurization process on biotrickling filters under anoxic conditions.

CHAPTER 7

MODELLING AN AEROBIC BIOTRICKLING FILTER FOR BIOGAS DESULFURIZATION THROUGH A MULTI-STEP OXIDATION MECHANISM

7. MODELLING AN AEROBIC BIOTRICKLING FILTER FOR BIOGAS DESULFURIZATION THROUGH A MULTI-STEP OXIDATION MECHANISM

In this chapter the development, calibration and validation of a biotrickling filter model was done. The model attempts to describe accurately, the behaviour of the BTF under constant and variable loading rate conditions. The development of a BTF model was especially interesting since the literature available describing H_2S removal at high loading rates in BTF is scarce. Moreover, it was also interesting that a kinetic model describing accurately intermediate and final products of H_2S oxidation was here used. The obtainment of the biotrickling filter model it is crucial in order to develop and apply control strategies towards the process optimization by improving the oxygen transfer to the liquid phase

Abstract

A dynamic model describing physical-chemical and biological processes for the removal of high loads of H_2S from biogas streams in biotrickling filters (BTFs) was developed, calibrated and validated for a wide range of experimental conditions in a lab-scale BTF. The model considers the main processes occurring in the three phases of a BTF (gas, liquid and biofilm) in a co-current flow mode configuration. Furthermore, this model attempts to describe accurately the intermediate (thiosulfate and elemental sulfur) and final products (sulfate) of H_2S oxidation through a kinetic model developed using respirometric techniques. A sensitivity analysis was performed in order to focus parameters estimation efforts on those parameters that showed the highest influence on modeling results over the main process variables. Biofilm and liquid layer thicknesses, specific growth rate of biomass over elemental sulfur and the H_2S mass transfer coefficient were the parameters that showed the highest influence on model outputs. Experimental data for model calibration corresponded to the operation of the BTF under stepwise increasing H_2S concentrations between 2000 and 10000 ppm_v. Once the model was calibrated, the validation was performed by simulating a pseudo- steady-state period of 42 days of operation of the BTF at an average concentration of 2000 ppm_v and a dynamic operation period where the BTF was operated under variable inlet H_2S concentration between 1000 and 5000 ppm_v to simulate load fluctuations occurring in industrial facilities. The model described the reactor performance in terms of H_2S removal and predicted satisfactorily the main intermediate and final products produced during the biological oxidation process.

A modified version of this chapter has been published as:

L.R. López, A.D. Dorado, M. Mora, X. Gamisans, J. Lafuente, D. Gabriel

Modeling an aerobic biotrickling filter for biogas desulfurization through a multi-step oxidation mechanism. Chem. Eng. J. (2016).

and presented as conference paper:

L.R. López., A.D. Dorado, M. Mora, Ll. Prades , X. Gamisans, J. Lafuente, D. Gabriel. Modelling biotrickling filters to minimize elemental sulfur accumulation during biogas desulfurization under aerobic conditions. 7th European Meeting on Chemical Industry and Environment (EMChIE 2015), Tarragona, Spain. June 2015.

7.1. INTRODUCTION

Obtaining energy from non-renewable sources is becoming too expensive or too environmentally damaging nowadays. An energy source with high potential for green energy production is biogas. However, in order to have a suitable biogas utilization, impurities such as H_2S and reduced sulfur compounds (RSC) produced during the anaerobic fermentation of S-bearing organic molecules must be removed (Abatzoglou and Boivin, 2009). Removal of H_2S is strictly necessary to avoid corrosion of internal combustion engines during co-generation processes as well as for proper performance of further biogas upgrading technologies (Cartwright, P.E., 2005). Biological technologies such as biotrickling filters (BTF) have demostrated to be a suitable, competitive treatment technology for biogas conditioning when compared to physical-chemical technologies. However, main efforts have focused on experimental works, studying different pollutant loads (Fortuny et al., 2011), using different packing materials (Fortuny et al., 2008), different oxygen mass transfer devices (Rodriguez et al., 2014), pH conditions (Montebello et al., 2013) or the gas-liquid flow pattern (López et al., 2016a). Altough process modelling has shown to be a crucial tool to evaluate the technical and economical feasibility of biological processes prior to full-scale implementation, few efforts have been made in this direction on biogas desulfurization in BTFs.

Multiphase biological processes, such as biofiltration in biofilters and biotrickling filters for the removal of different type of contaminants like volatile organic compounds (VOCs) (Álvarez-Hornos et al., 2009; Dorado et al., 2009; López et al., 2016a) and ammonia (Baquerizo et al., 2005; Cortus et al., 2008), have been modelled describing both transient and steady-state conditions. However, most BTF models have focused on VOCs removal (Ahmed et al., 2013), while literature available for H_2S BTFs modelling is scarce (Devinny and Ramesh, 2005; Kim and Deshusses, 2003; Li et al., 2002). Therefore, a model describing properly the removal of high loads of H_2S in BTFs is still lacking in literature. Previous models for H_2S removal in BTFs have focused on removal of H_2S at odor level concentrations (Kim and Deshusses, 2003; Li et al., 2002; Silva et al., 2012), while only few models in literature dealt with high loads of H_2S (Rodriguez, 2013; Sharvelle et al., 2008). In most cases, the inherent complexity of such plug-flow, heterogeneous, multiphase bioreactors has been strongly simplified to avoid facing a large number of unidentifiable parameters. Often, G-L mass transport, diffusion in the biofilm and biological degradation kinetics have been identified as the most relevant processes.

The heterogeneity of the water-biofilm layers as well as the kinetics and mechanisms considered to model H_2S removal in BTFs are the two main aspects that have been addressed differently by several authors. Most models consider an homogeneous biofilm density, a biofilm completely wetted along the packed bed height (Li et al., 2002; Liao et al., 2008; Sharvelle et al., 2008) and H_2S and O_2 mass transfer from the gas to the liquid phase prior to their diffusion to the biofilm were degradation takes place. Usually, only mass transfer resistance in the liquid phase is considered for modelling G-L mass transport due to the high interstitial gas velocity in the packed bed. However, biogas desulfurization requires of much longer gas contact times and, consequently, lower gas velocities that may increase mass transfer resistance in the gas phase. Also, several alternatives have been proposed to model such bioreactors such as considering a partially or a fully wetted biofilm as well as considering or not adsorption of a fraction of the pollutant by the biofilm (Bonilla-Blancas et al., 2015; Kim and Deshusses, 2003). Despite no clear consensus has been reached so far and a careful analysis from a modelling perspective must be performed, modelling of biotrickling filters using a wetted/non-wetted biofilm approach seems necessary when the trickling liquid velocity (TLV) is modified due to the variable amount of water in the packed bed.

One of the most critical parts in the development of a model is how biodegradation mechanisms and kinetics are described, since depending on the operational conditions, the process might become biodegradation rate-controlled (Devinny and Ramesh, 2005). Different biodegradation kinetics models and degradation mechanisms have been reported in order to describe the substrate consumption in BTFs models for H_2S removal. Eqs. 7.1 and 7.2 are usually lumped in a single equation describing the complete oxidation of sulfide to sulfate (Kim and Deshusses, 2003). However, partial oxidation to elemental sulfur has been often observed in BTFs for biogas desulfurization (Rodriguez et al., 2014). For this reason, a two-step mechanism (Eqs. 7.1 and 7.2) is needed for proper system modelling.

$$H_2S+0.5O_2 \rightarrow S^0+OH^- \quad (7.1)$$

$$S^0+1.5O_2+H_2O \rightarrow SO_4^{2-}+2H^+ \quad (7.2)$$

Obtaining an accurate model that describes well the production and accumulation of intermediate products of H_2S biological oxidation is crucial to describe accurately biogas desulfurization in BTFs. Recently, Mora et al. (Mora et al., 2016) have proposed a multi-step pathway for describing sulfide-oxidizing bacteria (SOB) as catalyst of H_2S oxidation to SO_4^{2-} considering the partial sulfide oxidation to elemental sulfur as an intracellular product, and the sulfite and thiosulfate production as additional intermediates. Such mechanistic model was calibrated and validated through homogeneous respirometric tests providing successful results in describing the main species of the H_2S oxidation process. From a practical point of view, prediction of desulfurizing BTFs performance is essential. Low sulfate production rates can lead to an excessive elemental sulfur formation that accumulates into the packed bed. Consequently, a significant increase in pressure drop inside the BTF bed occurs (Andreasen et al., 2012), with a considerable reduction of BTF operational life-span and process security. However, few works have addressed this topic so far. There is still the need for the development of tools that impulse the industrial application of this emerging biological-based technology. BTF models are essential in design steps, besides useful in the development of control strategies toward process optimization.

From the stated above, the aim of this work was to develop, calibrate and validate a dynamic model of an aerobic BTF for the removal of high-loads of H_2S from biogas streams. The BTF model attempts to describe intermediate and final products obtained from H_2S oxidation under stationary feeding periods, transient and dynamic conditions. It has to be remarked that no previous works have intended to model such range of intermediate products of biological sulfide oxidation in BTFs for biogas desulfurization

7.2. MATERIALS AND METHODS

7.2.1 Experimental setup and operating conditions

A laboratory-scale BTF reactor, with an ancillary unit for air supply, was used in this study to remove high loads of H_2S from biogas streams (Fig. 7.1). The synthetic biogas consisted of controlled mixtures of H_2S and nitrogen (N_2) fed at the top of the BTF (1). An air flow (2) was firstly fed to an aeration column (3) for air supply to increase the dissolved oxygen (DO) concentration in the liquid phase. Exhaust air (4) from the aeration column was fed at the top of the BTF under a co-current flow pattern and mixed with the biogas inlet stream at an O_2/H_2S supplied ratio of 41.2 (v v^{-1}). After biological degradation on the BTF bed (5), the treated biogas stream (6) leaves the reactor. The liquid phase was continuously

recycled from bottom-to-top of the BTF at a trickling liquid velocity (TLV) of 4.4 m h^{-1} (7). The liquid recirculation line (8) was previously oxygenated in an aeration column. The DO concentration in the recycle and purge lines was monitored in-situ in all the experiments. The reactor pH was also controlled at pHs of around 6.5 and 7 using an ON/OFF control system by automated addition of NaOH 1M or HCl 1 M. An empty bed residence time (EBRT) of 118 s and an average hydraulic retention time (HRT) of 9 ± 2 h were maintained throughout the study by regulating the purge pump (9) and the mineral medium pump (10).

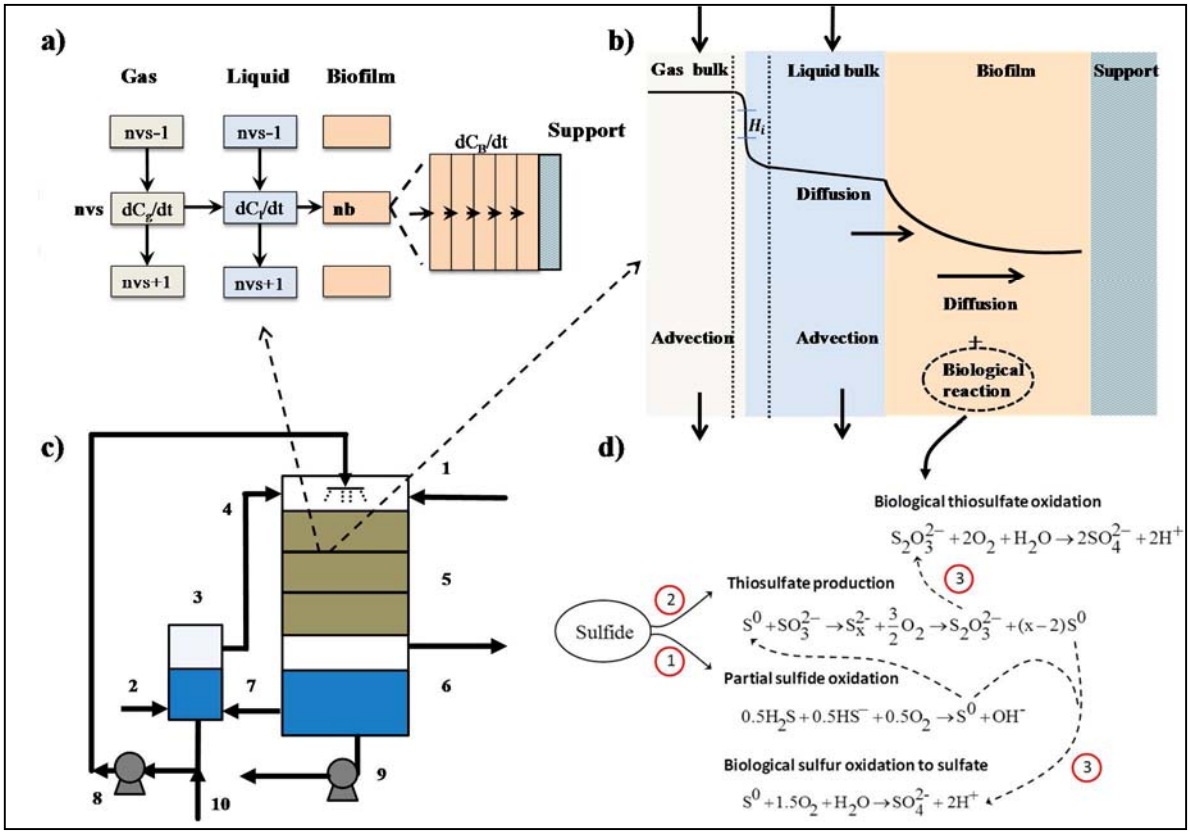

Figure. 7.1. Schematic of the (a) BTF discretization in *nvs* vertical layers and in *nb* subdivisions of the biofilm, (b) schematic of the main phenomena considered in the model, (c) co-current biotrickling filter setup, and (d) biological mechanisms for H_2S oxidation. In Fig. 7.1c numbers correspond to (1) the biogas inlet, (2) air inlet, (3) aeration column, (4) exhaust air from the oxygenation column, (5) main reactor, (6) biogas outlet from the BTF, (7) BTF liquid outlet , (8) liquid recycling pump, (9) liquid purge, (10) mineral medium and bicarbonate inlet. In Fig. 7.1d numbers correspond to (1) partial sulfide oxidation to elemental sulfur (2) thiosulfate production from polysulfide pathway (3) biological oxidation of thiosulfate and intracellular elemental sulfur.

Regarding the packed bed characteristics, the reactor diameter was 7.14 cm with a packed bed volume of $2.80 \cdot 10^{-3}$ m^3 (V_{bed}). Polypropylene Pall rings of 15.9 mm diameter (MACH engineering products, USA) with a specific surface area of 354 m^2 m^{-3} were used. Furthermore, H_2S, O_2 and carbon dioxide (CO_2) in the gas phase were measured by in three side streams and in the outlet gas stream. On-line monitoring was performed with an electrochemical H_2S gas sensor (Sure-cell, Euro-Gas Management Services, UK), O_2 gas sensor (O_2 SL sensor, Euro-Gas Management Services, UK) and a CO_2 gas sensor (CO_2 probe GMP343 Vaisala Carbocap, Vaisala, Finland). Sampling ports were located along the BTF height at 0.24 m, 0.51 m and 0.7 m in order to monitor the H_2S concentration profile along the BTF bed and therefore compare it with simulated data. Further information about gas concentration measurement, BTF inoculation, analytical methods and related information can be found on Chapter 4 (*see section 4.1.1*).

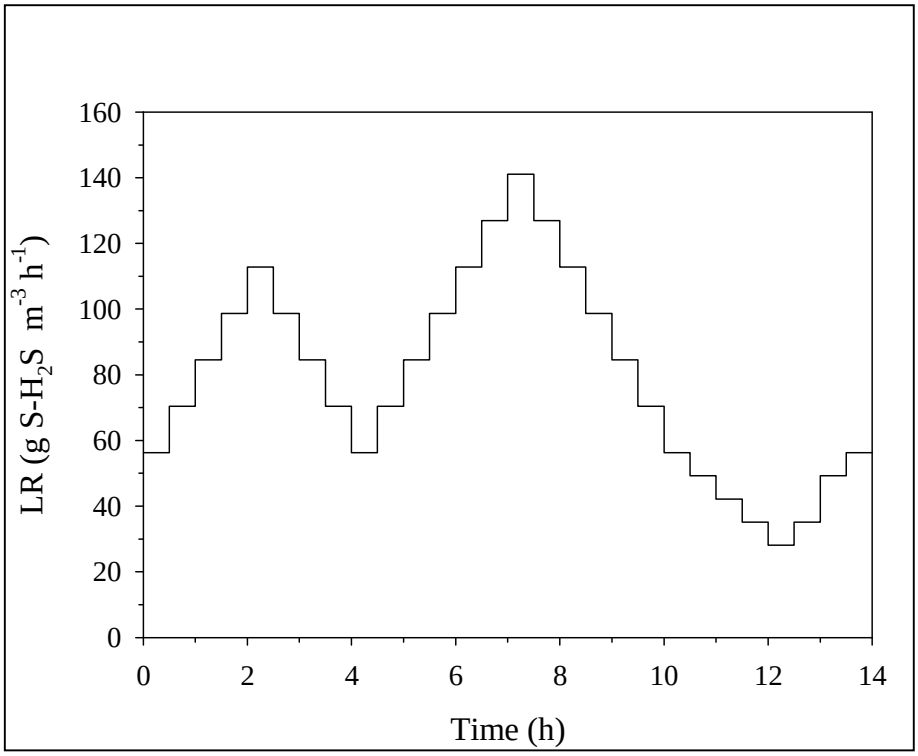

Figure 7.2 . Variable H_2S LR profile used for dynamic validation of the BTF model.

The calibration of model parameters was performed using data obtained during stepwise H_2S Loading Rate (H_2S LR) increments as a consequence of H_2S inlet concentration ($Cg_{in,H2S}$) increase (Period 1-Table 7.1) in the lab-scale BTF set up (Fig. 7.1a)

operating at constant EBRT and constant biogas flow. For model validation under stationary H_2S feeding, a period of 42 days was simulated at a constant $Cg_{in,H2S}$ of 2000 ppm_v (Period 2-Table 7.1). In addition, model was also validated under dynamic conditions (Period 3-table 7.1) by simulating variable H_2S LR conditions due to $Cg_{in,H2S}$ increase (Fig. 7.2) emulating daily load fluctuations as those commonly found in real facilities. The average, maximum and minimum H_2S LR are shown in Table 7.1. Periods in Table 7.1 do not correspond to consecutive periods. All experiments were performed in between a time span of 15 months.

Table 7.1. Experimental conditions for the simulated periods

Period	[H_2S] *(ppm_v)*	LR *(g S-H_2S m^{-3} h^{-1})*	O_2/H_2S *(% v v^{-1})*	Period simulated *(days)*
1: Calibration and sensitivity analysis	2000	56.3	42.2	5
	4000	112.9	21.0	
	6000	169.6	14.0	
	8000	226.6	10.5	
	10,000	283.8	8.4	
2: Stationary Validation	2000	56.3	42.2	42
3: Dynamic Validation	2758[a]	78.9	35.8	8
	5000[b]	141.1	84.4	
	1000[c]	28.1	16.8	

[a]Average concentration
[b]Maximum concentration
[c]Minimum concentration
n

7.2.2 Model development

A three phase model (gas, liquid and biofilm) was considered to model reactor dynamics under a co-current flow pattern configuration. The model also considered the main processes occurring in the aeration column attached to the bioreactor

Biotrickling filter model

The BTF model incorporates mathematical expressions for the following mechanisms occurring in the packed bed: mass transport by advective flow in the gas and liquid phases, mass transfer at the gas-liquid interface, mass transfer by diffusion at the liquid-biofilm interface, internal diffusion in the biofilm phase and biological reaction in the biofilm as schematized in Fig. 7.1. Also, the model considered oxygen mass transfer at the gas-liquid interface occurring in the aeration column. Model equations were built based on the above mentioned mechanisms and assumptions often assumed in BTF models in literature (Bonilla-Blancas et al., 2015; Kim and Deshusses, 2003; Li et al., 2002). Main model assumptions are described as follows:

(1) The whole biofilm is completely covered by liquid. **(2)** The adsorption capacity of the plastic packing material is neglected. **(3)** The packing material is entirely covered by a uniform layer of biofilm, which have a uniform thickness. **(4)** Biomass in the biofilm consists of active biomass responsible for substrate removal and no biomass growth is considered, therefore its distribution and density are considered to be uniform along the BTF packed bed. **(5)** Gas-Liquid mass transport is described by a gas-liquid global mass transfer coefficient referred to the liquid phase (K_L) that considers both the individual gas and liquid mass transfer resistances**(6)** According to the Henry's theory, gas-liquid interfaces are at equilibrium. **(7)** Mass transfer resistance in the liquid-biofilm interface was described by Fick's law considering that the whole thickness of the liquid phase acted as the liquid boundary layer for mass transport resistance.**(8)** Plug-flow mode without axial or radial dispersion was considered to describe the circulation of the gas flow through the BTF bed. **(9)** The mass flux through each finite division of the BTF bed is simulated as a single continuous stirred tank reactor (CSTR), therefore the complete BTF bed is simulated as a sequence of CSTRs (Fig 7.1a). All species and phases (gas, liquid, biofilm and packing material) were considered in each of the divisions. **(10)** Diffusion of the species through the biofilm is described by Fick's law.

Since transport of compounds in the axial direction is modeled as plug flow, the BTF bed was discretized in vertical layers in order to simulate a sequence of CSTR (Deshusses et al., 1995). Vertical layers (*nvs*) were numbered starting from the top of the BTF (*nvs*=1) to the biogas outlet (*nvso*). Similarly, the biofilm layers (*nb*) were also divided in different subdivisions starting from the biofilm surface (*nb*=1) to the biofilm subdivision in contact

with the packed material (*nbp*). The set of partial differential equations was discretized in space along the bed height and biofilm thickness. The conversion of the tubular reactor into a serial of stirred reactors was verified running simulations at different discretizations and optimizing results and computing time. As a result, an optimal discretization of the biofilter was found, resulting in eight nodes along the bed height (*nvs=8*) and ten nodes along the biofilm thickness (*nb=10*).

The following subsections describe the mass balances in the gas, liquid and biofilm phases and their initial conditions in the BTF:

- Mass balance for the gas phase in the BTF

$$\frac{dC_{g,i}^{nvs}}{dt} = \frac{F_T}{V_{g,\,nvs}} \cdot \left(C_{g,\,i}^{nvs-1} - C_{g,\,i}^{nvs}\right) - \frac{K_{L,i} \cdot a}{\varepsilon_g} \cdot \left(\frac{C_{g,\,i}^{nvs}}{H_i} - C_{L,i}^{nvs}\right) \tag{7.3}$$

initial conditions: $t=0,\ C_{g,\,i}^{nvs}=0$

at the BTF inlet (*nvs*=1): $C_{g,\,i}^{nvs-1}=C_{g,\,i}^{in}$

Where subscripts *i* refers to either gaseous H_2S or O_2, while $C_{g,\,i}^{nvs}$ and $C_{L,i}^{nvs}$ are the concentrations of component *i* in the bulk gas phase and bulk liquid phase for a certain layer (g m^{-3}), respectively; $V_{g,\,nvs}$ (m^3) is calculated as $V_{g,nvs}=\frac{V_{bed} \cdot \varepsilon_g}{nvs}$ where ε_g is the gas phase porosity, which represents the volume fraction occupied by the gas phase in the packed and V_{bed} is the empty volume of the packed bed. Notice that G-L mass transport is described by a gas-liquid global mass transfer coefficient referred to the liquid phase (K_L) that considers both the individual gas and liquid mass transfer resistances.

- Mass balance for the liquid phase in the BTF

$$\frac{dC_{L,i}^{nvs}}{dt} = \frac{F_L}{V_{L,nvs}} \cdot \left(C_{L,i}^{nvs-1} - C_{L,i}^{nvs}\right) + \frac{K_{L,i} \cdot a}{\varphi} \cdot \left(\frac{C_{g,\,i}^{nvs}}{H_i} - C_{L,i}^{nvs}\right) - \frac{a \cdot D_i}{\varphi \cdot \delta_L} \cdot \left(C_{L,i}^{nvs} - C_{B,i}^{nvs,1}\right) \tag{7.4}$$

initial conditions: $t=0,\ C_{L,\,i}^{nvs}=0$

at the BTF inlet (*nvs*=1): $C_{L,\,i}^{nvs-1}=C_{L,\,i}^{RE}$

subscripts *i* refers to S^{2-}, SO_4^{2-}, $S_2O_3^{2-}$ and DO concentration, the compounds considered in the liquid phase of the BTF; $V_{L,\ nvs}$ (m^3) is calculated as $V_{L,nvs}=\frac{V_b \cdot \varphi}{nvs}$ where φ is the volume fraction occupied by the liquid phase in the packed bed according to the dynamic hold-up measured (dimenssionless). Notice that mass transfer resistance in the liquid-biofilm interface was described by Fick's law considering that the whole thickness of the liquid phase acted as the liquid boundary layer for mass transport resistance.

- Mass balances for the biofilm in the BTF

For the first subdivision of the biofilm (*nb*=1) in all BTF layers (*nvs*=1 to *nvso*)

$$\frac{dC_{B,i}^{nvs,1}}{dt}=\frac{D_i}{\delta_B \cdot \delta_L}\cdot\left(C_{L,i}^{nvs}-C_{B,i}^{nvs}\right)-\frac{D_i}{\delta_{B\text{-}nb}{}^2}\cdot\left(C_{B,i}^{nvs,1}-C_{B,i}^{nvs,nb+1}\right)+\sum \nu_{ij}\cdot r_{B,j} \qquad (7.5)$$

For the inner subdivision of the biofilm (*nb*=2 to *nb=nbp-1*) in all BTF layers (*nvs*=1 to *nvso*)

$$\frac{dC_{B,i}^{nvs,nb}}{dt}=D_i\cdot\frac{\partial^2 C_{B,i}^{nvs,nb}}{\partial\delta_{B\text{-}nb}{}^2}+\sum \nu_{ij}\cdot r_{B,j} \qquad (7.6)$$

For the closest subdivision to the packing material (*nbp*) in all BTF layers (*nvs*=1 to *nvso*)

$$\frac{dC_{B,i}^{nvs,nbp}}{dt}=\frac{D_i}{\delta_{B\text{-}nb}{}^2}\cdot\left(C_{B,i}^{nvs,nb\text{-}1}-C_{B,i}^{nvs,nbp}\right)+\sum \nu_{ij}\cdot r_{B,j} \qquad (7.7)$$

initial conditions in Eqs. 7.5, 7.6 and 7.7: $t=0, \quad C_{B,\ i}^{nvs,nb}=0$

boundary conditions in Eqs. 7.5, 7.6 and 7.7: $x=0, \quad C_{B,i}=C_{l,i}$

$x=\delta_B, \quad \frac{\partial C_{B,i}^{nvs,nbp}}{\partial t}=0$

in Eqs. 7.5, 7.6 and 7.7, subscripts *i* refers to S^{2-}, SO_4^{2-}, $S_2O_3^{2-}$ and DO concentration, the compounds considered in the biofilm phase of the BTF, while subscripts *j* indicates the rate equation in which component *i* is participating.

- Mass balance for the liquid phase in the sump of the BTF

According to the BTF configuration, mass balances in the sump of the reactor (Eq. 7.8) and in the aeration column (Eqs. 7.9-7.10) were included.

$$\frac{dC_{L,i}^{P}}{dt} = \frac{F_L \cdot C_{L,i}^{nvs} - F_{L,P} \cdot C_{L,i}^{P} + F_{L,In} \cdot C_{L,i}^{In} - F_L \cdot C_{L,i}^{RE}}{V_{L,D}} \tag{7.8}$$

initial conditions: $t=0,\ C_{L,\,i}^{P}=0$

subscript *i* refers to S^{2-}, SO_4^{2-}, $S_2O_3^{2-}$ and DO concentration, the compounds considered in the liquid phase of the BTF. Notice that $C_{L,i}^{P}$ and $C_{L,i}^{RE}$ are equal except for dissolved oxygen because of the aeration column located in the recirculation line.

- Mass balance for the gas phase in the aeration column

$$\frac{dC_{g,\,O_2}^{out}}{dt} = \frac{F_{O_2}}{V_{g,\,AC}} \cdot \left(C_{g,\,O_2}^{AC} - C_{g,\,O_2}^{out}\right) - K_{L,O_2,AC}a' \left(\frac{C_{g,\,O_2}^{out}}{H_{O_2}} - C_{L,O_2}^{RE}\right) \tag{7.9}$$

initial conditions : $t=0,\ C_{g,\,O_2}^{AC}=0$

- Mass balance for the liquid phase in the aeration column

$$\frac{dC_{L,O_2}^{RE}}{dt} = \frac{F_L}{V_{L,\,AC}} \cdot \left(C_{L,O_2}^{P} - C_{L,i}^{RE}\right) + K_{L,O_2,AC} \cdot \left(\frac{C_{g,\,O_2}^{out}}{H_{O_2}} - C_{L,i}^{RE}\right) \tag{7.10}$$

initial conditions: $t=0,\ C_{L,O_2}^{P}=0$

- Elemental sulfur mass balance

In order to determine if elemental sulfur de-accumulation and, therefore, an increase in the sulfate concentration were due to an increase in the biological activity or due to an experimental error in sulfate concentration measurements by ionic chromatography (IC), an

extra mass balance was solved in order to determine the sulfate concentration in the BTF purge corresponding only to the elemental sulfur de-accumulation (Eq. 7.11).

$$\frac{dC^{s}_{L,i}}{dt} = \frac{F_{L,}}{V_L} \cdot \left(C^{e}_{L,i} - C^{s}_{L,i}\right) + \frac{\left(C_j^{t+1} - C_j^{t}\right)}{\left(t^{t+1} - t^{t}\right)} \quad (7.11)$$

subindex *i* refers to sulfate and subindex *j* refers to elemental sulfur, while F_L is the liquid flow rate in $m^3\ h^{-1}$; V_L is the total volume of liquid in the system (BTF+sump of the BTF) in m^{-3}; $C^e_{L,i}$ and $C^s_{L,i}$refers the concentration of sulfate in the liquid inlet and liquid outlet, respectively, in g m^{-3}; C_j^{t+1} refers to the concentration of compound *j* at time *t+1* and C_j^t refers to the compound *j* at time *t*.

Modelling of biological and chemical sulfur-compounds conversions

Biological degradation of H_2S described with a multi-step sulfide oxidation kinetic model (Fig. 7.1d) proposed by Mora et al. (Mora et al., 2016) was used herein. The multi-step sulfide oxidation mechanism (Fig. 7.1d) has been summarized in Tables 7.2 and 7.3, in which the stoichiometry and the kinetic expressions that describe each of the reactions occurring during the process have been specified. In short, the kinetic model considers that H_2S is partially oxidized to elemental sulfur, which is intracellularly stored, but also to sulfite, which in presence of sulfide reacts to subsequently form thiosulfate. Then, once sulfide is completely depleted, elemental sulfur and thiosulfate are further oxidized to sulfate, the end product of the reaction. Further information about the biological and chemical sulfide conversions can be found elsewhere (Mora et al., 2016).

According to Mora et al. (Mora et al., 2016), H_2S biodegradation kinetics were described by a Haldane equation since substrate inhibition caused by sulfide over sulfide oxidation was considered. Furthermore, oxygen limitation was described by including a Monod-type kinetic term in the rate equations. In addition, accumulation of intracellular elemental sulfur by SOB was considered in order to describe the experimental decrease of the sulfide oxidation rate observed due to accumulation of intracellular elemental sulfur. SOB in the BTF was *Thiotrix sp.* according to pyrosequencing analysis performed during the kinetic model development (Mora et al., 2016). Such filamentous γ-proteobacteria forms intracellular deposits of elemental sulfur as intermediary product during sulfide oxidation (Nielsen et al., 2000). Elemental sulfur biodegradation kinetics was described using a shrinking particle model analogous to that used for biological consumption of other solid

substrates such as Poly-hydroxy-butyrate (PHB). A non-competitive inhibition term was included in order to describe the substrate switch. Dissolved oxygen and thiosulfate limitation were described by a multi-substrate Monod-type kinetic expression. Similarly, thiosulfate oxidation to sulfate was described considering a Monod-type kinetic for substrate consumption, while potential chemical oxidation of sulfide to form thiosulfate was also considered.

Table 7.2. Process stoichiometry for the aerobic sulfide, thiosulfate and elemental sulfur oxidation by SOB

Process	**Compounds**				
	Sulfide	Thiosulfate	Sulfur	Sulfate	Oxygen
1. Growth on sulfide	$-\frac{1}{Y_{X/SS}}$		$\frac{1}{Y_{X/SS}}$		$-\frac{0.42^{*}}{Y_{X/SS}}$
2. Growth on elemental sulfur			$-\frac{1}{Y_{X/S}}$	$\frac{1}{Y_{X/S}}$	$-\frac{1.22^{*}}{Y_{X/S}}$
3. Growth on thiosulfate		$-\frac{1}{Y_{X/TS}}$		$\frac{2}{Y_{X/TS}}$	$-\frac{1.6\overset{*}{5}}{Y_{X/TS}}$
4. Thiosulfate production		1	-2		-1.5

* Mora et al., 2016.

Table 7.3. Process kinetics for the aerobic sulfide, thiosulfate and elemental sulfur oxidation by SOB

Process	**Process rate**
1. Growth on sulfide	$\mu_{\max,1}\cdot\left(\frac{C_{B,SS}}{k_{SS}+C_{B,SS}+\frac{C_{B,SS}{}^{2}}{k_{is}}}\right)\cdot\left(1-\left(\frac{\left(\frac{C_{B,S}}{X}\right)}{K_{max}}\right)^{\alpha}\right)\cdot\left(\frac{C_{B,DO}}{C_{B,DO}+k_{o}}\right)\cdot X$
2. Growth on elemental sulfur	$\mu_{max,2}\cdot\left(\frac{C_{B,S}}{X}\right)^{2/3}\cdot\left(\frac{K}{C_{B,SS}+K}\right)\cdot\left(\frac{C_{B,DO}}{C_{B,DO}+k_{o}}\right)\cdot X$
3. Growth on thiosulfate	$\mu_{max,3}\cdot\left(\frac{C_{B,TS}}{C_{B,TS}+K_{TS}}\right)\cdot\left(\frac{K}{C_{B,SS}+K}\right)\cdot\left(\frac{C_{B,DO}}{C_{B,DO}+k_{o}}\right)\cdot X$
4. Thiosulfate production	$k\cdot C_{B,SS}{}^{\beta}$

7.2.3 Model implementation

The resulting set of ordinary differential equations was solved using MATLAB in a home-made modelling environment. A variable order method was used for solving stiff differential equations based on numerical differentiation formulas (NDFs), which are generally more efficient than the closely related family of backward differentiation formulas (BDFs), also known as Gear's methods. Since the inlet H_2S concentration was changed throughout the BTF operation, inlet concentration profiles were used as input variable of the model. Model parameters were estimated during calibration by curve-fitting of experimental data to model predictions to describe the dynamics of a lab-scale BTF for biogas desulfurization.

A minimization routine on MATLAB, based on a non-lineal multidimensional minimization (Nelder-Mead) was used. The objective function to minimize was based on the H_2S removal efficiency (RE) and the concentration of sulfate in the liquid phase ($C_{L,SO4}^{2-}$) according to the sensitivity analysis, to take into account both the gas-phase and the liquid-phase dynamics, respectively. Also, the cumulative mass of elemental sulfur (m_S^0) was not included in the objective function because experimental m_S^0 was not analytically measured but determined through mass balances (López et al., 2016a).In order to evaluate the goodness of model predictions to experimental data, the efficiency criterion proposed by Nash and Sutcliffe (Nash and Sutcliffe, 1970) was used. Such efficiency criterion mathematically measures how well a model simulation fits the available experimental data. The efficiency coefficient (NSE) is defined as one minus the sum of the absolute squared differences between the predicted and observed data normalized by the variance of the observed data during the period under investigation according to Eq. 7.12. Essentially, the closer the model efficiency to 1, the more accurate the model is.

$$NSE=1-\frac{\sum_{i=1}^{i=n}(y_e-y_m)^2}{\sum_{i=1}^{n}(y_e-\bar{y}_e)^2} \quad (7.12)$$

7.3. RESULTS AND DISCUSSION

7.3.1 Sensitivity analysis.

Before model calibration, a sensitivity analysis was performed in order to determine the parameters that showed the highest influence on model outputs over the main process variables. Sensitivity was assessed by increasing and decreasing model parameters by 10%

and comparing the relative change of the output variables to a relative change of the model parameter. As stated in Deshusses et al. (Kim and Deshusses, 2003), model parameters fall in the following categories: physical-chemical properties, system specifications (dimensions), biokinetics and mass transfer parameters. In the present work, parameters belonging to all parameter categories were included to perform the relative sensitivity analysis of the main output variables on biofiltration such as RE, m_S^0 and $C_{L,SO4}^{2-}$. In order to determine the relative sensitivity, model parameters were varied 0.9 and 1.1 times the reference value while simulating the stepwise load increase of period 1 (Table 7.1). Relative sensitivity analysis results were chosen as those corresponding to the H_2S inlet concentration of 10000 ppm_v (Table 7.4) because of a larger relative sensitivity of the model at these inlet concentration. Only those parameters that showed a relative sensitivity higher than 0.10 in at least one of the output variables are shown in Table 7.4. Similar results in terms of relative sensitivity were obtained for the 4000, 6000 and 8000 ppmv concentration steps simulated (results not shown).

The most sensitive output variables were the RE and $C_{L,SO4}^{2-}$ that exhibited comparable sensitivities between them at a 10% increase while m_S^0 was the less sensitive output variable due to its cumulative nature. However, at a 10% decrease results indicated that RE was highly influenced by parameters of all categories abovementioned to a higher extent than $C_{L,SO4}^{2-}$. Thus, both RE and $C_{L,SO4}^{2-}$ were the sole output variables selected to be included in the objective function during the calibration stage. Despite the low relative sensitivity of m_S^0, the most sensitive parameters were those parameters related to its formation, *i.e.* O_2 and H_2S mass transfer coefficients $\left(K_{L,O_2}, K_{L,H_2S}, D_{O_2}\right)$, physical-chemical properties $\left(H_{O_2}, H_{H_2S}\right)$ and parameters related to its consumption ($\mu_{max,2}$).

This result was somehow expected since elemental sulfur formation directly depends on the oxygen availability and the S/DO ratio in the liquid phase that result from their transfer efficiency and solubility. Besides the system specific parameters and physical-chemical parameters, the relative sensitivity analysis showed that biokinetic and mass transfer parameters were the most sensitive, which are often the most difficult to determine experimentally (Mora et al., 2014b; Munz et al., 2009) and usually obtained by curve fitting of model estimations to experimental data (Dorado et al., 2015; Iliuta and Larachi, 2005).

Table 7.4. Sensitivity results for key BTF model parameters assessed at an inlet H_2S concentration of 10000 ppm_v

			Sensitivity, +Δ10 %			**Sensitivity, -Δ10 %**		
Parameter	**Symbol**	**Units**	RE (%)	m_S^0 (g-S)	$C_{L,SO4}^{2-}$ (g-S L^{-1})	RE (%)	m_S^0 (g-S)	$C_{L,SO4}^{2-}$ (g-S L^{-1})
Specific interfacial area	a	$m^2\ m^{-3}$	0,79	0,00	1,09	1,51	0,31	0,90
O_2 mass transfer coefficient	K_{L,O_2}	$m\ h^{-1}$	0,45	-0,30	0,68	1,20	-0,19	0,53
O_2 Diffusivity	D_{O_2}	$m^2\ h^{-1}$	0,40	-0,10	0,33	1,02	-0,05	0,25
Specific growth rate over sulfur	$\mu_{max,2}$	h^{-1}	-0,40	-0,22	0,27	-0,48	0,04	0,51
H_2S Henry's constant	H_{H_2S}	dimensionless	-0,30	-0,46	0,24	-0,08	-0,50	0,25
Biofilm layer thickness	δ_B	μm	-0,05	0,05	0,13	1,42	0,04	0,13
Biomass concentration	X	g VSS m^{-3}	0,06	0,12	0,11	1,31	0,12	0,11
Substrate switch	K_{max}	g S g VSS^{-1}	0,11	0,18	0,04	1,21	0,21	0,01
H_2S mass transfer coefficient	K_{L,H_2S}	$m\ h^{-1}$	-0,10	0,21	-0,04	-0,04	0,25	-0,07
O_2 half-saturation constant	k_o	g DO m^{-3}	0,14	0,08	-0,08	0,11	0,08	-0,09
Liquid layer thickness	δ_L	μm	-0,50	0,02	-0,25	-0,37	0,04	-0,31
O_2 Henry's constant	H_{O_2}	dimensionless	-1,41	0,22	-0,76	-0,72	0,55	-1,23

Both RE and $C_{L,SO4}^{2-}$ were mostly influenced by physical-chemical parameters such as O_2 and H_2S Henry coefficients (H_{O_2}, H_{H_2S}); system specific parameters such as the specific surface area (a); by mass transfer parameters such as the O_2 and H_2S mass transfer coefficients, liquid layer thickness and O_2 diffusivity $\left(K_{L,O_2}, K_{L,H_2S}, \delta_L, D_{O_2} \right)$; and by

kinetic parameters such as the specific growth rate for sulfur and the O_2 half-saturation constant ($\mu_{max,2}$, k_o).

Consequently, the relative sensitivity analysis indicated that H_2S removal was either influenced by gas-liquid mass transfer and by biological degradation. However, parameters related with O_2 mass transfer such as K_{L,O_2}, H_{O_2} and D_{O_2} exhibited a larger influence compared to the corresponding H_2S parameters. Such result is in consonance with previous works that reported that O_2 transport rather than H_2S transport is usually the limiting step in high-load H_2S biogas desulfurization (Fortuny et al., 2011; Montebello et al., 2012). In Chapter 5 of this thesis it was showed the effectiveness of O_2 G-L mass transfer due the TLV regulation was a key factor to improve H_2S oxidation in high-load H_2S biogas desulfurization.

Regarding the biokinetic parameters, $\mu_{max,2}$ was the most sensitive parameter, even if exhibited lower sensitivities compared with mass transport and physical-chemical parameters. This result indicates that elemental sulfur accumulation plays a major role as intermediate and that must be included and properly described by any kinetic model. Sulfide oxidation rate can be limited by excessive elemental sulfur accumulation, which is directly influenced by the rate at which elemental sulfur is consumed ($\mu_{max,2}$). In the kinetic model used in the present work, intermediate reactions such as elemental sulfur production and biodegradation are considered, which means that both the inhibitory or the catalytic effect caused by each species over other bioreactions are reflected.

Excluding those parameters that can be determined using correlations (K_{L,O_2}), or physical-chemical parameters that can be found in literature (D_{O2}, H_{H2S}, H_{O2}), or provided by the packing manufacturer (*a*), the most sensitive parameters were selected for model calibration. Five parameters were selected for curve-fitting estimation during model calibration: namely, biomass and liquid layer thickness (δ_B, δ_L), specific growth rate for sulfur ($\mu_{max,2}$), biomass concentration (X) and H_2S global mass transfer coefficient (K_{L,H_2S}). The number of parameters was selected according to the number of variables assessed (H_2S gas concentrations along the bed height, sulfate concentration and mass of elemental sulfur accumulated).

7.3.2 Model parameters estimation

A summary of the BTF model parameters is shown in Tables 7.5 and 7.6, while Fig. 7.3 and Fig. 7.4 show the comparison of model predictions using the parameters estimated and the experimental data corresponding to the calibration period (Table 7.1).

Table 7.5. Summary of main parameters of the BTF model for biogas desulfurization

Parameter	Symbol	Value	Units	Reference
Biomass concentration	X	$139.7 \cdot 10^{3}$	g VSS m^{-3}	Calibrated
Biofilm layer thickness	δ_B	200	μm	Calibrated
Liquid layer thickness	δ_L	10	μm	Calibrated
Specific growth rate for sulfur	$\mu_{max,2}$	$2.17 \cdot 10^{-2}$	g $VSS^{1/3}$ g $S^{-1/3}h^{-1}$	Calibrated
H_2S Global mass transfer coefficient	K_{L,H_2S}	0.23	m h^{-1}	Calibrated
O_2 global mass transfer coefficient in the BTF	K_{L,O_2}	0.38	m h^{-1}	(Billet and Schultes, 1999)
O_2 mass transfer coefficient in the Aeration column	$K_L a'_{,O2,AC}$	0.4	h^{-1}	Experimentally determined
Liquid hold-up	ϕ	$3.57 \cdot 10^{-2}$	dimensionless	Experimentally determined
Specific interfacial area	a	354.33	m^2 m^{-3}	Packing material
Packing material porosity	ε	0.85	dimensionless	manufacturer
H_2S diffusivity	D_{H_2S}	$5.80 \cdot 10^{-6}$	m^2 h^{-1}	(Perry et al., 1997)
O_2 diffusivity	D_{O_2}	$9.00 \cdot 10^{-6}$	m^2 h^{-1}	(Perry et al., 1997)
SO_4^{2-} diffusivity	$D_{SO_4^{2-}}$	$3.80 \cdot 10^{-3}$	m^2 h^{-1}	(Perry et al., 1997)
H_2S Henry's constant	H_{H_2S}	0.42	dimensionless	(Sander, 2014)
O_2 Henry's constant	H_{O_2}	32.80	dimensionless	(Sander, 2014)

Biomass concentration (X) estimated by the model (Table 7.5) was in agreement with the amount of elemental sulfur produced (22.37 g) and the K_{max} determined by Mora et al.

(Mora et al., 2016) (*see Table 7.6*). Since K_{max} is the relation between the maximum amount of elemental sulfur that could be accumulated inside SOB cells before this accumulation completely blocked the biological sulfide consumption, this maximum amount of elemental sulfur was determined using the substrate switch constant (K_{max}) and the biomass concentration estimated by the model (X) according to $K_{max}=\frac{m_{S^0max}}{X}$. Thus, under the calibration conditions, a maximum amount of 157 g of elemental sulfur could be accumulated inside SOB cells, well above the amount of elemental sulfur produced. The K_{L,H_2S} was in agreement with K_{L,O_2} since both K_L values were related by the square root of the diffusivity of each species (Li et al., 2002).

Table 7.6. Summary of main biokinetic parameters of the BTF model for biogas desulfurization calibrated by Mora et al. (Mora et al., 2016) through respirometry for the biotrickling filter modeled herein.

Parameter	Symbol	Value	Units
Specific growth rate for sulfide	$\mu_{max,1}$	0.41	h^{-1}
Specific growth rate for sulfide	$\mu_{max,3}$	0.012	h^{-1}
Sulfide affinity constant	k_{SS}	0.32	g S m^{-3}
Sulfide inhibition constant	k_{is}	42.4	g S m^{-3}
Oxygen affinity constant	k_o	0.11	g DO m^{-3}
Maximum intracellular elemental sulfur stored in the biomass	K_{max}	0.252	g S g^{-1} VSS
Thiosulfate affinity constant	K_{TS}	0.0023	g S m^{-3}
Kinetic constant for thiosulfate	k	6.35	h^{-1}
Substrate switch constant	K	0.014	g S m^{-3}
Kinetic constant for thiosulfate	β	0.530	dimensionless
Kinetic constant	α	1.71	dimensionless

The K_{L,O_2} was determined using the Billet and Schultes correlations (Billet and Schultes, 1999) for the gas and liquid individual mass transfer coefficients kg and kl, respectively, which was in close agreement with K_{L,O_2} determined by Dorado et al. (Dorado et al., 2009). It is worth highlighting that only the liquid-side resistance was significant since based on Billet and Schultes correlations the contribution of individual mass transfer resistances in the gas phase to the overall resistance for both gas species oxygen (O_2) and hydrogen sulfide (H_2S) were only 0.18% and 9.7% for O_2 and H_2S, respectively. In addition, $\mu_{max,2}$ lies close to the range of values determined by Mora et al. (Mora et al., 2016) ($5 \cdot 10^{-4}$ -$1.1 \cdot 10^{-2}$ h^{-1}). The δ_B denotes that the biofilm was thick enough to contain active and inactive biomass inside the biofilm and that δ_B is in the typical range of H_2S-degrading biofilms (Li et al., 2002). Kim and Deshusses (Kim and Deshusses, 2003) reported a δ_B of 23 μm concluding that, in order to perform the removal of high H_2S loads in biogas, higher δ_B must be achieved. The δ_L estimated during model calibration was in agreement with the value obtained by dividing D_{H_2S} by the K_{L,H_2S}. (Li et al., 2002).

In Fig. 7.3 and Fig. 7.4 experimental results and model predictions of the effect of stepwise LR increases due to H_2S inlet concentration increases corresponding to the model calibration period are presented. Experimental data in both figures indicate that the system was able to remove almost 100% of inlet H_2S at all H_2S LR (Fig. 7.3a and 7.3b). However, 100% sulfate production only occurred at the lowest H_2S LR corresponding to an inlet concentration of 2000 ppmv. Further information related to sulfate production in this experiment can be found elsewhere (López et al., 2016a). Thereafter, elemental sulfur was accumulated in the packed bed (Fig. 7.4a). At the highest H_2S LR tested the sulfate production was lower than the elemental sulfur produced, which lead to a decrease of the concentration of sulfate measured in the liquid phase (Fig. 7.4b). Such behavior was directly related to the oxygen availability and the S/DO ratio in the liquid phase. A linear decrease of the inlet O_2/H_2S volumetric ratio (from 42.2 down to 8.4 *% v* v^{-1}) along the experiment led to oxygen limiting conditions. Thus, elemental sulfur production over sulfate production was favored. No thiosulfate production was detected experimentally neither was predicted by the model.

Regarding the goodness of model predictions to experimental data, high NSE values were obtained for the fitting of H_2S concentration measured at different bed heights (Fig. 7.3a and 7.3b). In the range of 2000 to 10000 ppm_v, the model described well experimental

H_2S concentrations measured in the first and second sections, with NSE coefficients of E=0.90 and E=0.93, respectively. At an inlet concentration of 10000 ppmv, a Nash-Sutcliffe efficiency coefficient of 0.43 was obtained for the H_2S concentration measured at the BTF outlet, mainly due to a missmatch between model predictions and experimental data. However, the NSE coefficient at the BTF outlet in the range of 2000 to 8000 ppm_v was E=0.90.

A mismatch between model prediction and experimental data of the BTF outlet concentration during the 10000 ppm_v step mighty be related with the H_2S measurement system. At 10000 ppm_v a higher airflow rate is needed to dilute the biogas flow rate in order to measure H_2S concentrations inside the sensor measurement range. Therefore, less exact and precise experimental data is obtained. Additional details of BTF gas measurement system can be found in Chapter 4 (*see section 4.1.1*)

Regarding to the predictions on the elemental sulfur accumulation (m_S^0), a NSE coefficient of E=0.94 was obtained, indicating an accurate fit of the model to experimental data for the production of elemental sulfur. From Fig. 4b it can be observed how the predicted sulfate concentration values fits almost perfectly to all experimental points, although during the step concentration of 4000 ppmv the simulated $C_{L,SO4}^{2-}$ was a 15% higher than the experimental measure. Such difference was attributed to a biological delay time of microorganisms in the BTF to start to produce sulfate, since the first step-wise LR increment up to 4000 ppm_v was the first performed in the reactor after a long stationary feeding period at 2000 ppm_v of 42 days. The model reproduced well the sudden $C_{L,SO4}^{2-}$ concentration deacrease during the last concentration step of 10000 ppm_v as a consequence of both the unfavorable S/DO ratio and the amount of elemental sulfur accumulated in the BTF bed. A NSE coefficient of E=0.75 was calculated for sulfate concentration predicted considering the whole period of the 2000-10000 ppm_v stepwise increase experiment (Fig. 7.4b).

In Fig. 7.3 and Fig. 7.4 experimental results and model predictions of the effect of stepwise LR increases due to H_2S inlet concentration increases corresponding to the model calibration period are presented. Experimental data in both figures indicate that the system was able to remove almost 100% of inlet H_2S at all H_2S LR (Fig. 7.3a and 7.3b). However, 100% sulfate production only occurred at the lowest H_2S LR corresponding to an inlet concentration of 2000 ppmv. Further information related to sulfate production in this experiment can be found in Chapter 5. Thereafter, elemental sulfur was accumulated in the

packed bed (Fig. 4a). At the highest H_2S LR tested the sulfate production was lower than the elemental sulfur produced, which lead to a decrease of the concentration of sulfate measured in the liquid phase (Fig. 7.4b). Such behavior was directly related to the oxygen availability and the S/DO ratio in the liquid phase. A linear decrease of the inlet O_2/H_2S volumetric ratio (from 42.2 up to 8.4 % v v^{-1}) along the experiment led to limiting oxygen conditions. Thus, elemental sulfur production over sulfate production was favored. No thiosulfate production was detected experimentally neither was predicted by the model.

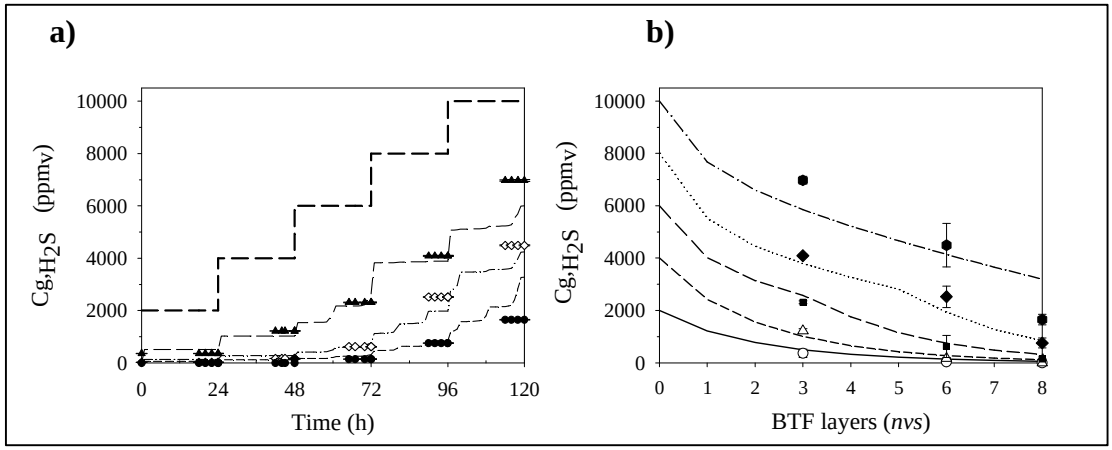

Figure 7.3. Experimental and predicted H_2S concentration during period 1 after model calibration. (a) Experimental and simulated H_2S concentration profiles at different BTF bed heights. (b) Experimental and simulated H_2S concentration along the BTF height. Fig. 7.3a: Inlet H_2S concentration (solid line), experimental and simulated data from the 1st bed (▲ and medium dashed line), the 2nd bed (◊ and dashed-dot line), and the 3rd bed (● and short dashed line). Fig. 7.3b: Experimental and simulated data at a LR of 56.3 g S-H_2S m^{-3} h^{-1} (○ and solid line), 112.9 g S-H_2S m^{-3} h^{-1} (△ and short dashed line), 169.6 g S-H_2S m^{-3} h^{-1} (■ and medium dashed line), 226.6 g S-H_2S m^{-3} h^{-1} (◆ and dot line), and 283.8 g S-H_2S m^{-3} h^{-1} (⬣ and dashed dot line).

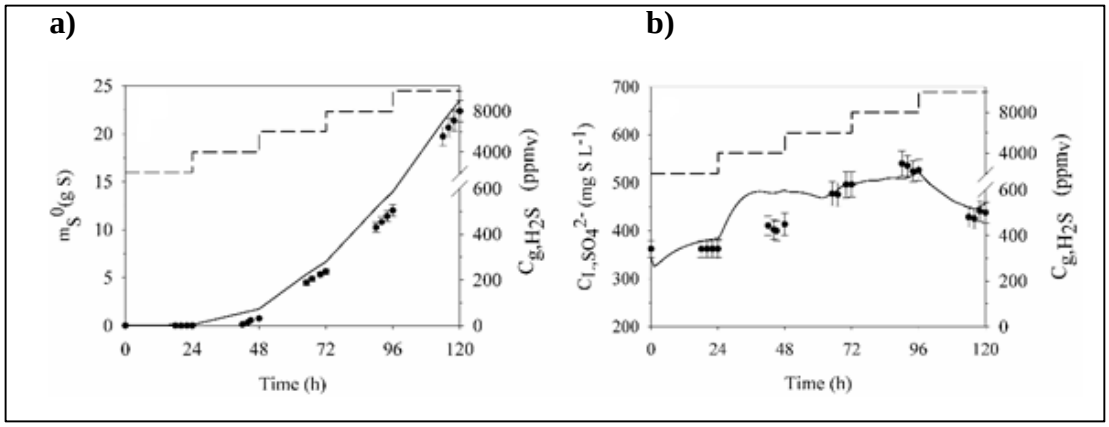

Figure 7.4. H_2S inlet concentration (dashed line) and experimental (simbols) and predicted profiles (solid lines) of cumulative mass of (a) elemental sulfur and (b) sulfate during model calibration.

Regarding the goodness of model predictions to experimental data, high NSE values were obtained for the fitting of H_2S concentration measured at different bed heights (Fig. 7.3a and 7.3b). In the range of 2000 to 10000 ppm_v, the model described well experimental H_2S concentrations measured in the first and second sections, with NSE coefficients of E=0.90 and E=0.93, respectively. At an inlet concentration of 10000 ppmv, a NSE coefficient of 0.43 was obtained for the H_2S concentration measured at the BTF outlet, mainly due to a missmatch between model predictions and experimental data. However, the NSE coefficient at the BTF outlet in the range of 2000 to 8000 ppm_v was E=0.90.Mismatch between model prediction and experimental data of the BTF outlet concentration during the 10000 ppm_v step mighty be related with the H_2S measurement system. At 10000 ppm_v a higher airflow rate is needed to dilute the biogas flow rate in order to measure H_2S concentrations inside the sensor measurement range. Therefore, less exact and precise experimental data is obtained.

Regarding to the predictions on the elemental sulfur accumulation (m_S^0), a NSE coefficient of E=0.94 was obtained, indicating an accurate fit of the model to experimental data for the production of elemental sulfur. From Fig. 7.4b it can be observed how the predicted sulfate concentration values fits almost perfectly to all experimental points, although during the step concentration of 4000 ppmv the simulated $C_{L,SO4}^{2-}$ was a 15% higher than the experimental measure. Such difference was attributed to a biological delay time of microorganisms in the BTF to start to produce sulfate, since the first step-wise LR increment up to 4000 ppm_v was the first performed in the reactor after a long stationary feeding period at 2000 ppm_v of 42 days. The model reproduced well the sudden $C_{L,SO4}^{2-}$ concentration deacrease during the last concentration step of 10000 ppm_v as a consequence of both the unfavorable S/DO ratio and the amount of elemental sulfur accumulated in the BTF bed. A NSE coefficient of E=0.75 was calculated for sulfate concentration predicted considering the whole period of the 2000-10000 ppm_v stepwise increase experiment (Fig. 7.4b).

7.3.3 Model Validation

After calibration, the response of the model was evaluated in a different experimental period from that used for calibration. A stationary feeding period of 42 days was used to validate the model, corresponding to period 2 in Table 7.1. Experimental data of cumulative mass of elemental sulfur and sulfate concentration and model predictions under the stationary feeding period for model validation are presented in Fig. 7.5.

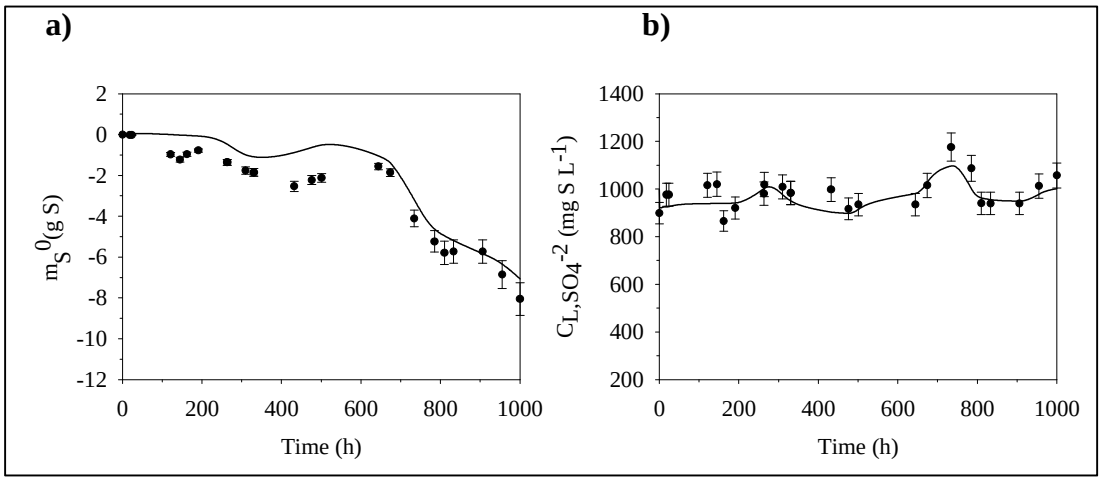

Figure 7.5. Experimental (symbols) and model predictions (solid lines) during the stationary feeding period: (a) cumulative mass of sulfur and (b) sulfate concentration.

The BTF performance during period 2 was always close to the optimal, since H_2S RE was 100% and sulfate selectivity higher than 100% was calculated. Since the H_2S LR during the experimental period corresponded to more than 100% sulfate production, elemental sulfur was progressively de-accumulated from the packed bed (Fig. 7.5a). The relatively small amount of sulfate produced from such elemental sulfur de-accumulation compared to that produced due to the H_2S fed led to a relatively constant sulfate profile along the monitored period. The above mentioned elemental sulfur de-accumulation was verified in order to determine if was due to a miscalculation in the mass balance or due to errors in the measurement of sulfate concentration by ionic chromatography (IC). For this reason sulfate concentration, directly related to elemental sulfur de-accumulation, was determined when sulfate production was higher than 100%.

Then, the ratio between the sulfate concentration related to elemental sulfur de-accumulation and sulfate concentration measured by IC was determined (Fig. 7.6). Results showed that the sulfate concentration produced from elemental sulfur de-accumulation was higher than the experimental error of IC (5%) (Fig. 7.6). Therefore the sulfate concentration increases during a stationary feeding period was confirmed to be due to elemental sulfur de-accumulation. The model was able to accurately reproduce the elemental sulfur de-accumulation along this period. Despite of experimental data variability, model predictions showed an excellent agreement with experimental data. NSE coefficients of E=0.87 and E= 0.92 were obtained along period 2 for the cumulative mass of sulfur and sulfate

concentration, respectively, reflecting that there were no significant difference between experimental sulfate concentration and that predicted by the model

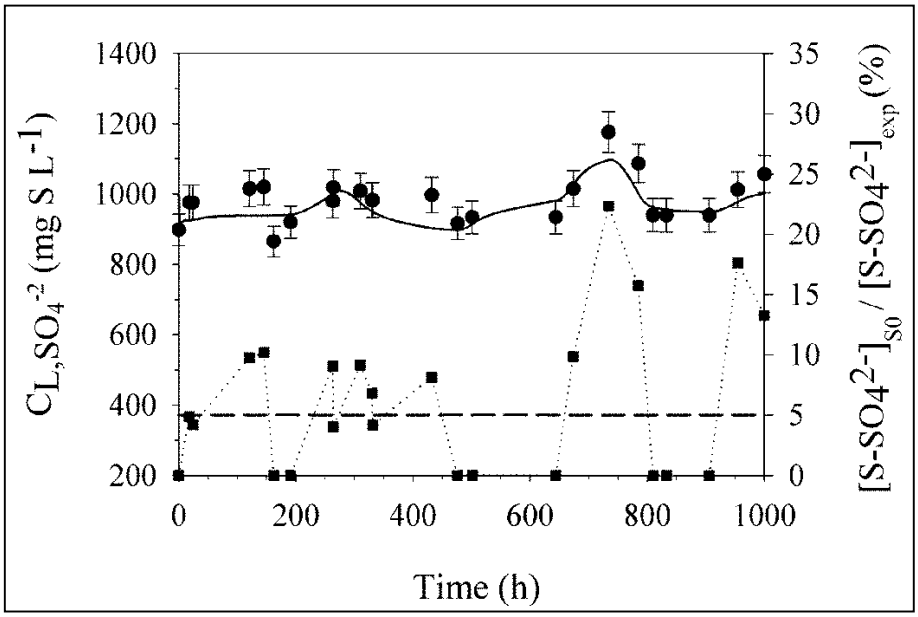

Figure 7.6. Ratio between sulfate concentration related to elemental sulfur de-accumulation and sulfate concentration measured with the ionic chromatography ($[S\text{-}SO_4^{2-}]_{S0}$ /$[S\text{-}SO_4^{2-}]_{exp}$). Experimental sulfate concentration (●), simulated sulfate concentration (solid line), experimental $[S\text{-}SO_4^{2-}]_{S0}$ to $[S\text{-}SO_4^{2-}]_{exp}$ ratio (■) and 5% of $[S\text{-}SO_4^{2-}]_{S0}$ to $[S\text{-}SO_4^{2-}]_{exp}$ ratio (dashed line).

Moreover, the model was used to simulate the performance of the reactor under dynamic conditions (Table 7.1), in order to simulate daily load fluctuations commonly found in real facilities. Dynamic model validation results are shown in Fig. 7.5. To properly assess the dynamics, the plant was fed a constant H_2S LR of 56 g m^{-3} h^{-1} during 190h. Thereafter, the inlet dynamic profile was activated at an average H_2S LR of 79 g m^{-3} h^{-1} with maximum and minimum peak H_2S LR of 141 and 28 g m^{-3} h^{-1}. The BTF model response properly fits the experimental data during the change of dynamics represented in Fig. 7.7. . During the first stage of 190h during the stationary feeding period, the model predicted correctly the $C_{L,SO4}^{2-}$ experimental data. When variable H_2S LR conditions were applied, a transient period with an increased sulfate concentration was observed until t=240h. Thereafter, $C_{L,SO4}^{2-}$ concentration remained oscilating in a constant range. The model was able to reproduce properly both the transient period and the pseudo steady-state period under a

variable inlet load. The goodness of the fitting was confirmed with a NSE coefficient of E=0.60.

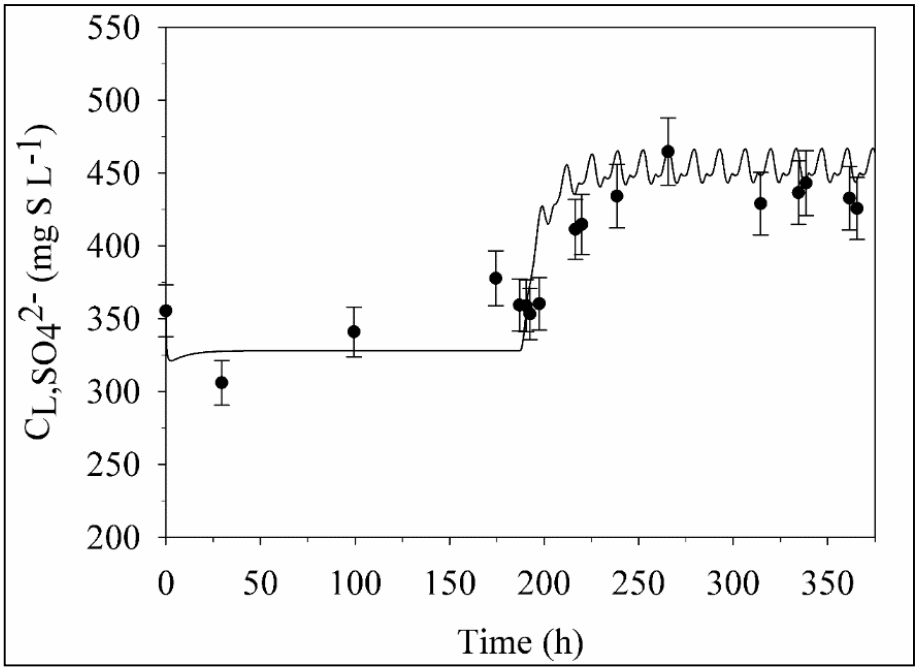

Figure 7.7. Sulfate concentration comparison betweeen experimental data (symbol) and model predictions (solid line) during dynamic validation.

Overall, the model showed to be valid to describe the main processes occurring in the three phases of a BTF, gas phase (Fig 7.3a and 7.3b), liquid phase (Fig.7. 4a, 7.5b and 7.6) and solid phase as elemental sulfur (Fig. 7.4b and 7.5a), in a co-current flow mode configuration. Thus, this model becomes a powerful tool to predict the main intermediate (elemental sulfur) and final product (sulfate) of H_2S oxidation along different operational conditions such as pseudo steady-state conditions and variable LR conditions. Especially, accurate model predictions under high H_2S LR and O_2 limiting conditions (period 1) could be useful for predicting elemental sulfur accumulation in industrial BTF.

Therefore, maintenance tasks can be strategically planned. Moreover, the BTF model can be used for the development and simulation of control strategies towards process optimization. Parameters related to O_2 transport are crucial in order to completely oxidize H_2S and avoid the formation of elemental sulfur in the BTF bed, since an excessive accumulation of elemental sulfur can significantly diminish the reactor performance.

Therefore, control strategies must be based on the improvement of the oxygen transfer to the liquid phase towards process optimization.

7.4. CONCLUSIONS

A dynamic model for a BTF for high H_2S LR biogas desulfurization in aerobic conditions was developed and successfully calibrated and validated, allowing a proper description of different operational scenarios such as LR increments due to H_2S concentration increases in the biogas stream. Furthermore the behavior of the different phases (gas, liquid, biofilm and elemental sulfur) involved in the biogas desulfurization were correctly predicted. Also the application of a two-step sulfide oxidation kinetic model was successfully performed in order to describe intermediate oxidation products.

A preliminary assessment through a relative sensitivity analysis allowed determining the most sensitive parameters of the model. Parameters related to O_2 mass transport exhibited a larger influence to model output variables considered (RE, $C_{L,SO4}^{2-}$ and m_S^0). The proposed model was calibrated using experimental data, which allowed describing accurately the outlet H_2S concentration profile along the BTF bed during H_2S LR increments. Besides describing properly sulfate production, elemental sulfur, the main intermediate product during H_2S oxidation, was correctly predicted. Mass transfer parameters (δ_B, δ_L, $K_{L,H2S}$) and kinetic parameters (X, $\mu_{max,2}$) were estimated during BTF model calibration.

Moreover, the BTF model was validated under a stationary feeding period and a dynamic H_2S LR period. Proper gas phase description during both periods was obtained. More importantly, elemental sulfur and sulfate were also in agreement with experimental data. Dynamic validation results demonstrated that the model is able to predict correctly the BTF operation when a variable H_2S LR profile is applied. Hence the BTF model here presented is capable to predict the BTF performance under similar conditions as those found in real plants, making it a suitable tool in order to develop and design control strategies towards process optimization of desulfurizing BTFs.

CHAPTER 8

MODEL-BASED ANALYSIS OF CONTROL STRATEGIES IN AN AEROBIC BIOTRICKLING FILTER FOR BIOGAS DESULFURIZATION

8. MODEL-BASED ANALYSIS OF CONTROL STRATEGIES IN AN AEROBIC BIOTRICKLING FILTER FOR BIOGAS DESULFURIZATION

Motivations

The finality of this chapter was, besides presenting another application of the BTF model calibrated and validated in the previous chapter, to study a range of feedback control strategies to control the outlet gas concentration of biogas desulfurization BTFs under aerobic conditions. Also, the study pursues to determine the controllability limits of the process under variable loading rate conditions and to study the added value of these strategies in increasing the selectivity of sulfate production. Moreover, in order to improve gas-liquid transfer at variable trickling liquid velocities a mass transfer correlation was added to the BTF model. Results obtained in this chapter were useful at the time of planning and designing control strategies in the lab-scale BTF reactor.

ABSTRACT

Further research is needed in order to optimize biological H_2S removal in biotrickling filters to enhance process reliability and, therefore, expand their field of application. To achieve robust operation, a larger degree of process monitoring and process control is required. Since H_2S loading rate on real plants may vary depending on many factors such as upstream conditions and seasonal or daily variations, process control is needed for a reliable operation. However, this is a topic not commonly addressed. The most common H_2S loading rate disturbances on a biotrickling filters are mainly due to biogas flow and H_2S inlet concentration variations, while the main manipulated variables in biotrickling filters are the air flowrate and the trickling liquid velocity. However, control loops are not widely implemented in industrial biotrickling filters to face such disturbances. In essence, O_2 outlet concentrations are controlled in feedback control loops to avoid excessive biogas dilution through the regulation of the air flowrate. Nevertheless, such control strategy often leads either to biogas dilution or to elemental sulfur accumulation. The aim of this study was to evaluate and to show the control limits, capabilities and added value of different control strategies, through biotrickling filters modelling. A model-based analysis was performed for a range of classical proportional and proportional integral feedback controllers (based on airflow regulation and O_2 measurements versus trickling liquid velocity regulation coupled to H_2S measurements) in order to determine the stability and controllability limits of the different strategies.

8.1. INTRODUCTION

Biogas desulfurization using biotrickling filters (BTFs) represents a significant technological innovation that serves to improve the quality of biogas produced by anaerobic digestion in WWTPs to be further used for energy recovery in downstream processes such as electricity production. Thus, the process optimization is relevant for improving the economical balance in WWTP's, since the energy obtained from a combined heat and power system would allow wastewater treatment facilities to produce some or all of their own electricity and space heating, which would turn the WWTP into a "net zero" energy consumer. Control strategies are needed in order to have a robust and reliable desulfurization process that allows obtaining a gaseous effluent with certain characteristics independently of the operational conditions.

Process control studies on BTFs is almost null if compared to other biological processes, from technologies with the a lower implementation level such as composting treatment (Puyuelo et al., 2010) up to the most advanced and developed technologies like wastewater treatment on WWTPs (Guerrero et al., 2011) and AD (Nguyen et al., 2015). However, lately more and more interest can be observed in recent works in the literature related to the understanding of the effect of the main manipulated variables involved in the control of biogas desulfurization on BTF's (López et al., 2016a; Rodriguez et al., 2014, 2013). Moreover the degree of knowledge of this technology has allowed the calibration and validation of models for BTF's for biogas desulfurization under aerobic conditions (Bonilla-Blancas et al., 2015; López et al., 2016b) as well as under anoxic conditions (Almenglo et al., 2015). These last efforts denote a serious intent of researchers to optimize technology performance through the development of control strategies, which is still required to warrant the stability of long-term operation. As it was mentioned in previous chapters, the main restriction for obtaining a stable long-term operation of BTF's for biogas desulfurization under aerobic conditions, is the elemental sulfur accumulation inside the BTF packed bed due to insufficient oxygen (O_2) mass transfer efficiency at high H_2S LR (*See chapter 5 section 5.3.1*).

Development and optimization of control strategies is still the main challenge before improving the scaling up of biogas desulfurization from lab- and pilot-scale into industrial scale. A wider industrial application of BTFs for biogas desulfurization would help to minimize the environmental impact (reduction of greenhouse gas footprint) and to reduce

WWTP economical costs (if BTF are compared to physical-chemical technologies), due to a longer lifespan of the BTF as a result of the reduction of elemental sulfur accumulation in the BTF bed and also lengthen the lifespan of cogeneration engines.

Control strategies are needed on BTFs for biogas desulfurization in order to mitigate process disturbances. In real scale BTFs for biogas desulfurization, not only one variable can be changed at the time. It can occur that both concentration and biogas flowrate can vary simultaneously. H_2S concentration increase may happen when the organic matter content of the feedstock to an anaerobic digester increases (Syed et al., 2006). In the other hand, biogas flowrate may vary, when there are small gasholders for biogas storage or when high amounts of biogas are produced due to an increase in the feedstock to AD (Nguyen et al., 2015; Walsh et al., 1988) , which is a less probable situation since AD are usually oversized to prevent this situation. Concentration increase is the most difficult situation to predict, even some chemicals can be added during the anaerobic digestion process or micro aeration can be done to avoid H_2S formation (Krayzelova et al., 2014) always is hard to strictly predict the percentage of H_2S present in the biogas stream.

Therefore, in both cases, a control system is needed in order to prevent environmental and technical problems when unexpected H_2S LR variations occurs due to H_2S concentration increases or due to biogas flowrate increases. Typical technical problems such as massive elemental sulfur accumulation on the packed bed can lead to bed clogging in the long-term operation (Andreasen et al., 2012), therefore reducing the lifetime of the BTF. Also, emission of sulfur as SO_x to the atmosphere may occur if biogas is burned in torches or in cogeneration engines to produce electricity (Rodriguez et al., 2014; Walsh et al., 1988).

Air flow increase is one of the most extended solutions in industrial facilities to provide additional O_2 to avoid massive sulfur accumulation (Rodriguez et al., 2014). Nevertheless, this strategy drives to biogas dilution and to the consequent loss of its heat capacity. For this reason, strategies based on the improvement of O_2 transfer from the gas to the liquid phase are key to optimize the complete oxidation of H_2S to sulfate (López et al., 2016a). The objective of the strategies would be to search the enhancement of the desulfurization process without diminish biogas calorific power, e.g. due to an increase in the air supply flow. As it was found on chapter 5, strategies based on the control of the Trickling Liquid Velocity (TLV) can provide interesting results in terms of sulfate

selectivity improvement, since increasing the TLV not only the dissolved oxygen load (DOL) is improved but the penetrability of the liquid through the BTF bed, thus reducing possible dissolved oxygen (DO) gradients inside the bed without the abovementioned biogas dilution. Regulation of TLV also modifies the global mass transfer coefficient (K_La.), since TLV has a strong linear relationship with K_La. Being the wettability factor and the liquid hold-up the governing factors for the effect of TLV. Since a feedforward control strategy is presented in the following chapter, a feedback control loop is herein studied.

Before implementing a PID feedback control on a certain process, there are two critical elections that must be done in order to have an optimal design: a) selection of the feedback controller type between the Proportional (P), Proportional Integral (PI) and Proportional Integral Derivative (PID) and b) selection of the controller parameters (c_s, K_c, τ_I and τ_D). The later is known as the controller tuning problem (Stephanopoulus, 1984). The controller parameters must be properly related to the process parameters to ensure closed-loop stability while still providing effective control (Perry et al., 1997). Time-integral criteria are based on the entire response of the process, unlike the simple criteria that use only isolated characteristics of the dynamic response (e.g. decay ratio, settling time, overshoot). The most used are Integral of the Square Error (ISE), Integral of the Absolute Error (IAE) and Integral of the Time-weighted Absolute Error (ITAE) as is described by Eq. 8.1. to Eq. 8.3, respectively.

$$ISE=\int_0^\infty \varepsilon^2(t)\cdot dt \qquad \text{(Eq. 8.1)}$$

$$IAE=\int_0^\infty |\varepsilon(t)|\, dt \qquad \text{(Eq. 8.2)}$$

$$ITAE=\int_0^\infty t\cdot|\varepsilon(t)|\, dt \qquad \text{(Eq. 8.3)}$$

The focus of this chapter was to perform a theoretical analysis of feedback controllers and control strategies in an aerobic BTF for biogas desulfurization. Control strategies derive from common actuations in real BTFs as well as from experimental results from

the influence of the main manipulated variables in aerobic BTFs for biogas desulfurization (Chapter 5). In this work, the analytical approach through the use of time-integral performance criteria was used to determine the most suitable controller parameters. In previous chapters (Chapter 7) a mathematical model of a BTF for biogas desulfurization under aerobic conditions was developed and calibrated under steady and dynamic loading rate conditions. Coupling modelling and simulation has a great importance since simulation of control strategies for BTFs for H_2S removal that properly improves reactor behavior during different operational scenarios (LR increments due to concentration increase or biogas inlet flowrate increments) are lacking in literature.

8.2. MATERIALS AND METHODS

8.2.1. Empirical Mass transfer correlations

Previously (Chapter 7), BTF was simulated at a constant trickling liquid velocity (TLV), therefore gas-liquid mass transfer was defined by a unique mass transfer coefficient for O_2 and H_2S $\left(K_{L,O_2}, K_{L,H_2S}\right)$. Gas-liquid mass transfer coefficient value relies on different system-specific parameters (dimensions of the packed bed), physical-chemical parameters and operational parameters. In order to have a proper description of gas-liquid mass transfer, the effect of the variation of the main manipulated variables (TLV and air flowrate) must be included in the estimation of K_{L,O_2} and K_{L,H_2S}. The effect of air flowrate variation on gas-liquid mass transfer coefficients was not considered since in chapter 7 (*see section 7.2.4*) it was demonstrated that only the liquid-side resistance was significant. The contribution of individual mass transfer resistances in the gas phase to the overall resistance for both gas species O_2 and H_2S were only 0.18% and 9.7%, respectively.

Experimentally (*Chapter 5, section 5.3.1*) and through sensitivity analysis (Chapter 7, section 7.3.1) it was found that the main process variables, such as removal efficiency (RE), elemental sulfur and sulfate selectivity are highly sensitive to the variation of O_2 and H_2S global mass transfer coefficients $\left(K_{L,O_2}, K_{L,H_2S}\right)$ in the packed bed. Therefore it is important to select a good correlation for the global mass transfer coefficients (K_{L,O_2} and K_{L,H_2S}). In this study two empirical mass transfer correlations for packed columns, Billet and Schultes and Onda's correlation (Eq. 8.4 and 8.5) (Billet and Schultes, 1999; Onda et

al., 1968), respectively were compared in order to select the most suitable correlation for describing gas-liquid mass transfer in our process.

$$K_{L,i}=C_L \left(\frac{\rho_L \cdot g}{\mu_L}\right)^{1/6} \left(\frac{D_L}{d_h}\right)^{0.5} \left(\frac{u_L}{a_p}\right)^{1/3} \quad \text{(Eq. 8.4)}$$

Where:

$K_{L,i}$= Global mass transfer coefficient in liquid for component *i*, m h^{-1}

C_L= Packing material specific constant

ρ_L= Liquid density, kg m^{-3}

g= Gravitational constant, m s^{-2}

μ_L= Liquid viscosity, kg m^{-1} s^{-1}

a_p= packing material specific surface area, m^{-1}

d_h= hydraulic diameter of packing material defined by $4\varepsilon/a_p$, m

u_L= superficial liquid velocity, m s^{-1}

D_L= Diffusion coefficient, m^2 s

$$K_{L;i}=0.0051 \left(\frac{L}{A_w \cdot \mu_L}\right)^{2/3} \left(\frac{\mu_L}{\rho_L \cdot D}\right)^{-0.5} \left(aD_p\right)^{0.4} \left(\frac{\rho_L}{\mu_L \cdot g_c}\right)^{-1/3} \quad \text{(Eq. 8.5)}$$

Where:

$K_{L;i}$= Mass transfer coefficient in liquid for component *i*, m h^{-1}

L= Superficial mass velocity of liquid, kg m^{-2} h^{-1}

ρ_L= Liquid density, kg m^{-3}

μ_L= Liquid viscosity, kg m^{-1} s^{-1}

g_c= Gravitational constant, m s^{-2}

A_w= wetted area, m^2

D= Diffusion coefficient, m^2 s^{-1}

a= packing material specific surface area, m^{-1}

In equation 8.4 and 8.5 TLV is named differently, in Eq. 8.4 as u_L, the superficial liquid velocity and in Eq. 8.5 as L, the superficial mass velocity of liquid which can be related to TLV through the liquid density and the cross sectional area of the bed. Operationally, TLV is regulated through the liquid recirculation flowrate. In order to choose the gas-liquid mass transfer coefficient, two different tests were performed. The first one aimed at evaluating how TLV affects K_L value for each mass transfer correlation while a second test aimed at evaluating the effect of the mass transfer correlation on the BTF model performance.

Effect of TLV on the gas-liquid mass transfer correlations

Firstly different TLV values in the typical range for BTF's between (5-30 m h^{-1}) (Kim and Deshusses, 2008), were evaluated directly on Billet and Schultes and Onda's correlation. Results here obtained where compared with the $K_{L,H2S}$ obtained during model calibration (López et al., 2016b).

Effect of the mass transfer correlation on the BTF model performance

Such effect was assessed in a range of simulations of a set of operational conditions (Table 8.1) similar to those presented for the constant TLV experiment on chapter 5 (*See table 5.2 section 5.2.4*).

Table 8.1. Operational conditions for K_{L,H_2S} evaluation

[H_2S] *(ppm_v)*	**[H_2S] LR** *(g S-H_2S m^{-3} h^{-1})*	**O_2/H_2S** *(% v v^{-1})*	**TLV** *(m h^{-1})*
2000	56.3	42.2	
4000	112.9	21.0	
6000	169.6	14.0	4.4
8000	226.6	10.5	
10000	283.8	8.4	

Afterwards, results predicted by the model obtained from evaluating both correlations where compared with experimental data obtained under similar operational

conditions. Further information about experimental conditions can be found in Chapter 5 (*see section 5.2*).

8.2.2. Framework for analysis of open-loop behavior: Effect of H_2S LR changes due to H_2S inlet concentration and biogas flowrate changes on BTF performance

Operational conditions were varied from reference conditions under open-loop conditions, as shown in table 8.2, in order to evaluate the BTF performance when a perturbation occurs. Further information about the reference conditions can be found in (López et al., 2016a). H_2SLR was first varied due to H_2S concentration increases and secondly due to biogas flowrate increases, two of the most common perturbations occurring during biogas desulfurization in BTFs.

In the first case, namely Open-loop Concentration, five H_2SLR were tested separately from 2000 ppm_v to 10000 ppm_v. Each H_2S LR was evaluated separately and simulated enough time in order to achieve steady-state conditions. H_2S LR was modified by increasing the H_2S gas flowrate while the carrier gas (N_2) flowrate was decreased in order to keep constant the biogas flowrate. The O_2/H_2S inlet volumetric ratio depends on the air flowrate and of the H_2S gas flowrate, and therefore during Open-loop concentration changes, the ratio decreases linearly from 42.2 until 8.4 *% v* v^{-1} due to H_2S flowrate increase under constant airflow conditions. The second case, namely Open-loop EBRT, five different H_2S LR were evaluated modifying the biogas flow rate from 61.5 L h^{-1} to 307.5 L h^{-1}, resulting in an EBRT decrease from 118 s to 48.4 s. Such EBRT reduction corresponds to a 59.3 % reduction of EBRT of the reference case.

Afterwards, sulfur and O_2 mass balances were performed in order to complete the evaluation of the process performance for both cases. Each H_2SLR was evaluated separately and simulated enough time in order to achieve steady-state conditions. Information related model performance obtained in this section was also useful to delimit the operational conditions for the closed-loop tests.

Table 8.2. Reference conditions for Open-loop tests

Variable	Reference case	Open-loop Concentration	Open-loop EBRT
[H_2S] *(ppm_v)*	2000	2000-10000	2000
[H_2S] LR *(g S-H_2S m^{-3} h^{-1})*	56.3	56.3-281.55	56.3-281.55
Q_{biogas} *(L h^{-1})*	61.5	61.5	61.5-307.5
Q_{air} *(L h^{-1})*	24.15	24.15	24.15
O_2/H_2S *(% v v^{-1})*	42.2	42.2-8.4	42.2-14.10
TLV *(m h^{-1})*	5.9	5.9	5.9
EBRT *(s)*	118	118	118-48.4
HRT *(h)*	9	9	9

8.2.3. Framework for analysis for Closed-loop behavior: Effect of H_2S LR changes due to H_2S inlet concentration and biogas flowrate changes on BTF performance

When perturbations such as an increase in the H_2S inlet concentration (Fortuny et al., 2008; López et al., 2016a) or an increase in the biogas flowrate (Montebello et al., 2012) occur process performance is diminished and, therefore, control is needed in order to improve process performance during variable H_2S LR conditions. Before evaluating how the process can be improved by coupling a feedback controller, the type of feedback controller Proportional (P), Proportional Integral (PI) or Proportional Integral Derivative (PID) and the values of the parameters of the controller must be selected.

Two case studies were analyzed in order to evaluate feedback control strategies in a BTF for biogas desulfurization when H_2S LR is varied from the reference conditions value 56.3 g S-H_2S m^{-3} h^{-1} until 168.9 g S-H_2S m^{-3} h^{-1} due to H_2S inlet concentration or due to biogas flowrate changes. H_2S LR conditions presented in this section were also tested under open-loop conditions in order to quantify process improvement when control loop is implemented. The first case evaluated was the effect of changes in the H_2S inlet concentration, which was step-wise increased from 2000 ppm_v until 6000 ppm_v as shown in Fig. 8.1a. As it was done in the Open-loop framework (*Section 8.2.2*), each concentration was evaluated enough time in order to achieve steady-state conditions as well as to study the long-term effect of the disturbances.

The second case evaluated was the effect of changes in the biogas flowrate performing step-wise increments from 61.5 L h^{-1} (EBRT=118 s) to 184.5 L h^{-1} (EBRT=48.4 s) as it can be observed in 8.1b. Since different perturbations lead to different controller designs, the conditions here tested were the closest conditions to those H_2S concentration ranges and EBRT ranges that can be found in BTF operating in real-scale facilities (Rodriguez et al., 2014). The first strategy studied, namely air flow regulation closed-loop (AFR-CL), is the traditional control strategy applied in BTFs (Rodriguez et al., 2014). In Fig. 8.2a a detailed description of control strategy for AFR closed-loop is presented. This strategy controls the O_2 outlet concentration through air flowrate regulation when H_2SLR is varied due to H_2S inlet concentration or biogas flowrate changes. In AFR-CL a set point (SP) of O_2 outlet concentration of 5.70 % (v v^{-1}) was established in order to calculate the error as is described in Eq. 8.6:

$$\varepsilon = y_{SP} - y_m \qquad \text{(Eq. 8.6)}$$

This SP value for the AFR-CL case was selected because under reference conditions the O_2 inlet was 5.90% and the outlet concentration is 5.70%, conditions at which complete H_2S oxidation and H_2S removal are achieved.

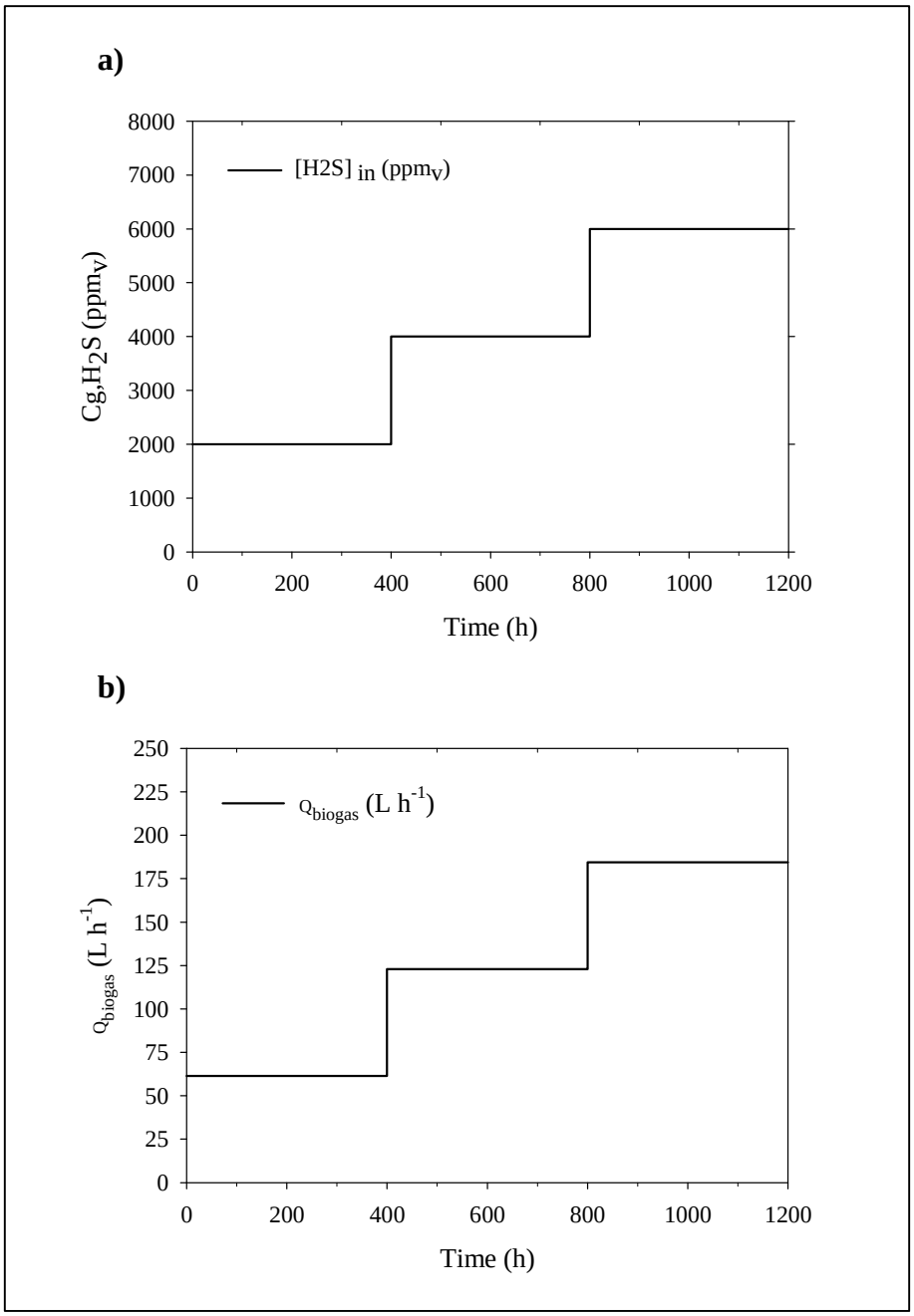

Figure 8.1. Inlet profile to simulate (a) H_2S inlet concentration changes and (b) biogas flow rate changes.

Therefore when H_2S LR increase, and consequently O_2 consume increases, the controller increases the air flowrate in order to provide more O_2 to the reactor. Regarding to the air flowrate range, this was regulated from the reference case value of 24.2 L h^{-1} to a maximum value of 120.8 L h^{-1}.

These values represent a dilution factor on biogas of 28.2 % and 66.3 % respectively. Considering that methane composition in biogas can be in the range of 50 to 70% (v v^{-1}) (Walsh et al., 1988), a minimum methane content in air of 16.88 % would be obtained when the above mentioned dilution factor is applied. According to Walsh et al. (Walsh et al., 1988), this value is higher than the percentage of methane required to obtain an explosive mixture, nonetheless a larger margin of safety should be applied for field application.

The second strategy studied, namely TLV regulation closed-loop (TLV-CL), is an innovative strategy to control biogas desulfurization in BTFs. In Fig. 8.2 (b) a detailed description of the TLV-CL control strategy is presented. This control loop aimed at controlling the H_2S gas outlet concentration through liquid recirculation flowrate regulation when H_2S LR is varied due to H_2S inlet concentration or biogas flowrate changes. In TLV-CL, the final control element is the liquid recirculation pump, which regulates the liquid recirculation flow rate that is related to TLV by Eq. 4.4 (*See Chapter 4*). A SP of H_2S outlet concentration of 100 ppm_v of H_2S was established in order to calculate the error as described in Eq. 8.6.

This SP was selected in order to produce a high-quality biogas effluent in order to enhance life time of co-generation engines or the engine where biogas is finally burned. Regarding TLV regulation limits, a minimum TLV of 5.9 m h^{-1} was applied when the H_2S outlet concentration was below the SP in order to provide nutrients and moisture to the packed bed. A maximum TLV of 28.3 m h^{-1} to prevent BTF bed flooding conditions was set. In the following Chapter (*Chapter 9*), it was proven that the BTF was able to work under TLVs higher than 28.3 m h^{-1}, but also it was found that over this value mass transfer in the aeration column was inefficient and therefore sulfate selectivity was affected.

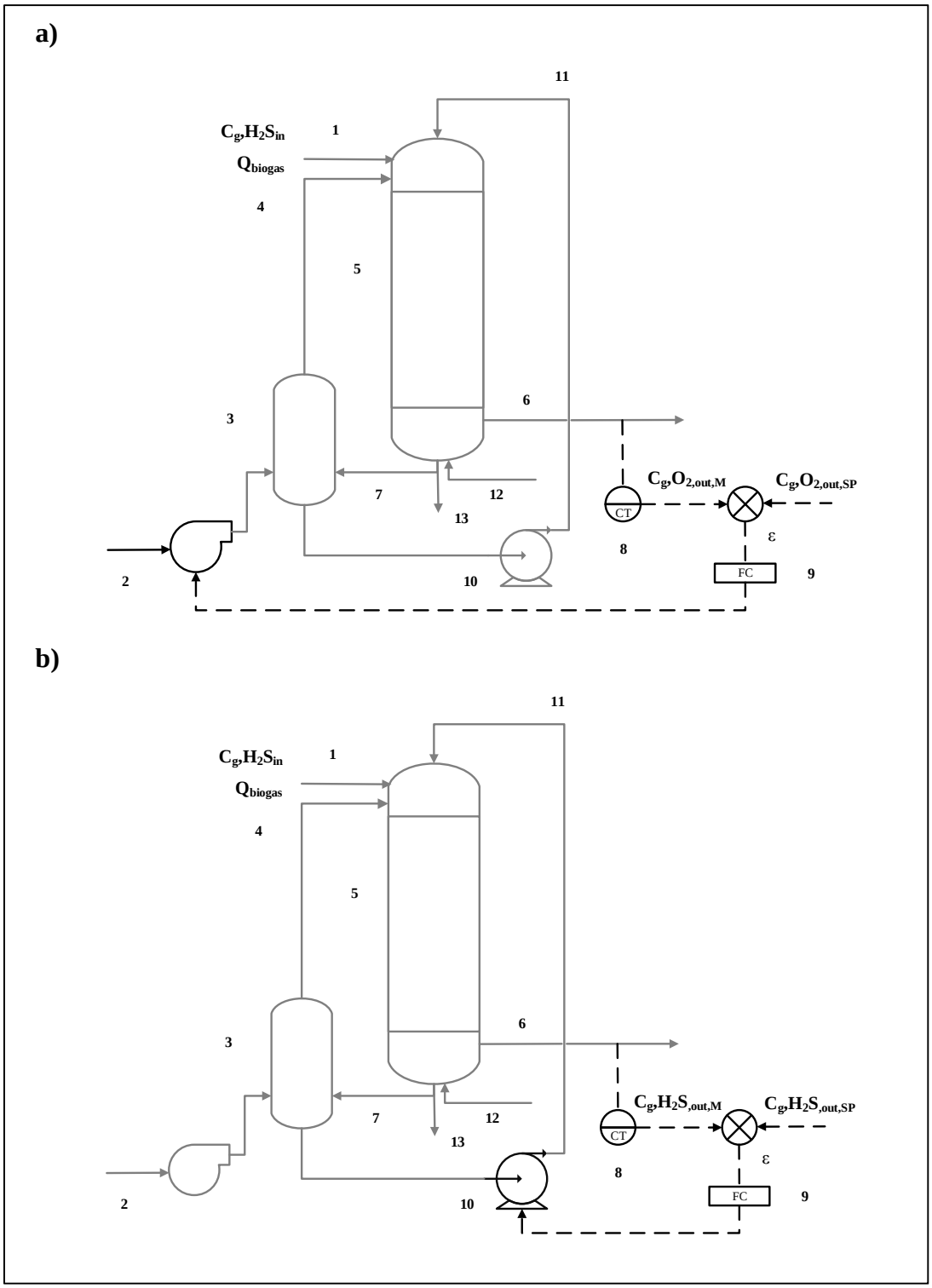

Figure 8.2 . Schematic of control strategy (a) for controlling $C_{g,O2,out}$ through gas flowrate regulation (b) for controlling $C_{g,H2S,out}$ through liquid recirculation flowrate in a co-current BTF set up: (1) biogas inlet , (2) Air flow inlet to the aeration column, (3) aeration column, (4) Air flow inlet to the BTF, (5) main reactor, (6) biogas outlet, (7) liquid recycled, (8) H_2S and O_2 transmitters, (9) feedback flow controller, (10) recycling pump, (11) recycling liquid line to the BTF (12) mineral medium and bicarbonate supply, (13) liquid purge. Q_{biogas}

8.2.4. Controllers tuning

Since in both closed-loop cases H_2S LR can be affected by the change of the H_2S inlet concentration or the biogas flowrate, different controller parameters must be applied for each case. Table 8.3 shows the different control loops that can be designed when different controlled variables and perturbations are combined with different types of feedback controllers. Note that in table 8.3 no derivative action was included because during previous tests was observed that due to the characteristics of the disturbances tested, the anticipative effect was null since the response of the process was a constant nonzero error, giving no action for the derivative term $\left(d\varepsilon/dt=0\right)$.

In order to tune the feedback controller parameters, time-integral performance criteria were used to evaluate the shape of the complete closed-loop response (Stephanopoulus, 1984). Time-integral criteria are based on the entire response of the process, unlike the simple criteria that use only isolated characteristics of the dynamic response (e.g. decay ratio, settling time, overshoot). Integral of the square error (ISE), Integral of the absolute value of the error (IAE) and integral of the time-weighted absolute error (ITAE) were determined as is described by Eq. 8.1 to Eq. 8.3, respectively.

Table 8.3. Closed-loop scenarios and control strategies studied.

Closed-loop Scenario	Controlled Variable	Manipulated Variable	Disturbances	Controller type	Parameter	Range
Air flowrate regulation	$C_{g,O2,out}$	Q_{air}	$C_{g,H_2S,in}$	P	K_c	0.005-0.2
				PI	K_c	0.005-0.2
					τ_I	1-5
TLV regulation	$C_{g,H_2S,out}$	FL	$C_{g,H_2S,in}$ & Q_{biogas}	P	K_c	1-1000
				PI	K_c	1-1000
					τ_I	0.1-10

Since the parameters that reduce the time-integral criteria may lead to any undesired process instability, production or not of oscillations in the response of the process was also considered to assess controllers response. Controller parameters ranges among the values showed in the last column of table 8.3. Lower gains were needed in order to control outlet O_2 concentration, denoting that the process was more sensitive to air flow rate changes.

While higher gain values were needed in order to control H_2S outlet concentration through TLV regulation, denoting that the process was less sensitive to TLV. This is mainly due to the gas and liquid phase dynamics, since in order to control O_2 concentration a gas phase variable is manipulated, while in order to control H_2S concentration a liquid phase variable is manipulated.

8.2.5. Added value of feedback control strategies on biogas desulfurization in aerobic BTFs

After studying the control limits and capabilities of the different control strategies presented on table 8.3, the main process performance variables such as RE, O_2 consumption, sulfate and elemental sulfur production, were included in the study. In order to evaluate the different feedback control strategies, mass balances of each simulation under closed-loop conditions were compared with mass balances of simulations under open-loop conditions. Sulfur and oxygen mass balances referred to the total amount of H_2S at the inlet were performed.

8.3. RESULTS AND DISCUSSION

8.3.1. Selection of a suitable oxygen mass transfer correlation

Effect of TLV on the gas-liquid mass transfer correlations

Dependency of $K_{L,H2S}$ on TLV for the Billet and Schultes correlation and Onda's correlation and the comparison with the K_{L,H_2S}. value obtained during BTF model calibration is presented in Fig 8.3. Billet and Schultes correlation resulted in higher $K_{L,H2S}$ than Onda's correlation. The K_L trend observed in Billet and Schultes correlation is more expected to occur in BTFs than the trend observed with Onda's correlation because when BTFs are operated at high TLV mass transfer is progressively reduced due to an increase

of water hold up in the packed bed. Also the K_{L,H_2S}. obtained during BTF model calibration is also closer to the Billet and Schultes K_{L,H_2S}. curve.

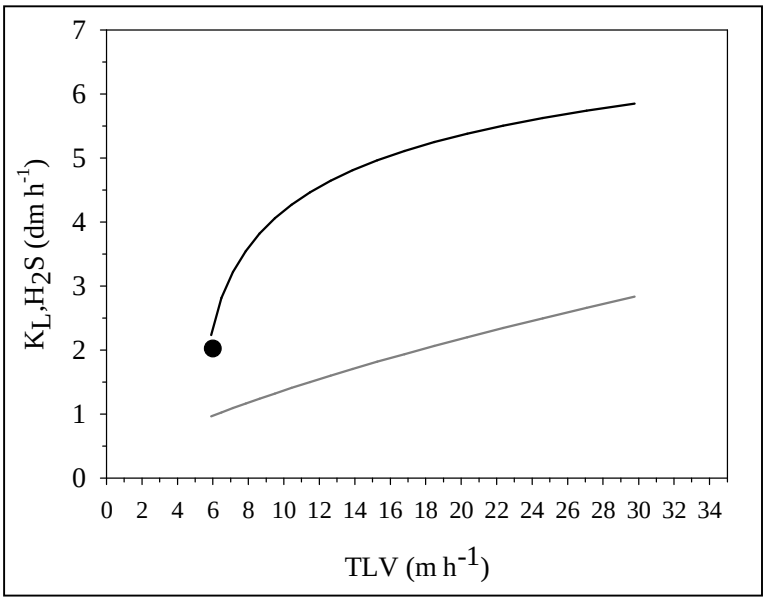

Figure 8.3. Mass transfer coefficient as a function of the TLV using the Billet and Schultes correlation (dark solid line), Onda's Correlation (gray solid line). The black dot corresponds to the K_{L,H_2S}. obtained during BTF model calibration (●) in chapter 7.

Effect of the mass transfer correlation on the BTF model performance

In Fig. 8.4 (a) and (b) experimental profiles for RE, sulfate and elemental sulfur obtained in an experiment where H_2S concentration was step-wise increased from 2000 ppm_v to 10000 ppm_v (*same experiment described in section 5.2.4, chapter 5*) performed under open-loop conditions in the lab-scale BTF are presented (López et al., 2016a) and compared with results predicted by the model under the same operational conditions using both correlations.

Fig. 8.4 shows that simulated data obtained with Billet and Schultes correlation fits better experimental data than when Onda's correlation is used. In order to evaluate the goodness of the fit to experimental data, the efficiency E criteria proposed by Nash and Sutcliffe (1970) is here used (Nash and Sutcliffe, 1970). The Nash-Sutcliffe efficiencies confirmed a better fit for the Billet and Schultes for all variables considered. The negative E value for Onda's correlation means that the average value of the experimental data is a

better predictor than the model. The reason why Onda's correlation resulted in smaller efficiencies compared to Billet and Schultes is explained in Fig. 8.4.

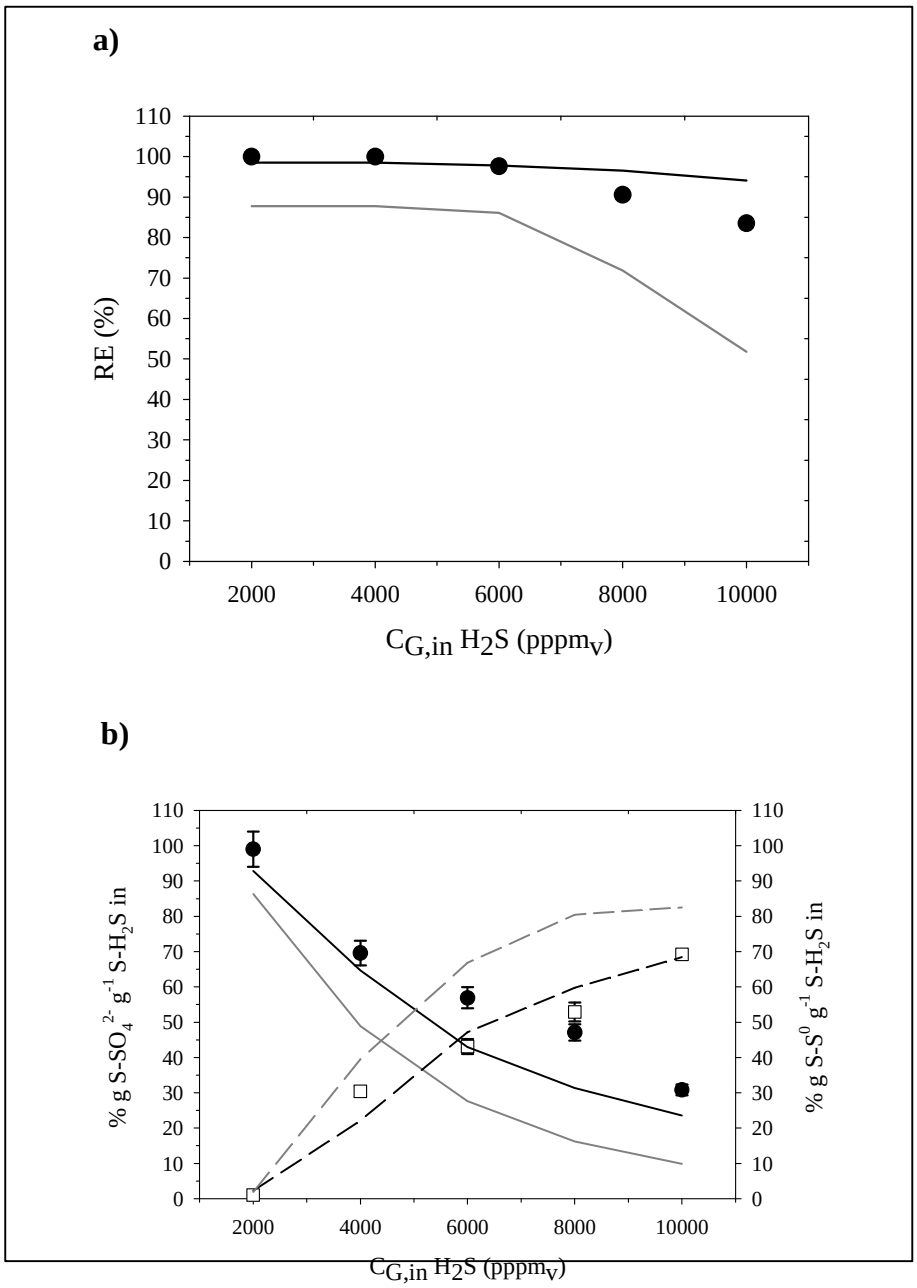

Figure 8.4. Comparison of experimental data and simulated results in open-loop condition. A) Experimental (●) and simulated RE profiles using the Billet & Schultes correlation (black solid line) and using Onda's correlation (solid dark line) and B) experimental sulfate (●) and elemental sulfur (□) selectivity; sulfate profiles simulated using Billet& Schultes (solid dark line) and Onda's correlation (solid gray line); and simulated elemental sulfur selectivity using Billet & Schultes (dashed dark line) and Onda's correlation (dashed gray line).

Table 8.5. Nash-Sutcliffe model efficiency values for Onda's and Billet and Schultes Correlation

	E,RE	E, g SO_4^{2-}g S-$H_2S_{in}^{-1}$	E, g S^0g S-$H_2S_{in}^{-1}$
Onda's Correlation	-7,65	0,26	0,70
Billet and Schultes Correlation	0,26	0,85	0,95

It can be observed that for the same TLV the Billet and Schultes correlation leads to a higher mass transfer coefficient, which results in higher gas-liquid global mass transfer and, therefore, higher values of the main variables describing BTF performance. According to the results, the Billet and Schultes correlation was chosen as the correlation to be used for simulating control strategies with the BTF model.

8.3.2. Analysis of open-loop behavior: Effect of H_2S LR changes due to H_2S inlet concentration and biogas flowrate changes on BTF performance

Steady-state results under the conditions described in section (8.2.2) are presented in Fig. 8.5. (a and b) for H_2S LR disturbances due to step-wise changes in the H_2S inlet concentration and biogas flowrate, respectively. Sulfate selectivity (g S-$SO_4^{2-}{}_{produced}$ g^{-1} S-$H_2S_{removed}$) decreased when the BTF H_2S LR increased stepwise. However, the reduction was more significant when H_2S LR increased due to biogas flowrate changes (Fig 8.5b) than to H_2S inlet concentration changes (Fig 8.5a). In the case of inlet concentration changes, sulfate selectivity was reduced from 99.8 to 80.3 %, meanwhile H_2S RE decreased from 98.5% to 42.6%. Elemental sulfur accumulation progressively increased from 0.1% to 17.8% at an inlet concentration of 10000 ppm_v of H_2S. In the case of biogas flowrate changes, sulfate selectivity was reduced from 99.8 to 75.4%, meanwhile H_2S RE decreased from 98.52% to 18.67%. Elemental sulfur accumulation progressively increased from 0.1% to 23.4% at an inlet concentration of 10000 ppm_v of H_2S.

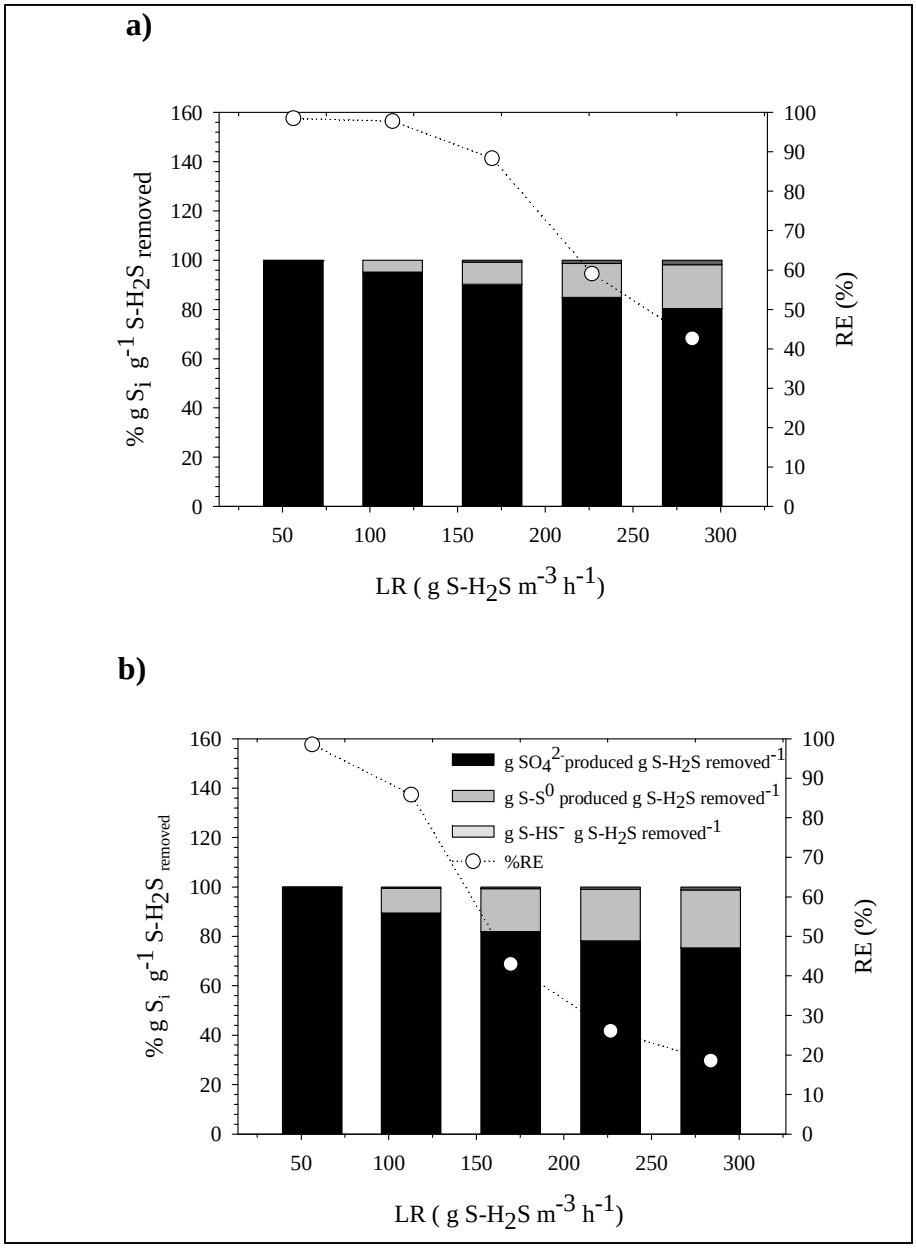

Figure 8.5. Sulfur species selectivity as function of H_2S LR step-wise changes of (a) H_2S inlet concentration and (b) biogas flowrate under open-loop conditions.

In BTFs for biogas desulfurization reduction of process performance is mainly related to biological limitation when concentration peaks occur because SOB cannot degrade the amount of contaminant transferred to the liquid phase. At some point, the dissolved H_2S concentration may even reduce the cell consumption capacity from their maximum capacity due to substrate inhibition. In addition, at increasing H_2S LR the O_2/H_2S volumetric ratio decreases, which means that the relative amount of O_2 present in the biogas, and concomitantly in the liquid phase, is reduced. Under this O_2 lack situation, elemental sulfur accumulation inside SOB cells is favored, affecting significantly the

sulfide consumption rate. If elemental sulfur is excessively accumulated inside the packed bed, the contact area for gas and liquid mass transfer may be also reduced, thus reducing the BTF performance due to a mass transfer limitation.

Moreover, Lopez et al. (López et al., 2016a) experimentally found that H_2S RE decrease could also be related to elemental sulfur accumulation inside SOB cells, even when the total contact area in the packed is not significantly modified. Instead, in BTFs for biogas desulfurization reduction of process performance is mainly related to mass transfer limitation when biogas flowrate peaks occur Operating at low EBRT values, reduces the contact time between gaseous compounds (O_2 and H_2S) and the liquid phase, affecting thus the mass transfer capacity of the process. Reducing the mass transfer efficiency of the process, affects the overall process performance as it can be observed on Fig. 8.5b.

This is reflected in the steep slopes of the H_2S-RE profile on Fig. 8.5 (b). Moreover also lower sulfate selectivities were obtained for the Open-Loop EBRT case since the process is principally mass-transfer limited due to an EBRT reduction. Regarding elemental sulfur, higher elemental sulfur selectivities are observed on Fig. 8.5b for the Open-Loop EBRT than those obtained for the Open-Loop Concentration case. Higher elemental sulfur selectivity values are obtained, since low EBRT values besides affecting H_2S RE, also affects O_2 transport. During chapter 7 (*See section 7.3.1*) it was demonstrated that parameters related to O_2 transport exhibit a larger influence on BTF process performance compared to the corresponding H_2S parameters. Results here obtained under open-loop conditions indicates that when a perturbation occurs in BTF's for biogas desulfurization, such as H_2S concentration increase or biogas flow increase the main process performance variables are significantly affected, and therefore process control need is clearly evidenced

8.3.3. Control strategies evaluation to face variable H_2S LR inlet changes

Proportional controller in a AFR-CL strategy to face H_2S inlet concentration changes.

When a proportional controller is applied to control the outlet O_2 concentration ($[O_2]_{out}$) through AFR-CL, stable actuations are obtained with Kc values lower than 0.1 and unstable/oscillating actuations with Kc values higher than 0.12 (Fig 8.6 (a and b)).

a) **b)**

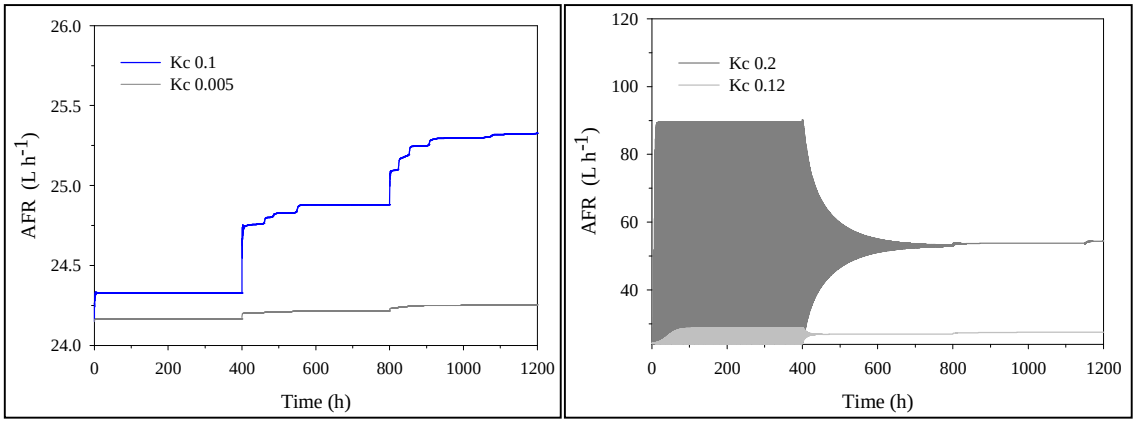

Figure 8.6. Air flowrate (manipulated variable) for oxygen control facing inlet H_2S concentration changes using a proportional controller showing stable (a) and oscillatory (b) behavior.

a) **b)**

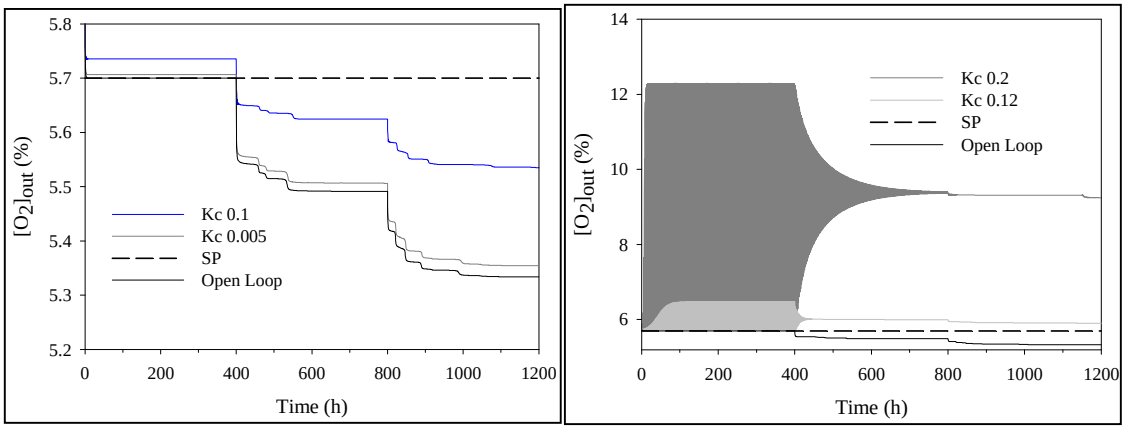

Figure 8.7. O_2 concentration (controlled variable) for O_2 control facing inlet H_2S concentration changes (Fig.8. 1 (a)) using a proportional controller showing stable (a) and oscillatory (b) behavior**.**

Regarding the controlled variable, Fig. 8.7a shows the offset between the $[O_2]_{out}$ concentration and the SP, which is reduced at increasing Kc values as expected. When Kc values higher than 0.12 are used in the proportional controller the $[O_2]_{out}$ exceeds the concentration required, and also specially during the first H_2S LR step, $[O_2]_{out}$ is unstable due to the oscillations in the actuator.

In addition, Fig. 8.8 (a and b) shows the outlet H_2S concentration found when the outlet O_2 concentration is the controlled variable when a P controller is used in the AFR-CL control strategy. When stable gain values are use, the outlet H_2S concentration is barely reduced if compared to the open-loop case. To reach significant reductions in the

outlet H_2S concentration, Kc values that lead to unstable actuations and responses should be used. Results found point at a poor added value of this strategy in terms of H_2S removal and sulfate selectivity increase since outlet H_2S reduction is mostly due to biogas dilution.

a) **b)**

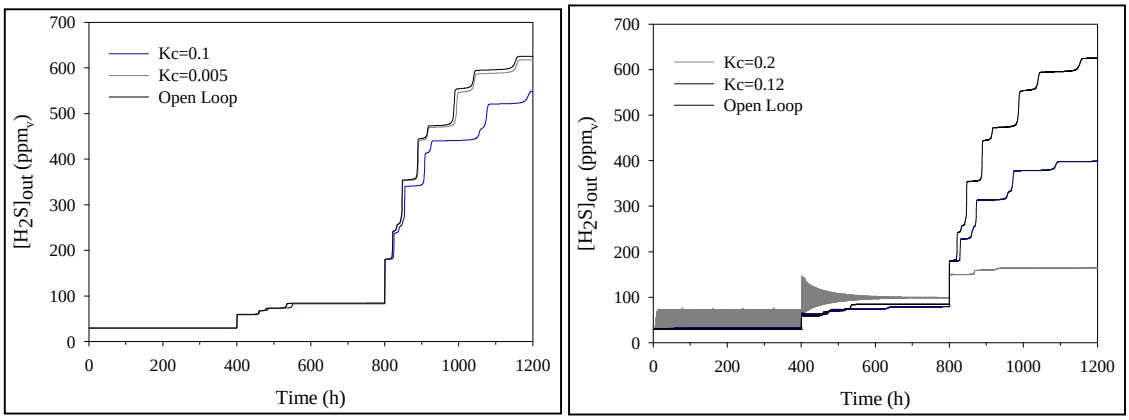

Figure 8.8. H_2S outlet concentration evolution (process variable) during O_2 control facing inlet H_2S concentration changes using a P controller showing stable (a) and oscillatory (b) behavior.

When time-integral criteria are evaluated to select the best Kc value for the proportional controller when air flowrate is regulated, two zones can be clearly distinguished in Fig. 8.9.

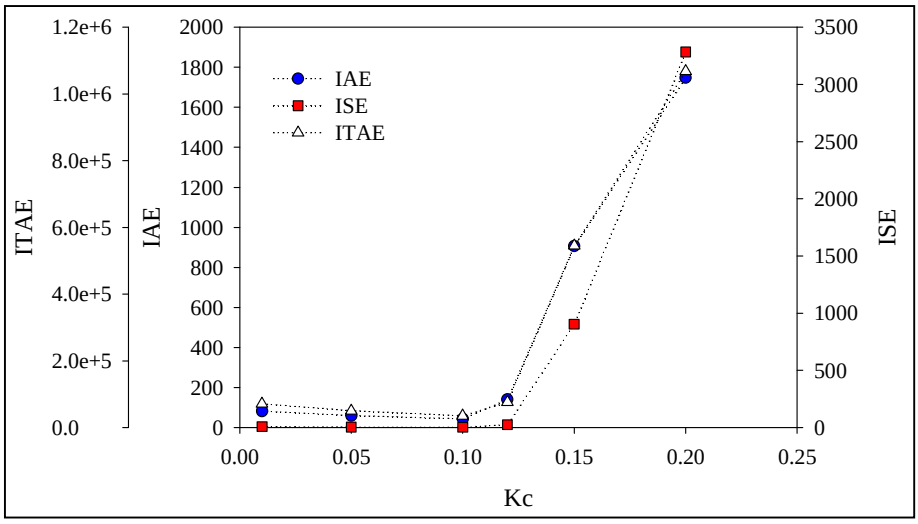

Figure 8.9 Time-integral criteria results for the different Kc values for the proportional controller for oxygen control facing inlet H_2S concentration changes (Fig.8. 1a).

Lower time-integral criteria values are obtained for Kc values lower than 0.12 for ISE and 0.10 for IAE and ITAE. In this sense the difference among integral criteria are due to ISE evaluation since the ISE criteria squares the error producing a much smaller result. Therefore IAE and ITAE seem to be more convenient criteria since the first one determines the absolute error and the second one amplifies the error by multiplying the error by the time.

Also it was important to consider simple performance criteria based on the characteristic features of the closed-loop response of the system. Since Kc higher than 0.12 produced an oscillatory actuation and therefore unstable controlled variable values, a Kc of 0.1 would be selected as the most suitable value for a proportional controller when the air flowrate is regulated during variable H_2S LR conditions due to inlet H_2S concentration increases.

Proportional-Integral controller in a AFR-CL strategy to face H_2S inlet concentration changes.

Results obtained in the previous section showed that a proportional action was not enough to control $[O_2]_{out}$ and that an integral action was needed to reduce the offset. Results of evaluating Kc and integral time (τ_I) for a PI feedback controller in the range presented in table 8.4 using an AFR-CL control strategy when H_2S LR is increased due to H_2S inlet concentration increase are presented in figures 8.10 to 8.12. For the AFR-CL control strategy, stable actuations are obtained for gain values smaller than 0.1 in combination of τ_I values smaller than 5.

As an example, Fig. 8.10a shows the results for gain values of 0.074 in combination with different values of τ_I between 1 and 5. A controller gain of 0.1 in combination with τ_I greater than 5 leads to process instability. A large τ_I means that the repetition time of the proportional action is longer. Then, the process has change dramatically when the time to apply the integral action comes, inducing the actuator to produce a strong action that destabilizes the system (Fig 8.10b).

a) **b)**

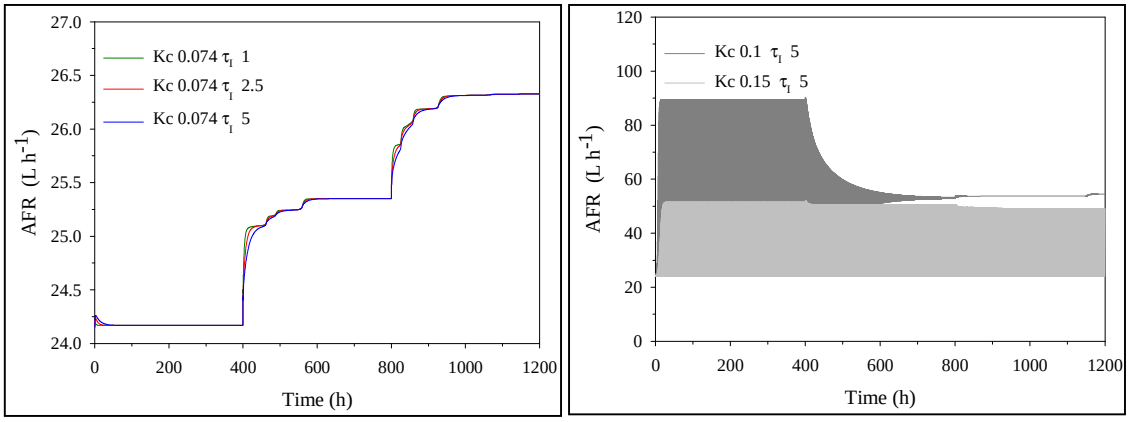

Figure 8.10. Air flowrate (manipulated variable) for O_2 control facing inlet H_2S concentration changes using a PI controller showing stable (a) and oscillatory (b) behavior.

a) **b)**

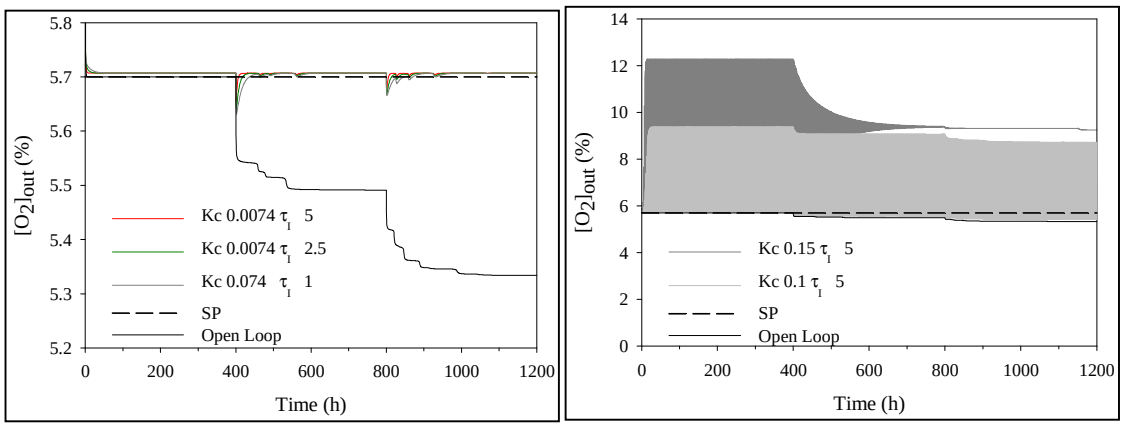

Figure 8.11. O_2 concentration (controlled variable) for O_2 control facing inlet H_2S concentration changes using a PI controller showing stable (a) and oscillatory behavior (b).

Regarding to the controlled variable, Fig. 8.11 shows different combinations of Kc and τ_I. As expected, complete offset removal was observed for Kc and τ_I values lower than 0.074 and 5, respectively. Unstable or oscillatory actuations are also translated to unstable/oscillatory process variable outputs. As abovementioned, different combinations of τ_I values with gain values equal or higher than 0.1 produces unstable actuations, which are also translated to unstable or oscillatory process variable outputs as (Fig 8.11b). Also, Fig. 8.12 shows the H_2S outlet concentration in comparison with the open-loop case when a PI controller is used in the AFR-CL control strategy.

As in the case of the P controller, stable signals produce a small reduction of the outlet H_2S concentration due to biogas dilution mainly. In the case of the proportional

integral (PI) controller, dilution increased only by 2.3% when stable responses were produced. Despite such low dilution increase, using a PI controller in the AFR-CL control strategy results useful in order to achieve the control strategy objective but is inefficient in terms of improving process variables such as H_2S removal when a set of parameters that produce a stable behavior are used.

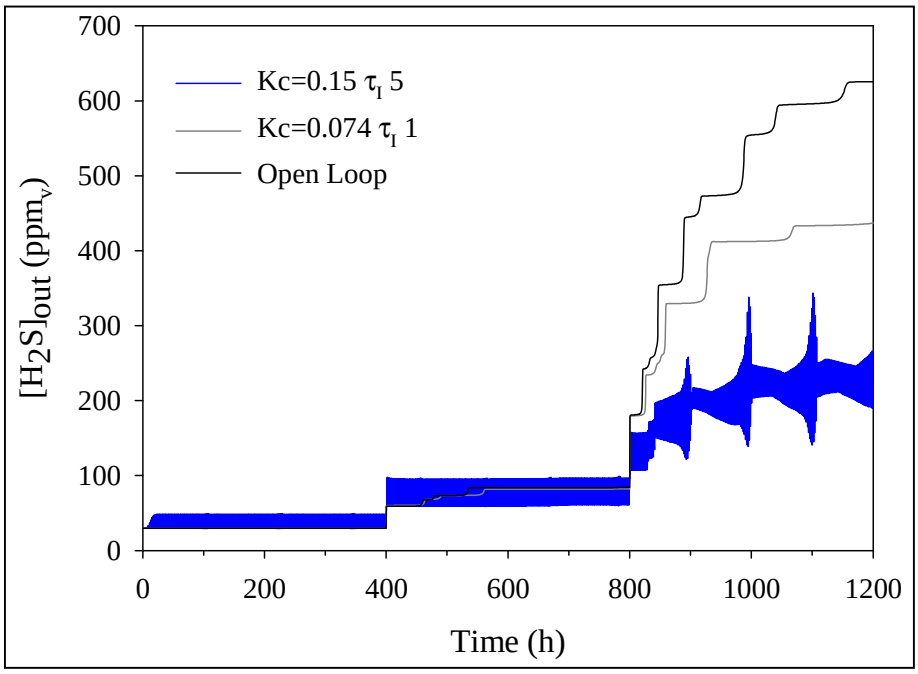

Figure 8.12. H_2S outlet concentration evolution (process variable) during O_2 control facing inlet H_2S concentration changes using a PI controller showing stable and oscillatory behavior.

Results of time-integral criteria evaluation for the PI feedback controller for the AFR-CL during variable H_2S LR conditions due to H_2S inlet concentration increase are presented in Fig. 8.13 (a,b and c). The three different criteria showed that lower time-integral criteria values (light blue area) were obtained for a Kc between 0.074 and 0.1, and $\tau_{I,}$ between 1 and 3. Dark blue areas corresponded to combinations where the parameters produces unstable/oscillating process performance, such as Kc values higher than 0.1 and $\tau_{I,}$ higher than 5.

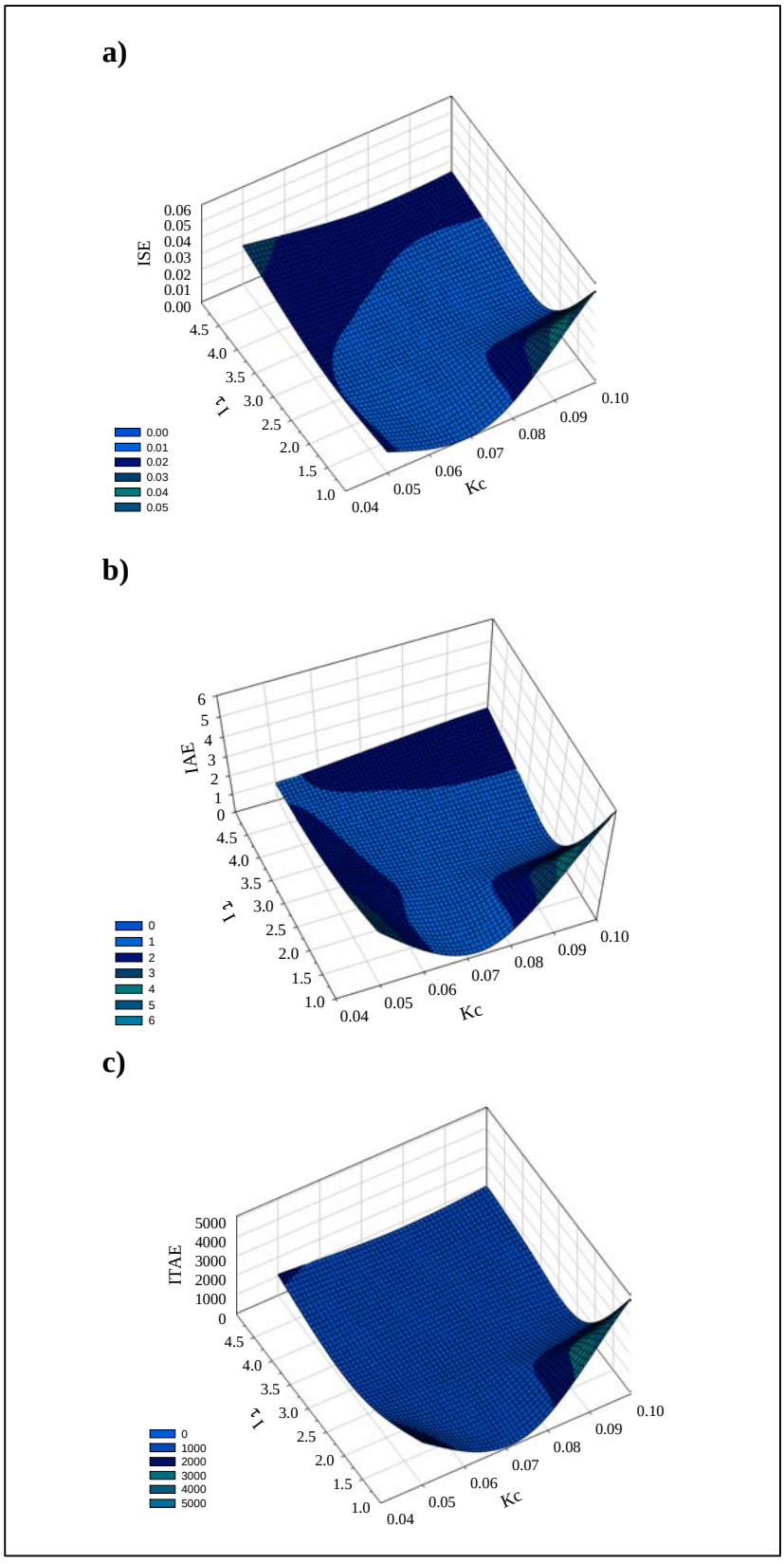

Figure 8.13. Time-integral criteria results for the different Kc and τ_I values for the values for the proportional integral controller for O_2 control facing inlet H_2S concentration changes (a) ISE mesh, (b) IAE mesh and (c) ITAE mesh.

Proportional controller in a TLV-CL strategy to face H_2S inlet concentration changes.

The TLV-CL control strategy is more complex than AFR-CL control strategy case since in order to reduce $[H_2S]_{out}$ concentration is first necessary to perform a gas-liquid mass transfer step, while for the AFR-CL control strategy the manipulated variable was acting directly in the phase of the controlled variable. As it was expected, no actuation in the controller output was observed during the first two concentration steps (Fig 8.14a) since $[H_2S]_{out}$ concentration (Fig 8.14b) was below the $[H_2S]_{out}$ setpoint. Only during the last concentration step the controller increased the TLV in order to reduce the offset between the $[H_2S]_{out}$ concentration and $[H_2S]_{out}$ SP.

a) **b)**

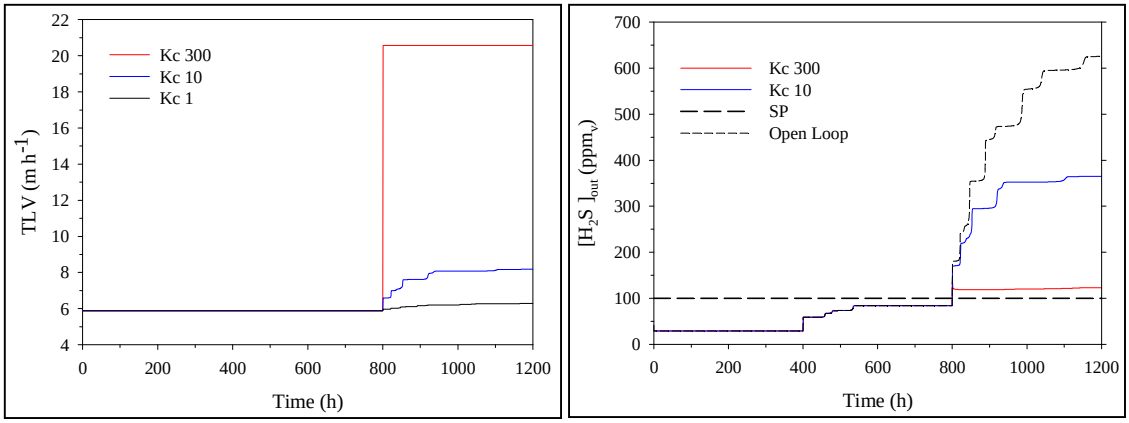

Figure 8.14. Trickling liquid velocity (a) and H_2S outlet concentration (b) for outlet H_2S concentration control using a P controller facing inlet H_2S concentration changes.

A similar behavior to that of the AFR-CL control strategy was found for the P controller in the TLV-CL control strategy. Fig. 8.14 (a and b) show that a Kc of 300 produces a significant reduction of the $[H_2S]_{out}$ offset down to values close to only 20 ppm_v. Smaller gains (blue and dark line) resulted in actuations close to the reference TLV value, producing almost no offset reduction (Fig. 8.14b). The time-integral criteria calculated at different Kc value (Fig 8.15) showed which range of Kc would be feasible to reduce the error criteria.

Fig. 8.15 shows that Kc values higher than 300 barely reduces the error criteria. Also, the higher the gain the more unstable the response was. A gain of 1000 produced an unstable response of the actuator (data not shown). Therefore, following the time-

integral criteria and the simple performance criteria, Kc values in the range of 200-300 would be selected for the proportional feedback controller in the present case.

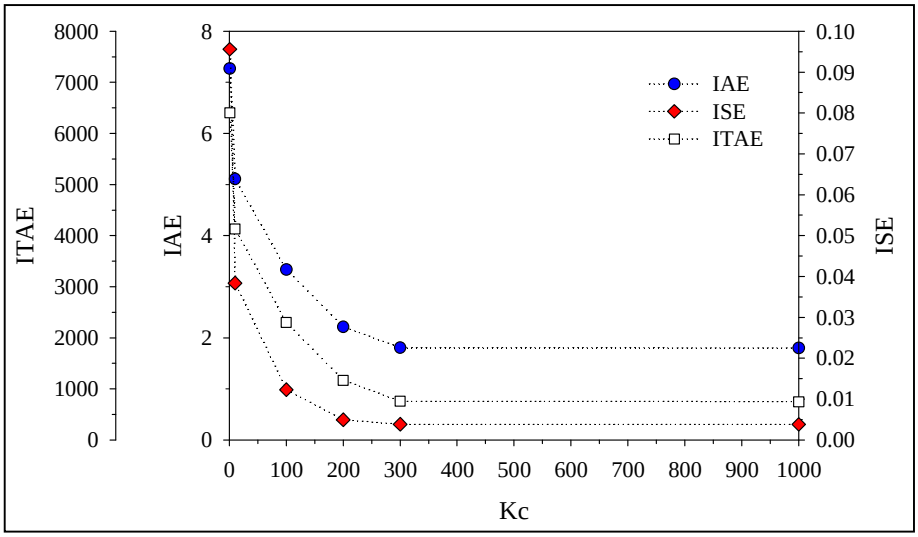

Figure 8.15. Time-integral criteria results for the different Kc values for the proportional controller for H_2S control facing inlet H_2S concentration changes.

Proportional Integral TLV control for variable H_2S LR inlet due to variable H_2S inlet concentration.

Since large Kc values in combination with low τ_I produce unstable actuations in a PI controller, Kc values for the PI controller were derived from results obtained for the P controller in the previous subsection. Unstable actuations were obtained with τ_I values lower than 0.1 for the highest Kc values tested (Kc=200 and Kc=147) as can be observed in Fig. 8.16a (dark gray and dark green lines). Instead, a stable actuation is observed for a Kc of 147 and τ_I of 1 (dark red line) (Fig. 8.16 (a)). It has to be noticed that lower actuations were obtained when the PI controller was applied, which was translated to higher offset values compared to the P controller.

At the end of the second concentration step, an offset of only 20 ppm_v was obtained with the P controller, while with the PI controller an offset of 40 ppm_v was obtained. Even if the Kc tested was increased using also a τ_I of 1 for the PI controller (data not shown), the $[H_2S]_{out}$ concentration reached was always the same. Why the same response was always obtained and, therefore, the $[H_2S]_{out}$ reached was always the same independently

of the parameters tested in the PI controller is explained by the characteristics of the error during the last H_2S inlet concentration step.

a) **b)**

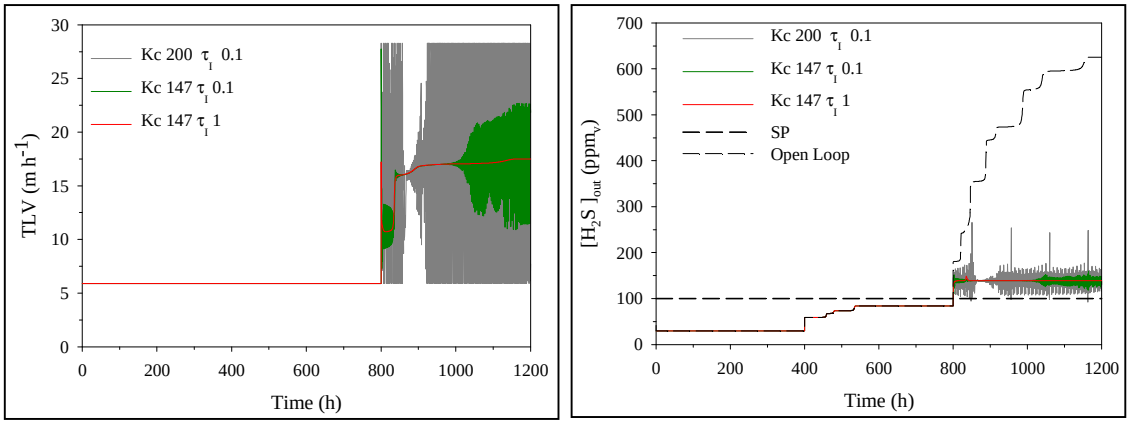

Figure 8.16. Trickling liquid velocity (manipulated variable) (a) and H_2S outlet concentration (controlled variable) (b) for H_2S control facing inlet H_2S concentration changes using a PI controller.

Once the error reached a constant value, the proportional action tends to zero and the PI controller turns to an integral (I) controller. Since during the conditions of the last step the error is constant or the increase in the error is not significant, the I action by itself is not capable to keep on increasing the TLV to decrease the outlet H_2S concentration. It has to be mentioned that this type of response of the controller is associated to the type of disturbance used in this study. In a real case, changes in the disturbance value would produce a constant error and therefore the proportional action would be canceled.

The reason why the PI controller required of lower TLV than the P controller was because during the first two H_2S concentrations tested the value of the error between the concentration measured and the SP value was negative. Thus, the sum of the proportional action plus the integral action was smaller than only the proportional action. Evaluation of time-integral criteria for the PI controller when TLV is regulated in order to control H_2S outlet concentration (Fig. 8.17) shows that there were small differences between all the cases tested for the PI controller for the three types of criteria studied. We can observe how the smaller error is obtained with the highest Kc value and the smaller τ_I value.

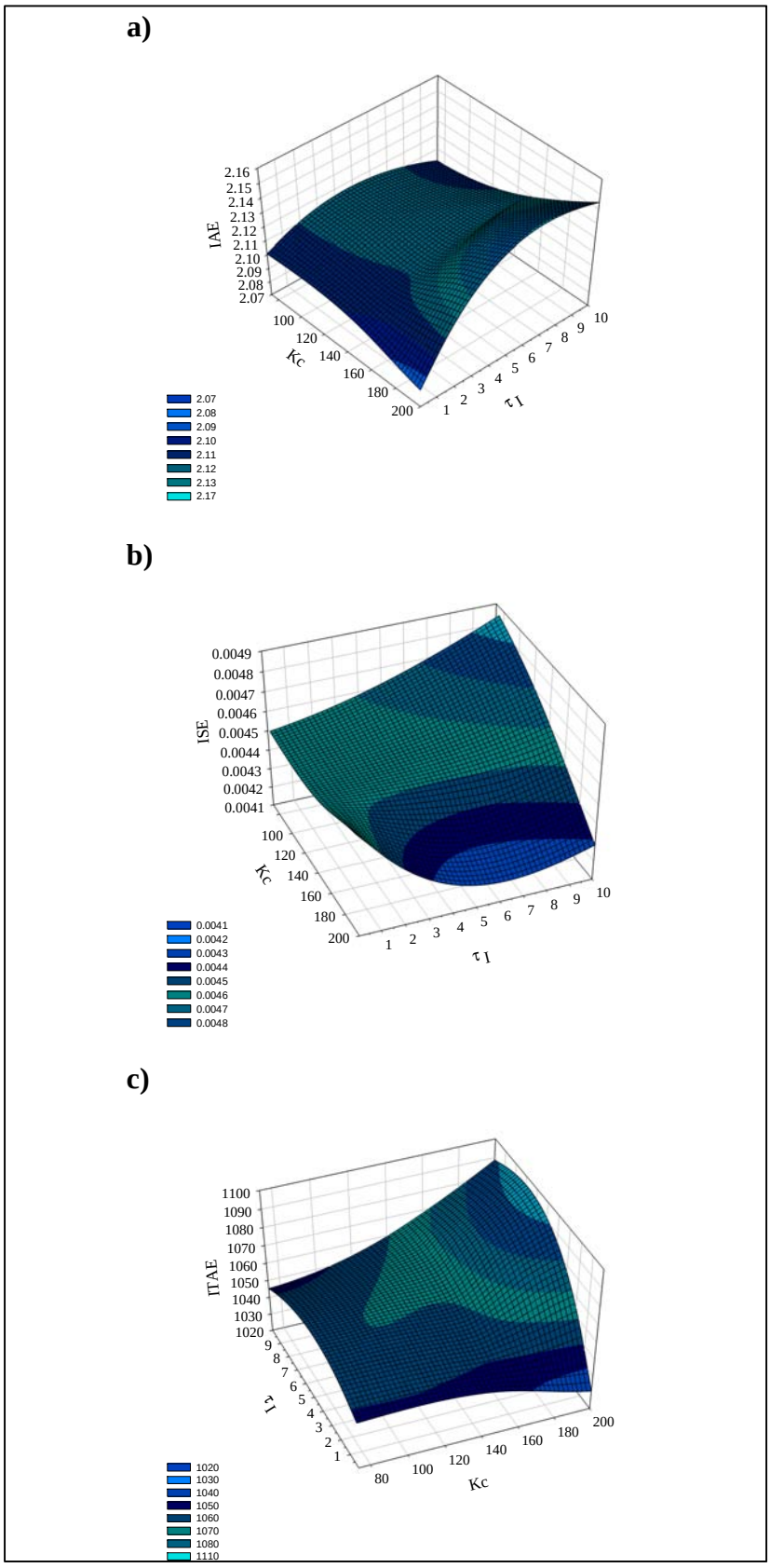

Figure 8.17. Time-integral criteria results for the different Kc and τ_I values for the values for the proportional integral controller for H_2S control facing inlet H_2S concentration changes (a) ISE mesh, (b) IAE mesh and (c) ITAE mesh.

However, considering only the time integral criteria would lead to erroneous conclusions since the parameters that provide the smaller error also lead to an unstable/oscillatory response of the controller. Hence, if stability of the actuation and time integral criteria were considered to select the most suitable pair of parameters, the parameters selected would be a Kc value of 147 and τ_I of 1.

Proportional controller in a TLV-CL strategy to face biogas flowrate changes.

Contrarily to the previous cases when TLV was regulated in order to control H_2S LR increase due to H_2S inlet concentration increases, the open-loop response shows that the $[H_2S]_{out}$ concentration was already higher than the SP during the first step change. Thus, the first biogas flowrate step provoked an actuation in the controller output (Fig 8.18a) denoting that the process is much more sensitive to the effect of reducing the EBRT (biogas flowrate increase) than to changes in the H_2S concentration. If actuation is evaluated as a function of the Kc tested, a Kc below 300 produces stable controller actuations and, therefore, a stable response of the controlled variable (Fig 8.18b). As an example of unstable response, a Kc of 500 is shown in Fig. 8.18a.

Interestingly, at the highest H_2S LR tested (169 g S-H_2S m^{-3} h^{-1}), the $[H_2S]_{out}$ concentration was reduced from 1100 ppmv (open-loop response) down to 550 ppm_v, which is far from the SP (100 ppm_v) meaning that changes on the H_2S LR due to a biogas flowrate increase corresponding to the highest H_2S LR tested were not controllable through a TLV-CL control strategy. However, the $[H_2S]_{out}$ was on the SP during the second H_2S LR tested (112.6 g S-H_2S m^{-3} h^{-1}), which means that under those H_2S LR and EBRT conditions the process was controllable.

The uncontrollability of the process during the last H_2S LR step was due to a limitation on the gas-liquid mass transfer when the EBRT is reduced. Therefore, mass transfer of gaseous compounds such as H_2S and O_2 is affected. Gas-liquid mass transfer could be improved by using intensive G-L mass transport devices such as Jet Venturi in order to produce an intensive contact between gas and liquid (Rodriguez et al., 2014). In this sense, model-based analysis of control strategies denotes their usefulness, since results such as the one shown in Fig. 8.18 warn to the designer that under those H_2S LR and EBRT conditions a redesign of the BTF would be needed in order to achieve higher H_2S transfer conditions.

a) **b)**

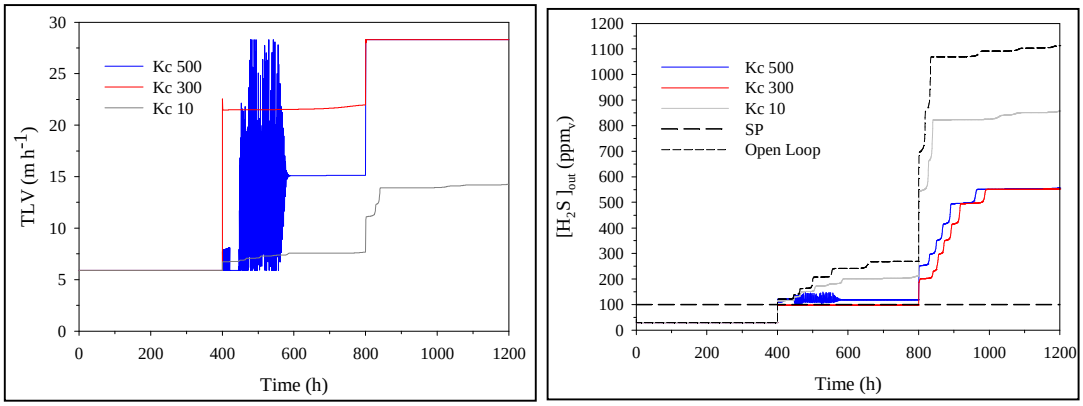

Figure 8.18. Trickling liquid velocity (manipulated variable) (a) and H_2S outlet concentration (controlled variable) (b) for H_2S control facing biogas flowrate changes using a P controller.

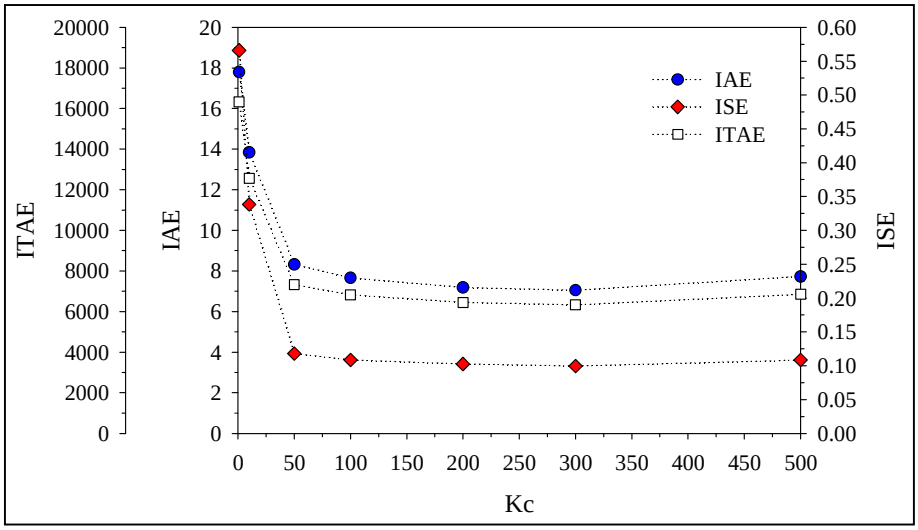

Figure 8.19. Time-integral criteria results for the different Kc values for the proportional controller for O_2 control facing biogas flowrate changes.

According to time-integral criteria and the simple performance criteria such as oscillation in the controller actuator in this case, a Kc value in the range of 100-300 would produce suitable results during the second H_2S LR tested for a proportional feedback controller. Instead, highest H_2S LR due to biogas flowrate changes would be hardly controllable using classical controllers.

Proportional-Integral controller in a TLV-CL strategy to face biogas flowrate changes

As in previous PI controllers, Kc for the PI controller were derived from observations and results obtained in the previous case for a P controller. Results for the PI controller were as expected and similar to the previous PI controller tested. Large Kc in combination with low τ_I produce unstable actuations. Unstable actuations were obtained for the highest Kc tested (Kc=300) with a τ_I of 0.1 (Fig. 8.20a). Therefore, lower Kc values and higher τ_I values were recommended to be used. Especially during the first biogas flowrate step, the error between the measured variable and the SP was small (Fig. 8.20a), therefore Kc higher than 300 produced oscillatory actuations. Therefore, lower Kc values (Kc = 110) resulted in a more suitable response.

a) **b)**

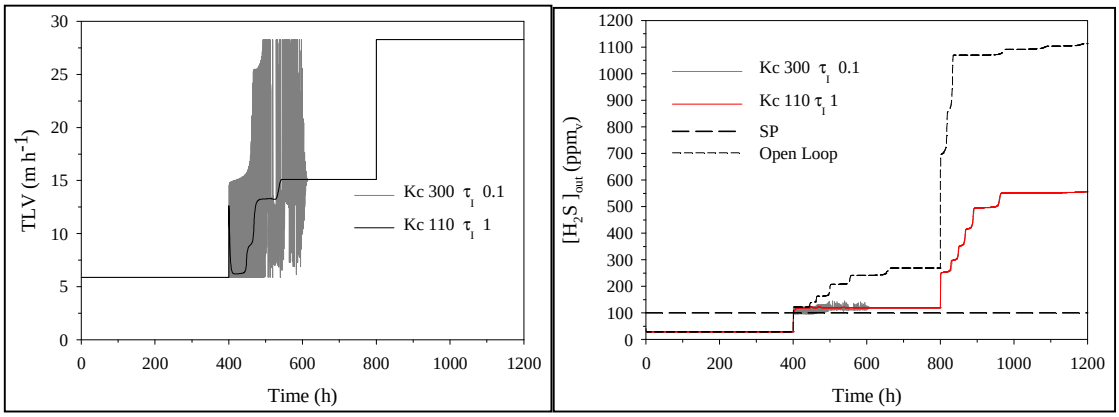

Figure 8.20. Trickling liquid velocity (manipulated variable) (a) and H_2S outlet concentration (controlled variable) (b) for H_2S control facing biogas flowrate changes using a PI controller.

Regarding τ_I, values between 1 and 10 were also tested (data not shown) in combination with a Kc of 110, demonstrating that the lowest the τ_I the fastest the answer of the controller was, as observed in Fig 8.20 (a) for a Kc value of 110 and τ_I value of 1. When the second biogas flowrate step occurs, the $[H_2S]_{out}$ obtained for the PI controller was again slightly higher than in the case of the P controller where offset was almost removed. Once more, this result was related to the characteristics of the disturbance that provoked the cancellation of the proportional action in the PI controller, and therefore only the I action was applied. However, the performance offered by the PI controller was acceptable, since the offset between the SP and the controlled variable was only 20 ppm_v.

Regarding the last biogas flowrate step, the process under those H_2S LR and EBRT conditions was again non-controllable with the PI controller.

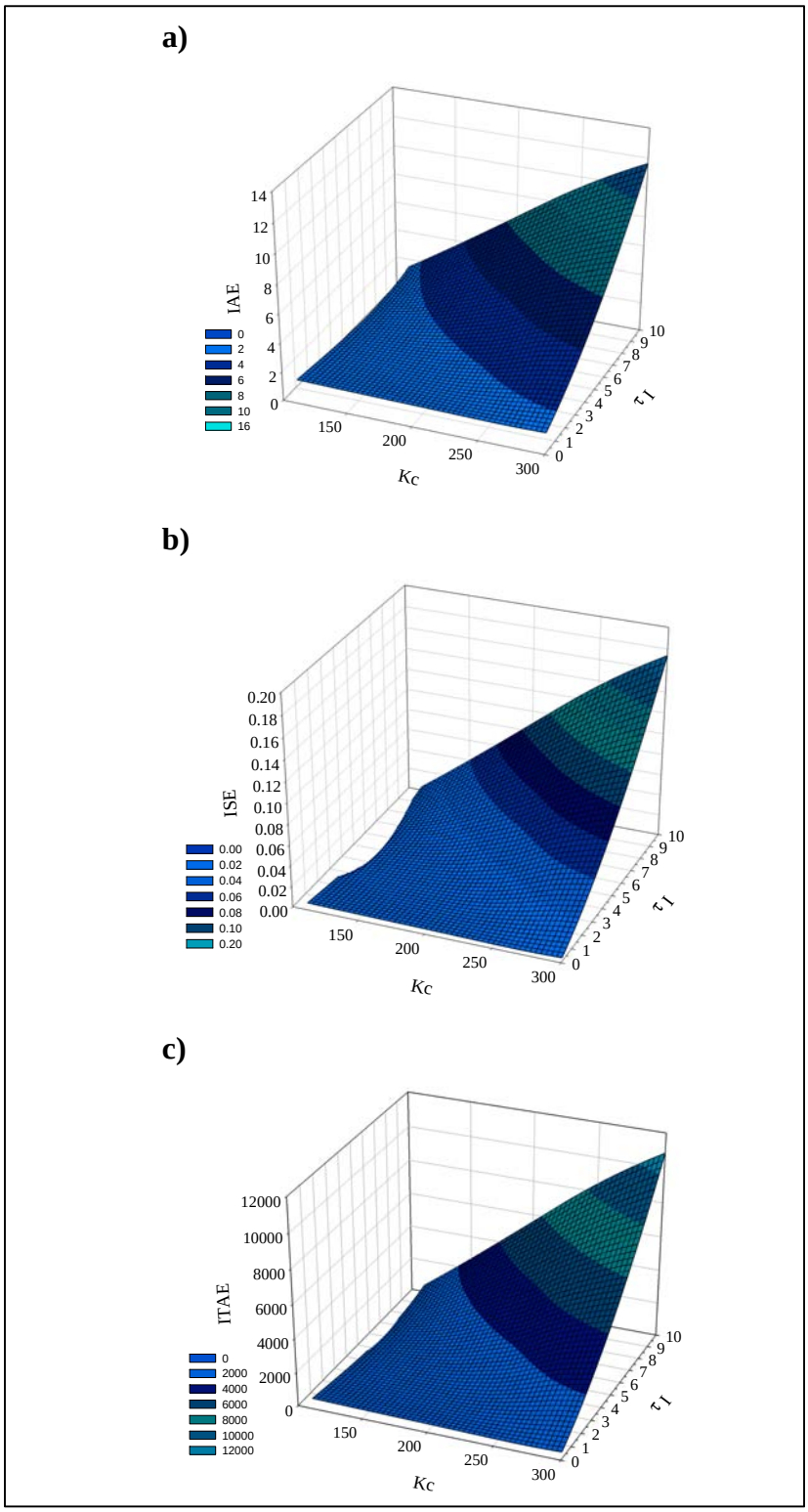

Figure 8.21. Time-integral criteria results for the different Kc and τ_I values for the values for the proportional integral controller for H_2S control facing biogas flowrate changes (a) ISE mesh, (b) IAE mesh and (c) ITAE mesh.

Evaluation of time-integral criteria for the PI controller when TLV is regulated in order to control H_2S outlet concentration is presented in Fig. 8.21, which was calculated based only on the H_2S LR where the process was controllable. According to Fig. 8.21, the smaller error (light blue area) was obtained for low τ_I (0.1-3) at all Kc values. However, a different set of parameters must be chosen when simple criteria such as oscillations are included. If stability of the actuation and time integral criteria are considered together to select the most suitable pair of parameters, Kc in the range of 100 to 200 in combination with τ_I between 1 and 10 would provide satisfactory results.

8.3.4. Added value of AFR-CL and TLV-CL control strategies for an aerobic biotrickling filter for biogas desulfurization

Besides finding the control limits of the different strategies studied on section 8.3.3, it is important to analyze the added value of the different feedback strategies on biogas desulfurization in an aerobic BTF. In order to have additional criteria to select control strategies, it is important to evaluate if the strategy studied, besides achieving the control objective (e.g. reaching the SP value), improves process performance significantly. A proper H_2S removal is necessary in full-scale BTFs for biogas desulfurization. However, a large product recovery as sulfate instead of elemental sulfur is a key factor to ensure process stability in the long run.

Sulfur species mass balance referred to the total amount of H_2S at the inlet and the amount of O_2 consumed during each simulation were calculated to evaluate the added value of the different feedback control strategies. Mass balances using each control strategy were compared with mass balances of simulations under open-loop conditions. In order to compare the BTF performance at each LR tested, mass balances were done integrating data of each LR step. Mass balances and the amount of O_2 consumed were determined according to Eq.8.8 to Eq. 8.11:

$$\%\ SO_{4,produced}^{2-} = \frac{g\ SO_{4,produced}^{2-}}{g\ S\text{-}H_2S_{in}} \cdot 100 \qquad (\%) \qquad \text{(Eq. 8.8)}$$

$$\%\ S_{produced}^{0} = \frac{g\ S_{produced}^{0}}{g\ S\text{-}H_2S_{in}} \cdot 100 \qquad (\%) \qquad \text{(Eq. 8.9)}$$

$$\%\ H_2S_{outlet} = \frac{g\ S\text{-}H_2S_{outlet}}{g\ S\text{-}H_2S_{in}} \cdot 100 \quad (\%) \quad \text{(Eq. 8.10)}$$

$$\%\ g\ O_{2,consumed} = g\ O_{2,inlet} - g\ O_{2,outlet} \cdot 100 \quad (\%) \quad \text{(Eq. 8.11)}$$

Therefore once the percentage of each specie and the O_2 consumed was determined, it was compared with the values obtained during the Open-loop case as described on Eq. 8.12 in order to determine the % of change (improvement or reduction).

$$\%\ Change = \frac{\%_{Open\text{-}loop} - \%_{Closed\text{-}loop}}{\%_{Open\text{-}loop}} \quad (\%) \quad \text{(Eq. 8.12)}$$

Selecting the most suitable feedback controller and control strategy to face a variable H_2S LR due to variable inlet H_2S concentrations

In table 8.6, the improvement in the main process variables for AFR-CL and TLV-CL control strategies facing H_2S inlet concentration changes using P and PI controllers are presented.

Table 8.6. Improvement on the main process performance variables for AFR-CL and TLV-CL facing H_2S inlet concentration changes using a feedback P and PI controller.

$Cg_{,in}$ H_2S (ppm_v)	Control type	Manipulated variable	Improvement $S\text{-}SO_4^{2-}{}_{produced}$ (%)	Reduction $S\text{-}S^0{}_{produced}$ (%)	Reduction g H_2S outlet (%)	Improvement g O_2 consumed (%)
4000	P Kc=0.1	AFR	0,4	4,5	1,6	0,3
6000			1,7	3,8	14,1	2,1
4000	PI Kc=0.074 τ_I=1	AFR	0,5	6,2	2,5	0,4
6000			3,1	8,5	23,7	3,0
6000	P Kc=300	TLV	17,5	91,0	75,6	9,0
6000	PI Kc=147 τ_I=1	TLV	14,9	70,7	71,9	8,7

Controller parameters for each control strategy were selected from the range of optimal parameters according to time-integral criteria and simple criteria results from section 8.3.3. Table 8.6 shows that the O_2 control through AFR regulation reduces the amount of H_2S in the outlet and the amount of elemental sulfur produced because of a larger oxygen consumption that leads to an increase in the amount of sulfate produced. However, reduction and improvement percentages are much lower compared to those obtained with the TLV-CL control strategy.

The AFR-CL control strategy showed less effective than TLV-CL control strategy since controlling O_2 outlet concentration does not ensure a better gas-liquid mass transfer, which is the main limiting step of the desulfurization process. Through TLV regulation, O_2 consumption is also substantially increased without any biogas dilution effect if compared to the AFR-CL control strategy. According to López et al. (López et al., 2016a), TLV regulation improves the penetrability of the liquid through the packed bed reducing possible DO gradients and, therefore, the formation of elemental sulfur.

Regarding the comparison between P and PI controllers, a PI control law performed better in the AFR-CL control strategy because the PI controller was able to remove completely the offset, thus improving the oxygen transport and consumption onto the packed bed. However, the P controller provided larger improvements than the PI controller in the TLV-CL control strategy. As stated previously this fact was mainly due to the type of disturbance employed in this study that turned the PI controller into an I controller. In any case, the TLV-CL control strategy offers interesting results in order to improve process performance since a reliable BTF operation can be obtained through the regulation of TLV, which does not involve biogas dilution.

Selecting the most suitable feedback controller using a TLV-CL control strategy to face a variable H_2S LR due to variable biogas flowrate

Table 8.7 shows the improvement in the process variables considered using P and PI control laws in a TLV-CL control strategy to face biogas flowrate changes. As discussed in section 8.3.3, the process was out the controllable limits using TLV as manipulated variable when the highest biogas flowrate was tested. Therefore, such results were excluded from the analysis herein. Results in table 8.7 show that the TLV regulation improved the main process performance variables during variable biogas flowrate conditions. Despite the lower EBRT of operation compared to the open-loop case, H_2S

RE and O_2 consumption were improved due to an enhancement of mass transfer along the packed bed caused by the TLV regulation. According to empirical correlations in section 8.3.1, a TLV increase improves the global mass transfer coefficients (K_La) for H_2S and oxygen, which correlates well with the reduction on H_2S outlet concentration and on the increase of O_2 consumption. Consequently, product selectivity towards sulfate is improved. The main difference between the P and PI control laws were related to the TLV applied in each case. If a P controller was used, a maximum TLV of 21.96 m h^{-1} was used by the controller while a maximum TLV of 15.12 m h^{-1} was reached with the PI controller during the first biogas flowrate step. Again, differences in the performance between both controllers was conditioned to the characteristics of the disturbance used in this work. Irrespective of the type of controller, process performance was positively improved through TLV regulation in order to face biogas flowrate changes. However, controlling biogas flowrate changes at lower EBRT values than 68.5 seconds can hardly be done using classical controllers.

Table 8.7. Improvement on the main process performance variables for TLV control strategy facing biogas flowrate changes using a using a P and PI feedback controllers

F_{biogas} (L h^{-1})	Control type	Manipulated variable	Improvement S-$SO_{4\ produced}^{2-}$ (%)	Reduction S-$S^0_{produced}$ (%)	Reduction g H_2S outlet (%)	Improvement g O_2 consumed (%)
123	P Kc=300	TLV	22,39	85,63	53,00	7,29
123	PI Kc=110 τ_I=1	TLV	15,23	51,52	43,22	6,67

8.4. CONCLUSIONS

The effect of different control strategies applied in an aerobic BTF for biogas desulfurization under different loading rate conditions was studied and the following conclusions were obtained:

A comparison of empirical correlations to calculate mass transfer coefficients showed that Billet and Schultes correlation fitted better the experimental data than Onda's correlation and was therefore implemented in the model.

Results obtained during open-loop tests indicated that process control in BTFs for biogas desulfurization is needed in order to mitigate disturbances such as H_2S inlet increase or biogas flowrate changes. Different control strategies, based on air flowrate and TLV regulation were here tested, demonstrating that process performance can be improved through manipulated variables regulation. However, if the two types of disturbances are compared, changes on H_2S inlet concentration have a higher controllability limit than biogas flowrate changes. The latter was found to be hardly controllable with classical controllers at EBRTs below 68.5 seconds.

The AFR-CL control strategy to control $[O_2]_{out}$ concentration demonstrated that a PI controller was able to completely remove the offset. However, this strategy was inefficient in terms of process improvement when added-value variables were considered because increasing the aeration flowrate does not ensure a proper gas-liquid mass transfer. Moreover, the AFR-CL control strategy involves a certain biogas dilution, which reduces the calorific power of the biogas produced. Therefore, AFR-CL strategy is not recommended in BTFs for biogas desulfurization.

The TLV-CL control strategy resulted as a proper strategy to regulate H_2S outlet concentration at H_2S LR below 169 g S-H_2S $m^{-3}h^{-1}$ when changes in the inlet H_2S concentration occur. When the biogas flowrate was the disturbance, TLV-CL was only able to control H_2S LR changes below 113 g S-H_2S $m^{-3}h^{-1}$. The TLV regulation also showed to be a feasible strategy to improve complementary BTF performance parameters such as RE, sulfate selectivity and O_2 consumption under variable H_2S LR conditions, independently of the type of feedback controller (P or PI).

If the two types of manipulated variables are compared, TLV showed better results than AFR regulation strategy since no biogas dilution is involved and because the percentage of process improvement compared to the open-loop case are much higher.

CHAPTER 9

APPLICATION OF FEEDBACK AND FEEDFORWARD CONTROL STRATEGIES BASED ON TRICKLING LIQUID VELOCITY REGULATION IN AN AEROBIC BIOTRICKLING FILTER FOR BIOGAS DESULFURIZATION

9 APPLICATION OF FEEDBACK AND FEEDFORWARD CONTROL STRATEGIES BASED ON TRICKLING LIQUID VELOCITY REGULATION IN AN AEROBIC BIOTRICKLING FILTER FOR BIOGAS DESULFURIZATION

The focus of this chapter was to test experimentally feedback and feedforward control strategies in an aerobic biotrickling filter for biogas desulfurization. Control strategies were based only on trickling liquid velocity in order to control H_2S outlet concentration, since in previous chapters (Chapter 5 and 8) it was already showed that this variables is a better alternative than air flowrate regulation. Design and parameters used in feedback control loops derive from results obtained in previous chapter, such the controllability limits obtained from the model based analysis of control strategies (Chapter 8). For the feedback control strategy, it was interesting to verify experimentally those controllability limits determined theoretically, for the two types of disturbances: variations in the H_2S inlet concentration and in biogas flowrate. For the feedforward control, besides focusing on the control strategy, it was interesting to evaluate the long term effect on process variables such as sulfate selectivity. Testing both types of control strategies would allow knowing more about the main contributions to process improvement and the main limitations of both types of control strategies.

ABSTRACT

In this work, feedback and feedforward control loops were implemented in a lab-scale, aerobic biotrickling filter (BTFs) operating under real H_2S LR fluctuating conditions in order to show the capabilities and added value of each strategy. BTF stability against inlet concentration and biogas flow rate changes was assessed experimentally. Regarding feedback control, two short tests with variable H_2S loading rate (LR) conditions due to biogas flowrate changes and H_2S inlet concentration changes were performed in order to study the regulatory response of the feedback control based on trickling liquid velocity (TLV) regulation. Tests had an average H_2S LR of 120 and 170 g S-H_2S m^{-3} h^{-1}, respectively. These values derive from controllability results obtained in chapter 8 of this thesis (see section 8.3.3, chapter 8). Regarding feedforward control, three long term tests with variable H_2S LR were performed to simulate disturbances in the inlet gas with and without the implementation of a feedforward control loop based on TLV manipulation. Tests had average load of 78, 98 and 116 g S-H_2S m^{-3} h^{-1}, respectively. Parameters as the

O_2 load, the ratio between O_2 load and H_2S load, the H_2S concentration in the outlet gas and the selectivity to sulfate were studied in order to assess the improvement of the operation with the implementation of the control strategy

Feedback control strategy to control H_2S inlet concentration variations through TLV regulation was also adequate to face fluctuating H_2S LR due to inlet concentration changes. However, biogas flowrate changes were hardly controllable with classical controllers. Despite system adaptation in the long-run, a feedforward control loop based on TLV regulation showed as an adequate strategy to reduce load perturbations impact. Feedforward control implementation improved removal efficiencies, sulfate selectivity (reducing elemental sulfur production) and mitigated H_2S peaks in the outlet gas of the desulfurizing biotrickling filter.

9.1. INTRODUCTION

Biological H_2S removal in biotrickling filters (BTFs) has been widely proved to be an efficient technology in order to clean biogas for upstream energy recovery processes (Syed et al., 2006; Tomàs et al., 2009). However, further research is needed in order to optimize biological desulfurization processes to enhance process reliability and, therefore, expand their application field. To achieve robust operation, a larger degree of process monitoring and process control is required (Montebello et al., 2012). Since H_2S loading rate (H_2S LR) on industrial plants may vary depending on many factors such as upstream conditions in anaerobic digesters and seasonal or daily variations (Gabriel and Deshusses, 2003a), process control is needed in order to have a stable operation.

Typically, hydrogen sulphide (H_2S) or oxygen (O_2) outlet concentrations are the controlled variables in feedback control loops and air flow is the main manipulated variable in industrial BTFs (Rodriguez et al., 2014). Nevertheless, such control strategy often leads to biogas dilution (Chaiprapat et al., 2011), which reduces its energy content and furthermore increases explosive risks associated to an increase of the air percentage in the energy-rich gas (Walsh et al., 1988) . On the other hand, such control strategy also leads to the reduction of the empty bed residence time (EBRT), which affects negatively the external mass transfer rate of O_2 and H_2S and, concomitantly, its removal efficiency (Kim and Deshusses, 2003; Montebello et al., 2012), favouring elemental sulfur accumulation in the trickling bed. Other authors have obtained successful results on the transference of O_2 from the gas to the liquid phase with intensive devices in order to

achieve better oxidation rates and lower production of elemental sulfur (Rodriguez et al., 2013, 2012). However, improvements on O_2 supply are still required not only to reduce even more elemental sulfur accumulation in the trickling bed but, specially, to mitigate shock loads of H_2S, typically present in industrial plants, which damage energy generation systems increasing maintenance requirements and decreasing systems lifespan (Pipatmanomai et al., 2009; Walsh et al., 1988).

The utilization of automatic control systems has improved the performance of numerous WWTPs (Guerrero et al., 2011) but few studies have been performed implementing control based strategies to improve pollutants degradation in BTFs (Almenglo et al., 2015). An alternative to the feedback control strategy is the feedforward control strategy. This strategy considers the inlet H_2S concentration ($[H_2S]_{in}$) as the measured variable and the trickling liquid velocity (TLV) as the manipulated variable.In chapter 5 it was showed that TLV regulation improves the dissolved oxygen load (DOL) and consequently the BTF performance, since improves the transference of O_2 to the liquid phase along the BTF packed bed and therefore improves sulfate production.

Also in Chapter 5 it was found that this strategy, reduces dissolved oxygen (DO) gradients along the packed bed without biogas dilutionThen, the implementation of this feedforward control loop could mitigate unusual loads of H_2S since disturbances are measured and accounted for before they have time to affect the system (Rieger et al., 2014). In order to apply this specific feedforward control strategy it is important to predict the effect of the disturbance over the main process variables.

In a desulfurizing BTF the effect of H_2S LR variations provoked by $[H_2S]_{in}$ increase or decrease is that the stoichiometric O_2/S ratio is moved from complete sulfide oxidation ($H_2S \rightarrow SO_4^{2-}$) values ($O_2/S \geq 2$) to partial sulfide oxidation values ($O_2/S \leq 2$), the latter leading to elemental sulfur production. Lopez *et al*. (López et al., 2016a) found that DOL control was crucial in order to improve the stoichiometric O_2/S and to achieve complete sulfide oxidation to sulfate, especially when high H_2S LR were treated in the BTF. Then, the feedforward control strategy that was analyzed in this thesis considered the $DOL/[H_2S]_{in}$ ratio as the process variable, which means that the $DOL/[H_2S]_{in}$ ratio will be maintained at a determined Set Point value despite the H_2S LR disturbances.

The aim of this study was therefore to show the potential of TLV as a manipulated variable in a feedback and feedforward control loop based on $[H_2S]_{in}$ measurements, to

control the outlet H_2S concentration ($[H_2S]_{out}$), besides the elimination capacity, of a biogas desulfurizing BTF operated under variable H_2S LR conditions. Additionally, process performance improvement in terms of sulfate selectivity increase was also assessed.

9.2 MATERIALS AND METHODS

9.2.1. Experimental conditions for evaluation of feedback control strategy

Two case studies were here analysed in order to evaluate feedback control in a lab-scale BTF for biogas desulfurization when H_2S LR is varied due to H_2S inlet concentration or due to biogas flow rate changes. Further details about the experimental setup and analytical methods can be found on chapter 4. Additionally to the BTF set up, a digital controller was programmed. The digital controller determined the controller action according to Equation 2.4 (Baeza, 2016), which is completely described in section chapter 2 (see section 2.3.1, Chapter 2).

Compared to the analogic controller, the digital controller does not requires to be initialized by a bias value (Cs), which is the value of the actuation of the controller when the error is zero. Moreover, this type of controller is protected against the controller saturation, which is known in control terminology as windup. The main reason why this type of controller was selected over the analogic controller was the facility to adapt it into the monitoring software. Feedback control applied in this section aimed at controlling the $[H_2S]_{out}$ concentration through liquid recirculation flowrate regulation when H_2S LR is varied due to H_2S inlet concentration or biogas flow rate changes. H_2S LR conditions presented in this section were derived from controllability limits obtained in the application of TLV regulation closed-loop (TLV-CL) (*see section 8.3.3, chapter 8*).

The first case studied was the evaluation of a feedback control loop in order to face changes in the H_2S inlet concentration, which was step-wise increased from 5180 ppm_v to 5450 ppm_v (Fig. 9.1a). The concentration profile shown in Fig. 9.1a corresponded to an average H_2S LR of 154 g S-H_2S m^{-3} h^{-1}.Tests were named according to the control strategy used, the disturbance applied, namely concentration (C) or biogas flowrate (EBRT), and according to the average LR of the test. Accordingly, the abovementioned test was defined as feedback-C-154 (FB-C-154). Table 9.1 shows the main characteristics of FB-C-154 profile tested in the BTF are described.

Table 9.1. Experimental conditions for feedback control evaluation under variable H_2S inlet concentration

Test	$[H_2S]$ LR_{avg} *(g S-H_2S m^{-3} h^{-1})*	$[H_2S]_{avg}$ *(ppm_v)*	$[H_2S]_{max}$ *(ppm_v)*	$[H_2S]_{min}$ *(ppm_v)*	Constant TLV tests *(m h^{-1})*	Variable TLV tests *(m h^{-1})*
FB-C-154	154	5460	5770	5283	5.9	5.9 - 13

The procedure followed to perform FB-C-154 was as follows. First, the BTF performance was assessed with fluctuant H_2S inlet concentration conditions at constant TLV (5.9 m h^{-1}). Then, the same H_2S LR profile was applied together with a feedback control strategy. Schematic of the feedback control loop for controlling $[H_2S]_{out}$ concentration through liquid recirculation flow rate can be found on previous chapters (see Fig 8.2b in section 8.2.3, chapter 8). In agreement with chapter 8, a $[H_2S]_{out}$ setpoint (SP) concentration of 100 ppm_v was defined. Also TLV regulations limits where fixed according to values defined in chapter 8, a minimum TLV of 5.9 m h^{-1} and a maximum TLV of 28.3 m h^{-1}.

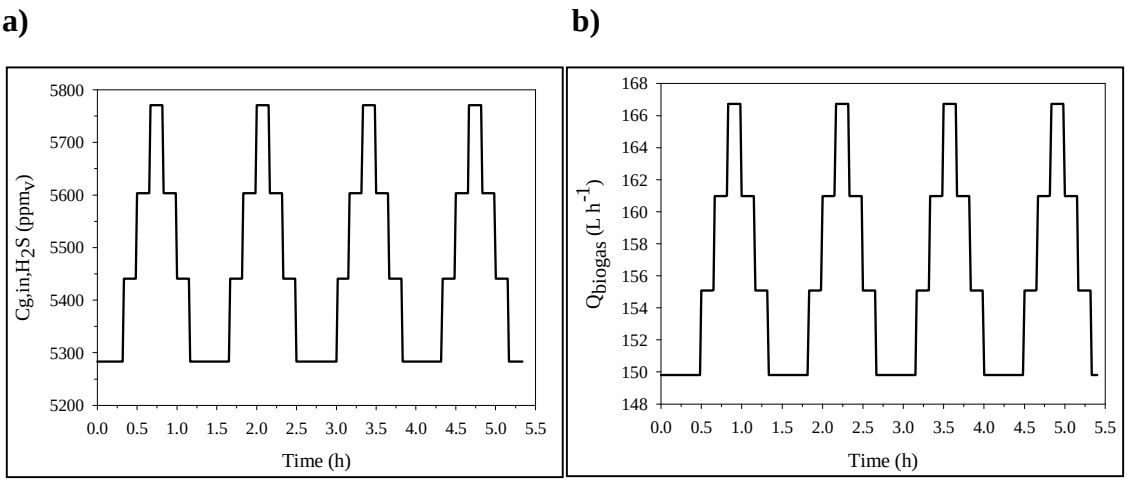

Figure 9.1. Inlet profile to simulate H_2S LR changes due to (a) H_2S inlet concentration variations and (b) to biogas flowrate changes.

The second case evaluated was the effect of biogas flowrate changes performing step-wise increments from 150 L h^{-1} (EBRT=67.4 s) to 166 L h^{-1} (EBRT=60.5 s) (Fig

8.1b). The application of the concentration profile shown in Fig. 9.1b corresponded to an average H_2S LR of 120 g S-H_2S m^{-3} h^{-1}, therefore this test was named feedback-120 (FB-EBRT-120). In table 9.2 the main characteristics of FB-EBRT-120 profile tested in the BTF are described. A similar procedure to that performed in the FB-EBRT-120 test was performed for the FB-C-154 test. First, the BTF performance was assessed with fluctuant biogas flowrate profiles at a constant TLV of 5.9 m h^{-1}. Then, the same biogas flowrate profile was applied together with a feedback control strategy.

Table 9.2. Experimental conditions for feedback control evaluation under variable biogas flowrate

Test	**[H_2S] LR_{avg}** *(g S-H_2S m^{-3} h^{-1})*	**$[EBRT]_{avg}$** *(s)*	**$[EBRT]_{max}$** *(s)*	**$[EBRT]_{min}$** *(s)*	**Constant TLV tests** *(m h^{-1})*	**Variable TLV tests** *(m h^{-1})*
FB-EBRT-120	120	64.9	67.4	60.5	5.9	5.9 - 17

The duration of the FB-C-154 and FB-EBRT-120 profiles were 1.3 hours (80 minutes) and 4 cycles were performed for each test. Since the effect of TLV over elemental sulfur and sulfate selectivity in the long-run was already assessed in previous chapters (*Chapter 5*), analysis in this chapter targeted the RE solely as process performance variable. Controller performance over RE was evaluated using the time-integral criteria (*see section 8.1, chapter 8*). In this section, the error was only quantified when the measured variable ($[H_2S]_{out}$ concentration) was above the SP.

9.2.2. Experimental conditions to evaluate a Feedforward control strategy

Variable H_2S LR profiles to evaluate the feedforward control loop were designed and tested in order to simulate daily H_2S LR fluctuations and elimination capacities commonly found in industrial facilities. Also changes in the H_2S inlet concentration and in the biogas flowrate were studied. The first case studied was the evaluation of a feedforward control loop in order to face H_2S LR variations due to biogas flowrate changes (Fig. 9.2). Application of the H_2S LR profile corresponded to an average H_2S LR of 98 g S-H_2S m^{-3} h^{-1}, therefore the test was named feedforward-EBRT-98 (FF-EBRT-

98). In table 9.3 the main characteristics of FF-EBRT-98 profile tested in the BTF are presented.

Table 9.3. Experimental conditions for feedforward control loop evaluation under variable biogas flowrate.

Test	**[H_2S] LR_{avg}** *(g S-H_2S m^{-3} h^{-1})*	**$[EBRT]_{avg}$** *(s)*	**$[EBRT]_{max}$** *(s)*	**$[EBRT]_{min}$** *(s)*	**Constant TLV tests** *(m h^{-1})*	**Variable TLV tests** *(m h^{-1})*
FF-EBRT-98	98	104	184	42	6.5	6.5 - 27

The procedure followed to perform FF-EBR-98 was as follows. First, the BTF performance was assessed with fluctuant H_2S LR conditions at constant TLV (6.5 m h^{-1}) following the profile described in Fig. 9.2. Then, the same H_2S LR profile was applied together with a feedforward control strategy, which consisted of manipulating the TLV as a function of the $[H_2S]_{in}$ (Fig 9.3).

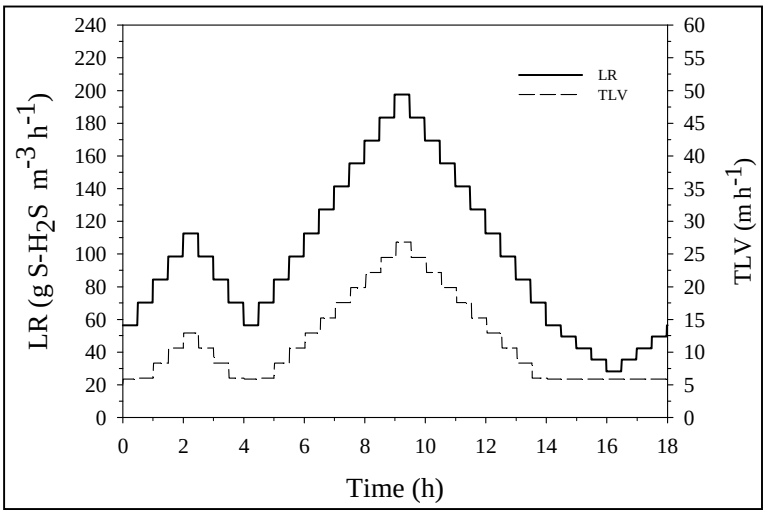

Figure 9.2. H_2S LR inlet profile(solid line) and TLV profile (dashed line) designed to simulate variable H_2S LR conditions due to biogas flow rate changes s for Test FF-EBRT-98

Experimental results obtained in chapter 5 (*See table 5.2, Chapter 5*) were useful to determine the relation between the DOL and TLV, since in order to have an optimal feedforward controller is important to know the effect of the manipulated variable over

the process. In consequence in this section a DOL/$[H_2S]_{in}$ ratio set point of 0.32 g O_2 g^{-1} S-H_2S_{in} was set seeing that experimentally it was found that 100% sulfate selectivity (S-SO_4^{2-}/S-$H_2S_{removed}$), and H_2S removal could be reached at this ratio value. In chapter 5 this ratio was can also be found as DOL/$[H_2S]_{removed}$ along the study of the effect of TLV in BTF performance, when is used to relate the effect of DOL with the RE of H_2S.

TLV regulation in a feedforward control strategy was also tested in order to face H_2S inlet concentration variations. To simulate variable H_2S LR conditions due to H_2S inlet concentration changes, three different cycles of 14, 18 and 20.5 hours were designed for each test and continuously repeated during the test period (≈200 h). However, in the results section, only four cycles for each test are presented in order to have a clearer perspective of the results. In table 9.4 the main characteristics of the different H_2S LR profile tested with a feedforward control loop are presented.

Tests were named according to the disturbance applied and the average LR of the test. e.g. for the test with an average LR of 78 g S-H_2S m^{-3} h^{-1} the test was named FF-C-78. The procedure followed to perform each test was the same as for the other tests. First, BTF performance was assessed with fluctuant H_2S LR conditions at constant TLV (6.5 m h^{-1}). Then, the same H_2S LR profile was applied together with a feedforward control strategy. In Fig. 9.4 the H_2S LR and TLV profiles corresponding to the cycle of test E-78 (14-hours cycle) are presented.

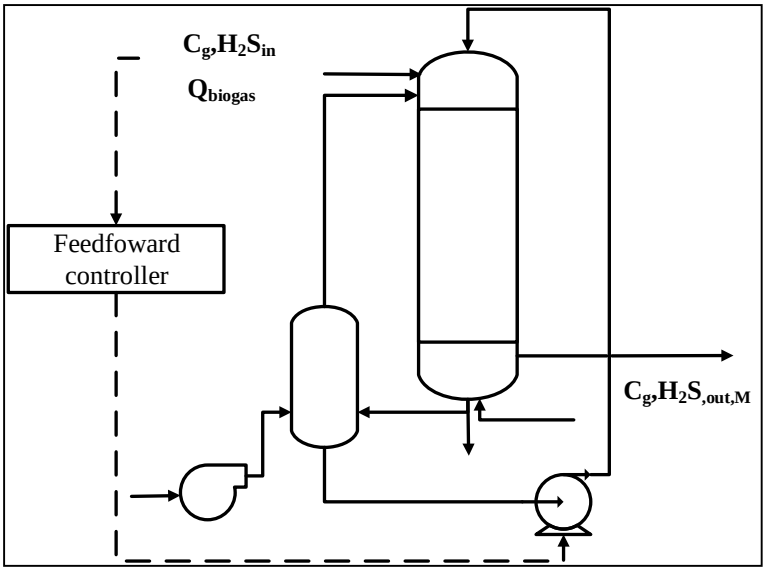

Figure 9.3. Schematic of feedforward control strategy for controlling H_2S LR variations due to H_2S inlet concentration or biogas flowrate changes through regulation of liquid recirculation flowrate.

Table 9.4. Experimental conditions for feedforward control loop evaluation under variable H_2S inlet concentration

Test	**$[H_2S]$ LR_{avg}** *(g S-H_2S m^{-3} h^{-1})*	**$[H_2S]_{avg}$** *(ppm_v)*	**$[H_2S]_{max}$** *(ppm_v)*	**$[H_2S]_{min}$** *(ppm_v)*	**Constant TLV tests** *(m h^{-1})*	**Variable TLV tests** *(m h^{-1})*
FF-C-78	78	2759	5000	1000		6.5 - 19
FF-C-98	98	3459	7000	1000	6.5	6.5 - 30
FF-C-116	116	4119	8500	1000		6.5 - 37

It must be mentioned that, before each test, the BTF was operating during 8 days at a pseudo steady-state in order to study the dynamics of the process in each test from similar starting conditions. Afterwards the sulfate selectivity was determined as the total amount of sulfate produced per amount of H_2S removed from the gas phase ($S\text{-}SO_4^{2-}/S\text{-}H_2S_{removed}$) along the whole test with and without feedforward control. Then, in order to evaluate the regulation limits of TLV along the three tests, sulfate selectivity increase for each test was determined as the increase of sulfate selectivity when the process was controlled related to the sulfate selectivity under Open-Loop conditions.

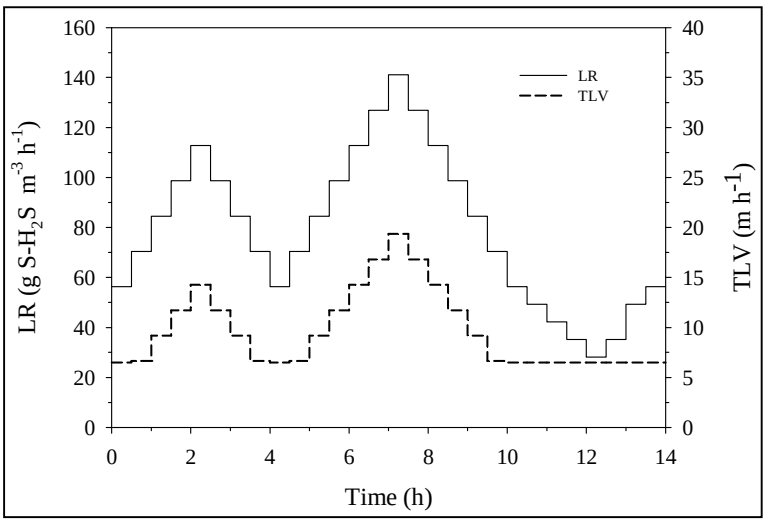

Figure 9.4. H_2S LR inlet profile (solid line) and TLV profile (dashed line) designed to simulate variable H_2S LR conditions due to H_2S inlet concentration

9.3. RESULTS AND DISCUSSION

9.3.1. Controller parameters re-adjustment to experimental conditions

According to the results obtained in chapter 8 (*see section 8.3.3, Chapter 8*), a proportional (P) controller was selected as the most suitable type of feedback controller to use in the TLV-CL control strategy. As showed in Fig. 9.1, H_2S LR profile was adjusted to the controllability limits founded in chapter 8 (see section 8.3.3, Chapter 8) and also the shape was modified in order to have a more realistic approach to disturbances founded in real-scale plants.

Therefore the set of parameters providing suitable results according to results obtained in chapter 8, were also modified according to experimental conditions. From time-integral criteria results in chapter 8, Kc values in the range of 200-300 would provide suitable results for H_2S outlet concentration control. However, values in that range produced unstable response of the actuator (data not shown), so lower Kc values in a lower test were studied. Higher Kc values were obtained through the model-based analysis since pronounced step changes in the H_2S LR were performed.

While experimentally, H_2S LR steps were done progressively (Fig 9.1) and therefore lowest Kc values were provided better results as showed in Fig. 9.5. Results of Kc evaluation (Fig 9.5a) in the range of 20 and 40, showed that for a P controller for H_2S control facing H_2S inlet concentration, a Kc value of 20 provided the lowest time-integral criteria value. Lowest values than 20 were tested but almost no controller actuation was obtained (data not showed). In the other hand, for a P controller for H_2S control facing biogas flowrate changes, a Kc value of 10 provided the lowest error (Fig.9.5b)

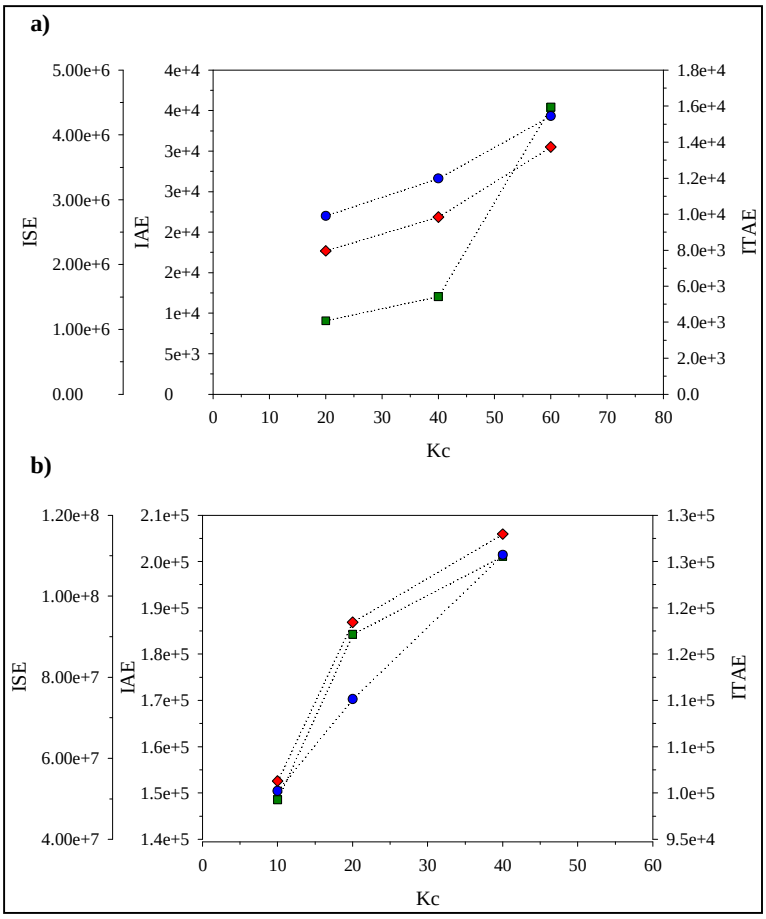

Figure 9.5. Time integral criteria results for the different Kc values for the proportional controller for H_2S control facing (a) inlet H_2S concentration changes and (b) biogas flowrate changes.

9.3.2. Evaluation of feedback control facing changes in the H_2S inlet concentration

For the FB-C-154 test, comparison of the $[H_2S]_{out}$ concentration profile between the Open-Loop and Closed-Loop case is presented in Fig. 9.6a, while the H_2S LR and the controller response (TLV) is presented In Fig. 9.6b. Fig. 9.6a shows that the $[H_2S]_{out}$ concentration of the process under Open-Loop conditions exceeds the setpoint during H_2S LR peaks. Under Closed-Loop conditions, $[H_2S]_{out}$ concentration remains below the setpoint instead. A significant reduction of the $[H_2S]_{out}$ concentration error, down to values close to 19.8 ppm_v at time 0.75h, was obtained for the process under Closed-Loop conditions, while error values up to 48.9 ppm_v were obtained at time 4.75 h during the Open-Loop case. Regarding the controller actuation, a stable controller response was obtained; TLV varied between 5.9 m h^{-1} and 13.3 m h^{-1}.

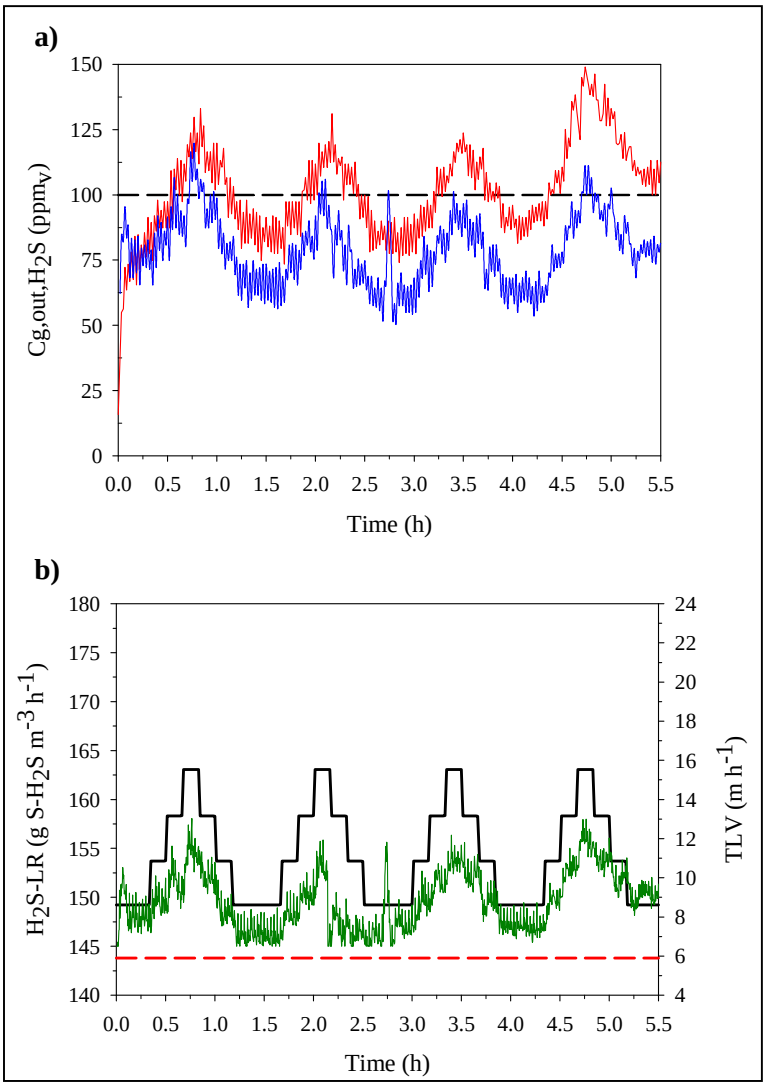

Figure 9.6. Experimental concentration profiles of Feedback control facing H_2S inlet concentration variations for test FB-C-154: (a) $[H_2S]_{out}$ concentration profiles under open-loop conditions (red line) and under closed-loop conditions (blue line) and SP value (back dashed line) and (b) H_2S LR profile (black line), TLV actuation under open-loop conditions (red dashed line) and controller actuation (TLV) (green line).The time-integral criteria results for the FB-C-154 tests are presented in table 9.5.

Table 9.5. Time-integral criteria results for the FB-C-154 test under Open-Loop and Closed-loop.

Criteria	Open-Loop	Closed-Loop	Improvement %
ISE	62106.2	1289.3	97.9
IAE	2638.6	123.9	95.3
ITAE	9881.7	250.3	97.5

Results in table 9.5 show that error criteria were successfully reduced when a feedback control loop was applied. Since time-integral criteria evaluate the error along all the experimental period, figures in table 9.5 indicate that the $[H_2S]_{out}$ concentration error was, on average, almost removed during all the experiment. Also is important to remark the fact that in biological processes control, such as in BTFs for biogas desulfurization, it must be taken into account the adaptability of the process to operational conditions and therefore the need of use of different set of controller parameters. When H_2S LR profiles were tested under closed-loop conditions along several hours, even during some days (data not showed), the processes increases its capability and therefore the parameters selected are less effective.

In the case of FB-C-154 test, even it's a short duration test, difference in H_2S outlet concentration along the time from the first to the third peak can be observed due to this phenomena. When the BTF is operated under Closed-Loop conditions, regulation of TLV increases the amount of water retained in the BTF packed bed which consequently increases the H_2S absorption. This is why the error is higher under Closed-Loop conditions during the valley periods of the H_2S LR profile. In the other hand, a difference in the H_2S outlet concentration between the first three cycles and the fourth cycle is observed, which could be explained by a a change in the preferential paths of the gaseous phase and probably also of the liquid phase paths, causing a diminution of the removal efficiency (RE). In spite of this phenomena which are common in multiphasic reactors such as BTFs, the controller was able to control H_2S outlet concentration during the last cycle. One particularity of the digital controller of our process is that there is a controller actuation even when the process does not exceeds the setpoint under Closed-Loop conditions.

This was explained because of the digital controller programming (equation 2.4). The digital controller considers the previous control action and the difference of errors between the present error (ε_n)and the previous error(ε_{n-1}). Therefore always that this difference of errors is different of zero, and the previous controller actuation is higher to the minimum control action, there is an controller's actuation. As it showed in Fig. 9.6b and 9.7b, TLV for the Closed-Loop does never returns to the minimum TLV value (red dashed line).

9.3.3. Evaluation of feedback control facing changes in the biogas flowrate

A comparison of the $[H_2S]_{out}$ concentration profiles between the Open-Loop and Closed-Loop case for the FB-EBRT-120 test is presented in Fig. 9.7a, while the controller response (TLV) and the H_2S LR profile are presented in Fig. 9.7b.

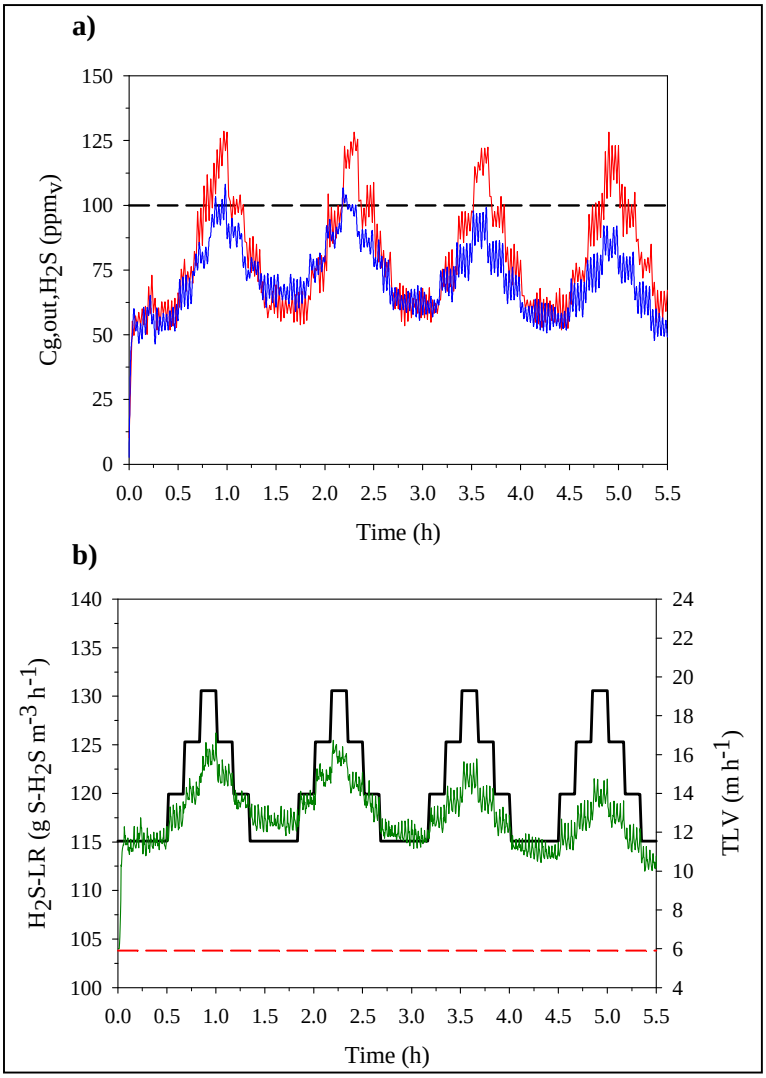

Figure 9.7. Experimental concentration profiles of Feedback control facing biogas flowrate variations for test FB-EBRT-120: (a) $[H_2S]_{out}$ concentration profiles under open-loop conditions (red line) and under closed-loop conditions (blue line) and SP value (back dashed line) and (b) H_2S LR profile (black line), TLV actuation under open-loop conditions (red dashed line) and controller actuation (TLV) (green line).

In Fig. 9.7(a) is observed how the $[H_2S]_{out}$ concentration for the process under Closed-Loop is well controlled during variable biogas flowrate conditions. Instead, the $[H_2S]_{out}$ concentration is above the setpoint for the Open-Loop case, especially during biogas flowrate peaks. Under Open-Loop conditions the highest $[H_2S]_{out}$ concentration error was around 28 ppm_v, meanwhile under Closed-Loop conditions, the highest error obtained was reduced to 8.1 ppm_v. Since FB-EBRT-120 test was performed at a lowest EBRT value ($EBRT_{average}$=64.9) than the reference EBRT value (EBRT=120 s), the process is under mass transfer limitation. Subject to this situation, variations of biogas flowrate are much more difficult to control compared to the previous test (FB-C-154) were H_2S inlet concentration was varied.

This difference can be observed in the fact that higher TLV values in the range of 5.9-17 m h^{-1} were applied, indicating that higher actuations are needed to attenuate the effect of this disturbance on the process. In addition, this mass transfer limitation effect in the FB-EBRT-120 test, can be observed in the minimum of the H_2S LR profile that for the Open-Loop and Closed-Loop case, the H_2S outlet concentration was almost the same. This evidence that the TLV applied in the valley periods of the H_2S LR profile for the Closed-Loop case is not capable to attenuate or improve the effect of the disturbance if high gas-liquid flowrate relations are applied, as it occurs in the FB-C-154 test.

However, in the maximum H_2S LR values of the FB-EBRT-120 profile, TLV actuations were effective to control H_2S outlet concentration, especially during the last cycle since the relation between the gas-liquid flowrate was lower. Time-integral criteria evaluation for the FB-EBRT-120 tests presented on table 9.6 also confirms the process performance improvement under Closed-Loop conditions.

Table 9.6. Time-integral criteria results for the FB-EBRT-120 test under Open-Loop and Closed-loop.

Criteria	Open-Loop	Closed-Loop	Improvement %
ISE	16967.2	141.6	99.17
IAE	921.6	26.1	97.17
ITAE	3064.1	39.8	97.70

9.3.4. Evaluation of feedforward control facing changes in the biogas flowrate

Fig. 9.8 shows the effect of the feedforward control loop implementation based on the DOL/$[H_2S]_{in}$ ratio control for the FF-EBRT-98 test. Under Open-Loop conditions, the DOL/$[H_2S]_{in}$ ratio was below the desired value most of the time, particularly during peak periods.

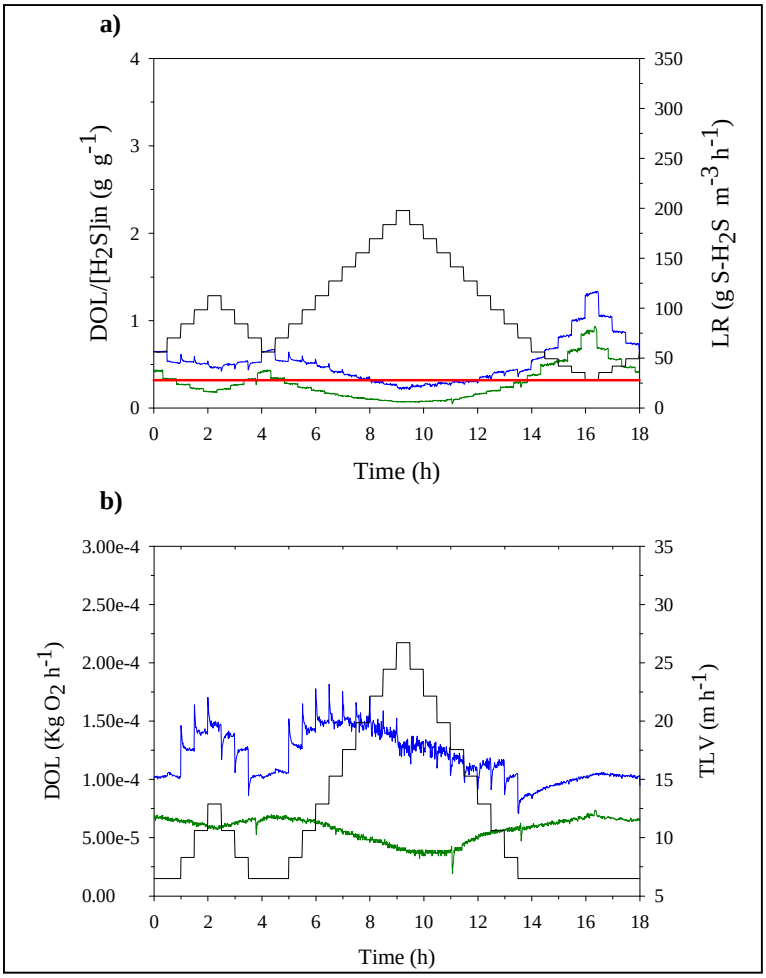

Figure 9.8. Experimental profiles for FF-EBRT-98 test with and without feedforward control. In Fig 9.8 (a): DOL/H_2S_{in} ratio, H_2S LR profiles under open-loop conditions (green solid line) and under Closed-Loop conditions (blue solid line) and setpoint (red solid line). In Fig. 9.8 (b): DOL profiles under Open-loop conditions (green solid line) and under Closed-Loop conditions (blue line), and TLV profile for the Closed-Loop case. (Black solid line).

Thus, the system was not performing under the optimum conditions for sulfate production due to oxygen limitation except during valley periods. Instead, under Closed-Loop conditions the DOL/$[H_2S]_{in}$ ratio was above the desired value most of the experimental time due to the TLV regulation, which lead to an increase in the amount of H_2S removed (Fig. 9.8a). Fig. 9.8b shows the significant DOL increase compared to the

Open-loop operation due to TLV regulation in the range of 5.9 m h^{-1} to 20 m h^{-1}. Interestingly, DOL decreased when TLV was higher than 20 m h^{-1} due to a reduction of the aeration column efficiency. Which can be explained due to a reduction in the liquid residence time that at the same time affects the gas-liquid mass transfer.

Reduction of the liquid residence time is directly related to the reduction of the liquid volume in the aeration column, which is explained by two phenomena that occurs at high TLV values (TVL>20 m h^{-1}). First due to an increase in the liquid recycling velocity and secondly due to increase of the liquid retention in the BTF packed bed. $[H_2S]_{out}$ concentration was barely improved at low H_2S LR as it can be observed during the first hours of the H_2S LR profile (Fig. 9.9a) and in the EC versus LR profile (Fig. 9.9b). At an H_2S LR above 100 g S-H_2S m^{-3} h^{-1}, biogas flowrate changes reduced significantly BTF performance. In that situation, the BTF was under mass transfer limitation due to a significant reduction of the EBRT.

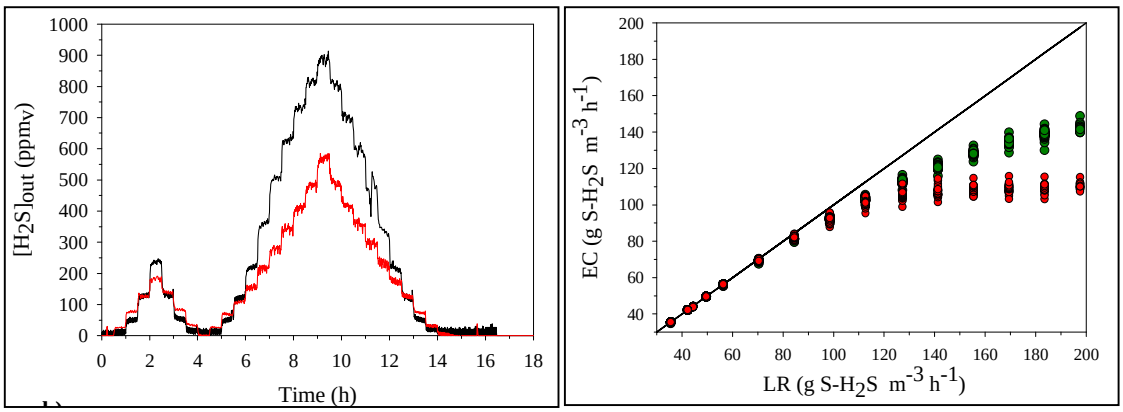

Figure 9.9. Experimental profiles for test FF-EBRT-98 with and without feedforward control. Fig. 9.9a: $[H_2S]_{out}$ concentration profile under Open-Loop (black solid line) and under Closed-loop (red solid line). In Fig. 9.9b: experimental EC profile under Open-Loop (red circles) and Closed-Loop (green circles) case, and 100% LR line (black solid line).

Application of a feedforward control when H_2S LR is increased due to variation on the biogas flowrate significantly reduces the $[H_2S]_{out}$ concentration (Fig. 9.9a) as it also improves the EC (Fig. 9.9b). The EC profile for the controlled process indicates that the BTF has not reached its maximum EC value. Contrarily to the EC profile of the Open-loop process that seemed to reach a plateau at LR over 150 g S-H_2S m^{-3} h^{-1}

9.3.5. Evaluation of feedforward control facing changes in the H_2S inlet concentration

Effect of TLV on O_2 load and the ratio DOL/$[H_2S]_{in}$

Fig. 9.10 shows the effect of the feedforward control loop implementation on DOL and the DOL/$[H_2S]_{in}$ ratio for the loading rates tested in this work (78, 98 and 116 g S-H_2S m^{-3} h^{-1}).

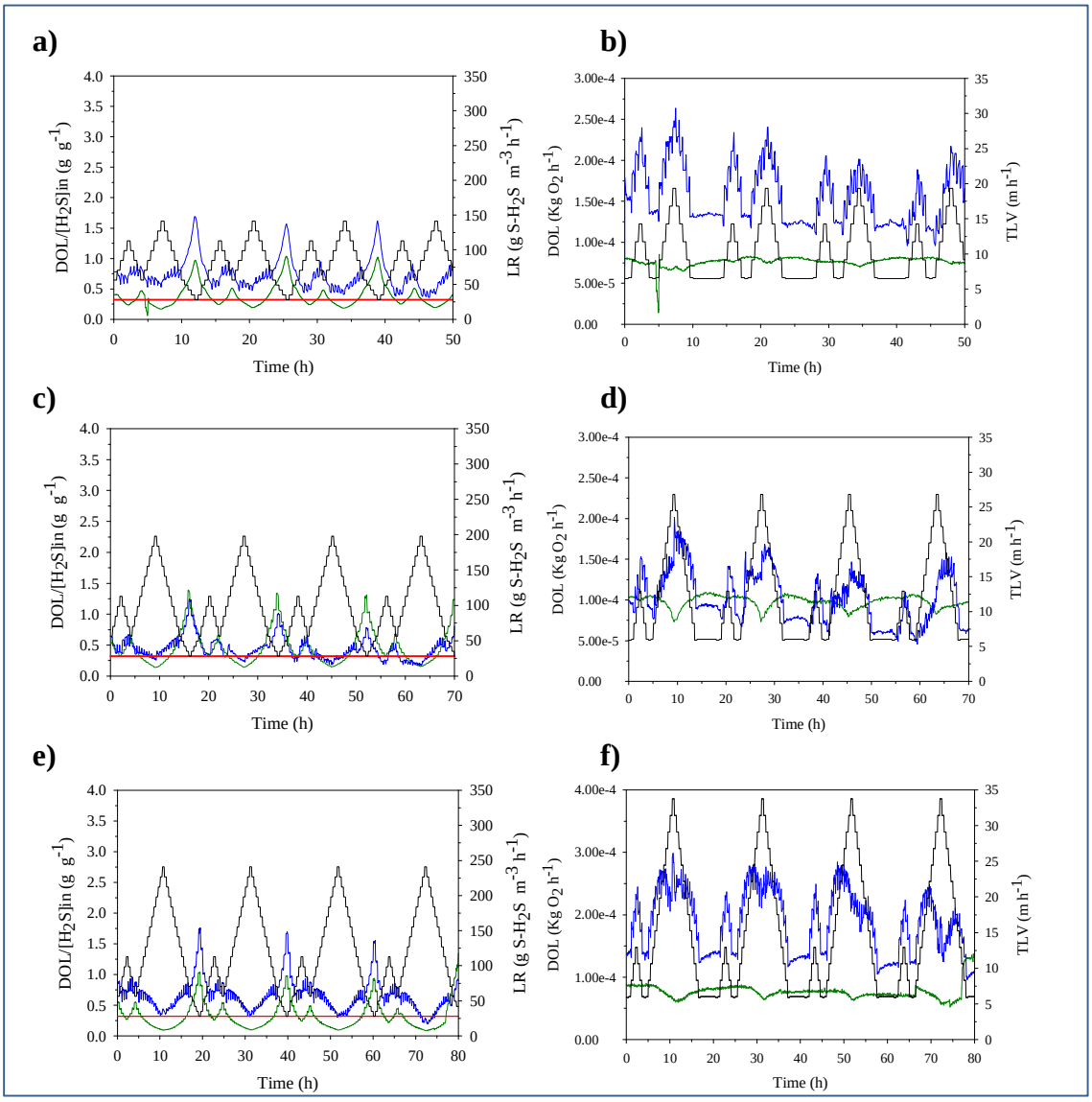

Figure 9.10. Experimental profiles obtained from tests FF-78, FF-98 and FF-116 with and without feedforward control. (a, b) Test FF-C-78 (c, d) Test FF-C-98 (e, f) Test FF-C-116. In Fig 9.10 (a,c,e): Open-Loop (green line), Close loop (blue solid line), Setpoint (red solid line) and loading rate (black solid line). In Fig. 9.10 (b.d.f): Open-Loop (green line), Close loop (blue solid line) and TLV (black solid line.

As it can be observed in Fig. 9.10 (a, c and e), tests performed in Close-loop show DOL/$[H_2S]_{in}$ above the setpoint (0.32 g O_2 g^{-1} S-H_2S_{in}) during most of the experimental time, which means that the complete oxidation of sulfide was favored. Tests performed without feedforward control (Open-loop) were whereas under the setpoint when [H_2S] LR was over 80-100 g S-H_2S m^{-3} h^{-1}. This means that the system will not have the capacity to completely oxidize sulfide at these loading rates. The implementation the feedforward control should improve theoretically the oxidation of sulfide to sulfate, since in chapter 5 it was showed that the O_2 availability increases with TLV regulation. This result was confirmed with Fig. 9.10 (b, d and f) in which the O_2 load is presented for each test with open and close loop. It is clearly shown that the DOL in Open-Loop tests was almost constant during each H_2S LR cycle. This means that, for higher H_2S LR elemental sulfur production was favored since the oxygen supply, and so the ratio DOL/$[H_2S]_{in}$, are essential to oxidize completely sulfide to sulfate.

Operating the BTF for long time periods under these conditions could lead to an excessive sulfur production and clogging of the packed bed. Meanwhile, in the case of close loop tests, the DOL increases following the TLV profile during most of the test time. Only during some hours in tests E-98 and E-116 DOL was under the setpoint due to operational problems.

Specifically due to a reduction of the liquid volume in the aeration column, since at TLV values higher than 20 m h^{-1}, the efficiency of the column was reduced. Between the two reasons that lead to the reduction of efficiency in the aeration column, increase in the liquid retention in the BTF packed bed could be the principal reason, due to biomass and solids (elemental sulfur) accumulation .This can be observed in Fig. 9.10d, were the DOL profile decreases when TLV exceeds the abovementioned value. In general terms, better results are obtained with the manipulation of TLV at higher H_2S LR because of the O_2 requirements for sulfide oxidation and the influence of mass transfer limitations.

Even so, the control must be improved since, although the DOL/$[H_2S]_{in}$ follows the setpoint trend, most of the experimental time is over the setpoint, which means higher power consumption by the recirculation pump.

Effect of TLV on H_2S removal and sulfate selectivity

Fig. 9.11 (a, b and c) shows the effect of feedforward control loop implementation on H_2S removal for the loading rates tested (78, 98 and 116 g S-H_2S m^{-3} h^{-1}). Mass transfer resistance could also increase with the accumulation of elemental sulfur since diminishes the superficial area of the packing material and decreases the absorption capacity. Interestingly, the profile obtained from E-98 (Fig. 9.11b) shows the effect of biomass growth and biomass density increment, since $[H_2S]_{out}$ decreases progressively along the test without any other change in the system both in constant and variable TLV experiments.

This behavior was not observed in tests E-78 and E-116. This fact demonstrate the difficulty of studying control strategies in BTFs with long-term operations, since factors like biomass growth and elemental sulfur accumulation modifies the BTF performance, making difficult the differentiation between the impact of disturbances and long-term effects.At the lowest $[H_2S]$ LR_{avg} (FF-C-78) the biomass concentration was probably increasing slowly, which did not increase the EC significantly, and the adaptation of the biomass was not necessary at such low load. At the highest H_2S LR_{avg} (FF-C-116) the problem was probably that, despite the biomass concentration was higher after previous tests, the maximum oxidation rate was already reached and the process was not controllable under those conditions.

Regardless the adaptation of the biomass, with the implementation of the control strategy the $[H_2S]_{out}$ was kept under 500 ppm_v in most of the cases after the first 25h of each test. This result is especially important since the control strategy proposed in this work avoids shock loads of H_2S to energy recovery processes which causes corrosion and damage of engines (Walsh et al., 1988).

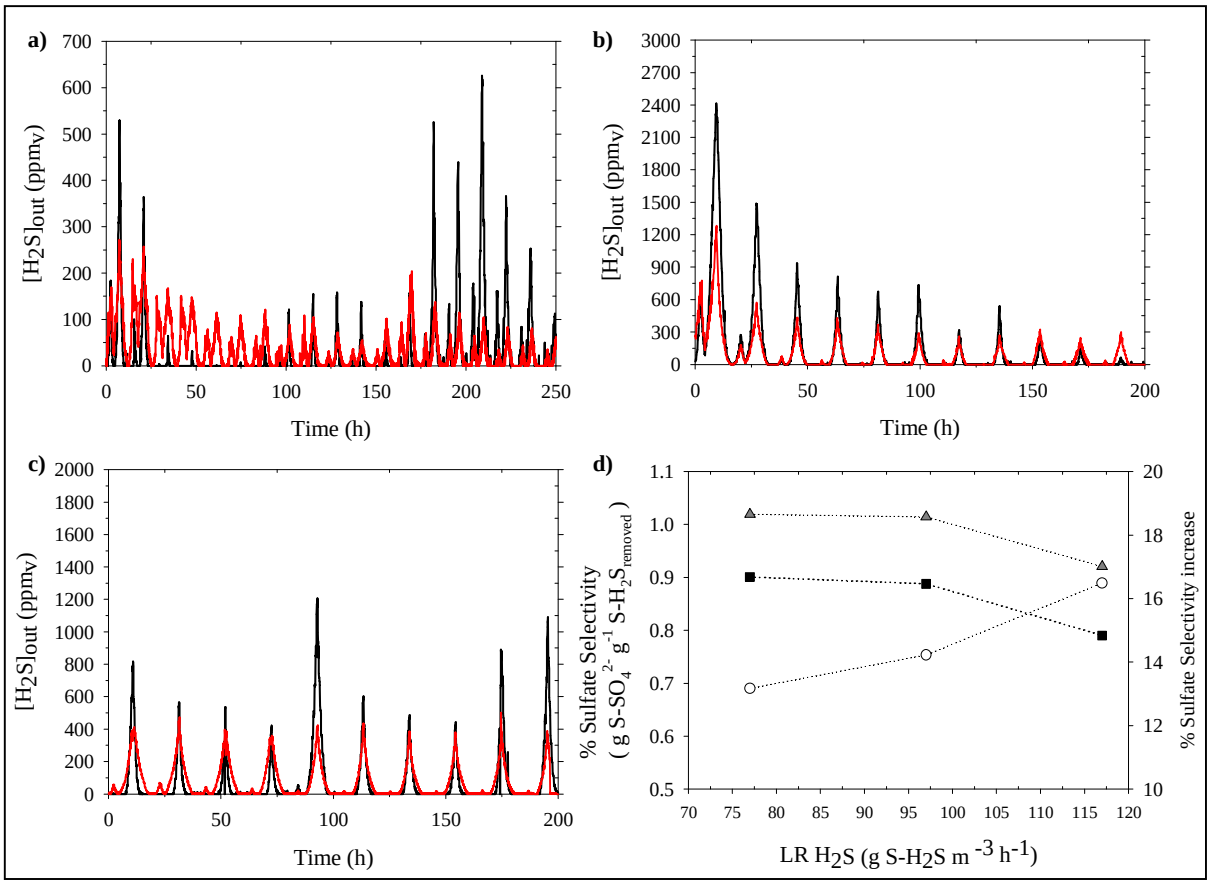

Figure 9.11. Concentration profiles and sulfate selectivity obtained from variable H_2S LR operations with and without the implementation of feedforward control. (a) $[H_2S]_{out}$ concentration for FF-C-78 experiment. (b) $[H_2S]_{out}$ concentration for FF-C-98 experiment. (c) $[H_2S]_{out}$ concentration for FF-C-116 experiment. Experiments with constant TLV (Open-Loop) are presented with solid black line and experiments with variable TLV (Closed-Loop) are presented with solid red line. (d) Sulfate selectivity (Open-Loop: black squares; Closed-Loop: grey triangles) and sulfate selectivity increment (white circles) obtained with and without the implementation of feedforward control.

In Fig. 9.11d sulfate selectivity, with and without feedforward control, is presented on the left y axis. It can be observed that increasing the TLV according to the H_2S LR increase leads to an enhancement of sulfate selectivity up to 92%, which corresponds to a relative sulfate selectivity increase up to 16.5 % (right y axis in Fig 9.1d). Similar results were obtained by Rodriguez et al. (Rodriguez et al., 2014) who obtained an increment of 17% on sulfate selectivity using a jet-venturi device to improve O_2 transfer efficiency. This means that the implementation of a feedforward control strategy together with the use of intensive transfer devices would improve significantly the operation of desulfurizing BTFs while reducing operational and maintenance costs. Also it must be noticed that sulfate selectivity for Open-Loop tests were considerably higher compared

to those values obtained when comparable step-wise H_2S LR increments were applied for short periods of time (Montebello et al., 2010). As it was seen before with the $[H_2S]_{out}$, sulfate selectivity during Open-Loop tests also support the fact that a better biomass density distribution is achieved along the BTF bed when a variable H_2S LR is applied to the BTF.

9.3.6. Overall assessment of feedback and feedforward control strategies

From the application of control strategies in desulfurizing BTF for biogas desulfurization under aerobic conditions several remarks must be done. Knowledge acquired in previous chapters through experimental and model-based analysis has allowed to test and evaluate experimentally different control strategies. As it was described in chapter 3, the main aim of control strategies is to improve O_2 transfer and therefore improve sulfate production, since elemental sulfur accumulation is the main drawback of this technology. In this chapter, control strategies were based on TLV regulation since experimentally and through model analysis, it was confirmed to be the most suitable manipulated variable. Even the added value of feedback control strategies was not quantified in this chapter, added value of feedforward control strategies also confirmed that TLV does haves a direct impact over H_2S removal and over sulfate production. Regarding feedback control it has to be mentioned that, TLV was better to control H_2S inlet concentration variations than biogas flowrate changes, since this last situation required highest TLV which in this BTF setup were difficult to apply.

Regarding the applicability of controller parameters obtained previously through model-based analysis, it must be remarked that the previous study performed in chapter 8 was helpful to delimit the range of the parameters. However, this cycle of model analysis and experimental validation, should be repeated in order to improve model predictions by implementing those new phenomena found through experimental validation of control strategies. Results here presented, are just the first iteration. In the other hand, feedforward results showed to also a suitable to control H_2S outlet concentration and to improve sulfate production. This strategy should be firstly applied in order to avoid that disturbances affect the BTF performance, as it occurs when feedback control is applied. However in most of the cases, it is recommended to have a secondary control loop in order to measure the H_2S outlet concentration and perform another actuation. Since in chapter 5 and chapter 8 it was demonstrated that air flowrate regulation

does not improves significantly process performance, this secondary measurement could be used to modify the feedforward controller parameters, according the error between a certain setpoint and the measured variable value. In some installations when biogas is not used for energy generation, air flowrate could be used as secondary actuation since the dilution effect would not be important.

Essentially, control strategies have showed to be effective to improve performance of BTF for biogas desulfurization under aerobic conditions, especially through TLV regulation since increases O_2 transport without any biogas dilution.

9.4. CONCLUSIONS

From experimental application of feedback and Feedforward control strategies based in TLV regulation in an aerobic BTF for biogas desulfurization the following conclusions were obtained:

Experimental application of feedback control strategy, showed that this strategy improved BTF stability against H_2S inlet concentration changes and biogas flowrate changes through TLV regulation.

TLV regulation in the H_2S LR range of 149-163 g S-H_2S m^{-3} h^{-1} when H_2S inlet concentration was the disturbance, provided satisfactory results in terms of reduction of the H_2S outlet concentration peaks compared to the Open-Loop case. This H_2S LR range is in agreement with controllable H_2S LR range predicted by the model-based analysis performed in chapter 8.

As well when biogas flowrate was the disturbance, TLV also demonstrated to be a suitable strategy to implement in a feedback control loop in the H_2S LR range of 115-130 g S-H_2S m^{-3} h^{-1}, which also correspond to the controllability range predicted by the theoretical analysis performed in chapter 8.

Despite that the process was under mass transfer limitation when biogas flowrate was changed, TLV was able to reduce H_2S concentration peaks applying higher TLV than when H_2S inlet concentration was changed. This demonstrate that biogas flowrate changes are more difficult to control than H_2S inlet concentration.

In the other hand, process performance was considerably improved when a feedforward control loop based in TLV regulation was implemented in a BTF for biogas desulfurization under aerobic conditions.

Satisfactory results of the application of feedforward control are due to rigorous and arduous study of the effect of TLV over the process performance done in chapter 5, one of the premises of feedforward control. Also study of the effect of the disturbance over the process helped to design a better control strategy.

Also in feedforward control, regulation of H_2S inlet concentration changes and biogas flowrate changes through TLV was studied. Even only gas phase gas was studied when biogas flowrate was changed, feedforward control loop based in TLV regulation displayed to improve the EC of the reactor compared to the Open-Loop case where the process is clearly mass transfer limited. When changes in the H_2S inlet concentration was studied, adaptation of biomass during the long-run operation was observed. Long-run operation, besides allowing to observe an H_2S removal improvement, TLV regulation in a feedforward control loop also allowed to minimize elemental sulfur production by increasing O_2 gas-liquid transport along the packed bed.

Feedforward control strategy allowed to maintain H_2S emissions most of the experimental time under 500 ppm_v, concentration under which the shortening of the energy recovery systems lifespan and the additional maintenance costs of the biogas valorization process are minimized.

In overall, this work demonstrates that TLV manipulation is a suitable strategy to implement in a feedback control loop, but especially in a feedforward control loop based on H_2S inlet concentration measurements. Control strategies based in TLV regulation improves BTF performance for biogas desulfurization under aerobic conditions without biogas calorific capacity reduction.

CHAPTER 10

GENERAL CONCLUSIONS AND FUTURE WORK

10. GENERAL CONCLUSIONS AND FUTURE WORK

10.1 CONCLUSIONS

Control strategies were studied from an experimental and modelling approach towards process optimization by improving the oxygen transfer to the liquid phase in a desulfurizing biotrickling filter under aerobic conditions.

Main conclusions related to Chapter 5 are:

- Experimental work allowed characterizing the effect of trickling liquid velocity and air flowrate modulation in an aerobic biotrickling filters for biogas desulfurization under different loading rate conditions.
- Trickling liquid velocity showed a higher influence over the main performance parameters such as removal efficiency, elimination capacity and sulfate selectivity, indicating that trickling liquid velocity is a suitable variable to manipulate in order to regulate dissolved oxygen load to the biotrickling filter.
- Air flowrate regulation barely improved performance parameters of the biotrickling filter, moreover air flowrate regulation involves biogas dilution and, concomitantly, a loss of calorific power. Therefore, air flowrate regulation is not recommended as manipulated variable in control strategies for desulfurizing biotrickling filters under aerobic conditions.

Main conclusions related to Chapter 6 are:

- Application of titrimetry allowed relating biological activity during different operating conditions with titrimetric variables such as the biological proton production and biological proton production rate.
- Proton production rate was influenced by the noise associated to pH control signal, while proton production showed to be a more suitable variable for process monitoring.
- Titrimetric variables were closely related to operational changes at the highest loading rate conditions tested.
- Carbon dioxide stripping occurring during autotrophic denitrification process was successfully characterized through the use of titrimetric techniques.
- The application of titrimetric techniques permitted obtaining the stoichiometry of the two-step autotrophic denit7rification and thiosulfate oxidation, but also

the biomass-substrate yields and the biological activities for respirometric tests under anoxic conditions.

Main conclusions related to Chapter 7 are:

- A dynamic model describing physical-chemical and biological processes for the removal of high loads of H_2S from biogas streams in biotrickling filters (BTFs) for a BTF for high H_2S loading rates biogas desulfurization in aerobic conditions was developed and successfully calibrated and validated allowing a proper description of different operational scenarios.
- The biotrickling filter model was validated under a stationary feeding period and a dynamic H_2S LR period.
- A two-step sulfide oxidation kinetic model was successfully integrated in a complete model of a biotrickling filter o describe intermediate oxidation products.
- Sensitivity analysis showed that the most sensitive parameters of the model were those parameters related to O_2 mass transport, which exhibited a larger influence to model output variables considered.
- Model allowed an accurate description of the outlet H_2S concentration profile along the BTF bed, intermediate products accumulation like elemental sulfur, and sulfate production during pseudo-steady and dynamic operating conditions. of the biotrickling filter.

Main conclusions related to Chapter 7 are:

- Billet and Schultes correlation was selected when compared with Onda's correlation in order to determine the global G-L mass transfer coefficient.
- Simulations under Open-Loop conditions indicated that process control in desulfurizing biotrickling filters is needed in order to mitigate disturbances in the H_2S loading rate.
- Strategies based on air flowrate regulation for controlling oxygen outlet concentration showed to be inefficient in terms of process improvement when added-value variables such as sulfate selectivity were considered.
- Controlling oxygen concentration through air flowrate regulation did not only barely improve added-value variables but also involved biogas dilution, which was negative in terms of energy recovery.

- Trickling liquid velocity regulation for controlling H_2S outlet concentration showed to be a feasible strategy to improve complementary biotrickling filter performance parameters such as removal efficiency, sulfate selectivity and oxygen consumption.
- The type of disturbance used to study control strategies did not allow evaluating the proportional integral controller properly in all the cases studied.
- Comparison between the two manipulated variables showed that better results are obtained through trickling liquid velocity regulation since no biogas dilution is involved and because higher percentage of process improvement is achieved.

Main conclusions related to Chapter 9 are:

- Experimental application of a feedback control strategy showed that this strategy improved BTF stability against H_2S inlet concentration changes and biogas flowrate changes through TLV regulation.
- H_2S LR ranges studied in Chapter 9 are in agreement with controllability ranges predicted by the model-based analysis performed in Chapter 8.
- TLV regulation allowed reducing H_2S concentration peaks despite the BTF was under mass transfer limitation during biogas flowrate changes.
- H_2S outlet concentration was properly controlled through trickling liquid velocity when a feedback control strategy was coupled to a desulfurizing biotrickling filter operating under variable H_2S loading rate conditions, especially in the case when biogas flowrate was varied since the process was under mass transfer limitation.
- Satisfactory results of the application of feedforward control requires of a previous rigorous analysis of the effect of TLV over the process performance under open-loop conditions.
- TLV regulation in a feedforward control loop during long-run operation allowed, besides allowing observing an H_2S removal improvement, minimizing elemental sulfur production by increasing O_2 gas-liquid transport along the packed bed.

Overall, the main conclusion of this thesis is that the use of control strategies based on TLV regulation can be used to improve BTF performance for biogas desulfurization under aerobic conditions without biogas calorific capacity reduction.

Development and application control strategies towards the optimization of biogas desulfurization in BTFs under aerobic conditions have allowed acquiring sufficiently information to set this work as a reference for future work in this field. However, in this work only a certain number of strategies under a defined operational conditions have been performed, and therefore there is still different areas in this field which could be further investigated.

Regarding the characterization of the manipulated variables involved in an aerobic BTF for biogas desulfurization (Chapter 5), the following improvements could be done in future research in order to improve or obtain further information:

- Improving or modifying the design of the aeration column, since at high TLV values, reduction of the volume in the aeration column affects the gas-liquid mass transfer efficiency.

- More effective devices such as jet-venture could be implement in the BTF set up in order to improve oxygen mass transfer to the liquid phase in the aeration column.

- Test the alternation of co-current flow pattern and counter-current flow pattern during non-regulated experiments to achieve a more homogeneous biomass distribution along the packed bed, and therefore be able to attenuate loading rate fluctuations.

- Improve the gas phase measurement system of the BTF setup up, since when high dilution air flowrates were used, high errors were observed in the experimental measures.

- Implementation of an off-line FIA monitoring system to monitor total dissolved sulfide in the liquid phase in order to have a better estimation of sulfur mass balances.

- Experimentally it was observed that the liquid lines have a considerable amount of biomass, father study to determine the percentage of degradation that

corresponds to this part of the BTF could be useful at the time of modelling the BTF performance.

Regarding the evaluation of titrmetry as a possible measured variable in control loops (Chapter 6), especially for the application in continuous processes such as BTF for biogas desulfurization, the following tasks could be done in future research in order to improve this technique:

- Implementation of a pH controller different from ON/OFF control is required, such as a proportional (P) or proportional integral controller (PI). The type of controller installed should avoid control the pH between the LSP and HSP band.

- The equations describing the different contributions to the $HP_{observed}$ are already defined and biological HP and HPR could be determine on-line in order to evaluate the suitability of titrimetry in a long-term operation.

- Further knowledge and evaluation of the characterization of the different physical-chemical contributions affecting the pH must be performed, such as the characterization of CO_2 stripping under abiotic conditions in the BTF.

In relation with the development of the BTF model performed in Chapter 7, several improvements could be done, by studying some of the assumptions performed, and therefore obtain a more realistic model.

- Since in the BTF model a homogeneous biofilm density along the packed bed height of the BTF was considered, a function describing a variable biofilm density could be implemented.

- Including a wetted/non-wetted biofilm description could be necessary when TLV regulations are done, since the amount of water in the packed bed varies, affecting then the gas-liquid mass transfer.

- Include in the model the variation of the liquid volume of the aeration column in function of the liquid recycling flowrate.

- Implement titrimetric equations to the BTF model in order to determine the biological HP and HPR.

Also further research could be done in the model-based analysis (Chapter 8), in order to examine through simulation, different control strategies, which were not included in this work. Implementation of these improvements in the model-based study would help to approximate results obtained through simulations with results obtained later in the experimental evaluation of control strategies (Chapter 9). In this sense, further el research about experimental control strategies development and application is needed.

- Evaluate the use of oxygen concentration as a possible controlled variable through TLV regulation.

- Include the DOL in the liquid recycling line as a possible measured variable in a secondary control loop of a cascade control loop, where the primary loop would be based in TLV regulation for H_2S outlet concentration control.

- Analyze feedback control strategies using dynamic H_2S LR profiles, instead of step-wise H_2S LR increments, since it was observed that the shape of the disturbance affected PI controller's performance.

- Alternative control rules for controller parameters tuning could be tested and compared with the methodology used in this work.

CHAPTER 11

REFERENCES

Abatzoglou, N., Boivin, S., 2009. A review of biogas purification. Biofuels, Bioprod. Biorefining 3, 42–71.

Ahmed, W., Shareefdeen, Z.M., Jabbar, N.A., 2013. Dynamic modeling and analysis of biotrickling filters in continuous operation for H2S removal. Clean Technol. Environ. Policy 16, 1757–1765.

Alcántara, S., Pedret, C., Vilanova, R., 2010. On the model matching approach to PID design: Analytical perspective for robust Servo/Regulator tradeoff tuning. J. Process Control 20, 596–608.

Alex, J., Benedetti, L., Copp, J., Gernaey, K. V, Jeppsson, U., Nopens, I., Pons, M., Rieger, L., Rosen, C., Steyer, J.P., Vanrolleghem, P., Winkler, S., 2008. Benchmark Simulation Model No . 1 (BSM1).

Almenglo, F., Ramírez, M., Gómez, M., Cantero, D., David, A., 2015. Modeling and control strategies for anoxic biotrickling filtration in biogas purification. J. Chem. Technol. Biotechnol.

Alonso, C., Suidan, M.T., Sorial, G. a, Smith, F.L., Biswas, P., Smith, P.J., Brenner, R.C., 1997. Gas treatment in trickle-bed biofilters: biomass, how much is enough? Biotechnol. Bioeng. 54, 583–94.

Alonso, C., Zhu, X., Suidan, M.T., Kim, B.R., Kim, B.J., 2001. M ATHEMATICAL M ODEL OF B IOFILTRATION OF VOC S : 127, 655–664.

Álvarez, J.A., Otero, L., Lema, J.M., 2010. Bioresource Technology A methodology for optimising feed composition for anaerobic co-digestion of agro-industrial wastes. Bioresour. Technol. 101, 1153–1158.

Álvarez-Hornos, F.J., Gabaldón, C., Martínez-Soria, V., Marzal, P., Penya-roja, J.-M., 2009. Mathematical modeling of the biofiltration of ethyl acetate and toluene and their mixture. Biochem. Eng. J. 43, 169–177.

Andreasen, R.R., Nicolai, R.E., Poulsen, T.G., 2012. Pressure drop in biofilters as related to dust and biomass accumulation. J. Chem. Technol. Biotechnol. 87, 806–816.

Araya, P., Aroca, G., Chamy, R., 1999. Anaerobic treatment of effluents from an industrial polymers synthesis plant 19, 141–146.

Ariunbaatar, J., Panico, A., Esposito, G., Pirozzi, F., Lens, P.N.L., 2014. Pretreatment methods to enhance anaerobic digestion of organic solid waste. Appl. Energy 123, 143–156.

Artiga, P., González, F., Mosquera-Corral, A., Campos, J.L., Garrido, J.M., Ficara, E., Méndez, R., 2005. Multiple analysis reprogrammable titration analyser for the kinetic characterization of nitrifying and autotrophic denitrifying biomass. Biochem. Eng. J. 26, 176–183.

Åström, K.J., Hägglund, T., 2004. Revisiting the Ziegler-Nichols step response method for PID control. J. Process Control 14, 635–650.

Baeza, J.A., 2016. Principles of bioprocess control. In: Current Developments In Biotechnology and Bioengineering. Elsevier.

Baeza, J.A., Gabriel, D., Lafuente, J., 2004. Effect of internal recycle on the nitrogen removal efficiency of an anaerobic/anoxic/oxic (A2/O) wastewater treatment plant (WWTP). Process Biochem. 39, 1615–1624.

Baeza, J.A., Gabriel, D., Lafuente, J., 2002. Improving the nitrogen removal efficiency of an A2/O based WWTP by using an on-line Knowledge Based Expert System. Water Res. 36, 2109–2123.

Baltzis, B.C., Mpanias, C.J., Bhattacharya, S., 2001. Modeling the removal of VOC mixtures in biotrickling filters. Biotechnol. Bioeng. 72, 389–401.

Baquerizo, G., Maestre, J.P., Sakuma, T., Deshusses, M.A., Gamisans, X., Gabriel, D., Lafuente, J., 2005. A detailed model of a biofilter for ammonia removal: Model parameters analysis and model validation. Chem. Eng. J. 113, 205–214.

Barjenbruch, M., Kopplow, O., 2003. Enzymatic , mechanical and thermal pre-treatment of surplus sludge 7, 715–720.

Bartrolí, A., Pérez, J., Carrera, J., 2010. Applying ratio control in a continuous granular reactor to achieve full nitritation under stable operating conditions. Environ. Sci. Technol. 44, 8930–8935.

Basu, S., Khan, A.L., Cano-odena, A., 2010. Membrane-based technologies for biogas separations 750–768.

Betlach, M.R., Tiedje, J.M., 1981. Kinetic Explanation for Accumulation of Nitrite , Nitric Oxide , and Nitrous Oxide During Bacterial Denitrificationt 42, 1074–1084.

Billet, R., Schultes, M., 1999. Prediction of mass transfer columns with dumpled and arranged packings Updated Summary of the Calculation Method of Billet and Schultes. Chem. Eng. Res. Des. 77, 498–504.

Boden, T.A., Marland, G., Andres, R.J., 2015. National CO2 Emissions from Fossil-Fuel Burning, Cement Manufacture, and Gas Flaring: 1751-2011

Bonilla-Blancas, W., Mora, M., Revah, S., Baeza, J.A., Lafuente, J., Gamisans, X., Gabriel, D., González-Sánchez, A., 2015. Application of a novel respirometric methodology to characterize mass transfer and activity of H2S-oxidizing biofilms in biotrickling filter beds. Biochem. Eng. J. 99, 24–34.

Bouallagui, H., Lahdheb, H., Romdan, E. Ben, Rachdi, B., Hamdi, M., 2009. Improvement of fruit and vegetable waste anaerobic digestion performance and stability with co-substrates addition. J. Environ. Manage. 90, 1844–1849.

British Petroleum, 2015. BP Statistical Review of World Energy.

Campos, J.L., Carvalho, S., Portela, R., Me, R., 2008. Kinetics of denitrification using sulphur compounds : Effects of S / N ratio , endogenous and exogenous compounds 99, 1293–1299.

Carroll, B.W., Ostlie, D.A., 2007. An Introduction to Modern Astrophysics. Pearson Eduction, Inc.

Cartwright, P.E., P.S., 2005. Water Reuse. Water Encyclopedia, 1st ed.

Caulet, C., Bujo, B., Philippe, J., Lefevre, F., Audic, J., 1998. Upgrading of wastewater treatment plants for nitrogen removal: industrial application of an automated aeration management based on ORP evolution analysis. Water Sci. Technol. 37, 41–47.

Cavinato, C., Fatone, F., Bolzonella, D., Pavan, P., 2010. Bioresource Technology Thermophilic anaerobic co-digestion of cattle manure with agro-wastes and energy crops : Comparison of pilot and full scale experiences. Bioresour. Technol. 101, 545–550.

Chaiprapat, S., Charnnok, B., Kantachote, D., Sung, S., 2015. Bio-desulfurization of biogas using acidic biotrickling filter with dissolved oxygen in step feed recirculation. Bioresour. Technol. 179, 429–35.

Chaiprapat, S., Mardthing, R., Kantachote, D., Karnchanawong, S., 2011. Removal of hydrogen sulfide by complete aerobic oxidation in acidic biofiltration. Process Biochem. 46, 344–352.

Chaisson, E., McMillan, S., 1999. Astronomy Today, 5th ed. Prentice Hall.

Cohen, Gh., Coon, G.A., 1953. Theoretical consideration of retarded control. Trans. Asme 75, 827–834.

Corriou, J.P., Pons, M.N., 2004. Model predictive control of wastewater treatment plants: Application to the BSM1 benchmark. Comput. Aided Chem. Eng. 18, 625–630.

Cortus, E.L., Lemay, S.P., Barber, E.M., Hill, G.A., Godbout, S., 2008. A dynamic model of ammonia emission from urine puddles 99, 390–402.

Couvert, A., Renner, C., Levasseur, J., 2010. Wet Scrubbing Intensification Applied to Hydrogen Sulphide Removal in Waste Water 88, 682–687.

Deshusses, M.A., Cox, H.H.J., 2002. Biotrickling filters for air pollution control, in: The Encyclopedia of Environmental Microbiology. J. Wiley & Sons, pp. 782–792.

Deshusses, M.A., Hamer, G., Dunn, I.J., 1995. Behavior of Biofilters for Waste Air Biotreatment. 1. Dynamic Model Development. Environ. Sci. Technol. 29, 1048–1058.

Deublein, D., A. Steinhauser, 2008. Biogas from Waste and Renewable Resources, Wiley-VCH . ed. Weinheim, Germany.

Devinny, J., Armstrong, C., 1999. Biological Treatment of Industrial Waste A 2–5.

Devinny, J.S., Deshusses, M.A., Webster., T.S., 1999. Biofiltration for Air Pollution Control. CRC Lewis Publishers.

Devinny, J.S., Ramesh, J., 2005. A phenomenological review of biofilter models. Chem. Eng. J. 113, 187–196.

Diks, R.M.M., Ottengraf, S.P.P., 1991. Verification studies of a simplified model for the

removal of dichloromethane from waste gases using a biological trickling filter O-o. Bioprocess Eng. 6, 93–99.

Doan, H.D., Wu, J., Eyvazi, M.J., 2008. Effect of liquid distribution on the organic removal in a trickle bed filter. Chem. Eng. J. 139, 495–502.

Dorado, A.D., Dumont, E., Muñoz, R., Quijano, G., 2015. A novel mathematical approach for the understanding and optimization of two-phase partitioning bioreactors devoted to air pollution control. Chem. Eng. J. 263, 239–248.

Dorado, A.D., Rodriguez, G., Ribera, G., Bonsfills, A., Gabriel, D., Lafuente, J., Gamisans, X., 2009. Evaluation of Mass Transfer Coefficients in Biotrickling Filters: Experimental Determination and Comparison to Correlations. Chem. Eng. Technol. 32, 1941–1950.

Duan, H., Koe, L.C.C., Yan, R., Chen, X., 2006. Biological treatment of H2S using pellet activated carbon as a carrier of microorganisms in a biofilter. Water Res. 40, 2629–36.

Environmental Protection Agency, U.. D. of E., 2014. Biogas Opportunities Roadmap.

Estrada, J.M., Kraakman, N.J.R. (Bart), Lebrero, R., Muñoz, R., 2012. A sensitivity analysis of process design parameters, commodity prices and robustness on the economics of odour abatement technologies. Biotechnol. Adv. 30, 1354–1363.

European Commission, 2013. Report from the commission to the european parliament and the council progress towards achieving the Kyoto and EU 2020 objectives. Brussels, Belgium.

Eurostat, 2015. The EU in the world 2015.

Fernández, M., Ramírez, M., Gómez, J.M., Cantero, D., 2013a. Biogas biodesulfurization in an anoxic biotrickling filter packed with open-pore polyurethane foam. J. Hazard. Mater. 1–7.

Fernández, M., Ramírez, M., Pérez, R.M., Gómez, J.M., Cantero, D., 2013b. Hydrogen sulphide removal from biogas by an anoxic biotrickling filter packed with Pall rings. Chem. Eng. J. 225, 456–463.

Ficara, E., Rozzi, A., Cortelezzi, P., 2003. Theory of pH-stat titration. Biotechnol. Bioeng. 82, 28–37.

Fortuny, M., 2009. Expanding the application range of conventional biological gas treatment techniques: Development of a biotechnological reactor for energy-rich gases desulfurization. Universitat Autònoma de Barcelona. PhD Thesis.

Fortuny, M., Baeza, J.A., Gamisans, X., Casas, C., Lafuente, J., Deshusses, M.A., Gabriel, D., 2008. Biological sweetening of energy gases mimics in biotrickling filters. Chemosphere 71, 10–17.

Fortuny, M., Gamisans, X., Deshusses, M.A., Lafuente, J., Casas, C., Gabriel, D., 2011. Operational aspects of the desulfurization process of energy gases mimics in biotrickling filters. Water Res. 45, 5665–5674.

Fortuny, M., Guisasola, A., Casas, C., Gamisans, X., Lafuente, J., Gabriel, D., 2010. Oxidation of biologically produced elemental sulfur under neutrophilic conditions. J. Chem. Technol. Biotechnol. 85, 378–386.

Gabriel, D., Cox, H.H.J., Deshusses, M.A., 2004. Conversion of Full-Scale Wet Scrubbers to Biotrickling Filters for H 2 S Control at Publicly Owned Treatment Works 1110–1117.

Gabriel, D., Deshusses, M. a, 2003a. Retrofitting existing chemical scrubbers to biotrickling filters for H2S emission control. Proc. Natl. Acad. Sci. U. S. A. 100, 6308–12.

Gabriel, D., Deshusses, M.A., 2003b. Performance of a Full-scale Biotrickhg Fflter Treating H2S at a Gas Contact Time of 1 . 6 t o 2 . 2 Seconds 111–118.

García-Diéguez, C., Molina, F., Roca, E., 2011. Multi-objective cascade controller for an anaerobic digester. Process Biochem. 46, 900–909.

Gernaey, K. V., Van Loosdrecht, M.C.M., Henze, M., Lind, M., Jørgensen, S.B., 2004. Activated sludge wastewater treatment plant modelling and simulation: State of the art. Environ. Model. Softw. 19, 763–783.

Gernaey, a. K., Petersen, B., Ottoy, J.P., Vanrolleghem, P., 2001. Activated sludge monitoring with combined respirometric-titrimetric measurements. Water Res. 35,

1280–1294.

Gernaey, K., Petersen, B., Dochain, D., Vanrolleghem, P.A., 2002. Modeling aerobic carbon source degradation processes using titrimetric data and combined respirometric?titrimetric data: Structural and practical identifiability. Biotechnol. Bioeng. 79, 754–767.

Gonzaléz, A., Arellano García, L., Bonilla-Blancas, W., Baquerizo, G., Hernandéz, S., Gabriel, D., Revah, S., 2014. Kinetic Characterization by Respirometry of Volatile Organic Compound-Degrading Bio fi lms from Gas-Phase Biological Filters.

Gonzalez, G., Richards, J., 2004. The Privileged Planet: How Our Place in the Cosmos is Designed for Discovery. Regnery Publishing.

Guerrero Camacho, F.J., 2014. Improving EBRT stability in WWTPs aiming at simultaneous carbon and nutrient removal: from modelling studies to experimental validation. Universitat Autonoma de Barcelona.

Guerrero, J., Guisasola, A., Baeza, J. a, 2014. A novel control strategy for efficient biological phosphorus removal with carbon-limited wastewaters. Water Sci. Technol. 70, 691–7.

Guerrero, J., Guisasola, A., Vilanova, R., Baeza, J. a., 2011. Improving the performance of a WWTP control system by model-based setpoint optimisation. Environ. Model. Softw. 26, 492–497.

Guimerà, X., Moya, A., Dorado, A.D., Villa, R., Gabriel, D., Gabriel, G., Gamisans, X., 2014. Biofilm dynamics characterization using a novel DO-MEA sensor: mass transport and biokinetics. Appl. Microbiol. Biotechnol. 5

Guisasola, A., Marcelino, M., Lemaire, R., Baeza, J.A., Yuan, Z., 2010. Modelling and simulation revealing mechanisms likely responsible for achieving the nitrite pathway through aeration control. Water Sci. Technol. 61, 1459–65.

Guisasola, A., Petzet, S., Baeza, J. a, Carrera, J., Lafuente, J., 2007a. Inorganic carbon limitations on nitrification: experimental assessment and modelling. Water Res. 41, 277–86.

Guisasola, A., Petzet, S., Baeza, J.A., Carrera, J., Lafuente, J., 2007b. Inorganic carbon limitations on nitrification: Experimental assessment and modelling. Water Res. 41,

277–286.

Guisasola, A., Vargas, M., Marcelino, M., Lafuente, J., Casas, C., Baeza, J.A., 2007c. On-line monitoring of the enhanced biological phosphorus removal process using respirometry and titrimetry. Biochem. Eng. J. 35, 371–379.

Gujer, W., Henze, M., Mino, T., Van Loosdrecht, M.C.M., 1999. Activated Sludge Model No. 3. Water Sci. Technol. 39, 183–193.

Hartmans, S., Tramper, J., 1991. Dichloromethane removal from waste gases with a trickle-bed bioreactor. Bioprocess Eng. 6, 83–92.

Hendriks, A.T.W.M., Zeeman, G., 2009. Bioresource Technology Pretreatments to enhance the digestibility of lignocellulosic biomass 100, 10–18.

Henze, M., Grady, C.P.L., J., Gujer, W., Marais, G.V.R., Matsuo, T., 1987. Activated Sludge Model No. 1. IAWQ Scientific and Techni- cal Report No. 1. London, UK.

Heredia-Molinero, M.C., Sánchez-Prieto, J., Briongos, J. V., Palancar, M.C., 2014. Feedback PID-like fuzzy controller for pH regulatory control near the equivalence point. J. Process Control 24, 1023–1037.

Hodge, D.., Devinny, J.S., 1995. Modeling removal of air contaminants by biofiltration. J. Environ. Eng. 121, 21–32.

Holubar, P., Zani, L., Hager, M., Fröschl, W., Radak, Z., Braun, R., 2002. Advanced controlling of anaerobic digestion by means of hierarchical neural networks. Water Res. 36, 2582–2588.

Horikawa, M.S., Rossi, F., Gimenes, M.L., Costa, C.M.M., Silva, M.G.C., 2004. Chemical Absorption of H2S For Biogas Purification 21, 415–422.

Iliuta, I., Larachi, F., 2005. Modeling simultaneous biological clogging and physical plugging in trickle-bed bioreactors for wastewater treatment. Chem. Eng. Sci. 60, 1477–1489.

Intenational Gas Union, 2015. Biogas - From Refuse to Energy.

Isanta, E., Figueroa, M., Mosquera-Corral, A., Campos, L., Carrera, J., Pérez, J., 2013. A novel control strategy for enhancing biological N-removal in a granular sequencing

batch reactor: A model-based study. Chem. Eng. J. 232, 468–477. doi:10.1016/j.cej.2013.07.118

Janssen, A., Meijer, S., Bontsema, J., Lettinga, G., 1998. Application of the redox potential for controling a sulfide oxidizing bioreactor. Biotechnol. Bioeng. 60, 147–55.

Jemaat, Z., Bartrolí, A., Isanta, E., Carrera, J., Suárez-Ojeda, M.E., Pérez, J., 2013. Closed-loop control of ammonium concentration in nitritation: Convenient for reactor operation but also for modeling. Bioresour. Technol. 128, 655–663.

Jenkins, B.M., Williams, R.B., Adams, L.S., Peace, C., Petersen, G., Leary, M., 2008. Current Anaerobic Digestion Technologies Used for Treatment of Municipal Organic Solid Waste.

Jimenez, J., Latrille, E., Harmand, J., Robles, A., Ferrer, J., Gaida, D., Wolf, C., Mairet, F., Bernard, O., Alcaraz-Gonzalez, V., Mendez-Acosta, H., Zitomer, D., Totzke, D., Spanjers, H., Jacobi, F., Guwy, A., Dinsdale, R., Premier, G., Mazhegrane, S., Ruiz-Filippi, G., Seco, A., Ribeiro, T., Pauss, A., Steyer, J.P., 2015. Instrumentation and control of anaerobic digestion processes: a review and some research challenges. Rev. Environ. Sci. Biotechnol. 14, 615–648.

Jin, Y., Veiga, M.C., Kennes, C., 2005. Effects of pH, CO2, and flow pattern on the autotrophic degradation of hydrogen sulfide in a biotrickling filter. Biotechnol. Bioeng. 92, 462–71.

Joseph S. Devinny, Marc A. Deshusses, T.S.W., 1998. Biofiltration for air pollution control., CRC Press. ed. Lewis Publishers, Florida.

Jou, D., 2013. Introducción al mundo cuántico. Pasado&Presente, Barcelona,Spain.

Kennes, C., Veiga, M.C., 2001. Bioreactors for Waste Gas Treatment. Kluwer Academic Publishers, Dordrecht, The Netherlands.

Khalid, A., Arshad, M., Anjum, M., Mahmood, T., Dawson, L., 2011. The anaerobic digestion of solid organic waste. Waste Manag. 31, 1737–1744.

Kim, S., Deshusses, M. a., 2008. Determination of mass transfer coefficients for packing materials used in biofilters and biotrickling filters for air pollution control. 1.

Experimental results. Chem. Eng. Sci. 63, 841–855.

Kim, S., Deshusses, M.A., 2005. Understanding the limits of H 2 S degrading biotrickling filters using a differential biotrickling filter 113, 119–126.

Kim, S., Deshusses, M.A., 2003. Development and Experimental Validation of a Conceptual Model for Biotrickhg Ffltration of H2S 119–128.

Kraakman, N.J.R., Rocha-Rios, J., van Loosdrecht, M.C.M., 2011. Review of mass transfer aspects for biological gas treatment. Appl. Microbiol. Biotechnol. 91, 873–86.

Krayzelova, L., Bartacek, J., Kolesarova, N., Jenicek, P., 2014. Bioresource Technology Microaeration for hydrogen sulfide removal in UASB reactor. Bioresour. Technol. 172, 297–302.

Kristensson, I., 2007. Biogas på gasnätet utan propantillsats.

Kymäläinen, M., Lähde, K., Arnold, M., Kurola, J.M., Romantschuk, M., Kautola, H., 2012. Biogasi fi cation of biowaste and sewage sludge e Measurement of biogas quality. J. Environ. Manage. 95, S122–S127. doi:10.1016/j.jenvman.2011.01.003

Langenhove, H. Van, De, B., 2001. Biotechnological treatment of sewage odours. Control.

Lau, a. K., Lo, K.V., Liao, P.H., Yu, J.C., 1992. Aeration experiments for swine waste composting. Bioresour. Technol. 41, 145–152.

Lau, C.S., Tsolakis, A., Wyszynski, M.L., 2010. Biogas upgrade to syn-gas (H2 -CO) via dry and oxidative reforming. Int. J. Hydrogen Energy 36, 397–404.

Li, H., Crittenden, J.C., Mihelcic, J.R., Hautakangas, H., 2002. Optimization of Biofiltration for Odor Control: Model Development and Parameter Sensivity 74, 5–16.

Liao, Q., Tian, X., Chen, R., Zhu, X., 2008. Mathematical model for gas–liquid two-phase flow and biodegradation of a low concentration volatile organic compound (VOC) in a trickling biofilter. Int. J. Heat Mass Transf. 51, 1780–1792.

Lo, H.M., Kurniawan, T.A., Sillanpää, M.E.T., Pai, T.Y., Chiang, C.F., Chao, K.P., Liu, M.H., Chuang, S.H., Banks, C.J., Wang, S.C., Lin, K.C., Lin, C.Y., Liu, W.F.,

Cheng, P.H., Chen, C.K., Chiu, H.Y., Wu, H.Y., 2010. Bioresource Technology Modeling biogas production from organic fraction of MSW co-digested with MSWI ashes in anaerobic bioreactors. Bioresour. Technol. 101, 6329–6335.

López, L.R., Bezerra, T., Mora, M., Lafuente, J., Gabriel, D., 2016a. Influence of trickling liquid velocity and flow pattern in the improvement of oxygen transport in aerobic biotrickling filters for biogas desulfurization. J. Chem. Technol. Biotechnol. 91, 1031–1039.

López, L.R., Dorado, A.D., Gabriel, D., Mora, M., Gamisans, X., Lafuente, J., 2016b. Modeling an aerobic biotrickling filter for biogas desulfurization through a multi-step oxidation mechanism. Chem. Eng. J. 294, 447–457.

Lu, C., Lin, M.-R., Chu, C., 2002. Effects of pH, moisture, and flow pattern on trickle-bed air biofilter performance for BTEX removal. Adv. Environ. Res. 6, 99–106.

Luyben, M.L., Luyben, W.L., 1997. Essentials of Process Control, Chemical Engineering. McGraw-Hill.

Maat, H., Hogendoorn, J.A., Versteeg, G.F., 2005. The removal of hydrogen sulfide from gas streams using an aqueous metal sulfate absorbent Part I . The absorption of hydrogen sulfide in metal sulfate solutions 43, 183–197.

Mannucci, A., Munz, G., Mori, G., Lubello, C., 2012. Biomass accumulation modelling in a highly loaded biotrickling filter for hydrogen sulphide removal. Chemosphere 88, 712–7.

Marcelino, M., Guisasola, A., Baeza, J.A., 2009. Experimental assessment and modelling of the proton production linked to phosphorus release and uptake in EBPR systems. Water Res. 43, 2431–2440.

Martín-González, L., Castro, R., Pereira, M.A., Alves, M.M., Font, X., Vicent, T., 2011. Thermophilic co-digestion of organic fraction of municipal solid wastes with FOG wastes from a sewage treatment plant : Reactor performance and microbial community monitoring. Bioresour. Technol. 102, 4734–4741.

Martín-González, L., Colturato, L.F., Font, X., Vicent, T., 2010. Anaerobic co-digestion of the organic fraction of municipal solid waste with FOG waste from a sewage treatment plant : Recovering a wasted methane potential and enhancing the biogas

yield. WASTE Manag. d

Mc Crone, A., 2013. Global Trends in Renewable Energy Investment. Frankfurt, Germany.

Meena, V., Rajendran, L., Kumar, S., Jansi Rani, P.G., 2015. Mathematical modeling of gas phase and biofilm phase biofilter performance. Egypt. J. Basic Appl. Sci. 3, 94–105.

Meyer, T., Edwards, E.A., 2014. ScienceDirect Anaerobic digestion of pulp and paper mill wastewater and sludge. Water Res. 65, 321–349.

Montebello, A.M., Baeza, M., Lafuente, J., Gabriel, D., 2010. Monitoring and performance of a desulphurizing biotrickling filter with an integrated continuous gas/liquid flow analyser. Chem. Eng. J. 165, 500–507.

Montebello, A.M., Bezerra, T., Rovira, R., Rago, L., Lafuente, J., Gamisans, X., Campoy, S., Baeza, M., Gabriel, D., 2013. Operational aspects, pH transition and microbial shifts of a H2S desulfurizing biotrickling filter with random packing material. Chemosphere 93, 2675–82.

Montebello, A.M., Fernández, M., Almenglo, F., Ramírez, M., Cantero, D., Baeza, M., Gabriel, D., 2012. Simultaneous methylmercaptan and hydrogen sulfide removal in the desulfurization of biogas in aerobic and anoxic biotrickling filters. Chem. Eng. J. 200–202, 237–246.

Montebello, A.M., Mora, M., López, L.R., Bezerra, T., Gamisans, X., Lafuente, J., Baeza, M., Gabriel, D., 2014. Aerobic desulfurization of biogas by acidic biotrickling filtration in a randomly packed reactor. J. Hazard. Mater. 280, 200–8.

Montebello, A.M., 2013. AEROBIC BIOTRICKLING FILTRATION FOR BIOGAS DESULFURIZATION. Universitat Autonoma de Barcelona PhD thesis

Mora, M., 2014. Characterization of S-Oxidizing Biomass Through Respirometric Techniques Under Anoxic and Aerobic Conditions. Universitat Autonoma de Barcelona. PhD thesis

Mora, M., Fernández, M., Gómez, J.M., Cantero, D., Lafuente, J., Gamisans, X., Gabriel, D., 2014a. Kinetic and stoichiometric characterization of anoxic sulfide oxidation by SO-NR mixed cultures from anoxic biotrickling filters. Appl. Microbiol.

Biotechnol.

Mora, M., Guisasola, A., Gamisans, X., Gabriel, D., 2014b. Examining thiosulfate-driven autotrophic denitrification through respirometry. Chemosphere 113, 1–8.

Mora, M., López, L.R., Gamisans, X., Gabriel, D., 2014c. Coupling respirometry and titrimetry for the characterization of the biological activity of a SO-NR consortium. Chem. Eng. J. 251, 111–115.

Mora, M., López, L.R., Lafuente, J., Pérez, J., Kleerebezem, R., Loosdrecht, M. Van, Gamisans, X., Gabriel, D., 2016. Respirometric characterization of aerobic sulfide, thiosulfate and elemental sulfur oxidation by S-oxidizing biomass. Water Res. 89, 282–292.

Munz, G., Gori, R., Mori, G., Lubello, C., 2009. Monitoring biological sulphide oxidation processes using combined respirometric and titrimetric techniques. Chemosphere 76, 644–650.

Murphy, J., Bochmann, G., 2011. Biogas from Crop Digestion Biogas from Crop Digestion.

Murphy, J.D., Mckeogh, E., Kiely, G., 2004. Technical / economic / environmental analysis of biogas utilisation 77, 407–427.

Namini, M.T., Abdehagh, N., Heydarian, S.M., Bonakdarpour, B., Kooki, D.Z.B., 2013. Hydrogen sulfide removal performance of a bio-trickling filter employing Thiobacillus thiparus immobilized on polyurethane foam under various starvation regimes. Biotechnol. Bioprocess Eng. 17, 1278–1283.

Nash, J.E., Sutcliffe, J. V, 1970. River flow forecasting through conceptual models part I: A discussion of principles. J. Hydrol. 10, 282–290.

Nguyen, D., Gadhamshetty, V., Nitayavardhana, S., Khanal, S.K., 2015. Automatic process control in anaerobic digestion technology: A critical review. Bioresour. Technol. 193, 513–522.

Nielsen, P.H., de Muro, M. a, Nielsen, J.L., 2000. Studies on the in situ physiology of Thiothrix spp. present in activated sludge. Environ. Microbiol. 2, 389–98.

Norbert Pfenning, Friedrich Widdel, H.G.T., 1981. The Dissimilatory Sulfate-Reducing

Bacteria, in: Starr MP (Ed.), The Prokaryotes, Vol 1. Springer Verlag., Stolp H, Trupper HG,Balows A, Schlegels H., New York, USA., pp. 926–940.

Onda, K., Takeuchi, H., Okumoto, Y., 1968. Mass transfer coefficients between gas and liquid phases in packed columns. J. Chem. Eng. Japan 1, 56–62.

Perry, R., Green, D., Maloney, J., 1997. Perry's chemical engineers' handbook, Journal of Chemical Education.

Persson, M., Wellinger, A., Braun, R., Holm-nielsen, J.B., Seadi, T.A.L., Baxter, D., Jormanainnen, M., 2006. Biogas Upgrading to Vehicle Fuel Standards and Grid Injection.

Persson, T., Baxter, D., 2015. IEA Bioenergy Task 37 Country Reports Summary.

Pipatmanomai, S., Kaewluan, S., Vitidsant, T., 2009. Economic assessment of biogas-to-electricity generation system with H2S removal by activated carbon in small pig farm. Appl. Energy 86, 669–674.

Popat, S.C., Deshusses, M. a., 2010. Analysis of the rate-limiting step of an anaerobic biotrickling filter removing TCE vapors. Process Biochem. 45, 549–555.

Pöschl, M., Ward, S., Owende, P., 2010. Evaluation of energy efficiency of various biogas production and utilization pathways. Appl. Energy 87, 3305–3321.

Puyuelo, B., Gea, T., Sánchez, A., 2010. A new control strategy for the composting process based on the oxygen uptake rate. Chem. Eng. J. 165, 161–169.

Ravina, M., Genon, G., 2016. Global and local emissions of a biogas plant considering the production of biomethane as an alternative end-use solution. J. Clean. Prod. 102, 115–126.

Rieger, L., Jones, R.M., Dold, P.L., Bott, C.B., 2014. Ammonia-Based Feedforward and Feedback Aeration Control in Activated Sludge Processes. Water Environ. Res. 86, 63–73.

Rincón, A., Erazo, C., Angulo, F., 2012. A robust adaptive controller for an anaerobic digester with saturated input: Guarantees for the boundedness and convergence

properties. J. Process Control 22, 1785–1792.

Rintala, J., Kinnunen, V., Yl, A., 2015. Mesophilic anaerobic digestion of pulp and paper industry biosludge e long-term reactor performance and effects of thermal pretreatment 87, 105–111.

Rodriguez, G., 2013. Eliminació de H2S mitjançant biofiltres percoladors: millora de la transferencia d'oxygen. Universitat Politecnica de Catalunya. PhD Thesis

Rodriguez, G., Dorado, a. D., Bonsfills, a., Gabriel, D., Gamisans, X., 2013. Optimization of Oxygen Transfer through Membrane Diffusers for Biological Sweetening of Biogas. Chem. Eng. Technol. 36, 513–518.

Rodriguez, G., Dorado, A.D., Bonsfills, A., Sanahuja, R., Gabriel, D., Gamisans, X., 2012. Optimization of oxygen transfer through venturi-based systems applied to the biological sweetening of biogas. J. Chem. Technol. Biotechnol. 87, 854–860.

Rodriguez, G., Dorado, A.D., Fortuny, M., Gabriel, D., Gamisans, X., 2014. Biotrickling filters for biogas sweetening: Oxygen transfer improvement for a reliable operation. Process Saf. Environ. Prot. 92, 261–268.

Roosta, A., Jahanmiri, A., Mowla, D., Niazi, A., 2011. Mathematical modeling of biological sulfide removal in a fed batch bioreactor. Biochem. Eng. J. 58-59, 50–56.

Ruano, M.V., Ribes, J., Seco, a., Ferrer, J., 2012. An advanced control strategy for biological nutrient removal in continuous systems based on pH and ORP sensors. Chem. Eng. J. 183, 212–221.

Ryckebosch, E., Drouillon, M., Vervaeren, H., 2011. Techniques for transformation of biogas to biomethane. Biomass and Bioenergy 35, 1633–1645.

Salehahmadi, R., Halladj, R., Zamir, S.M., 2012. Unsteady-State Mathematical Modeling of a Fungal Biofilter Treating Hexane Vapor at Different Operating Temperatures. Ind. Eng. Chem. Res. 51, 2388–2396. doi:10.1021/ie2014718

Saltelli, A., Chan, K., Scott, E., 2000. Sensitivity analysis. John Wiley & Sons, Ltd., New York.

Sander, R., 2014. Compilation of Henry's law constants. Atmos. Chem. Phys. Discuss. 14. doi:10.5194/acpd-14-29615-2014

Santin, I., Pedret, C., Vilanova, R., 2015. Applying variable dissolved oxygen set point in a two level hierarchical control structure to a wastewater treatment process. J. Process Control 28, 40–55. doi:10.1016/j.jprocont.2015.02.005

Sharvelle, S., Arabi, M., Mclamore, E., Banks, M.K., 2008. Model Development for Biotrickling Filter Treatment of Graywater Simulant and Waste Gas . I. J. Environ. Eng. 130, 813–825.

Shu, F., 1982. The Physical Universe, An Introduction to Astronomy. University Science Books.

Silva, J., Morales, M., Cáceres, M., Morales, P., Aroca, G., 2012. Modelling of the biofiltration of reduced sulphur compounds through biotrickling filters connected in series: Effect of H2S. Electron. J. Biotechnol. 15.

Soreanu, G., Falletta, P., Béland, M., Edmonson, K., Ventresca, B., Seto, P., 2010. Empirical modelling and dual-performance optimisation of a hydrogen sulphide removal process for biogas treatment. Bioresour. Technol. 101, 9387–90.

Spanjers, H., Vanrolleghem, P., Nguyen, K., Vanhooren, H., Patry, G.G., 1998. Towards a simulation-benchmark for evaluating respirometry-based control strategies. Water Sci. Technol.

Spanjers, H., Vanrolleghem, P., Olsson, G., Dold, P., 1996. Respirometry in control of the activated sludge process. Water Sci. Technol. 34, 117–126.

Starr, K., Gabarrell, X., Villalba, G., Talens, L., Lombardi, L., 2012. Life cycle assessment of biogas upgrading technologies. Waste Manag. 32, 991–999.

Stephanopoulos, G., 1984. Chemical Process Control, An introduction to Theory and Practice. Prentice Hall New Jersey, Englewood Cliffs, New Jersey.

Stephanopoulus, G., 1984. Chemical Process Control An Introduction to Theory and Practice. Prentice Hall, Englewood Cliffs, New Jersey.

Steudel, R., Eckert, B., 2004. Solid Sulfur Allotropes. ChemInform 35.

Stewart, P.S., 2003. Diffusion in Biofilms. J. Bacteriol. 185, 1485–1491.

Steyer, J.-P., Buffière, P., Rolland, D., Moletta, R., 1999. Advanced control of anaerobic digestion processes through disturbances monitoring. Water Res. 33, 2059–2068.

Swedish Gas Association, 2011. Biogas in Sweden.

Syed, M., Soreanu, G., Falletta, P., Béland, M., 2006. Removal of hydrogen sulfide from gas streams using biological processes - A review. Can. Biosyst. Eng. 2.1.

Tajima, H., Yamasaki, A., Kiyono, F., 2004. Energy consumption estimation for greenhouse gas separation processes by clathrate hydrate formation. Energy 29, 1713–1729.

Tomàs, M., Fortuny, M., Lao, C., Gabriel, D., Lafuente, J., Gamisans, X., 2009. Technical and economical study of a full-scale biotrickling filter for H 2 S removal from biogas. water Pract. Technol. 4.

Torà, J.A., Lafuente, J., Baeza, J.A., Carrera, J., 2010. Combined effect of inorganic carbon limitation and inhibition by free ammonia and free nitrous acid on ammonia oxidizing bacteria. Bioresour. Technol. 101, 6051–8.

Trejo-Aguilar, G., Revah, S., Lobo-Oehmichen, R., 2005. Hydrodynamic characterization of a trickle bed air biofilter. Chem. Eng. J. 113, 145–152.

Tremier, A., De Guardia, A., Massiani, C., Paul, E., Martel, J.L., 2005. A respirometric method for characterising the organic composition and biodegradation kinetics and the temperature influence on the biodegradation kinetics, for a mixture of sludge and bulking agent to be co-composted. Bioresour. Technol. 96, 169–180.

Trenberth, K.E., Fasullo, J.T., Kiehl, J., 2008. Earth's Global energy budget. Am. Meteorol. Soc. 90, 311–324.

United Nations, 1998. Kyoto Protocol To the United Nations Framework Kyoto Protocol To the United Nations Framework. Rev. Eur. Community Int. Environ. Law 7, 214–217.

Van den Bosch, P.L.F., van Beusekom, O.C., Buisman, C.J.N., Janssen, A.J.H., 2007. Sulfide oxidation at halo-alkaline conditions in a fed-batch bioreactor. Biotechnol. Bioeng. 97, 1053–1063.

Waewsak, C., Nopharatana, A., Chaiprasert, P., 2010. Neural-fuzzy control system

application for monitoring process response and control of anaerobic hybrid reactor in wastewater treatment and biogas production. J. Environ. Sci. 22, 1883–1890.

Walsh, J., Ross, C., Smith, M., Harper, S., Wilkins, W., 1988. Handbook on Biogas Utilization. Georgia.

Weiland, P., 2010. Biogas production : current state and perspectives 849–860.

Whitman, W.G., 1923. The Two-Film Theory of Gas Absorption. Chem. Metall. Eng. 29, 146–148.

Wilcox, S.J., Hawkes, D.L., Hawkes, F.R., Guwy, A.J., 1995. A neural network, based on bicarbonate monitoring, to control anaerobic digestion. Water Res. 29, 1465–1470.

Winkler, M.-K.H., Ettwig, K.F., Vannecke, T.P.W., Stultiens, K., Bogdan, a, Kartal, B., Volcke, E.I.P., 2015. Modelling simultaneous anaerobic methane and ammonium removal in a granular sludge reactor. Water Res. 73, 323–31.

Wood, B.D., Quintard, M., Whitaker, S., 2002. Calculation of effective diffusivities for biofilms and tissues. Biotechnol. Bioeng. 77, 495–516.

Yan, S., He, Q., Zhao, S., Wang, Y., Ai, P., 2014. Chemical Engineering and Processing : Process Intensi fi cation Biogas upgrading by CO 2 removal with a highly selective natural amino acid salt in gas – liquid membrane contactor. Chem. Eng. Process. Process Intensif. 85, 125–135.

Yang, C., Chen, H., Zeng, G., Yu, G., Luo, S., 2010. Biomass accumulation and control strategies in gas biofiltration. Biotechnol. Adv. 28, 531–40.

Zhang, C., Su, H., Baeyens, J., Tan, T., 2014. Reviewing the anaerobic digestion of food waste for biogas production. Renew. Sustain. Energy Rev. 38, 383–392.

Zhang, P., Yuan, M., Wang, H., 2008. Improvement of nitrogen removal and reduction of operating costs in an activated sludge process with feedforward–cascade control strategy. Biochem. Eng. J. 41, 53–58.

Ziegler, J.G., Nichols, N.B., 1942. Optimum Settings for Automatic Controllers. Transacction of the A.S.M.E 64, 759–768.